frontiers | Research Topics

Community series in new insights in sepsis pathogenesis and renal dysfunction: Immune mechanisms and novel management strategies, volume II

Edited by
Alessandra Stasi and Patrick M. Honore

Published in
Frontiers in Immunology
Frontiers in Medicine

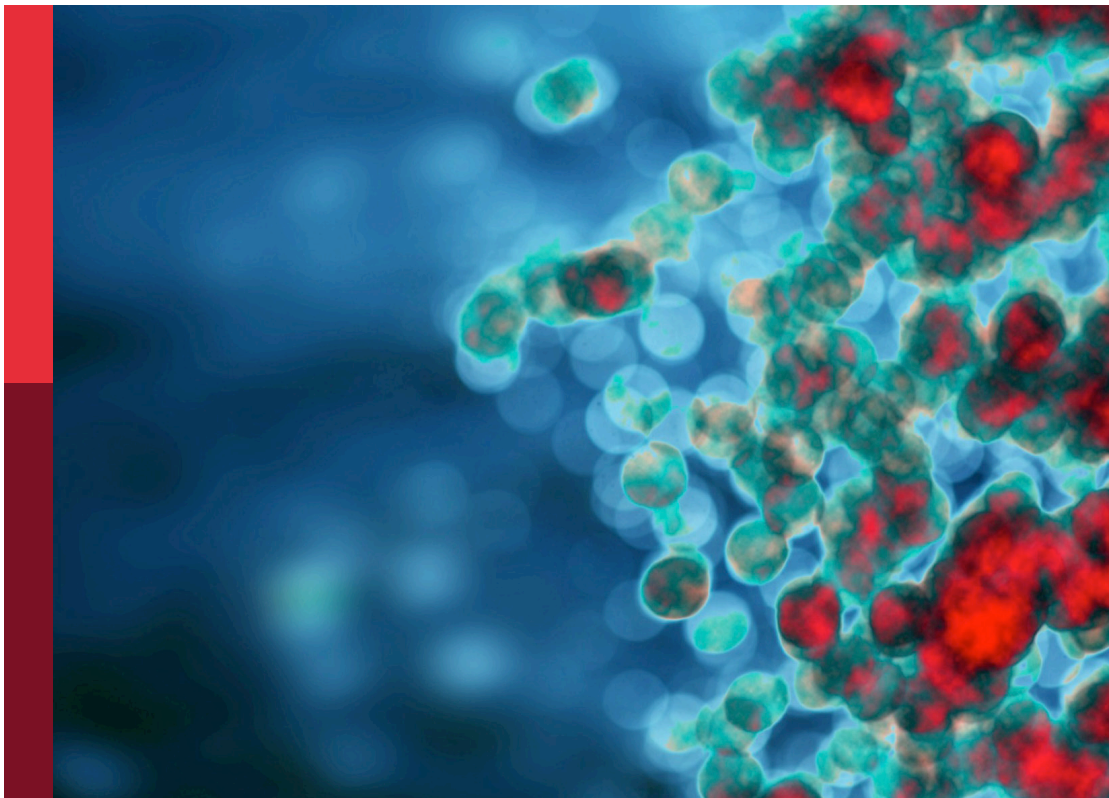

ISSN 1664-8714
ISBN 978-2-8325-3904-0
DOI 10.3389/978-2-8325-3904-0

About Frontiers

Frontiers is more than just an open access publisher of scholarly articles: it is a pioneering approach to the world of academia, radically improving the way scholarly research is managed. The grand vision of Frontiers is a world where all people have an equal opportunity to seek, share and generate knowledge. Frontiers provides immediate and permanent online open access to all its publications, but this alone is not enough to realize our grand goals.

Frontiers journal series

The Frontiers journal series is a multi-tier and interdisciplinary set of open-access, online journals, promising a paradigm shift from the current review, selection and dissemination processes in academic publishing. All Frontiers journals are driven by researchers for researchers; therefore, they constitute a service to the scholarly community. At the same time, the *Frontiers journal series* operates on a revolutionary invention, the tiered publishing system, initially addressing specific communities of scholars, and gradually climbing up to broader public understanding, thus serving the interests of the lay society, too.

Dedication to quality

Each Frontiers article is a landmark of the highest quality, thanks to genuinely collaborative interactions between authors and review editors, who include some of the world's best academicians. Research must be certified by peers before entering a stream of knowledge that may eventually reach the public - and shape society; therefore, Frontiers only applies the most rigorous and unbiased reviews. Frontiers revolutionizes research publishing by freely delivering the most outstanding research, evaluated with no bias from both the academic and social point of view. By applying the most advanced information technologies, Frontiers is catapulting scholarly publishing into a new generation.

What are Frontiers Research Topics?

Frontiers Research Topics are very popular trademarks of the *Frontiers journals series*: they are collections of at least ten articles, all centered on a particular subject. With their unique mix of varied contributions from Original Research to Review Articles, Frontiers Research Topics unify the most influential researchers, the latest key findings and historical advances in a hot research area.

Find out more on how to host your own Frontiers Research Topic or contribute to one as an author by contacting the Frontiers editorial office: frontiersin.org/about/contact

Community series in new insights in sepsis pathogenesis and renal dysfunction: Immune mechanisms and novel management strategies, volume II

Topic editors

Alessandra Stasi — University of Bari Aldo Moro, Italy

Patrick M. Honore — CHU UCL Namur Site Godinne, Belgium

Citation

Stasi, A., Honore, P. M., eds. (2023). *Community series in new insights in sepsis pathogenesis and renal dysfunction: Immune mechanisms and novel management strategies, volume II*. Lausanne: Frontiers Media SA.

doi: 10.3389/978-2-8325-3904-0

Table of contents

frontiers | Frontiers in Immunology

TYPE Editorial
PUBLISHED 27 October 2023
DOI 10.3389/fimmu.2023.1322571

OPEN ACCESS

EDITED AND REVIEWED BY
Pietro Ghezzi,
University of Urbino Carlo Bo, Italy

*CORRESPONDENCE
Patrick M. Honore
Patrick.Honore@CHUUCLNamur.UCLouvain.be

RECEIVED 16 October 2023
ACCEPTED 23 October 2023
PUBLISHED 27 October 2023

CITATION
Honore PM, Stasi A and Cantaluppi V (2023) Editorial: Community series in new insights in sepsis pathogenesis and renal dysfunction: immune mechanisms and novel management strategies: volume II. *Front. Immunol.* 14:1322571. doi: 10.3389/fimmu.2023.1322571

Editorial: Community series in new insights in sepsis pathogenesis and renal dysfunction: immune mechanisms and novel management strategies: volume II

Patrick M. Honore[1]*, Alexandra Stasi[2] and Vincenzo Cantaluppi[3]

[1]Intensive Care Department, Université Catholique de Louvain (UCL) Louvain Medical School of Medicine, Centre Hospitalier Universitaire (CHU) UCL Mont-Godinne Namur, Yvoir, Belgium, [2]Nephrology, Dialysis and Transplantation Unit, Department of Precision and Regenerative Medicine and Ionian Area, University of Bari "Aldo Moro", Bari, Italy, [3]Nephrology and Kidney Transplantation Unit, Department of Translational Medicine (DIMET), University of Piemonte Orientale (UPO), "Maggiore della Carità" University Hospital, Novara, Italy

KEYWORDS

sepsis, COVID 19, subarachnoid bleeding, immunology, macrohemodynamics, autophagy, biomarkers, neutrophils and acupuncture

Editorial on the Research Topic

Community series in new insights in sepsis pathogenesis and renal dysfunction: immune mechanisms and novel management strategies: volume II

Sepsis, trauma, COVID-19-disease and subarachnoid hemorrhage (SAH) can cause severe organ failure, such as Acute Kidney Injury (AKI) and encephalopathy, among others (1). The mechanisms behind this induced organ failure are diverse and not limited to immune mechanisms, emphasized in Volume I of this series (2). In the second volume of the Research Topic "*New Insights in Sepsis Pathogenesis and Renal Dysfunction: Immune Mechanisms and Novel Management Strategies*" published in Frontiers in Immunology, we delve into a broader spectrum of mechanisms associated with life-threatening organ dysfunction. This includes exploring aspects such as macrohemodynamics and autophagy, which have been extensively studied in conditions such as severe trauma and sepsis (3). We also examine the intricate role of neutrophils and other contributing factors (2). Additionally, biomarkers for aiding in diagnosis and assessing organ function will be discussed. Furthermore, innovative approaches are considered, with a focus on acupuncture as a therapeutic intervention within this context, showing promise in mitigating organ damage and enhancing patient outcomes (4). Within this comprehensive exploration of mechanisms associated with life-threatening organ dysfunction in the second volume, noteworthy studies shed light on vital aspects.

One such study, led by Guo et al., has focused on AKI datasets GSE30718 and GSE44925. Their findings reveal that the hub gene Afamin (AFM) is significantly downregulated in AKI samples and correlates with the development of this syndrome. In another intriguing investigation, Zhao et al. explore the blood pressure target in sepsis-associated AKI (SA-AKI). Their conclusions suggest that, in order to ensure optimal renal perfusion, AKI patients with hypertension may benefit from a higher mean arterial pressure range (MAP), specifically in the range of 70-80 mmHg, as opposed to the traditional range of 65-73 mmHg.

Autophagy has gained attention for its crucial role in immune disorders after major trauma (3). Chen et al. demonstrated its significance in the early stages of trauma-induced immune disorders. Furthermore, their study showed a comprehensive single-cell immune profile for major trauma patients, unveiling how autophagy profoundly affects innate immune cell functions, providing insight into post-trauma immune dysregulation.

Sepsis-associated encephalopathy (SAE) has garnered significant research attention. A meta-analysis conducted by Hu et al. reveals a moderate association between elevated serum S100 calcium binding protein B (S100B) levels in septic patients and SAE, particularly concerning unfavorable outcomes including mortality. These findings suggest that serum S100B levels could serve as valuable diagnostic and prognostic biomarkers for SAE.

Recently, a compelling link has emerged between heightened levels of neutrophil extracellular traps (NETs) and adverse clinical outcomes in patients affected by COVID-19 disease. Kim et al. demonstrated that elevated NETs are closely tied to AKI, that in turn represents a robust predictor of mortality. This close connection between NETs and plasma von Willebrand factor raises the possibility of NETs playing a role in COVID-19-associated vasculopathy, potentially contributing to the development of AKI.

Pylephlebitis refers to an infective and suppurative thrombosis that affects the portal vein and its branches. When concurrent pylephlebitis and subarachnoid hemorrhage (SAH) occur in patients with sepsis, it presents a rare yet life-threatening situation. Managing both coagulation and bleeding simultaneously poses a significant challenge for clinicians. In a case report, Zhao et al. describe the successful treatment of an octogenarian with E. coli bacteremia who faced concurrent pylephlebitis, SAH, and multiple organ dysfunction syndrome (MODS). In such cases of critical complications, early and decisive use of LMWH (Low Molecular Weight Heparin) proves essential for resolving thrombosis and ultimately leads to a favorable prognosis.

Biomarkers are playing an increasingly vital role in the diagnosis of sepsis, as well as in understanding the intricate connections between genes and immune cells with differential expression in specimens from sepsis patients compared to healthy controls. In their study, Wang et al. pinpointed COMMD9, CSF3R, and NUB1 as potential genes that could serve as sepsis biomarkers—a hypothesis corroborated by ROC analysis. Furthermore, their research unveiled correlations between the expression of these three genes and the composition of immune cell infiltrates. Specifically, COMMD9 exhibited correlations with regulatory T cells, follicular helper T cells, CD8 T cells, and more. Similarly, CSF3R showed associations with regulatory T cells, follicular helper T cells, and CD8 T cells, while NUB1 correlated with regulatory T cells, gamma delta T cells, and follicular helper T cells. These collective findings not only identify promising new diagnostic markers for sepsis but also shed light on novel disease pathogenetic mechanisms, paving the way to potential therapeutic interventions.

In the realm of sepsis treatment, acupuncture has gained widespread acceptance and utilization, with notable advancements in understanding its mechanisms in recent years. In a breakthrough study, Yang et al. unveiled the pivotal role played by the cholinergic anti-inflammatory pathway of the vagus nervous system, the adrenal dopamine anti-inflammatory pathway, and the sympathetic nervous system in transmitting acupuncture's therapeutic effects and suppressing systemic inflammation. Particularly in cases of Multiple Organ Dysfunction Syndrome (MODS), acupuncture serves as a protective shield against sepsis-induced organ damage. It achieves this by curbing excessive inflammatory responses, fortifying resistance against oxidative stress, safeguarding mitochondrial function, and diminishing apoptosis and tissue or organ damage.

The second volume of the "*New Insights in Sepsis Pathogenesis and Renal Dysfunction: Immune Mechanisms and Novel Management Strategies*" Research Topic in Frontiers in Immunology show the multifaceted landscape of sepsis and related conditions, encompassing mechanisms like immunology, macrohemodynamics, autophagy, and the impact of neutrophils. Studies by Guo et al., Zhao et al., Chen et al., Hu et al., Kim et al., Wang et al., and Yang et al. contribute valuable insights, revealing underlying mechanisms, potential diagnostic markers, novel pathways, and therapeutic interventions. This holistic perspective underscores the complexity of sepsis management, emphasizing the importance of diverse mechanisms and innovative strategies to improve patient outcomes.

Author contributions

PH: Conceptualization, Writing – original draft, Writing – review & editing. AS: Writing – review & editing. VC: Writing – review & editing.

Funding

The author(s) declare that no financial support was received for the research, authorship, and/or publication of this article.

Acknowledgments

The authors would like to thanks a lot the incredible help of Dr Sydney Blackman,MD,ULB, in this manuscript.

Conflict of interest

The authors declare that the research was conducted in the absence of any commercial or financial relationships that could be construed as a potential conflict of interest.

The author(s) declared that they were an editorial board member of Frontiers, at the time of submission. This had no impact on the peer review process and the final decision.

Publisher's note

References

1. Kozlov AV, Grillari J. Pathogenesis of multiple organ failure: the impact of systemic damage to plasma membranes. *Front Med (Lausanne)* (2022) 9:806462. doi: 10.3389/fmed.2022.806462

2. Stasi A, Honore PM. Editorial: New insights in sepsis pathogenesis and renal dysfunction: Immune mechanisms and novel management strategies. *Front Immunol* (2023) 14:1176620. doi: 10.3389/fimmu.2023.1176620

3. Ren C, Zhang H, Wu TT, Yao YM. Autophagy: A potential therapeutic target for reversing sepsis-induced immunosuppression. *Front Immunol* (2017) 8:1832. doi: 10.3389/fimmu.2017.01832

4. Matsuda A, Jacob A, Wu R, Aziz M, WL Y, Matsutani T, et al. Novel therapeutic targets for sepsis: regulation of exaggerated inflammatory responses. *J Nippon Med Sch* (2012) 79(1):4–18. doi: 10.1272/jnms.79.4

frontiers | Frontiers in Immunology

TYPE Original Research
PUBLISHED 15 December 2022
DOI 10.3389/fimmu.2022.1060612

OPEN ACCESS

EDITED BY
Patrick Honore,
University Hospital Brugmann, Belgium

REVIEWED BY
Akram M. Zaaqoq,
MedStar Washington Hospital Center, United States
Wenfei Tan,
The First Affiliated Hospital of China Medical University, China

*CORRESPONDENCE
Keliang Xie
xiekeliang2009@hotmail.com
Yun Li
cfsyy_liyun@126.com
Lina Zhao
18240198229@163.com

SPECIALTY SECTION
This article was submitted to Inflammation, a section of the journal Frontiers in Immunology

RECEIVED 03 October 2022
ACCEPTED 25 November 2022
PUBLISHED 15 December 2022

CITATION
Zhao L, Fan Y, Wang Z, Wei Z, Zhang Y, Li Y and Xie K (2022) The blood pressure targets in sepsis patients with acute kidney injury: An observational cohort study of multiple ICUs.
Front. Immunol. 13:1060612.
doi: 10.3389/fimmu.2022.1060612

The blood pressure targets in sepsis patients with acute kidney injury: An observational cohort study of multiple ICUs

Lina Zhao[1*], Yan Fan[1], Zhiwei Wang[1], Zhiyong Wei[1], Ying Zhang[1], Yun Li[2*] and Keliang Xie[1,2,3*]

[1]Department of Critical Care Medicine, Tianjin Medical University General Hospital, Tianjin, China, [2]Department of Anesthesiology, Tianjin Medical University General Hospital, Tianjin, China, [3]Department of Anesthesiology, Tianjin Institute of Anesthesiology, Tianjin, China

Background: The maintenance of blood pressure is pivotal in preventing sepsis with acute kidney injury (AKI). Especially in sepsis patients treated with vasopressors. The optimal the blood pressure has been controversial to maintain renal perfusion. This study aims to explore the blood pressure target in sepsis with AKI.

Methods: We retrieved patient data from the MIMIC IV and eICU databases. The Lasso regression model was used to identify the relationship between blood pressure and sepsis in patients with AKI and remove collinearity among variables. Generalized additive models were used to estimate the blood pressure range in patients with sepsis with AKI. Statistical methods such as multivariable logistic regression, propensity score analysis, inversion probability-weighting, and doubly robust model estimation were used to verify the target blood pressure for patients with sepsis and AKI.

Results: In total, 17874 patients with sepsis were included in this study. the incidence of AKI may be related to the level of mean article pressure (MAP) and diastolic blood pressure (DBP) in sepsis patients. The range of MAPs and DBPs may be 65-73 mmHg and 50-60 mmHg in AKI patients without hypertension. The range of MAPs and DBPs may be 70-80 mmHg and 54-62 mmHg in AKI patients with hypertension. The prognosis of sepsis with AKI was unaffected by MAP or DBP. Systolic blood pressure is not associated with sepsis in patients with AKI.

Conclusions: To ensure renal perfusion, AKI patients with hypertension may require a higher MAP [70-80] versus (65-73), mmHg] and DBP [(54-62) vs (50-60), mmHg] than patients without hypertension.

KEYWORDS

sepsis, mean arterial pressure, diastolic blood pressure, acute kidney injury, hemodynamics

Introduction

Acute kidney injury (AKI) has been a global concern in the field of acute and critical diseases (1). According to a multinational cross-sectional survey, over 50% of intensive care unit (ICU) patients suffer from AKI, with hospital mortality being linked to severity (2). The incidence of AKI is high, and it is associated with short-term as well as long-term mortality among severe patients especially patients with sepsis and shock. In the ICU, sepsis with AKI develops in 50%-70% of patients and acts as an independent risk factor for mortality in hospitalized patients (3, 4). AKI patients with Sepsis usually develop more severe symptoms with higher mortalities, resulting in a significant economic burden on patients, families, and society. This is an urgent clinical problem that needs to be resolved in the field of acute and severe diseases (5).

Despite receiving adequate fluid resuscitation and vasopressors, many patients with sepsis still suffer from organ hypoperfusion. Insufficient renal perfusion and low blood pressure are health risks that contribute to AKI. The Surviving Sepsis Campaign recommends that patients with low blood pressure receive vasopressors to raise their blood pressure (6) where lactate levels were used to determine this recommendation. Maintaining renal perfusion in sepsis requires higher MAP (>75 mmHg) levels, according to Martin Dünser et al. (7). According to a multicenter randomized controlled trial (RCT) study focusing on sepsis patients with AKI prognosis, patients were divided into two groups according to MAP level, with high MAP levels of 80 to 85 mmHg, and low MAP levels of 65 to 70 mmHg whose results showed that AKI patients do not have any difference in prognosis. Patients with AKI and chronic hypertension who had high MAP levels were less likely to develop AKI and required fewer CRRT treatments than those with low MAP levels (8). Saito et al. reported measurement of ICU hemodynamic parameters including systolic blood pressure (SBP), DBP, MAP, and central venous pressure while calculating the mean perfusion pressure as well as diastolic perfusion pressure according to these hemodynamics parameters where they found that there was no difference in the percentage of SBP or MAP between AKI+ and AKI-. The DBP, diastolic perfusion pressure, and mean perfusion pressure, however, showed significant variations (9). An MAP that maintains renal perfusion remains controversial. Hemodynamic management of sepsis with AKI has always been a hot topic of discussion (10).

The effects of MAP on renal injury have been studied through RCTs, but the effects of SBP and DBP have been poorly investigated. The effects of SBP and DBP have been studied in a small sample size but the impact of extremely high blood pressure on patients has rarely been considered. Thus, there are still no a large-scale study with comprehensive blood pressure assessments in patients with sepsis and AKI. The effect of blood pressure on kidney is still a hot topic and controversial. Sepsis patients with AKI with chronic hypertension may and without hypertension need different blood pressure levels to maintain kidney function. As a result of the above study, sepsis patients with AKI were categorized into patients with chronic hypertension and those without chronic hypertension. Through large multiple databases, we explored the blood pressure of sepsis patients with AKI who had hypertension and those who did not have hypertension using the incidence of AKI as the main research result, and atrial fibrillation as an adverse event caused by high blood pressure.

Materials and methods

Study settings

This study was a large observational study from the multicenter database eICU Collaborative Research Database (eICU-CRD v2.0) from 2014 to 2015 and Medical Information Mart for Intensive Care IV (MIMIC-IV version 1.0) database from 2008 to 2019 (11, 12). The author of this study has completed the collaborative institutional training initiative examination (certification number 33690380) and can access the database. They all have passed the review of the ethics committee.

Patients

This study population conforms to the diagnostic criteria of sepsis 3.0 (13). In this study, sepsis was defined as a suspected infection in conjunction with an acute increase in the Sequential Organ Failure Assessment (SOFA) score ≥ 2. If the patient was suspected of having an infection or was prescribed antibiotics, bodily fluids were sampled for microbiological culture. After the antibiotic is administered, a microbiological sample must be obtained within 24 hours; after the microbiological sample is collected, the antibiotic must be administered within 72 hours. In this study, sepsis patients with AKI were included during the hospitalizationg, and AKI was defined according to the Kidney Disease Improving Global Outcomes (KDIGO) criteria (14). This study focused on adult patients (aged >18) who stayed in the intensive care unit for more than 48 hours. Sepsis patients without vasopressors drugs in the period of hospitalization, missing blood pressure values were

Abbreviations: AKI, acute kidney injury; GCS, Glasgow coma scale; MIMIC-IV, Medical Information Mart for Intensive Care IV; ICU, intensive care unit; SOFA, sequential organ failure assessment; MAP, mean arterial pressure; DBP, diastolic blood pressure; SBP, systolic blood pressure; RRT, renal replacement therapy; KDIGO, Kidney Disease Improving Global Outcomes; IPTW, inverse probability of treatment weighting; IQR, interquartile range; XGBoost, Gradient Boosting; SMD, standardized mean difference.

excluded from the study. Furthermore, this study looked for patients with atrial fibrillation in sepsis based on previous studies that showed a high MAP led to atrial fibrillation. A secondary diagnosis of atrial fibrillation was made during hospitalization, and the patient was treated with antiarrhythmic drugs. Patients with atrial fibrillation who meet the above conditions are considered atrial fibrillation.

Data collection

We collected patient age, gender, coexisting illnesses, infection site, and microbiological infection type data. During hospitalization and treatment with vasopressor drugs, the mean value of vital signs and urine output as well as the worst laboratory parameters were recorded. Patient's disease severity score, including SOFA and GCS. In addition to recording if the patients were treated with mechanical ventilation, the patients' length of stay, length of stay in the ICU, and their hospital mortality were also recorded. Only the first admission was considered for patients who are admitted to the ICU repeatedly.

Statistical analysis

The Shapiro Wilk test was used in this study to detect distributions of data. This study uses continuous variables with non-normal distributions. Several continuous variables are described by the median and interquartile range (IQR). There are also categorical variables that are expressed as a count and a percentage. The two groups of continuous variables were compared using a nonparametric test. The categorical variables were compared using Fisher's exact test.

To reduce multicollinearity between variables, the Lasso regression model was used to select variables that were significantly different from each other in Table 1 (15). To determine which blood pressure range is most for different AKI populations in terms of the incidence of AKI and atrial fibrillation, the generalized additive model was used to estimate the range of blood pressure-related variables selected by the lasso regression model (16).

We tested the relationship between blood pressure and AKI patients using a multivariate Logistic Regression model. An independent association between optimal blood pressure levels and patients' AKI was inferred through the doubly robust estimation method (17). Multivariate Logistic regression and Extreme Gradient Boosting (XGBoost) were used to create propensity score models for the 29 covariables in sepsis patients with AKI and chronic hypertension. A cohort of inverse probability of treatment weighting (IPTW) was generated from the estimated propensity scores (18). Afterward, we performed a Logistic Regression on the weighted cohort to adjust for remaining unbalanced variables in the propensity score model between AKI groups and non-AKI groups, resulting in a double robust analysis. To determine whether IPTW reduced the imbalance of covariate distribution, the standardized mean difference (SMD) of the original cohort was compared with the SMD of the IPTW cohort. R software was used to carry out all statistical analyses, and $P < 0.05$ is considered statistically significant.

Results

Baseline characteristics

A total of 51395 sepsis patients were retrieved from MIMIC IV and the eICU databases. Of these, 33521 patients were excluded based on the exclusion criteria. A total of 17874 patients were included in the study. The number of patients with Sepsis with AKI was 5833 while the number of patients with sepsis without AKI was 12041 (Figure 1).

Table 1 are described the baseline characteristics of the patients. The incidence of multiple site infections and multiple microbiology was higher in patients with AKI compared with sepsis patients without AKI whereas the level of sodium, potassium, glucose, hemoglobin, and blood urea nitrogen was worse in patients with AKI. Compared to sepsis patients without AKI, sepsis patients with AKI had higher SOFA scores, higher rates of mechanical ventilation and RRT, longer hospital stays, ICU stays, and higher hospital mortality (Table 1).

Characteristic variable for incidence of AKI

In Table 1 the results show that there are differences in many variables between sepsis patients with AKI and without AKI. The patients' diseases are very serious, and many significant differences variables are likely to have collinearity. To remove collinearity between the variables, we used the Lasso regression model to screen the significantly different variables. As shown in Figure 2B, two models are obtained after removing the existing collinearity variable. The dotted line at the left represents the minimum model, which contains 33 variables [Log(λ): -8.06]. As shown in Figure 2A, the dotted line on the right represents the streamlined model, which contains 29 variables [Log(λ): -5.27].

Generalized additive models to estimate the blood pressure targets for incidence of AKI

We divided the patients into two groups according to whether they had hypertension so that we could evaluate the SBP, DBP, and MAP of the incidence of AKI using a generalized additive model. According to the results of the study, MAP≥70 mmHg (Figure 3A), DBP≥54 mmHg (Figure 3C) and SBP≥92 mmHg (Figure 3E) reduced the incidence of AKI among sepsis patients with hypertension. In patients with sepsis without chronic hypertension,

10.3389/fimmu.2022.1060612

TABLE 1 Baseline characteristics and outcomes of patients with sepsis.

	Non-AKI patients (n = 12041)	AKI patients (n = 5833)	P
Baseline variables			
Age(years) (median [IQR])	68.00 [58.00, 77.00]	71.00 [61.00, 80.00]	<0.001
Gender, M (%)	5136 (42.7)	2256 (38.7)	<0.001
Coexisting illness, (n(%))			
Hypertension	2212 (18.4)	1587 (27.2)	<0.001
Diabetes	2123 (17.6)	1850 (31.7)	<0.001
Chronic lung disease	1494 (12.4)	1218 (20.9)	<0.001
Cardiovascular disease	3430 (28.5)	2683 (46.0)	<0.001
Site of infection, (n (%))			
Urinary	1284 (10.7)	855 (14.7)	<0.001
Lung	996 (8.3)	653 (11.2)	<0.001
Catheter	109 (0.9)	206 (3.5)	<0.001
Skin soft tissue	668 (5.5)	434 (7.4)	<0.001
Abdominal cavity	490 (4.1)	373 (6.4)	<0.001
Microbiology type, (n (%))			
Acinetobacter baumannii	7 (0.1)	32 (0.5)	<0.001
Klebslella	191 (1.6)	571 (9.8)	<0.001
Escherichia Coli	453 (3.8)	959 (16.4)	<0.001
Pseudomonas aeruginosa	120 (1.0)	361 (6.2)	<0.001
Staphylococcus aureus	1118 (9.3)	1617 (27.7)	<0.001
Fungus	399 (3.3)	1355 (23.2)	<0.001
Vital signs, (median [IQR])			
Heart rate(bpm)	93.00 [83.00, 106.00]	100.00 [87.00, 116.00]	<0.001
Respiratory rate (bpm)	23.00 [20.00, 28.00]	27.00 [22.00, 32.00]	<0.001
Systolic blood pressure (mmHg)	96.00 [85.00, 113.00]	88.00 [78.00, 100.00]	<0.001
Diastolic blood pressure (mmHg)	53.00 [45.00, 62.00]	47.00 [40.00, 55.00]	<0.001
Mean arterial pressure(mmHg)	70.00 [60.00, 84.00]	58.00 [52.00, 67.00]	<0.001
Laboratory parameters (median [IQR])			
White blood cell ($\times 10^9$ /L)	15.30 [11.00, 20.60]	14.30 [10.00, 20.10]	<0.001
Hemoglobin(g/dL)	9.50 [8.20, 10.90]	9.00 [7.80, 10.60]	<0.001
Platelet ($\times 10^9$ /L)	153.00 [109.00, 213.00]	152.00 [102.00, 223.00]	0.217
Creatinine (mg/dL)	1.10 [0.80, 2.00]	1.80 [1.20, 3.00]	<0.001
Blood urea nitrogen (mg/dL)	23.00 [15.00, 40.00]	36.00 [23.00, 58.00]	<0.001
Glucose(mg/dL)	140.00 [115.00, 186.00]	152.00 [121.00, 210.00]	<0.001
Sodium (mmol/L)	138.00 [135.00, 141.00]	139.00 [135.00, 142.00]	<0.001
Potassium(mmol/L)	4.50 [4.10, 5.00]	4.70 [4.20, 5.60]	<0.001
Lactates (mmol/L)	2.30 [1.50, 3.90]	2.00 [1.30, 3.50]	<0.001
Urine output(mL)	611.00 [150.00, 1757.00]	1012.00 [325.00, 1760.00]	<0.001
The score system, (median [IQR])			
SOFA	6.00 [4.00, 9.00]	7.00 [5.00, 10.00]	<0.001
GCS	12.00 [12.00, 14.00]	13.00 [10.00, 15.00]	0.009
Mechanical ventilation, (n(%))	5959 (49.5)	4137 (70.9)	<0.001
Outcome			
Atrial fibrillation, (n (%))	4086 (33.9)	1742 (29.9)	<0.001
RRT, (n (%))	1412 (11.7)	1211 (20.8)	<0.001
Length of ICU stays, days (median [IQR])	2.80 [1.37, 5.60]	3.40 [1.80, 7.73]	<0.001
Length of hospital stays, days (median [IQR])	8.00 [5.10, 14.20]	11.60 [6.40, 20.70]	<0.001
Hospital mortality, (n (%))	2353 (19.5)	1625 (27.9)	<0.001

GCS, Glasgow coma scale; SOFA, sequential organ failure assessment; RRT, renal replacement therapy; ICU, intensive care unit.

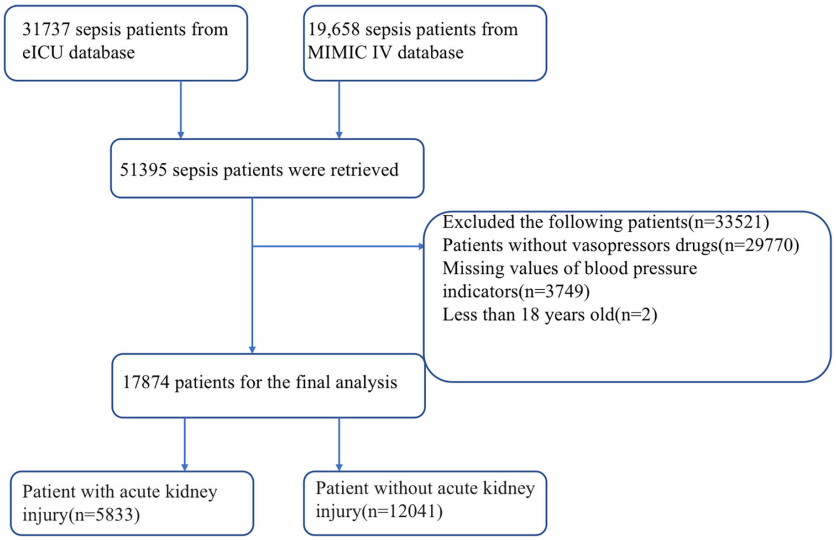

FIGURE 1
Flow chart for patient selection. ICU, intensive care unit; MIMIC-IV, Medical Information Mart for Intensive Care IV.

this study showed a nonlinear relationship between DBP, MAP, and the incidence of AKI. For AKI incidence (P<0.001), the MAP ranged from 65 to 177 mm Hg (Figure 3G), DBP was 50 to 132mmHg (Figure 3I) and SBP was more than 94mmHg (Figure 3K).

A high MAP was linked to atrial fibrillation in previous RCT studies. A high MAP, DBP, and SBP of patients were limited in the above population when atrial fibrillation incidence is taken as the endpoint. There was an increased incidence of atrial fibrillation in patients having sepsis with chronic hypertension who had MAP ≥80mmHg (Figure 3B), DBP ≥62mmHg (Figure 3D), and SBP≥101mmHg (Figure 3F) whereas there was an increased incidence of atrial fibrillation in patients with sepsis without chronic hypertension who had MAP ≥73 mmHg (Figure 3H), DBP ≥60 mmHg (Figure 3J), and SBP ≥108 mmHg (Figure 3L).

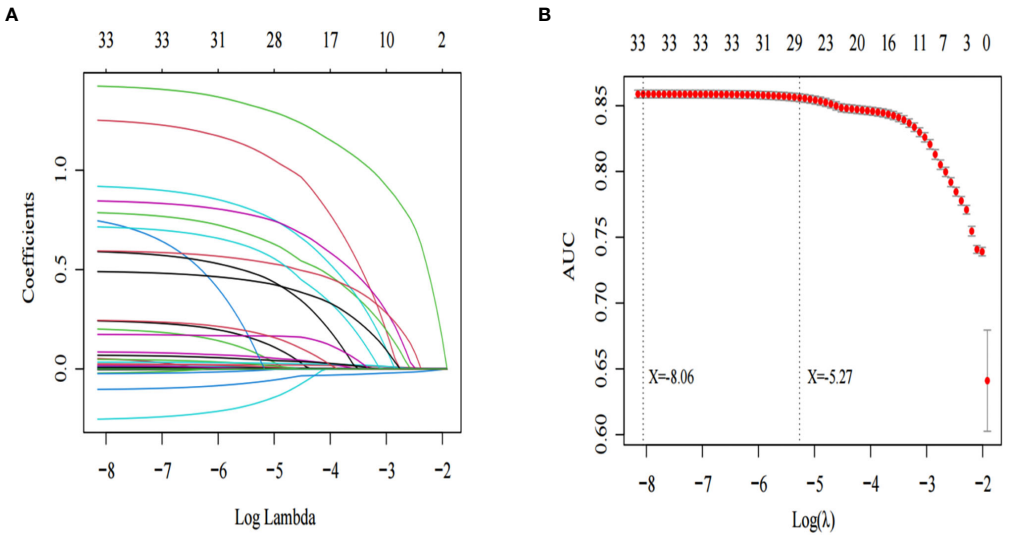

FIGURE 2
Lasso regression was used to screen the characteristic variables. **(A)** shows that with the increase of log lambda value, the punishment to the model increases, and fewer characteristic variables are included in the model. The dotted line on the left of **(B)** indicates the inclusion of the minimum model independent variables, the dotted line on the right indicates the inclusion of independent variables in the most concise model.

Multivariate logistic analysis for incidence of AKI in sepsis patients

According to the results of the generalized additive model, the range of MAP, DBP, and SBP of AKI patients with hypertension was (70-80) mmHg, (54-62), and (92-101) mmHg, respectively. In patients with AKI without hypertension disease, the MAP, DBP, and SBP ranges (65-73) mmHg, (50-60) mmHg, and (94-108) mmHg, respectively. Moreover, we selected variables that were contained in the most streamlined model screened by Lasso regression for multivariate analysis (Supplementary Material 1). The results of Table 2 show that MAP (70-80) mmHg [OR: 0.60, 95% CI: 0.45-0.80, P<0.001], DBP (54-62) mmHg [OR: 0.65, 95% CI: 0.54-0.77, P<0.001] were independent protective factors in sepsis patients with AKI with chronic hypertension. It was found that the MAP (65-73) mmHg [OR: 0.82, 95% CI: 0.72-0.93, P=0.033], and the DBP (50-60) mmHg [OR: 0.89, 95% CI: 0.77-0.99, P=0.038] were independent protective factors in sepsis patients with AK without chronic hypertension. SBP is not an independent protective factor for septic AKI (Table 2).

Propensity match analysis

In terms of AKI incidence, the double-robust analysis showed that MAP, DBP, and SBP had a significant beneficial effect. A propensity matching scoring model was constructed using 29 covariates with statistically significant differences in Table 1 except platelets, creatinine, blood urea nitrogen, urine output, RRT, length of ICU stays, length of hospital stays, ICU mortality, systolic blood pressure, diastolic blood pressure, and mean arterial pressure. For standardizing the differences between the AKI group and the non-AKI group, the estimated propensity scores were used. Covariates were well balanced between classes after IPTW (<0.1) (Figure 4). To evaluate the relationship between the MAP, DBP, and SBP levels (estimated as per generalized additive model) and AKI incidence, we used four different models: statistical analysis, propensity matching score, proportion score IPTW and doubly robust model. The estimation models led to the same conclusion: MAP (70-80) mmHg and DBP (54-62) mmHg were protective factors for patients with AKI with hypertension disease; MAP (65-73) mmHg and DBP (50-60) mmHg are protective factors of patients with AKI without hypertension disease (Table 2).

Prognostic analysis of blood pressure and sepsis patients with AKI

In septic patients with AKI without chronic hypertension, MAP (65-73) mmHg and DBP (50-60) mmHg were associated with less atrial fibrillation and lower creatinine and blood urea nitrogen levels; whereas, among sepsis patients having AKI with chronic hypertension, MAP (70-80) mmHg and DBP (54-62)

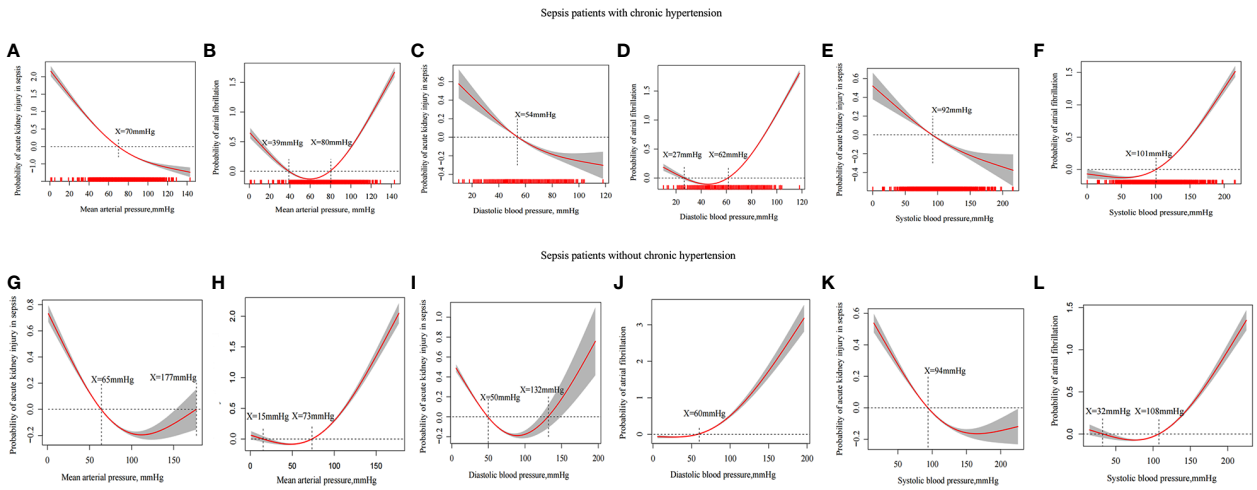

FIGURE 3
Generalized additive model evaluates the relationship between MAP, DBP, SBP and incidence in sepsis patients with AKI and incidence of atrial fibrillation. The relationship between MAP **(A)**, DBP **(C)** and SBP **(E)** and the incidence of AKI in sepsis patients with hypertension. The relationship between MAP **(G)**, DBP **(I)** and SBP **(K)** and the incidence of AKI in sepsis patients without hypertension. The relationship between MAP **(B)**, DBP **(D)** and SBP **(F)** and the incidence of atrial fibrillation in sepsis patients with chronic hypertension. The relationship between MAP **(H)**, DBP **(J)** and SBP **(L)** and the incidence of atrial fibrillation in sepsis patients with chronic hypertension.

10.3389/fimmu.2022.1060612

TABLE 2 Application of multiple models to explore blood pressure indicators to predict the occurrence of sepsis with AKI.

Models	OR	CI		P
		2.5%	97.5%	
Patients without hypertension disease				
Lasso regression + Multivariate Logistic analysis				
Mean arterial pressure (65-73) mmHg	0.82	0.72	0.93	0.003
Diastolic blood pressure (50-60) mmHg	0.89	0.78	0.99	0.038
SBP(94-108)mmHg	0.91	0.82	1.02	0.101
Propensity score matching				
Mean arterial pressure (65-73) mmHg	0.88	0.80	0.97	0.008
Diastolic blood pressure (50-60) mmHg	0.73	0.66	0.79	<0.001
SBP(94-108)mmHg	0.83	0.76	0.91	<0.001
Propensity score IPTW				
Mean arterial pressure (65-73) mmHg	0.83	0.75	0.93	0.001
Diastolic blood pressure (50-60) mmHg	0.85	0.77	0.94	0.002
SBP(94-108)mmHg	0.96	0.87	1.07	0.472
Doubly robust with all covariates				
Mean arterial pressure (65-73) mmHg	0.84	0.77	0.91	<0.001
Diastolic blood pressure (50-60) mmHg	0.89	0.82	0.95	0.001
SBP(94-108)mmHg	0.94	0.87	1.02	0.133
Patients with hypertension disease				
Lasso regression + Multivariate Logistic analysis				
Mean arterial pressure (70-80) mmHg	0.60	0.45	0.80	<0.001
Diastolic blood pressure (54-62) mmHg	0.65	0.54	0.77	<0.001
SBP(92-101)mmHg	0.99	0.80	1.23	0.959
Propensity score matching				
Mean arterial pressure (70-80) mmHg	0.72	0.55	0.94	0.018
Diastolic blood pressure (54-62) mmHg	0.82	0.68	0.98	0.028
SBP(92-101)mmHg	0.96	0.77	1.12	0.729
Propensity score IPTW				
Mean arterial pressure (70-80) mmHg	0.57	0.44	0.73	<0.001
Diastolic blood pressure (54-62) mmHg	0.54	0.46	0.63	<0.001
SBP(92-101)mmHg	0.93	0.76	1.13	0.456
Doubly robust with all covariates				
Mean arterial pressure (70-80) mmHg	0.76	0.63	0.91	0.004
Diastolic blood pressure (54-62) mmHg	0.73	0.66	0.80	<0.001
SBP(92-101)mmHg	0.97	0.86	1.10	0.643

mmHg were linked to less atrial fibrillation, lower creatinine, and lower urea levels. There was no association with length of hospital stays, ICU stays, and hospital mortality in patients with sepsis AKI (Supplementary Material 2).

Discussion

The incidence of AKI was 32.63%. Sepsis patients with AKI had poor clinical outcomes. The range of MAP and DBP may be (65-73) mmHg and (50-60) mmHg in sepsis patients with AKI who did not have hypertension. The range of the MAP and DBP may be (70-80) mmHg and (54-62) mmHg in sepsis patients with AKI having hypertension. It was found that MAP and DBP were not linked with the prognosis of sepsis patients with AKI.

Sepsis with AKI has always been a disease of global concern, it has a high incidence rate and is associated with poor clinical outcomes. Sean m Bagshaw et al. found that the incidence of AKI was 64.4% and AKI was mainly associated with significant ICU mortality and hospital mortality (OR 1.73 and OR 1.62), respectively (3). A Korean population cohort study found that patients with AKI had higher hospital mortality, longer ICU stays, and higher total costs (4). This study is based on a large multicenter cohort study that indicated that the incidence of AKI was 32.63%, and sepsis patients with AKI had higher SOFA scores, more patients use mechanical ventilation, longer hospital

stay, ICU stays, and shown higher hospital mortality as compared to sepsis patients without AKI. The results of this study are consistent with similar studies conducted in the past. However, the incidence of septic AKI in this study is found to be lower than that of the investigation performed by Bagshaw et al. This difference may be attributed to the use of different AKI diagnostic methods. In this study, KDIGO criteria were adopted, while Bagshaw et al. adopted RIFLE criteria. Recent research by Zhang and coworkers found that the incidence of AKI in sepsis was 41.1% in the mimic IV database (19), the results of this study support the findings of Luming Zhang and other colleges. The above studies indicate that patients with Sepsis AKI are still diseases that require urgent attention in critical care medicine.

Most sepsis patients are known to have low blood pressure and insufficient tissue perfusion. These two parameters (low blood pressure levels and renal hypoperfusion) are the important mechanisms of AKI in sepsis (20). It has always been a clinical hot topic to maintain blood pressure levels of renal perfusion, but it is still controversial. Martin WD ü nser et al. proposed that MAP > 75 mmHg may be sufficient to maintain kidney function (7). The study made a better proposal for maintaining kidney function, however, it did not consider whether the patients had chronic hypertension or the adverse effect caused by patients with high MAP. Pierre asfar et al. conducted an RCT study after the study of Martin W D ü nser et al. Pierre asfar et al. made up for the study limitation of Martin W D ü nser et al. in sepsis AKI, they considered that AKI patients with chronic hypertension may need higher MAP levels and the harm that caused by higher MAP to the patient's body. Asfar et al. suggested that patients suffering from chronic hypertension, target a MAP of 80 to 85 mm Hg, and patients without a history of chronic hypertension, target a MAP of 65 to 70 mm Hg. It was an observation that higher MAP did not have any significant impact on the prognosis of AKI patients; however, in addition, it will enhance the incidence of atrial fibrillation (8). The study led by Asfar et al. provides strong evidence for the control of MAP levels among patients with sepsis AKI. However, in the same study, the mortality of AKI patients was the primary outcome with an exploration of the MAP level, not AKI incidence, which may deviate from the MAP level for the incidence of AKI in sepsis. Besides, the study only considered MAP and did not consider the impact of SBP and DBP levels on AKI patients. The study also classifies the high MAP group (80-85) mmHg and the low MAP group (65-70) mmHg on the bases of clinical observation, there may be bias in the accurate MAP level. In another study by Forni and coworkers, the impact of MAP on AKI was questioned and discussed. They provided the detailed suggestion that why one should not only pay attention to MAP, DBP, renal systolic perfusion pressure and diastolic perfusion pressure, but other indicators also play a key role which should also be given proper attention (20, 21). Based on the results of previous studies, in this study, AKI incidence and atrial fibrillation as an outcome were explored for levels of SBP, DBP, and sepsis MAP in patients with AKI. The blood

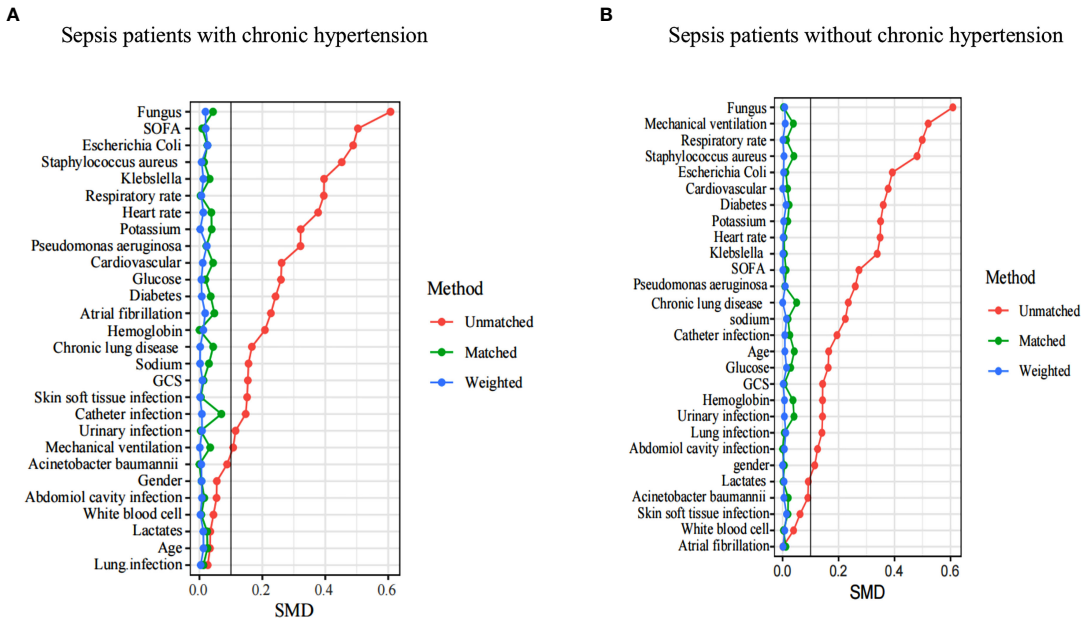

FIGURE 4
A SMD of the original cohort was compared with the SMD of the IPTW cohorts. In sepsis AKI incidence, sepsis patients with hypertension **(A)** and sepsis patients without hypertension **(B)** showed that covariates were well balanced between classes after IPTW(<0.1). SMD, standardized mean difference, IPTW, inverse probability of treatment weighting .

pressure level was estimated by a generalized additive model rather than by dividing by clinical experience. In many articles, the generalized additive model is used in evaluating the index level (22, 23).

The surprising finding of this study was that there was a nonlinear relationship between MAP, DBP, and the incidence of sepsis in patients with AKI without chronic hypertension. They did, however, have a linear relationship with sepsis patients with AKI with chronic hypertension. It may be attributed to the increase of anterior glomerular arteriole resistance and intraglomerular hypertension and the continuous increase of anterior glomerular artery resistance which brings the glomerular capillaries into a state of high perfusion, high filtration, and high transmembrane pressure and ultimately in the state of long-term chronic hypertension (24). Glomerular capillaries are in a state of high perfusion and high filtration for a long time, which can withstand the level of high blood pressure in sepsis. MAP > 177 mmHg and DBP > 132 mmHg will cause an increase in glomerular pressure leading to kidney damage in sepsis patients without chronic hypertension. Furthermore, MAP < 65 mmHg and DBP <50 mmHg can lead to insufficient renal perfusion and renal injury in sepsis patients without chronic hypertension. We need to control the patient's MAP ≥ 65 mmHg and DBP ≥ 50 mmHg to maintain the patient's renal perfusion in the condition of sepsis without chronic hypertension. MAP ≥ 65 mmHg is almost in line with the guidelines of the surviving sepsis campaign, expert opinion of the working group on prevention, AKI section, European Society of intensive care medicine (25-27). Sepsis patients with hypertension need to maintain a higher MAP (≥ 70 mmHg) and DBP (≥54 mmHg), which is basically in line with the study conducted by Pierre as far et al, which says that higher MAP can lead to atrial fibrillation. This study shows that MAP>73 mmHg and DBP>60 mmHg can lead to atrial fibrillation in sepsis patients without chronic hypertension, and MAP>80 mmHg and DBP>62 mmHg can lead to atrial fibrillation in sepsis patients having chronic hypertension. In summary, we suggest that the MAP range is 65 to 73 mmHg and the DBP range is 50 to 60 mmHg in sepsis patients with AKI without chronic hypertension; the MAP range is 70 to 80 mmHg and the DBP range is 54 to 62 mmHg in sepsis patients having AKI along with chronic hypertension (Table 2). Patients with blood pressure within the range had significantly lower levels of creatinine and blood urea nitrogen than those with AKI outside the range (Supplementary Material 3). Unfortunately, this study found that the blood pressure range level was not associated with the prognosis of patients with AKI. This study not only provides the range of MAP but also provides the range of DBP too. It also established that DBP may play an important role in the occurrence of AKI. We have found results that are potentially impactful and that support the resulting study of Pierre et al. However, the highest value of the range of MAP level is higher than Pierre et al. suggested MAP≤ 70 mmHg in sepsis without chronic hypertension, and MAP range is lower than Pierre et al. suggested MAP from 80 to 85 mmHg. The difference could be explained by the different methods of estimating MAP ranges and the different primary outcomes of the studies. Another difference can be as Pierre et al. studied the mortality of sepsis patients with AKI, and we studied the incidence of sepsis in patients with AKI. Although our findings support the blood pressure target for sepsis patients with AKI, the target would not apply in some instances, for example, in patients with severe shock and disturbance of consciousness who may need higher blood pressure levels to maintain their consciousness. Severe shock cannot be corrected and is life-threatening. In addition, our results do not extend to patients who do not take vasopressor drugs.

Through a large observational study, we provide a reference range for blood pressure levels, but it is important to demonstrate the limitations of such studies. First of all, since this is a retrospective study, our results could not provide a causal relationship between the blood pressure level and AKI incidence in sepsis. Secondly, based on previous studies, we chose atrial fibrillation caused by high blood pressure to be the endpoint of blood pressure level control, which may have caused a deviation in the research results. Thirdly, the dose and type of the vasopressors, and the amount of fluid used for residence, were not included in this study, which are important for AKI of sepsis patients, their absence may cause information bias to the study results. We provide a certain reference range for the blood pressure level control of AKI patients based on large-scale data, but some patients don't fit into this range.

Conclusion

Based on previous studies, we reassessed the blood pressure range in sepsis patients with AKI using multiple large databases. Through this study, we recommend that the MAP range may be 65 to 73 mmHg and the DBP range may be 50 to 60mmHg in sepsis patients with AKI without chronic hypertension; however, the MAP range may be 70 to 80 mmHg and the DBP range may be 54 to 62 mmHg in sepsis patients with AKI with chronic hypertension.

Data availability statement

The original contributions presented in the study are included in the article/Supplementary Material. Further inquiries can be directed to the corresponding authors.

Ethics statement

The studies involving human participants were reviewed and approved by MIMIC-IV and eICU-CRD databases were approved by the institutional review boards of the

Massachusetts Institute of Technology and Beth Israel Deaconess Medical Center. Written informed consent for participation was not required for this study in accordance with the national legislation and the institutional requirements.

Author contributions

LZ, YL, and KX conceived the central ideas of the study. YF and ZWang collected the data. LZ wrote the first draft of the manuscript. YL and KX revised the paper, worked on the English, and drafted the final version of the manuscript. ZWei and YZ revised the paper. All authors contributed to the article and approved the submitted version.

Funding

This work was supported by a grant from the Medical and Health Science and Technology Plan Project of Inner Mongolia Autonomous Region Health Commission (serial number 202202326) and Inner Mongolia natural science foundation (serial number 2022MS08002). Science and Technology Support Key Program Affiliated to the Key Research and Development Plan of Tianjin Science and Technology Project (18YFZCSY00560), National Natural Science Foundation of China (81772043, 81971879).

Conflict of interest

The authors declare that the research was conducted in the absence of any commercial or financial relationships that could be construed as a potential conflict of interest.

Publisher's note

Supplementary material

The Supplementary Material for this article can be found online at: https://www.frontiersin.org/articles/10.3389/fimmu.2022.1060612/full#supplementary-material

SUPPLEMENTARY MATERIAL 1
The variables contained in the most streamlined model screened by the lasso regression model.

SUPPLEMENTARY MATERIAL 2
Blood pressure effect on the prognosis of sepsis patients with acute kidney injury.

References

1. Lameire NH, Bagga A, Cruz D, De Maeseneer J, Endre Z, Kellum JA, et al. Acute kidney injury: an increasing global concern. *Lancet* (. 2013) 382(9887):170–9. doi: 10.1016/S0140-6736(13)60647-9

2. Hoste EA, Bagshaw SM, Bellomo R, Cely CM, Colman R, Cruz DN, et al. Epidemiology of acute kidney injury in critically ill patients: the multinational AKI-EPI study. *Intensive Care Med* (2015) 41(8):1411–23. doi: 10.1007/s00134-015-3934-7

3. Bagshaw SM, Lapinsky S, Dial S, Arabi Y, Dodek P, Wood G, et al. Cooperative antimicrobial therapy of septic shock database research g. acute kidney injury in septic shock: clinical outcomes and impact of duration of hypotension prior to initiation of antimicrobial therapy. *Intensive Care Med* (2009) 35(5):871–81. doi: 10.1007/s00134-008-1367-2

4. Hwang S, Park H, Kim Y, Kang D, Ku HS, Cho J, et al. Changes in acute kidney injury epidemiology in critically ill patients: a population-based cohort study in Korea. *Ann Intensive Care* (2019) 9(1):65. doi: 10.1186/s13613-019-0534-7

5. Bagshaw SM, George C, Bellomo R, Committee ADM. Early acute kidney injury and sepsis: A multicentre evaluation. *Crit Care* (2008) 12(2):R47. doi: 10.1186/cc6863

6. Dellinger RP, Levy MM, Rhodes A, Annane D, Gerlach H, Opal SM, et al. Surviving sepsis campaign guidelines committee including the pediatric s. surviving sepsis campaign: international guidelines for management of severe sepsis and septic shock: 2012. *Crit Care Med* (2013) 41(2):580–637. doi: 10.1097/CCM.0b013e31827e83af

7. Dunser MW, Takala J, Ulmer H, Mayr VD, Luckner G, Jochberger S, et al. Arterial blood pressure during early sepsis and outcome. *Intensive Care Med* (2009) 35(7):1225–33. doi: 10.1007/s00134-009-1427-2

8. Asfar P, Meziani F, Hamel JF, Grelon F, Megarbane B, Anguel N, et al. High versus low blood-pressure target in patients with septic shock. *N Engl J Med* (2014) 370(17):1583–93. doi: 10.1056/NEJMoa1312173

9. Saito S, Uchino S, Takinami M, Uezono S, Bellomo R. Postoperative blood pressure deficit and acute kidney injury progression in vasopressor-dependent cardiovascular surgery patients. *Crit Care* (2016) 20:74. doi: 10.1186/s13054-016-1253-1

10. Suarez J, Busse LW. New strategies to optimize renal haemodynamics. *Curr Opin Crit Care* (2020) 26(6):536–42. doi: 10.1097/MCC.0000000000000774

11. Pollard TJ, Johnson AEW, Raffa JD, Celi LA, Mark RG, Badawi O. The eICU collaborative research database, a freely available multi-center database for critical care research. *Sci Data* (2018) 5:180178. doi: 10.1038/sdata.2018.178

12. Johnson A, Bulgarelli L, Pollard T, Horng S, Celi LA, Mark, R. (2022) *MIMIC-IV (version 2.0)*. PhysioNet. doi: 10.13026/7vcr-e114

13. Singer M, Deutschman CS, Seymour CW, Shankar-Hari M, Annane D, Bauer M, et al. The third international consensus definitions for sepsis and septic shock (Sepsis-3). *JAMA* (2016) 315(8):801–10. doi: 10.1001/jama.2016.0287

14. Ricci Z, Romagnoli S. Acute kidney injury: Diagnosis and classification in adults and children. *Contrib Nephrol* (2018) 193:1–12. doi: 10.1159/000484956

15. Tibshirani R. Regression shrinking and selection *via* the lasso. *J R Stat Soc Ser B Methodol* (1996) 58:267–88. doi: 10.1111/j.2517-6161.1996.tb02080.x

16. Wood SN. Generalized additive models: An introduction with r, *J Roy Statist Soc Ser A Stat* (2017).

17. Mccaffrey DF, Griffin BA, Almirall D, Slaughter ME, Burgette LF. A tutorial on propensity score estimation for multiple treatments using generalized boosted models. *Stat Med* (2015) 32(19):3388–414. doi: 10.1002/sim.5753

18. Cole SR, Hernan MA. Constructing inverse probability weights for marginal structural models. *Am J Epidemiol* (2008) 168(6):656–64. doi: 10.1093/aje/kwn164

19. Zhang L, Xu F, Han D, Huang T, Li S, Yin H, et al. Influence of the trajectory of the urine output for 24 h on the occurrence of AKI in patients with sepsis in intensive care unit. *J Transl Med* (2021) 19(1):518. doi: 10.1186/s12967-021-03190-w

20. Sato R, Luthe SK, Nasu M. Blood pressure and acute kidney injury. *Crit Care* (2017) 21(1):28. doi: 10.1186/s13054-017-1611-7

21. Forni LG, Joannidis M. Blood pressure deficits in acute kidney injury: not all about the mean arterial pressure? *Crit Care* (2017) 21(1):102. doi: 10.1186/s13054-017-1683-4

22. van den Boom W, Hoy M, Sankaran J, Liu M, Chahed H, Feng M, et al. The search for optimal oxygen saturation targets in critically ill patients: Observational data from Large ICU databases. *Chest* (2020) 157(3):566–73. doi: 10.1016/j.chest.2019.09.015

23. Chang WT, Wang CH, Lai CH, Yu HY, Chou NK, Wang CH, et al. Optimal arterial blood oxygen tension in the early postresuscitation phase of extracorporeal cardiopulmonary resuscitation: A 15-year retrospective observational study. *Crit Care Med* (2019) 47(11):1549–56. doi: 10.1097/CCM.0000000000003938

24. Mennuni S, Rubattu S, Pierelli G, Tocci G, Fofi C, Volpe M. Hypertension and kidneys: unraveling complex molecular mechanisms underlying hypertensive renal damage. *J Hum Hypertens* (2014) 28(2):74–9. doi: 10.1038/jhh.2013.55

25. Joannidis M, Druml W, Forni LG, Groeneveld A, Honore PM, Hoste E, et al. Prevention of acute kidney injury and protection of renal function in the intensive care unit: update 2017. *Intensive Care Med* (2017) 43(6):730–49. doi: 10.1007/s00134-017-4832-y

26. Kellum JA, Lameire N, Aspelin P, Barsoum RS, Burdmann EA, Goldstein SL, et al. Kidney disease: Improving global outcomes (KDIGO) acute kidney injury work group KDIGO clinical practice guideline for acute kidney injury. *Kidney Int Suppl* (2012) 2:1–138. doi: 10.1038/kisup.2012.1

27. Joannidis M, Metnitz B, Bauer P, Schusterschitz N, Rui M, Druml W, et al. Acute kidney injury in critically ill patients classified by AKIN versus RIFLE using the SAPS 3 database. *Intensive Care Med* (2009) 35(10):1692–702. doi: 10.1007/s00134-009-1530-4

frontiers | Frontiers in Immunology

TYPE Original Research
PUBLISHED 12 January 2023
DOI 10.3389/fimmu.2022.1090358

OPEN ACCESS

EDITED BY
Alessandra Stasi,
University of Bari Aldo Moro, Italy

REVIEWED BY
Lu Wang,
Renmin Hospital of Wuhan University, China
Peter A. Ward,
University of Michigan, United States

*CORRESPONDENCE
Teding Chang
changtd@tjh.tjmu.edu.cn
Zhao-hui Tang
tangzh@tjh.tjmu.edu.cn

SPECIALTY SECTION
This article was submitted to Inflammation, a section of the journal Frontiers in Immunology

RECEIVED 05 November 2022
ACCEPTED 15 December 2022
PUBLISHED 12 January 2023

CITATION
Chen D, Zhang C, Luo J, Deng H, Yang J, Chen S, Zhang P, Dong L, Chang T and Tang Z-h (2023) Activated autophagy of innate immune cells during the early stages of major trauma.
Front. Immunol. 13:1090358.
doi: 10.3389/fimmu.2022.1090358

Activated autophagy of innate immune cells during the early stages of major trauma

Deng Chen, Cong Zhang, Jialiu Luo, Hai Deng, Jingzhi Yang, Shunyao Chen, Peidong Zhang, Liming Dong, Teding Chang* and Zhao-hui Tang*

Department of Traumatic Surgery, Tongji Trauma Center, Tongji Hospital, Tongji Medical College, Huazhong University of Science and Technology, Wuhan, China

Background: Trauma-induced immune dysfunction has been a major barrier to achieving reduced mortality, which is poorly understood. Autophagy is a crucial catabolic mechanism of immune cells during times of stress. Few studies have investigated the immune regulatory effects induced by autophagy after trauma. Here, we use single-cell transcriptomics analysis in a major trauma cohort to demonstrate the dominant role of autophagy in innate immune cells during the early stages of major trauma.

Method: Single-cell transcriptional profiling of peripheral blood mononuclear cells (PBMCs) was performed, which were sampled from three control participants and five major trauma patients within 6 hours of injury. In detail, after single-cell RNA-sequence data processing, cell type annotation and cluster marker identification were performed. A genetic toolbox with 604 autophagy-related genes was used to monitor the autophagy levels in immune cells. In addition, all transcriptome RNA sequencing data obtained from PBMCs in a cohort of 167 major trauma patients were downloaded from gene expression omnibus (GEO) datasets (GSE36809). Key deregulated biological processes and important autophagic hub genes involved in immune cells were identified by weighted gene co-expression network analysis and gene ontology enrichment analysis.

Results: A total of 20,445 differentially expressed genes were identified and five co-expression modules were constructed. Enrichment analysis indicated that activated autophagy is the most important biological process during the early stages of major trauma, and JMY (autophagy-related genes) were identified as hub genes. The single-cell transcriptional profiling of PBMCs demonstrated that all components of adaptive immune cells were significantly decreased, whereas components of innate immune cells (monocytes and neutrophils) were significantly increased in major trauma patients compared with control participants. Activated autophagy was detected in monocytes and neutrophils by monitoring the dynamic transcriptional signature of the autophagy-related genetic toolbox. Biological process analysis shows that antigen uptake, processing presentation, and major histocompatibility complex (MHC) class II protein complex assembly pathways were up-regulated in autophagy-positive

monocytes, whereas antigen processing and presentation of endogenous antigen and type I interferon signaling pathways were up-regulated in autophagy-positive neutrophils during the early stages of major trauma.

Conclusion: Our study demonstrated that autophagy is a biological process crucial to the development of immune disorders in the early stages of major trauma. Furthermore, the results of our study generated a comprehensive single-cell immune landscape for major trauma patients, in which we determined that autophagy profoundly affects the main functions of innate immune cells and provides insight into the cellular basis of immune dysregulation after major trauma.

KEYWORDS

autophagy, innate immune cells, major trauma, trauma-induced immune dysfunction, single-cell sequencing, monocyte, neutrophil

1 Introduction

Trauma is a leading cause of global mortality and accounts for 10.1% of the global burden of disease. Annually, nearly 4.8 million people die from trauma-related injuries (1–3). Major trauma accounts for 3%–5% of total trauma incidents and is characterized by serious complications and a higher mortality rate, primarily because of fatal damage and unmanageable complications (4, 5). Hemorrhagic shock and overwhelming injury to vital organs are responsible for early mortality in major trauma, and more than half of delayed deaths are caused by complex immune dysfunction and secondary infections. Systemic inflammatory response syndrome, caused by the release of endogenous factors termed damage-associated molecular patterns (DAMPs) and pathogen-associated molecular patterns (PAMPs) (6, 7), commonly follows traumatic injury. Recognition of DAMPs and PAMPs by the innate immune system triggers both an intense pro-inflammatory and an anti-inflammatory immune response. The anti-inflammatory immune response leads to host defense impairment and sepsis, which increases the risk of multiple organ dysfunction syndrome (MODS) and of death (8, 9). Much money worldwide has been invested in new biological therapeutics for trauma-induced immune dysfunction, but the results are mostly disappointing. The current pro-inflammatory immune paradigm, which is based on an incomplete understanding of the functional integration of the complicated host immune response, remains a major impediment to the establishment of effective, innovative therapies. It is imperative that immunological mechanisms in the pathogenesis of major trauma, particularly the molecular and cellular basis of immune regulation during the early stages of major trauma, are accurately elucidated.

There is growing evidence indicating the existence of a close relationship between autography machinery and immune cells. Autophagy is a crucial catabolic mechanism of non-selective, lysosome-mediated degradation of cytosolic cargo during times of stress. The cytoplasmic cleanup function of autophagy is, by default, anti-inflammatory, in any type of cell capable of activating a cell-autonomous inflammatory response (10, 11). A complementary autophagical function is its involvement in aligning the endoplasmic reticulum (ER) and mitochondrial content with immune cell functions to sculpt the interior of immune cells. In addition, autophagy-dependent metabolic adjustments contribute to immunometabolic states, affecting macrophage and T-cell polarization (12). All of the above findings indicate that different forms of autophagy play key roles in regulating innate and adaptive immunity through affecting inflammatory outputs and resolution (13). A considerable number of studies have been performed to

Abbreviations: ARDS, acute respiratory distress syndrome; ATG, autophagy related gene; BP, biological process; DAMPs, damage-associated molecular patterns; DCs, dendritic cells; DEGs, differentially expressed genes; ER, endoplasmic reticulum; FDR, false discovery rate; GCS, Glasgow Coma Scale; GEO, gene expression omnibus; GO, gene ontology; GSEA, gene set enrichment analysis; HIV, human immunodeficiency virus; ISS, injury severity score; KEGG, Kyoto Encyclopedia of Genes and Genomes; WGCNA; MHC, major histocompatibility complex; MODS, multiple organ dysfunction syndrome; MOF, multiple organ failure; MTOR, mammalian target of rapamycin; NK cells, natural killer cells; ORA, over-representative analysis; PAMPs, pathogen-associated molecular patterns; PBMCs, peripheral blood mononuclear cells; PBS, phosphate buffer solution; PCA, principal component analysis; PCs, principal components; RNA, ribonucleic acid; scRNA-seq, single-cell RNA sequencing; SICU, surgical intensive care unit; SOM, self-organizing map; t-SNE, t-stochastic neighbor embedding; UMAP, uniform manifold approximation and projection; UMIs, unique molecular identifiers; WGCNA, weighted gene co-expression network analysis.

elucidate post-traumatic immune dysfunction over the past few decades, most of which were focused on apoptosis, pyroptosis, depletion, and the generation of immune cells. Few studies have investigated the relationship between autophagy and immunological dysfunction after major trauma. Trauma-induced immunological dysfunction is an extremely complex pathological process, which involves almost all types of immune cells. As autophagy involves many biological processes and signal regulatory pathways, it is difficult to comprehensively analyze its variances and mechanisms using traditional research methods.

At present, little is known about autophagy machinery in immunological regulation after major trauma. To address this issue, we performed single-cell transcriptomics analyses of peripheral blood mononuclear cells (PBMCs) in major trauma patients. The present study aims to explore the transcriptomic profiling of autophagy-related genes in immune cells and to understand how autophagy processes are involved in trauma-induced immune dysfunction. Specifically, the key deregulated biological process and some important hub genes of autophagy involved in immune cells of trauma patients were investigated. Our study indicated that activated autophagy plays a critical role in regulating innate immune responses during the early stages of major trauma. Therefore, our study provides new evidence of autophagy-related mechanisms in the function of innate immune cells after trauma, which may in turn help in the development of new strategies for immune dysfunction prevention and to improve prognoses in the major trauma population.

2 Patients and method

2.1 Patient information

From April 2021 to February 2022, patients presenting with major trauma and admitted to the SICU (surgical ICU) of Tongji Hospital were eligible for enrollment in this study. Diagnostic criteria for major trauma were based on published guidelines (14, 15). Patients with active malignancy, who were younger than 18 years of age or older than 50 years of age, infected with HIV, receiving immunosuppressive therapy or blood transfusions, and who died within 48 hours of admission were excluded. Patients who had been treated with corticosteroids or other immune regulatory agents before enrollment were also excluded. Finally, five patients, whose characteristics covered a wide range of age and injury severity, were selected for analysis. Control subjects, without significant concomitant acute or chronic illness, were also selected to ensure age and sex comparability in the healthy population. Standard treatments according to published guidelines were provided to all patients (14, 15). The procedures involving human participants were reviewed and approved by the ethics committee at Tongji Hospital and Tongji Medical College. Written informed consent was obtained from patients' legally authorized representatives or from patients themselves.

2.2 Sample collection and isolation of peripheral blood mononuclear cells

Peripheral venous blood samples were obtained within 6 hours of injury and stored under suitable conditions. PBMCs were isolated by density gradient centrifugation using the Ficoll-Paque™ Plus medium (GE Healthcare, Chicago, IL, USA). After centrifugation, the PBMC layer was collected and washed twice in phosphate buffer solution (PBS) at room temperature.

2.3 Droplet-based single-cell sequencing

Our small condition RNA (scRNA)-sequencing datasets can be downloaded from the Gene Expression Omnibus (GEO) database (GSE197552). Single-cell RNA sequencing (scRNA-seq) was performed using the Chromium single cell platform (10X Genomics) combined with cell hashing. Approximately 10,000 cells were contained in each channel and 5,000 target cells were recovered. The target cells were lysed and released RNA was barcoded by HTO-barcodes through reverse transcription in individual single-cell gel beads in the emulsion (16). Complementary DNA (cDNA) was generated and amplified following the manufacturer's protocol, with additional steps for the amplification of HTO barcodes, after which quality was assessed using an Agilent 4200. in accordance with the manufacturer's instructions, cDNA libraries were sequenced to a depth of 20,000 reads per cell on a Novaseq6000 sequencer (Illumina).

2.4 Single-cell RNA-seq data processing

Raw data were aligned to the GRCh38 reference genome using the Cell Ranger v7.0.1 (10X Genomics, Pleasanton, CA, USA) pipeline to generate the unique molecular identifiers (UMIs) count matrices. The output filtered gene expression matrices were analyzed using R software (v.4.0.1 https://www.r-project.org/) with Seurat packages (reference1) (v4.1.1). Low-quality cells were filtered out if they met the following criteria: (1) between <200 and >2,500 unique gene features; (2) between <800 and >10,000 gene counts; and (3) >5% UMIs derived from the mitochondrial genome. The filtered matrix was normalized by employing a global-scaling normalization method ("LogNormalize" in the "NormalizeData" function) and 2,000 highly variable features were identified by the "FindVariableFeatures" function for reducing dimensionality of the datasets. To perform comparative scRNA-seq analysis across experimental conditions, the scRNA-seq integration procedure was commenced by finding the anchors between each cell pair dataset using the "FindIntegrationAnchors" function. After anchors were generated, the integration was performed by using these anchors to generate a comparable scRNA-seq Seurat object (labelled as "integrated") which contained the integrated gene count matrix of each cell pair dataset. Principal component

analysis (PCA) by way of the "RunPCA" function was conducted with default parameters on linear-transformation scaled data generated by the "ScaleData" function. The elbow plot was used to identify the effective number of principal components (PCs) to reflect the difference and the top 10 PCs were chosen for further downstream analyses. Based on the top 10 significant PCs, cells were clustered by FindNeighbors and "FindClusters" function, and we performed t-stochastic neighbor embedding (t-SNE) non-linear dimensional reduction using the "RunTSNE" function with default settings.

2.5 Cell type annotation and cluster marker identification

After non-linear dimensional reduction and projection into two-dimensional space by tSNE, cells were clustered together according to similarities in their gene expression profiles. The "FindAllMarker" function with default parameters was used to identify marker genes for each cluster. Cluster annotation was performed based on the canonical markers of particular cell types and excluded clusters expressing two or more canonical cell-type markers.

2.6 Autophagy-related gene acquisition

The ATG (autophagy-related genes) genetic toolbox was formed using a well-established methodology designed by Dr. F. Cecconi et al. to monitor autophagy-related genetic transcription (17). A genetic toolbox of 604 autophagy-related genes [including MTOR and upstream pathways (135 genes), autophagy core (197 genes), autophagy regulators (68 genes), mitophagy (80 genes), docking and fusion (22 genes), lysosome (162 genes), and lysosome-related genes (34 genes)] was used to assess the autophagy machinery in cells (17). The ATG genetic toolbox for monitoring autophagy transcription and gene signature enrichment analysis website contains details of genes from these three gene lists: (GOBP_AUTOPHAGY_CELL_DEATH.v.7.5.1, GOBP_REGULATION_OF_AYTOPHAGY_CELL_DEATH.v.7.5.1, and WP_NANOPARTICLE_TRIGGERED_AUTOPHAGIC_CELL_DEATH.v.7.5.1).

2.7 Differential gene expression analysis

The standard workflow of differential expression analysis was performed on the bulk RNA gene sets and pseudo-bulk RNA gene sets by using the "DESeq" function in "DESeq2" package (18) (v1.32.1). The log2 fold change (log_2FC), *p*-values and adjusted *p*-values were extracted using the Result function. Differences in gene expression were considered significant and important if their associated adjusted *p*-value was < 0.05 and they had a |log2 fold change| value of > 1. Volcano plots were created using ggplot2 packages (v3.3.6). As for scRNA-seq differential gene expression analysis, the pseudo-bulk RNA gene matrix was generated according to the aggregation procedure (that is, each individual cell was treated as its own replicate). We then performed differential gene expression analysis, as described above.

2.8 Self-organizing map algorithm

Of the 604 genes in the ATG genetic toolbox, 39 genes crucial to processes in autophagy were selected for self-organizing map (SOM) analysis to explore the dynamic expression signature of autophagy, as previously described (17). The expression level of each gene was recorded as the median value for each stage. SOM was constructed by kohonen (v3.0.7) packages and yielded smooth toroidal boundary conditions. The map grid was reset with the top two principal components (PCs) of the data multiplied by the sinusoidal function and visualized by R.

2.9 Functional gene enrichment analysis

Gene set enrichment analysis (GSEA) and over-representative analysis (ORA) were performed on the relevant genes using the ClusterProfiler packages (19, 20)(v.4.0.5). Gene ontology (GO) enrichment analysis was performed using the "gseGO" and "enrichGO" functions. Kyoto Encyclopedia of Genes and Genomes (KEGG) enrichment was performed using the "gseKEGG" and "enrichKEGG" functions.

2.10 Dataset download and data acquisition

RNA sequencing data from the PBMCs of control participants and severely traumatized patients were downloaded from Gene Expression Omnibus Data Sets (GSE36809, GEO, https://ncbi.nlm.mih.gov/geo/). Peripheral venous blood was sampled from a cohort of 167 severe blunt trauma patients between the ages of 18 and 55 years. Serial blood samples were taken at 12 hours and at 7 and 28 days after injury.

2.11 Weighted gene co-expression network analysis

Differentially expressed genes (DEGs) were identified to construct gene co-expression networks using weighted gene co-expression network analysis (WGCNA) packages (21) (v.3.3.4). The co-expression similarity matrix was generated using Pearson correlations and transformed into an adjacency

matrix using the soft-thresholding power (β) to ensure a good scale-free topology fit and a large number of connections (the latter was achieved using the "pickSoftThreshold" function). Gene networks were constructed with the condition β = 6 using the "blockwiseModules" function. Autophagy-related modules were identified by detecting the correlation between patient status (control participants and critical trauma patients) and module eigengenes using "cor" functions and the significance of student *p*-values was determined using the "corPvalueStudent" function. The network of most significant modules was constructed by using graph packages (v2.0.5).

2.12 Quantification and statistical analysis

For comparison between two independent groups represented as bar plots, the *p*-value was determined with an unpaired two-tailed Student's *t*-test, with a 95% confidence interval in R. For data in violin plots, a two-tailed Wilcoxon rank-sum test was performed using R. To compare the differential gene expression analysis between bulk transcriptome and pseudo-bulk transcriptome RNA, the false discovery rate (FDR) was determined using R. Data are presented as the mean ± standard deviation if consistent with normal distribution. A value of $p<0.05$ for the differential gene expression analysis indicated statistically significant differences.

3 Results

3.1 Autophagy: an essential biological process in immune cells' response to trauma

The abnormal regulation of autophagy in immune processes has been implicated in the development of infectious diseases and cancer (22). However, few studies focus on the impact of autophagy on immune cells after trauma, and little is known about and reported on the precise role of autophagy in trauma-induced immunological dysfunction. The following study aims to demonstrate that autophagy is an essential biological process in immune cells' response to trauma by way of single-cell transcriptomics analysis.

Both gene expression profiles from the GSE36809 dataset and clinical data were downloaded from the GEO database. All transcriptome RNA sequencing data were obtained from PBMCs in a cohort of 167 major trauma patients and control participants. Serial blood samples were taken at 12 hours and at 7 and 28 days after injury. After data filtering, the "DEseq" package in R was used to compare the DEGs in PBMCs for trauma patients with those of control participants. 20,445 DEGs were identified, which are represented visually as both a heatmap (Figure 1A) and a dendrogram (Figure 1C). A false discovery rate (FDR) of < 0.05 was defined as the threshold for screening DEGs (Figure 1B).

Weighted gene co-expression network analysis (WGCNA) was performed to categorize DEGs into different gene modules, and 5 gene modules were randomly assigned color labels (Figure 1D). The blue module was significantly correlated with DEGs in PBMCs of the control group ($r = 0.7$, $p < 0.05$), the light-green module was significantly correlated with DEGs in PBMCs taken 12h after injury ($r = 0.68$, $p < 0.05$), and the light-yellow module was significantly correlated with DEGs in PBMCs taken 7 days after injury ($r = 0.67$, $p < 0.05$) (Figure 1D). Kyoto Encyclopedia of Genes and Genomes (KEGG) analysis was performed on the light-yellow module (7 days after injury) and light-green module (12h after injury). DEGs in the light-yellow module were significantly enriched in the cell cycle (Figure 2A), and those in the light-green module genes were significantly enriched in the presence of autophagy pathways and levels of endocytosis (Figure 2C). In terms of BP (biological process) enrichment analysis, DEGs in the light-yellow module (7 days after injury) were significantly associated with nuclear division and organelle fission (Figure 2B) and those in the light-green module (12h after injury) were mainly involved in the autophagy process (Figure 2D). The hub genes networks of the light-green module (12h after injury) showed that JMY (junction mediating and regulatory protein gene) was identified as a hub gene (Figure 2E).

3.2 Activated autophagy in innate immune cells during the early stages of major trauma

The above-mentioned findings demonstrate that autophagy is an essential biological process in the development of immune disorders in the early stages of major trauma (12h), and subsequent studies have further evaluated the levels of expression profiling of ATG (autophagy-related genes) in innate and adaptive immune cells of patients after major trauma through single-cell transcriptome analysis.

3.2.1 Characteristics of major trauma patients

From April 2021 to February 2022, a total of five patients meeting the study's eligibility requirements were admitted to the SICU (surgical ICU) of Tongji Hospital. The mean age of the cohort was 37 ± 8.5 years, and all patients were male. The mean Injury Severity Score (ISS) was 28.4± 3.1, indicating a severely injured population, and the mean Glasgow Coma Scale (GCS) score was 11.2 ± 1.3, indicating moderate consciousness disorders. Overall, 40% (2/5) patients suffered from a cerebral injury, 80% (4/5) patients suffered from a chest injury, 40% (2/5) patients suffered from a spine injury, 60% (3/5) patients suffered from pelvic fractures, and 100% (5/5) patients suffered from extremities fractures. Injuries were mainly caused by traffic

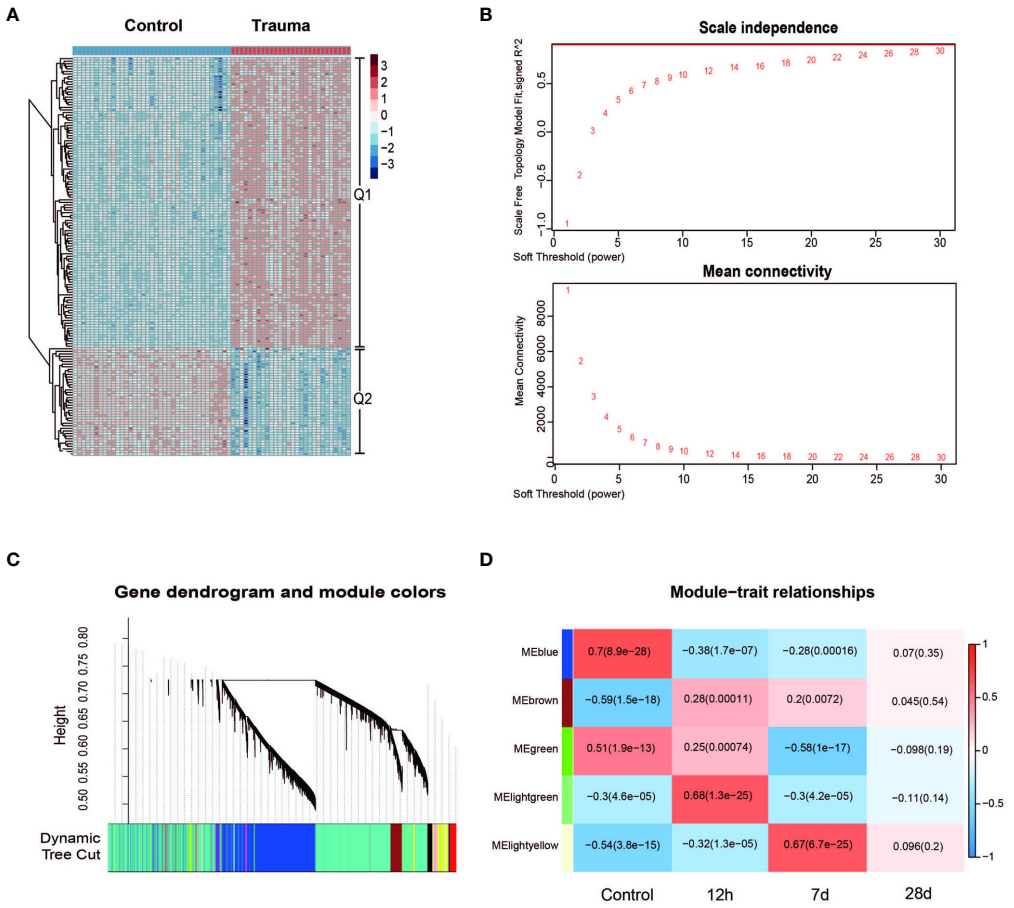

FIGURE 1
Gene network analysis of trauma patients. **(A)** Heatmap of processed differentially expressed genes (DEGs) expression profiles in trauma patients and control participants. **(B)** Scale independence and mean connectivity under the different soft threshold values. **(C)** Gene co-expression modules, represented by different colors under the gene cluster tree. Each color represents a different co-expression module. **(D)** Heatmap of the correlations between module and the injury time of trauma patients (control, injury after 12 hours, injury after 7 days and injury after 28 days). Five modules that were randomly assigned color labels were identified (blue, brown, green, light green and light yellow). The color of the square area represents the MS (module significance). When the MS value approaches +1, there is a positive correlation between the module and trait; otherwise, when the MS value approaches −1, there is a negative correlation between the module and trait. The *p*-values are shown in parentheses and were calculated using the Student's *t*-test.

accidents ($n = 3$), followed by falls ($n = 1$), then crushing ($n = 1$). Peripheral venous blood samples were obtained from three control participants and from five major trauma patients within 6 hours of injury.

3.2.2 Single-cell transcriptional profiling of PBMCs after major trauma

To elucidate the cytologic characteristics of immune cells, scRNA-seq dataset of PBMCs were analyzed as a discovery cohort; this cohort included five patients who had been diagnosed with major trauma. After data filtering, samples with less than 500 cells were excluded. After the quality control process, 167,897 single cells were obtained, with an average of 3,694 unique molecular identifiers (UMIs) and 14,587 genes represented.

Fifteen types of major cells were annotated by expressions of canonical gene markers (23), which included monocytes (LYZ+ and S100A9+), natural killer (NK) cells (GNLY+ and NKG7+), neutrophils (FCGR3B+ and IFITM2+), macrophages (IL7R+ and TCF7+), memory CD8+ *t*-cells (CD8A+, CD8B+ and GNLY+), B cells (MS4A1+ and CD79A), naive CD4+ *t*-cells (CD3+, CD4+ and TCF7+), plasmablasts (PPBP+ and TUBB1+), myeloid dendritic cells (STMN1+ and H4C3+), regulatory *t*-cells (IL7R+ and IL32+), naive CD8+ *t*-cells (CD8B+ and CRR7+), natural killer T (NKT) cells (IL32+, NKG7+ and CD3+), erythroid cells (HBB+ and HBA2+), plasmacytoid dendritic cells (LILRA+), and progenitor cells (SPINK2+ and SOX4+) (Figures 3A–C). Fifteen clusters of PBMCs were identified using unsupervised hierarchical clustering and visualized with uniform manifold approximation and projection (UMAP); the cells of each group were then visualized with UMAP

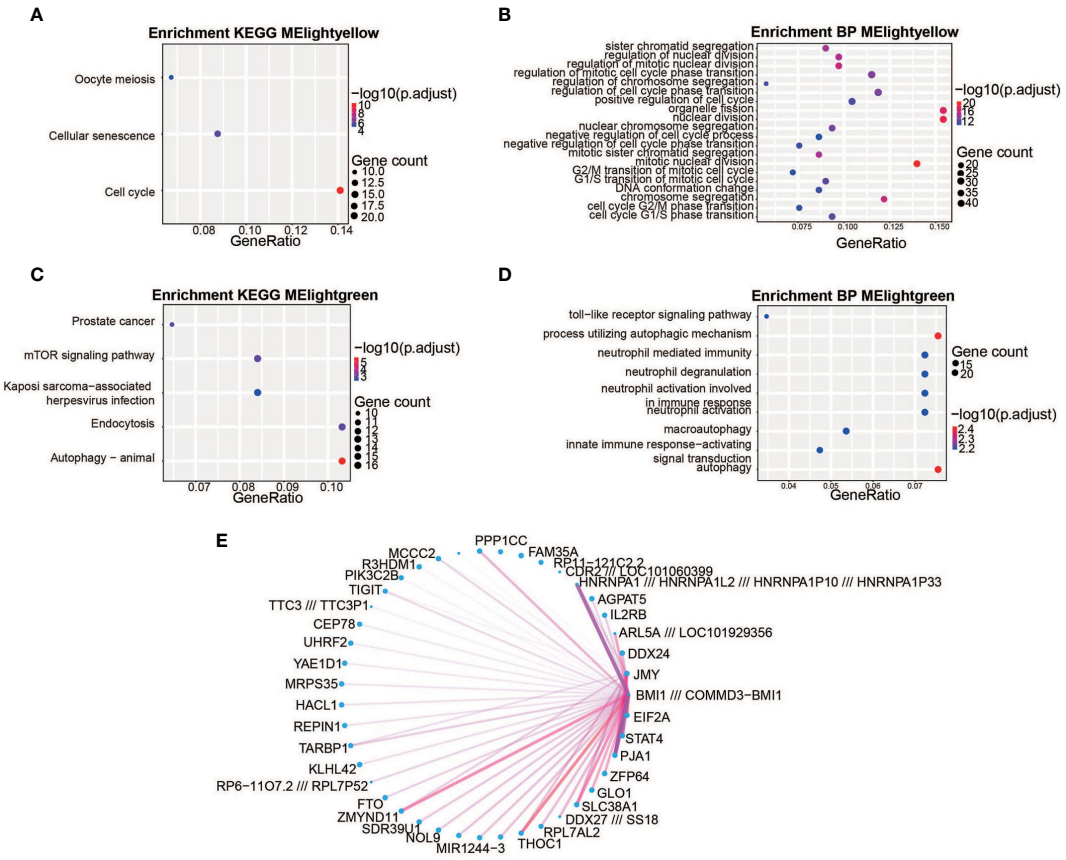

FIGURE 2
The biological significance of the light-yellow and light-green module genes. **(A, C)** Kyoto Encyclopedia of Genes and Genomes (KEGG) enrichment analysis. The light-yellow module genes were significantly enriched in the cell cycle **(A)** and the light-green module genes were significantly enriched in their autophagy pathways and endocytosis **(C)**. The color represents the -$\log_{10}$(adjustment of *p*-value) values and the size of the dot represents the size of corresponding pathways and gene counts. **(B, D)** Gene Ontology (GO) enrichment analysis. The light-yellow module was significantly associated with nuclear division and organelle fission **(B)** and the light-green module was mainly involved in the autophagy process **(D)** The different colors represent the -$\log_{10}$(adjustment of *p*-value) values and the size of the dot represents the size of corresponding pathways and gene counts. **(E)** Weighted co-expression gene networks are represented by the light-yellow module. The width of the line represents gene−gene interaction weight and the size of the dot represents the gene degree. JMY is the hub gene for the light-green module.

plots, individually (Figures 3D, E). We further explored the effect of major trauma on the composition of immune cells in PBMCs according to the scRNA-seq data analysis. Only cell types with a number of cells that met the statistical requirement were included in the analysis. As is shown in Figures 3F, G, the proportion of NK cells, CD8+ memory *t*-cells, CD4+ naive *t*-cells, CD8+ naive *t*-cells, B cells, Tregs and NKT cells decreased during the early stages of major trauma. The proportion of DCs did not significantly change. Compared with control participants, major trauma patients had significantly increased proportions of monocytes/macrophages and neutrophils (Figure 3G).

3.2.3 Expression profiling of autophagy-related genes in immune cells after major trauma

Given the critical role of autophagy during the early stages of trauma (Figures 2B, D), the expression profiling of ATG (autophagy-related genes) was measured in innate and adaptive immune cells of patients within 6 hours of injury. We followed the well-established methodology designed by Dr. F. Cecconi et al. to monitor autophagy-related gene transcription (17). A genetic toolbox with 604 ATG, containing almost all signaling pathways involved in autophagy, was used to assess autophagy in immune cells by single-cell transcriptomics analysis (17). Self-organized mapping (SOM) was performed on each cell type gene expression profile to explore the dynamic transcriptional signature of genes crucial to processes in autophagy (including 39 genes crucial to processes in autophagy) by dimensionality reduction and image analysis. Dynamic expression patterns of genes crucial to processes in autophagy were observed in memory CD8+ *t*-cells, naive CD4+ *t*-cells, neutrophils, NK cells and plasma DC (Figure 4A). The total ATG analysis expression analysis outlines the ATG expression profile in each cell type (Figure 4B). In the context of trauma patients, the autophagy was significantly activated in innate immune cells, especially in monocytes and

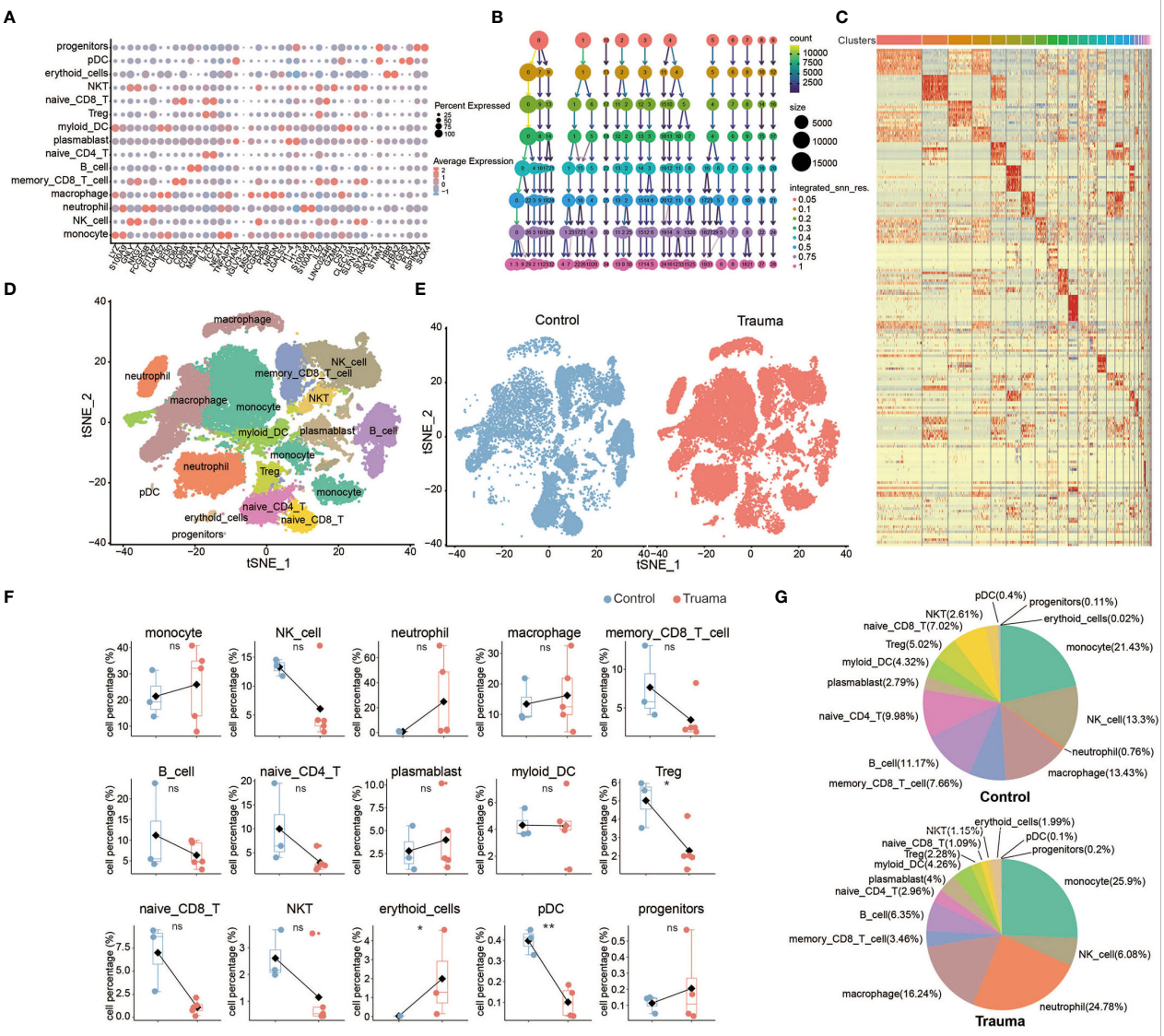

FIGURE 3
Single-cell transcriptional profiling of peripheral blood mononuclear cells (PBMCs) after major trauma. **(A)** A dot graph showing the expression of hallmark genes by different cell clusters. **(B)** Cluster tree graph of the number of clusters under the conditions of different resolutions. **(C)** Heatmap of the expression of the top 10 hallmark genes by different cell clusters. **(D)** t-distributed stochastic neighbor embedding (t-SNE) of small conditional RNA sequencing (scRNA-seq) of PBMCs from control participants and early-stage major trauma patients. **(E)** t-SNE plot of immune cells in control participants (n = 3) and major trauma patients (n = 5). **(F)** Quantification of percentage different immune cells from control participants (n=3) and major trauma patients (n=5). p values were calculated using an unpaired two-tailed Student's t-test. *p < 0.05, **p < 0.01. **(G)** Proportion of each population out of all immune cells in control participants and major trauma patients. ns, not statistically significant.

neutrophils (Figure 4C). No significant change of autophagy level was observed in adaptive immune cells, including memory CD8+ T cells, naive CD4+ T cells, naive CD8+ T cells, Tregs, DCs, and NKT cells.

3.2.4 Activated autophagy in monocytes

To figure out the influence of the autophagy in monocytes, ATG core gene sets (six core autophagy-related genes, namely *ATG14*, *ATG7*, *NBR1*, *ULK1*, *ULK2*, and *WDR45*, were identified as being fundamental to the effective initiation of the autophagy cascade) were used to classify the monocytes (17) (24). The monocytes were divided into two subsets according to the expression of ATG core gene sets, namely ATG positive monocytes (total ATG core genes expression > 10) and ATG negative monocytes (total ATG core genes expression < 10) (24). The percentage of ATG-positive monocytes was greater in major trauma patients than in control participants (Figure 5A). Under the condition of resolution=0.05, monocytes were divided into four subsets based on defined stages of cells differentiation, and then the

10.3389/fimmu.2022.1090358

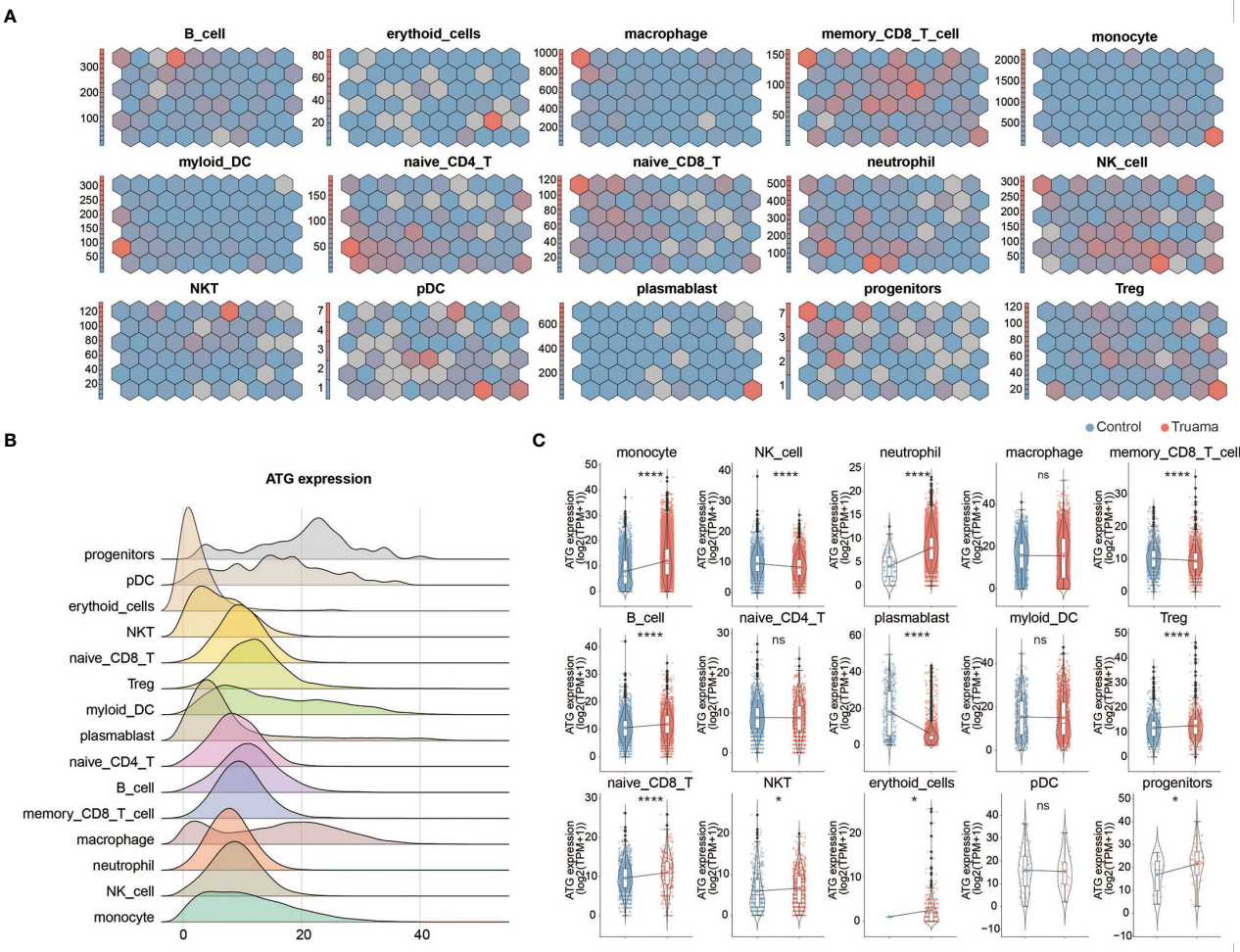

FIGURE 4
Expression profiling of autophagy-related genes in immune cells after major trauma. **(A)** Expression of autophagic genes represented by the self-organizing map (SOM) algorithm. Each cell cluster represents a subset of autophagy-related genes (ATG). **(B)** Ridges graph showing ATG expression levels in different immune cells. **(C)** The difference in total ATG expression levels of different immune cells between early-stage major trauma patients and control participants. *p* values were calculated using an unpaired two-tailed Student's *t*-test. *$p < 0.05$, ****$p < 0.0001$. ns, not statistically significant.

ATG expression levels were determined in each monocyte subset. The quantity of ATG positive monocytes significantly increased in the Mon1 subtype of monocyte after major trauma (Figures 5B, C). A total of 645 DEGs were identified in ATG-positive monocytes *via* pseudo-bulk RNA differential gene analysis (Figure 5D). Gene ontology enrichment analysis shows that antigen uptake, processing presentation, and MHC class II protein complex assembly pathways were up-regulated in ATG positive monocytes, whereas different types of metabolic processes were down-regulated (Figure 5E).

3.2.5 Activated autophagy in neutrophils

To explore the function alteration in autophagy positive neutrophils, we separated the neutrophils into ATG-positive and ATG-negative neutrophils according to ATG core gene sets (as mentioned above) (17) (24). The percentage of ATG-positive neutrophils significantly increased in major trauma patients compared with control participants (Figure 6A). Neutrophils were divided into two subsets according to cellular differentiation (resolution = 0.05). The quantity of ATG positive neutrophils was upregulated in each of the subtypes individually (Figures 6B, C). As shown in Figure 6D, 109 DEGs were identified in ATG positive neutrophils *via* pseudo-bulk RNA differential gene analysis (Figure 6B). To explore the biological meaning of these DEGs, GO enrichment analysis was performed on DEGs and indicated that there was positive regulation of antigen processing and presentation of endogenous antigen, and that type I interferon signaling pathways were up-regulated in ATG-positive neutrophils. On the contrary, the expression levels of tRNA processing, cell recognition, mitochondrial, phagocytosis and recognition genes were down-regulated (Figure 6E).

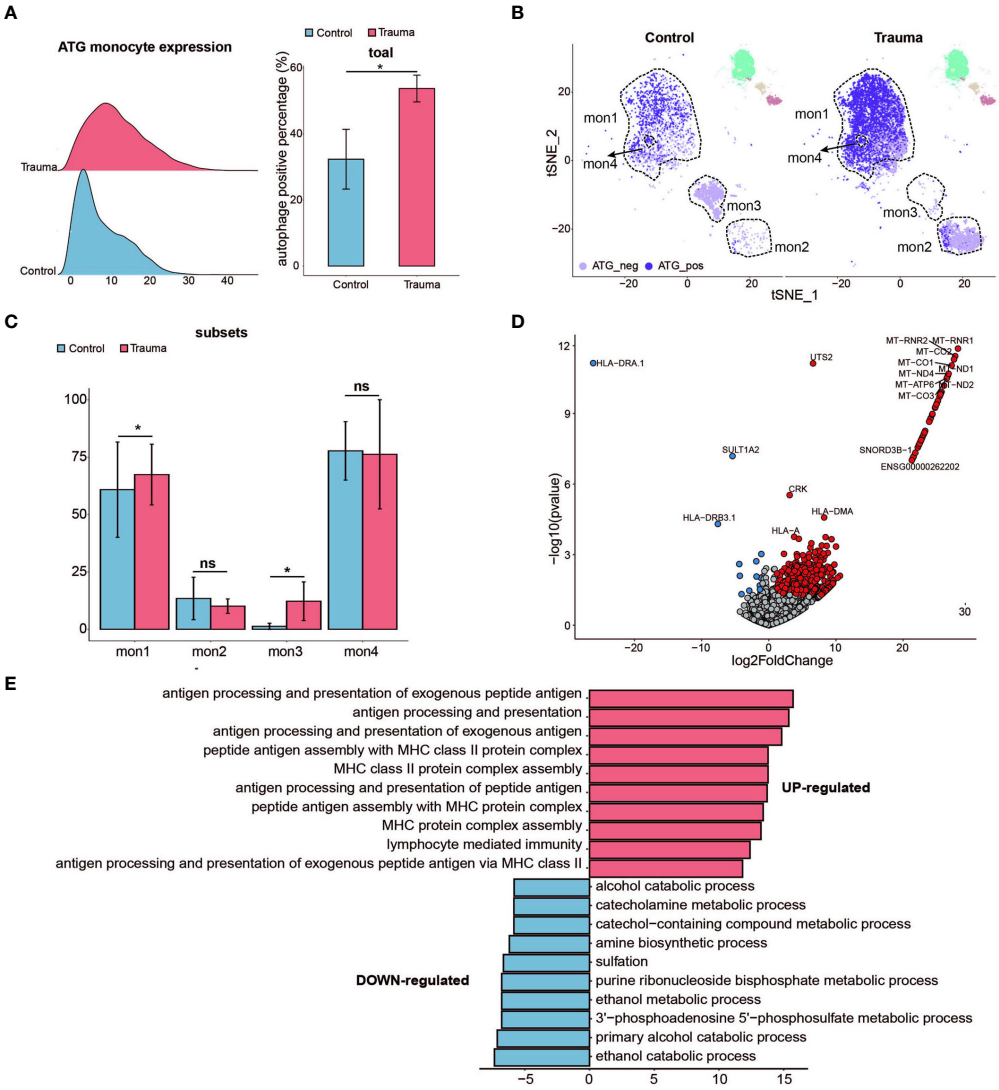

FIGURE 5
Activated autophagy in monocytes. **(A)** Ridge plot showing the autophagy-related gene (ATG) expression levels of monocytes (left panel) and the percentage of ATG positive monocytes alteration (right panel) in major trauma patients. *p*-values were calculated using an unpaired two-tailed Student's *t*-test. **p* < 0.05. **(B)** t-distributed stochastic neighbor embedding (t-SNE) projection of ATG expression levels of monocytes in major trauma patients. **(C)** The percentage alteration of autophagy-positive monocytes in major trauma patients. *p*-values were calculated using an unpaired two-tailed Student's *t*-test. **(D)** Volcano graph displaying differential expressed genes of monocytes in major trauma patients and control participants. Genes with $\log_2$FC values of > 1 and *p*- values of < 0.05 are highlighted in red, and genes with $\log_2$FC values of < −1 and *p*-values of < 0.05 are highlighted in blue. **(E)** GO analysis of up-regulated differentially expressed genes (DEGs) (red) and down-regulated DEGs (blue) in autophagy-positive monocytes. ns, not statistically significant.

4 Discussion

Hemorrhagic shock and overwhelming injuries of vital organs are responsible for early mortality in major trauma, whereas more than half of delayed deaths are associated with multiple organ failure or severe sepsis induced by the severe repression of immunological functions. Over the past few decades, considerable efforts have been invested on the study of limited pathways or single components in trauma-induced immune dysfunction. However, contradictory findings have been reported, which has always been a major barrier to achieving widely reproducible clinical benefits. Therefore, the underlying molecular mechanism and physiological implications of trauma-induced immunological dysfunction need to be further understood.

In the present study, large-scale single-cell transcriptome analysis and weighted gene co-expression network analysis (WGCNA) provided new insight into the landscape of PBMCs in patients with major trauma. The results of our study demonstrated that the DEGs of the light-green module (12h after injury) were mainly involved in the biological process

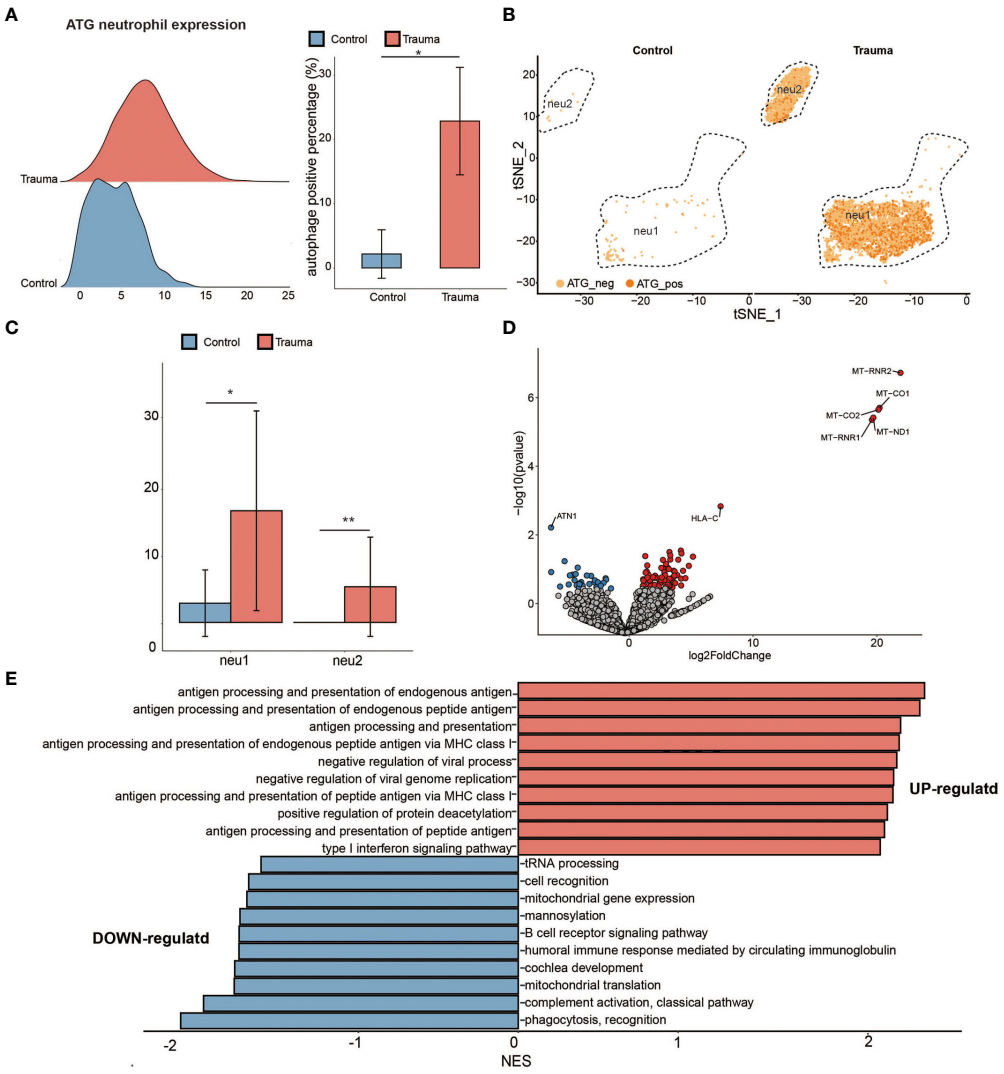

FIGURE 6
Activated autophagy in neutrophils. **(A)** Ridge plot showing the autophagy-related genes (ATG) expression levels of neutrophils (left panel) and the percentage of ATG-positive neutrophils alteration (right panel) in major trauma patients. *p*-values were calculated using an unpaired two-tailed Student's *t*-test. *$p < 0.05$. **(B)** t-distributed stochastic neighbor embedding (t-SNE) projection of ATG expression levels of neutrophils in major trauma patients. **(C)** The percentage alteration of the autophagy positive neutrophils in major trauma patients. *p*-values were calculated using an unpaired two-tailed Student's *t*-test. **(D)** Volcano graph displaying differentially expressed genes (DEGs) of neutrophils in major trauma patients and control participants. Genes with log_2FC values of > 1 and *p*-values of < 0.05 are highlighted in red, and genes with log_2FC values of < −1 and *p*-values of < 0.05 are highlighted in blue. **(E)** GO enrichment analysis of up-regulated DEGs (red) and down-regulated DEGs (blue) in autophagy-positive neutrophils. **$p < 0.01$.

relating to the autophagy pathways and endocytosis. The Kyoto Encyclopedia of Genes and Genomes (KEGG) pathway analysis and GO enrichment analysis revealed that light-green module (12h after injury) genes were highly enriched in the autophagy pathways, which in turn indicates that autophagy-related genes dominate the expression change in PBMCs during the early stage of major trauma. JMY was screened as the hub gene in light-green modules, and was closely related to the autophagy machinery (25–28). The aforementioned results suggest that autophagy activation is the most significant change occurring in the biological processes of PBMCs during the early stage of major trauma. Previous studies have also observed activated autophagy after trauma, but the majority of findings reach the conclusion that trauma contributes to activated autophagy in osteoblasts, cardiomyocytes or lung tissue using animal models of trauma (29–31). To our knowledge, ours is the first study to investigate autophagy in PBMC after trauma, and to propose that there exists a potential relationship between activated autophagy and trauma-induced immune dysfunction in patients with major trauma.

Autophagy functions broadly in immunity, ranging from cell-autonomous defense to coordination of multicellular

immune responses (22). However, there is a lack of study on the role of autophagy in immune cells after major trauma. To simultaneously reveal the autophagy levels in various types of immune cells after trauma, PBMC single-cell sequencing was performed. Single-cell RNA sequencing analysis represents an effective means of obtaining an unbiased and comprehensive visualization of the immunological profiles of PBMCs in patients with major trauma. Compared with bulk RNA sequencing, it has a single-cell level resolution, which can estimate the whole changes of cell subsets, the immune cell function of individual cell, and the correlation between different cell subsets. In using this approach, we observed significantly higher expression levels of autophagy-related gene (ATG) in monocytes and neutrophils accompanying increased cell numbers after major trauma. Identification of ATG genes has provided the impetus for a molecular understanding of autophagy. The findings indicated that autophagy was significantly activated in the innate immune cells of trauma patients. However, almost no significant change in autophagy levels was observed in adaptive immune cells, including naive or memory CD8+ *t*-cells, naive CD4+ *t*-cells, Tregs NKT cells, and B cells. Meanwhile, obviously decreased numbers of adaptive immune cells were observed during the early stages of major trauma. It has been reported that activated autophagy reduced cell damage caused by pathogens, and protected against monocyte death during virus infection (32). Considering the above-mentioned findings, we speculate that alteration in levels of autophagy activation is associated with the function and survival of monocytes after major trauma.

Monocytes possess the potential for differentiation into macrophages and myeloid lineage dendritic cells, which serve three main functions in the immune system: phagocytosis, antigen processing and presentation, and cytokine production (32). There are growing findings which emphasize that aberrations in the function of monocytes are pivotal to the development of trauma-induced immunopathology. Since monocytes bridge innate and adaptive immunity, their dysfunction profoundly affects the whole immune system (33, 34). Activated monocytes and their macrophage and dendritic-cell progeny can directly present antigens to *t*-cells and promote Th1-type immunity. The extremely up-regulated antigen processing and presentation will trigger an intense systemic inflammatory response and excessive release of pro-inflammatory mediators, inevitably leading to unfavorable clinical outcomes in trauma patients. Growing evidence has already confirmed that monocytes pathology contributes to unfavorable clinical outcomes for trauma patients (34, 35). However, few studies reveal the underlying mechanisms behind this.

In the present study, our findings indicated that autophagy was significantly activated in monocytes after major trauma. Previous studies have revealed that the induction of autophagy is essential for the differentiation of monocytes in viral or bacterial infections (32). Autophagy is also important in the induction of pathogen killing by monocytes/macrophages. Preventing the induction of autophagy hinders differentiation and cytokine production in monocytes (32). However, the regulatory effects mediated by autophagy in monocytes are poorly investigated in major trauma patients. In following study, we further elucidated the mechanism of autophagy in regulating monocytes function after major trauma.

GO enrichment analysis further indicated that activated autophagy contributes to the up-regulated major function of monocytes in patients with major trauma, including antigen uptake, processing, presentation, and MHC class II protein complex assembly. Activated autophagy also results in the down-regulation of partial monocytes function, such as ribosome assembly and hydrogen peroxide catabolic process. Our findings indicate that activated autophagy is heavily involved in the pathological changes of monocytes during the early stages of major trauma.

Neutrophils are another important component of the innate immune system and serve as the first line of defense against infiltrating pathogens. There is emerging evidence that the modulated functions of neutrophils play a core role in the development of inflammatory complications after major trauma (36). Hyperactive neutrophils were found to elicit severe inflammatory tissue damage, contribute to develop acute respiratory distress syndrome (ARDS) and multiple organ failure, thus exacerbating outcome after major trauma (37). Over the past decades, the deregulated activation of neutrophils in PBMCs of trauma patients was observed mainly through changes in the phenotypic and intracellular markers of neutrophils in their dynamic response to traumatic insult. At present, little is known about the molecular mechanisms which could potentially regulate neutrophil function and maintain homeostasis in neutrophils after trauma.

As was observed with monocytes, our findings indicated that autophagy was also significantly activated in neutrophils after major trauma. Previous studies have established that autophagy is an important regulator of neutrophil functions, including degranulation, cytokine production and the elimination of invading pathogens in animal models infected with the *Streptococcus* or *Rickettsia* bacterial strains (32). The current evidence around trauma-associated autophagy in neutrophils is inconclusive; however, a correlation between neutrophils and autophagy activation can be observed after major trauma.

In our study, 109 DEGs were identified in ATG-positive neutrophils *via* pseudo-bulk RNA differential gene analysis. To explore the biological significance of these 109 DEGs, GO enrichment analysis was performed. Our findings indicated that activated autophagy contributes to up-regulation in the major function of neutrophils in patients with major trauma, including antigen processing and presentation, and type I interferon signaling pathways. Our findings also indicate that

activated autophagy is heavily involved in the pathological changes of monocytes during the early stages of major trauma.

Our study suggests that activated autophagy plays a core role in regulating the pathological processes of innate immune cells during the early stages of major trauma. Activated autophagy causes the hyperaction of innate immune cells, through up-regulating pivotal functions, including antigen uptake, processing, presentation, MHC class II protein complex assembly, and type I interferon signaling pathways. Hyperactive innate immune cells in turn contribute to the development of immunological disorders, which further lead to complex complications such as ARDS, sepsis, MOF, and so on, ultimately exacerbating negative survival outcomes in patients with major trauma.

5 Conclusion

In summary, by analyzing single-cell transcriptomics data, our findings suggest the autophagy is significantly activated in monocytes and neutrophils during the early stages of major trauma. Activated autophagy contributes to up-regulated major functions of monocytes and neutrophils. Thus, we contend that well-regulated autophagy activation in neutrophils and monocytes has the potential to optimize post-traumatic immune treatment strategies, which may in turn improve survival outcomes in major trauma patients. Further research investigating the molecular mechanisms of autophagy, and how it affects innate immune cell functions after major trauma need to be conducted in the near future.

Data availability statement

The datasets presented in this study can be found in online repositories. The names of the repository/repositories and accession number(s) can be found below: https://www.ncbi.nlm.nih.gov/, GSE197522.

Ethics statement

The studies involving human participants were reviewed and approved by Medical Ethics Committee of Tongji Hospital Affiliated to Tongji Medical College, Huazhong University of Science and Technology. The patients/participants provided written informed consent to participate in this study.

Author contributions

Z-hT supervised the study. Z-hT and TC designed the experiments, analyzed the data, and co-wrote the manuscript. DC performed the experiments, analyzed the data and co-wrote the manuscript. CZ, HD, JL, SC, PZ, JY, and LD performed the experiments and analyzed the data. All authors contributed to the article and approved the submitted version.

Funding

This work was supported in part by National Natural Science Foundation of China 81873870 (Z-hT).

Acknowledgments

We thank the staff at Department of Immunology, Tongji Medical College for their assistance in the task of data pre-processing.

Conflict of interest

The authors declare that the research was conducted in the absence of any commercial or financial relationships that could be construed as a potential conflict of interest.

Publisher's note

References

1. Haagsma JA, Graetz N, Bolliger I, Naghavi M, Higashi H, Mullany EC, et al. The global burden of injury: incidence, mortality, disability-adjusted life years and time trends from the global burden of disease study 2013. *Inj Prev* (2016) 22:3–18. doi: 10.1136/injuryprev-2015-041616

2. Leilei D, Pengpeng Y, Haagsma JA, Ye J, Yuan W, Yuliang E, et al. The burden of injury in China, 1990-2017: findings from the global burden of disease study 2017. *Lancet Public Health* (2019) 4:e449–61. doi: 10.1016/S2468-2667(19)30125-2

3. Pape HC, Halvachizadeh S, Leenen L, Velmahos GD, Buckley R, Giannoudis PV. Timing of major fracture care in polytrauma patients - an update on principles, parameters and strategies for 2020. *Injury* (2019) 50:1656–70. doi: 10.1016/j.injury.2019.09.021

4. Sikand M, Williams K, White C, Moran CG. The financial cost of treating polytrauma: implications for tertiary referral centres in the united kingdom. *Injury* (2005) 36:733–7. doi: 10.1016/j.injury.2004.12.026

5. Bardes JM, Inaba K, Schellenberg M, Grabo D, Strumwasser A, Matsushima K, et al. The contemporary timing of trauma deaths. *J Trauma Acute Care Surg* (2018) 84:893–9. doi: 10.1097/TA.0000000000001882

6. Raymond SL, Holden DC, Mira JC, Stortz JA, Loftus TJ, Mohr AM, et al. Microbial recognition and danger signals in sepsis and trauma. *Biochim Biophys Acta Mol Basis Dis* (2017) 1863:2564–73. doi: 10.1016/j.bbadis.2017.01.013

7. Relja B, Land WG. Damage-associated molecular patterns in trauma. *Eur J Trauma Emerg Surg* (2020) 46:751–75. doi: 10.1007/s00068-019-01235-w

8. Tsukamoto T, Chanthaphavong RS, Pape HC. Current theories on the pathophysiology of multiple organ failure after trauma. *Injury* (2010) 41:21–6. doi: 10.1016/j.injury.2009.07.010

9. McBride MA, Owen AM, Stothers CL, Hernandez A, Luan L, Burelbach KR, et al. The metabolic basis of immune dysfunction following sepsis and trauma. *Front Immunol* (2020) 11:1043. doi: 10.3389/fimmu.2020.01043

10. Deretic V, Levine B. Autophagy balances inflammation in innate immunity. *Autophagy* (2018) 14:243–51. doi: 10.1080/15548627.2017.1402992

11. Deretic V. Autophagy in inflammation, infection, and immunometabolism. *Immunity* (2021) 54:437–53. doi: 10.1016/j.immuni.2021.01.018

12. Riffelmacher T, Richter FC, Simon AK. Autophagy dictates metabolism and differentiation of inflammatory immune cells. *Autophagy* (2018) 14:199–206. doi: 10.1080/15548627.2017.1362525

13. O'Neill LA, Kishton RJ, Rathmell J. A guide to immunometabolism for immunologists. *Nat Rev Immunol* (2016) 16:553–65. doi: 10.1038/nri.2016.70

14. Palmer CS, Gabbe BJ, Cameron PA. Defining major trauma using the 2008 abbreviated injury scale. *Injury* (2016) 47:109–15. doi: 10.1016/j.injury.2015.07.003

15. Spahn DR, Bouillon B, Cerny V, Duranteau J, Filipescu D, Hunt BJ, et al. The European guideline on management of major bleeding and coagulopathy following trauma: fifth edition. *Crit Care* (2019) 23:98. doi: 10.1186/s13054-019-2347-3

16. Bacher M, Metz CN, Calandra T, Mayer K, Chesney J, Lohoff M, et al. An essential regulatory role for macrophage migration inhibitory factor in T-cell activation. *Proc Natl Acad Sci U.S.A.* (1996) 93:7849–54. doi: 10.1073/pnas.93.15.78492

17. Bordi M, De Cegli R, Testa B, Nixon RA, Ballabio A, Cecconi F. A gene toolbox for monitoring autophagy transcription. *Cell Death Dis* (2021) 12:1044. doi: 10.1038/s41419-021-04121-9

18. Love MI, Huber W, Anders S. Moderated estimation of fold change and dispersion for RNA-seq data with DESeq2. *Genome Biol* (2014) 15:550. doi: 10.1186/s13059-014-0550-8

19. Wu T, Hu E, Xu S, Chen M, Guo P, Dai Z, et al. clusterProfiler 4.0: A universal enrichment tool for interpreting omics data. *Innovation (Camb)* (2021) 2:100141. doi: 10.1016/j.xinn.2021.100141

20. Yu G, Wang LG, Han Y, He QY. clusterProfiler: an r package for comparing biological themes among gene clusters. *OMICS* (2012) 16:284–7. doi: 10.1089/omi.2011.0118

21. Zhang B, Horvath S. A general framework for weighted gene co-expression network analysis. *Stat Appl Genet Mol Biol* (2005) 4:17. doi: 10.2202/1544-6115.1128

22. Levine B, Mizushima N, Virgin HW. Autophagy in immunity and inflammation. *Nature* (2011) 469:323–35. doi: 10.1038/nature09782

23. Deguine J, Breart B, Lemaitre F, Di Santo JP, Bousso P. Intravital imaging reveals distinct dynamics for natural killer and CD8(+) T cells during tumor regression. *Immunity* (2010) 33:632–44. doi: 10.1016/j.immuni.2010.09.016

24. Turei D, Foldvari-Nagy L, Fazekas D, Modos D, Kubisch J, Kadlecsik T, et al. Autophagy regulatory network - a systems-level bioinformatics resource for studying the mechanism and regulation of autophagy. *Autophagy* (2015) 11:155–65. doi: 10.4161/15548627.2014.994346

25. Liu X, Klionsky DJ. Regulation of JMY's actin nucleation activity by TTC5/STRAP and LC3 during autophagy. *Autophagy* (2019) 15:373–4. doi: 10.1080/15548627.2018.1564417

26. Hu X, Mullins RD. LC3 and STRAP regulate actin filament assembly by JMY during autophagosome formation. *J Cell Biol* (2019) 218:251–66. doi: 10.1083/jcb.201802157

27. Coutts AS, La Thangue NB. Actin nucleation by WH2 domains at the autophagosome. *Nat Commun* (2015) 6:7888. doi: 10.1038/ncomms8888

28. Liu Y, Gu ZY, Miao XY, Gong YP, Xiao YJ, Li J, et al. [The effects and mechanisms of BTBD10 on the proliferation of islet beta cell]. *Zhonghua Nei Ke Za Zhi* (2012) 51:136–9. doi: 10.3760/cma.j.issn.0578-1426.2012.02.016

29. Din FV, Valanciute A, Houde VP, Zibrova D, Green KA, Sakamoto K, et al. Aspirin inhibits mTOR signaling, activates AMP-activated protein kinase, and induces autophagy in colorectal cancer cells. *Gastroenterology* (2012) 142:1504–15.e3. doi: 10.1053/j.gastro.2012.02.050

30. Liu J, Hao G, Yi L, Sun TS. [Protective effects of 3-methyladenine on acute lung injury caused by multiple trauma in rats]. *Zhongguo Gu Shang* (2015) 28:350–3. doi: 10.3969/j.issn.1003-0034.2015.04.013

31. Zahm AM, Bohensky J, Adams CS, Shapiro IM, Srinivas V. Bone cell autophagy is regulated by environmental factors. *Cells Tissues Organs* (2011) 194:274–8. doi: 10.1159/000324647

32. Germic N, Frangez Z, Yousefi S, Simon HU. Regulation of the innate immune system by autophagy: monocytes, macrophages, dendritic cells and antigen presentation. *Cell Death Differ* (2019) 26:715–27. doi: 10.1038/s41418-019-0297-6

33. Huber-Lang M, Lambris JD, Ward PA. Innate immune responses to trauma. *Nat Immunol* (2018) 19:327–41. doi: 10.1038/s41590-018-0064-8

34. Laudanski K, Wyczechowska D. Monocyte-related immunopathologies in trauma patients. *Arch Immunol Ther Exp (Warsz)* (2005) 53:321–8.

35. Marcos-Morales A, Barea-Mendoza JA, Garcia-Fuentes C, Cueto-Felgueroso C, Lopez-Jimenez A, Martin-Loeches I, et al. Elevated monocyte distribution width in trauma: An early cellular biomarker of organ dysfunction. *Injury* (2022) 53:959–65. doi: 10.1016/j.injury.2021.11.026

36. Hazeldine J, Hampson P, Lord JM. The impact of trauma on neutrophil function. *Injury* (2014) 45:1824–33. doi: 10.1016/j.injury.2014.06.021

37. Janicova A, Relja B. Neutrophil phenotypes and functions in trauma and trauma-related sepsis. *Shock* (2021) 56:16–29. doi: 10.1097/SHK.0000000000001695

frontiers | Frontiers in Immunology

TYPE Systematic Review
PUBLISHED 27 January 2023
DOI 10.3389/fimmu.2023.1102126

OPEN ACCESS

EDITED BY
Alessandra Stasi,
University of Bari Aldo Moro, Italy

REVIEWED BY
Vladimir M. Pisarev,
Federal Research and Clinical Center of Intensive Care Medicine and Rehabilitation, Russia
Gianvito Caggiano,
University of Bari Aldo Moro, Italy

*CORRESPONDENCE
Lina Zhang
zln7095@163.com

SPECIALTY SECTION
This article was submitted to Inflammation, a section of the journal Frontiers in Immunology

RECEIVED 18 November 2022
ACCEPTED 13 January 2023
PUBLISHED 27 January 2023

CITATION
Hu J, Xie S, Li W and Zhang L (2023) Diagnostic and prognostic value of serum S100B in sepsis-associated encephalopathy: A systematic review and meta-analysis.
Front. Immunol. 14:1102126.
doi: 10.3389/fimmu.2023.1102126

Diagnostic and prognostic value of serum S100B in sepsis-associated encephalopathy: A systematic review and meta-analysis

Jiyun Hu[1,2], Shucai Xie[1,2], Wenchao Li[1,2] and Lina Zhang[1,2]*

[1]Department of Critical Care Medicine, Xiangya Hospital, Central South University, Changsha, China, [2]National Clinical Research Center for Geriatric Disorders, Xiangya Hospital, Central South University, Changsha, Hunan, China

Background: In sepsis, brain dysfunction is known as Sepsis-associated encephalopathy (SAE), which often results in severe cognitive and neurological sequelae and increases the risk of death. Our systematic review and meta-analysis aimed to explore the diagnostic and prognostic value of serum S100 calcium-binding protein B (S100B) in SAE patients.

Methods: We conducted a systematic search of the databases PubMed, Web of Science, Embase, Cochrane databases, CNKI, VIP, and WFSD from their inception dates until August 20, 2022. A Meta-analysis of the included studies was also performed using Review Manager version 5.4 and Stata16.0.

Results: This meta-analysis included 28 studies with 1401 serum samples from SAE patients and 1591 serum samples from no-encephalopathy septic (NE) patients. The Meta-Analysis showed that individuals with SAE had higher serum S100B level than NE controls (MD, 0.49 [95% CI (0.37)-(0.60), Z =8.29, $P < 0.00001$]), and the baseline level of serum S100B in septic patients with burn was significantly higher than average (1.96 [95% CI (0.92)-(2.99), Z =3.71, P < 0.0002]) In addition, septic patients with favorable outcomes had lower serum S100B levels than those with unfavorable outcomes (MD, -0.35 [95% CI (-0.50)-(-0.20), Z =4.60, $P < 0.00001$]).

Conclusion: Our Meta-Analysis indicates that higher serum S100B level in septic patients are moderately associated with SAE and unfavorable outcomes (The outcomes here mainly refer to the mortality). The serum S100B level may be a useful diagnostic and prognostic biomarker of SAE.

KEYWORDS

sepsis-associated encephalopathy, biomarker, outcome, meta-analysis, S100B

1 Introduction

Sepsis is one of the leading causes of death in Intensive Care Unit (ICU) patients who are critically ill. Each year, sepsis affects approximately 49 million people, resulting in 11 million deaths, which accounts for 20% of all deaths worldwide (1). In 2017, World Health Organization (WHO) declared sepsis a global health priority and the greatest unmet

medical need of our time (2). Sepsis-associated encephalopathy (SAE) is an underlying brain dysfunction that frequently occurs in the absence of overt infection of the central nervous system (3). Because the complex etiology and pathophysiological pathogenesis of SAE are poorly understood, the clinic lacks specific and effective treatment. As a result, there is a pressing need for an accurate, rapid, and simple test, such as biomarkers, to assess the diagnosis and prognosis of SAE.

Biomarkers are objective indicators used to evaluate the physiological or pathological state and to judge the occurrence, development, and prognosis of diseases. They can reflect characteristic changes that can be measured in the environmental interactions of organisms (4). It is possible to identify, predict, or develop new treatment strategies for SAE by using a biomarker or a panel of biomarkers (5); the small size of miRNAs allows them to pass through the blood-brain barrier (BBB) more easily than other biomolecules in SAE (6); the levels of zonula-occludens (ZO-1) were positively correlated with the APACHE II score, SOFA score as well as lactate levels of SAE patients (7); high mobility group box 1 (HMGB1) mediates cognitive impairment in sepsis survivors, and it may be possible to prevent or reverse cognitive impairments by administering anti-HMGB 1 antibodies (8).

In addition to these biomarkers, the role of S100 calcium-binding protein B (S100B) in the guidance of therapeutic options and surveillance strategies in SAE has also been demonstrated in recent studies (9–11). S100B is a calcium-binding protein, predominantly synthesized in and constitutively secreted by astrocytes, oligodendrocytes of the central nervous system, and Schwann cells of the peripheral nervous system (12, 13). It is mainly present in the cytoplasm in a normal state and regulates protein phosphorylation, cell proliferation and apoptosis, energy metabolism, and inflammatory response through the calcium signaling pathway; in a pathological state, it is mainly secreted into the cell in the form of autocrine and paracrine (14). S100B protein plays a crucial role in Alzheimer's disease, Parkinson's disease, multiple sclerosis, Schizophrenia and epilepsy because the high expression of this protein directly targets astrocytes and promotes neuroinflammation (15, 16). Experimental animal studies have revealed that the brain is the primary source of S100B during endotoxemia (17) and play a crucial role in acute brain injury and long-term cognitive impairment during sepsis by regulating mitochondrial dynamics through RAGE/ceramide pathway (18); these findings make S100B a candidate as an essential biomarker of SAE. The purpose of our Systematic Review and Meta-Analysis was to evaluate the potential diagnostic and prognostic value of S100B in SAE patients.

2 Methods

2.1 Search strategy

All studies published before August 20, 2022, were searched in PubMed, Web of Science, Embase, Cochrane databases, CNKI (China National Knowledge Infrastructure), VIP (China Science and Technology Journal Database) and WFSD (Wanfang Data Knowledge Service Platform). The Medical Subject Heading (Mesh) headings or keywords as: ("S100B," or "S100 calcium binding protein B," or "S100," or "S100-B," or "S100Beta," or "S100B,") AND ("sepsis," or "severe sepsis," or "septic shock"). There were no restrictions on language. All cited references were reviewed to identify additional studies.

2.2 Inclusion and exclusion criteria

The meta-analysis was limited to studies dealing with the serum S100B in SAE patients. Studies that met the following criteria were identified (1): all patients should meet the confirmed sepsis or septic shock definition, and experiments should be Sepsis-associated encephalopathy patients (SAE), controls should no-encephalopathy septic patients (NE) (2); evaluation of S100B in serum samples. We included both prospective and retrospective studies without restrictions. The exclusion criteria were as follows (1): duplicate publications or other types of patients (2); studies lacking original or complete data (3); animal studies or reviews; and (4) not involving the selected biomarker.

2.3 Quality assessment

Two independent reviewers (J-YH and S-CX) performed a study quality assessment. The quality and risk of bias of the selected studies were assessed using the Quality Assessment of Diagnostic Accuracy Studies version 2 (QUADAS-2) assessment tool according to the recommendation by the Cochrane Collaboration (19). We analyzed the following two domains: risk of bias and applicability. Each category had its assessment protocol. We identified the risk of bias in each domain as low, unclear, or high risk based on the methods used to ensure that each form of bias was minimized. Any disagreements were discussed and resolved by the entire review team.

2.4 Data extraction

Three reviewers independently extracted data from each included study according to the selection criteria. After extraction, data were reviewed and compared by the first author. Disagreements were resolved by consensus. The data extracted included study characteristics (first author and year), participant characteristics (age, sex ratio, and sample size), and methodological characteristics (assay, cutoff and collection time, and clinical trial design types). We unified serum S100B levels to (ng/mL). Additional information can be obtained by directly questioning the primary authors when possible to acquire and verify the data. If there were several serum S100B collection time points in one study, we marked them separately at different time points, such as Feng 2017(1d) and Feng 2017(3d).

2.5 Statistical analysis

Parametric variables were described as means and SDs, and nonparametric variables were described as medians and

interquartile ranges (IQRs). If mean data were not reported, we used the method by Wan et al. to estimate the mean and SD using the median and IQR or median and range to estimate the mean and SD (20, 21). I-squared (I^2) statistics and Q test were used to evaluate the effect of study heterogeneity on the Meta-Analysis results (22). According to the Cochrane review guidelines, if severe heterogeneity was present at P<0.1 or I^2>50%, a random-effects model was selected; otherwise, a fixed-effects model was used. Moreover, Subgroup analyses were performed according to serum sample collection time or serum S100B measurement assay. Potential publication bias was assessed using Begg's and Egger's tests and funnel plots. A sensitivity analysis was performed to determine the stability and consistency of the meta-analysis results. All analyses were performed using Review Manager version 5.4 (RevMan, The Cochrane Collaboration, Copenhagen) and STATA software (version 16.0, StataCorp, College Station, TX). For all analyses, P<0.05 was considered significant. For publication bias, P>0.1 was considered significant.

3 Results

3.1 Search results

Figure 1 illustrates the study selection process. There were 1143 relevant studies under the search words (PubMed 137, Web of Science 205, EMBASE 390, Cochrane Library 5, CNKI 27, WFSD 350, VIP 26), of which 440 were excluded due to duplicates. A total of 703 studies were identified through a literature search and screening of titles and/or abstracts. Of these, 641 studies were unrelated to the topic and excluded. After the assessment of eligibility using full text, 62 studies were excluded. Finally, 28 studies met all inclusion criteria and were included in the meta-analysis: 12 studies from the English database (23–34); 16 studies from the Chinese database (35–50). The selected details of the individual studies are listed in Table 1. In the current meta-analysis, there were 1401 serum samples from patients with SAE and 1591 serum samples from septic patients without encephalopathy.

3.2 Quality assessment

Twenty-eight studies examined the risk of bias and applicability concerns using a modified QUADAS-2 assessment tool, as displayed in Figures 2 and 3. There were 15 studies with a low risk of patient selection, two studies with low risk, and 22 with unclear risk on index test; seven studies had low risk on the reference standard; ten studies had a low risk of flow and timing. There were 15 studies with low concern regarding patient selection, 14 with low concern about the index test, and 5 with low concern about the reference standard. In short, high-risk was mainly focused on index tests, flow, and timing items.

3.3 Meta-analysis results

3.3.1 Comparison of serum S100B levels between SAE and NE

Because we unified serum S100B units to (ng/mL), the Mean Difference (MD) rather than Standardized Mean Difference (SMD) was used to estimate serum S100B levels in both groups. The results of the pooled MD analysis are revealed in Figure 4. The heterogeneity test demonstrated significant differences among studies (Chi^2 = 10551.25, I^2 = 100%, P < 0.00001); therefore, the random-effects

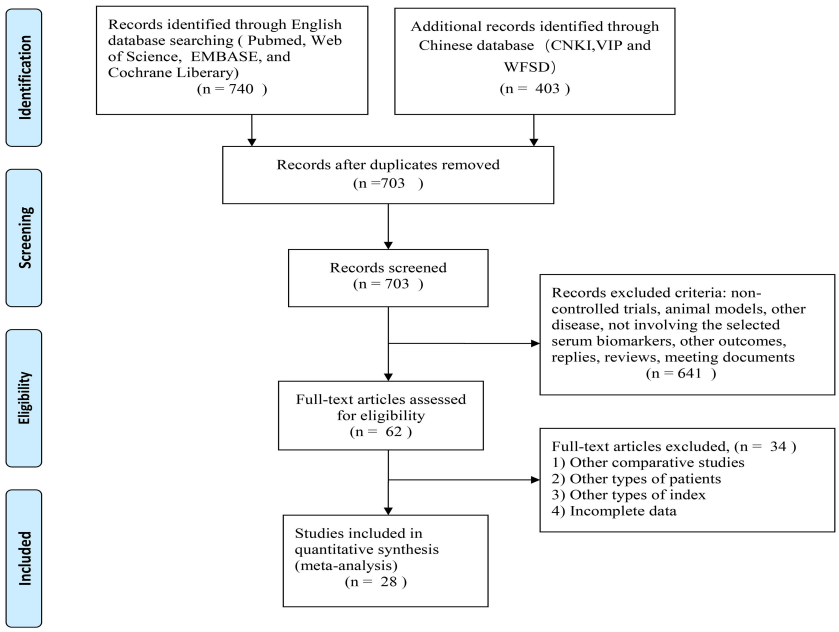

FIGURE 1
Literature search strategy and screening process.

10.3389/fimmu.2023.1102126

TABLE 1 Specific basic characteristics of the included studies (SAE, Sepsis-associated encephalopathy patients; NE, no–encephalopathy septic patients; NA, not announce; h, hour; d, day; m, month; ELISA, enzyme-linked immunosorbent assay; ECLIA, electrochemiluminescence immunoassay; CLIA, chemiluminescence immunoassay; ICA, immunochromatography assay; FICA, fluorescence immunochromatography assay; RIA, radioimmunoassay; WB, western blotting).

study and year	SAE sample size (Males/ Female)	NE sample size (Males/ Female)	Age	Sample Collection time	Assay	SAE S100B cutoff (ng/mL)	Design
Chen 2019 (45)	42(-) All patients: 100 (56/44)	58 (–)	68 ± 5.4	ICU admission	ELISA	0.53 ± 0.28	NA
Cui 2022 (46)	79(45/34)	121(70/51)	SAE:72.78 ± 4.01 NE:72_86 ± 4.60	Within 48 h	FICA	0.53 ± 0.09	Retrospective study
Erikson 2019 (29)	10(4/6)	12(10/2)	SAE: 62.4 (49-70.5) NE: 61.8 (60.1-78.5)	When CAM-ICU assessed	CLIA	0.30 (0.19-0.59)	Prospective observational study
Feng 2017 (31)	36(21/15)	23(14/9)	SAE:52 ± 14 NE:57 ± 15	1,3 d	CLIA	1d:0.33(0.15,0.54) 3d:0.19(0.10,0.29)	Retrospective study
Guo 2021 (26)	30(17/13)	90(42/48)	SAE:57.61 ± 4.16 NE:56.91 ± 4.85	NA	ELISA	0.27 ± 0.06	NA
Hamed 2009 (25)	16(-) All patients: 40(24/16)	24(-)	51.75 ± 4.09 months	NA	ELISA	0. 24 ± 0.07	NA
Hu 2020 (47)	40(-)	40(-)	NA	1 h,3 d,5 d	ELISA	1h:0.50351 ± 0.41551 3d:0.36315 ± 0.2466 5d:0.0683 ± 0.02235	NA
Jiang 2021 (35)	26(18/8)	38(27/11)	SAE:42.45 ± 3.48 NE:41.2 ± 3.5	4 h	ELISA	0.16446 ± 0.02921	Retrospective study
Kang 2022 (40)	22(14/8)	25(14/11)	SAE:27.5(11.3-54.5) months NE:21.0(9.0-32.5) months	Within 24 h	ELISA	1.8 ± 0.2	Retrospective study
Li 2019 (42)	28(-) All patients: 100(56/44)	102(-)	58.6 ± 6.7	1 d	ELISA	0.92 ± 0.15	Retrospective study
Li 2022 (23)	21(13/8)	20(12/8)	SAE: 37 ± 5 NE: 38 ± 4	12,24,48 h	NA	12h:2.38 ± 0.21 24h:3.52 ± 0.16 48h:2.45 ± 0.18	Retrospective study
Liao 2017 (37)	28(20/8)	10(8/2)	SAE: 55 ± 13 NE: 51 ± 16	1 h,3 d	ELISA	1h: 0.5 ± 0.24 3d:0.58 ± 0.33	NA
Lu 2016 (27)	34(24/10)	52(33/19)	SAE: 59.15 ± 8.8 NE: 58.39 ± 8.14	NA	NA	1.21 ± 0.15	Retrospective study
Nguyen 2014 (33)	107 (-) All patients: 128 (83/45)	21(-)	65 ± 14	ICU admission,4 d	RIA	ICU admission:0.13 (0.06, 0.49) 4d:0.12 (0.08, 0.24)	Prospective observational study
Pfister 2008 (34)	All patients: 16(10/6)	NA	73.08 ± 8.78	NA	CLIA	NA	NA
Wang 2019 (48)	48(20/28)	12(7/5)	SAE: 55 ± 13 NE: 56 ± 7	1 h,3 d	ELISA	NA	NA
Wang 2020 (41)	30(17/13)	30(19/11)	SAE: 50.5 ± 2.3 NE: 50.8 ± 2.5	1 d	WB	0.28 ± 0.04	NA
Wang 2022 (49)	45(29/16)	35(22/13)	SAE:55.42 ± 14.63 NE: 56.37 ± 15.74	1 d,3 d	ELISA	1d:0.32(0.162, 0.579) 3d:0.18(0.116, 0.307)	NA
Wu 2020 (30)	59(38/21)	45(32/13)	SAE: 54 ± 15 NE: 58 ± 14	1,3d	ECLIA	1d:0.291(0.174–0.478) 3d:0.226(0.129–0.447)	Prospective and cohort study
Yan 2019 (28)	58(44/14)	94(60/34)	SAE: 55.8 ± 16.4 NE: 55.0 ± 18.3	Within 24 h	ELISA	0.5(0.3, 1.3)	Retrospective study

(Continued)

TABLE 1 Continued

study and year	SAE sample size (Males/ Female)	NE sample size (Males/ Female)	Age	Sample Collection time	Assay	SAE S100B cutoff (ng/mL)	Design
Yao 2014 (24)	48(33/15)	64(40/24)	SAE: 56 ± 16 NE: 52 ± 17	1 d	ECLIA	0.306 (0.157,0.880)	Prospective observational study
Yu 2020 (39)	90(49/41)	90(47/43)	SAE: 53.61 ± 12.74 NE: 52.89 ± 11.65	NA	ELISA	0.96 ± 0.14	NA
Yu 2022 (38)	67(37/30)	95(51/44)	SAE:70.3 ± 8.3 NE: 69.7 ± 8.6	NA	ICA	1.03 ± 0.32	Retrospective study
Zhang 2015 (36)	38(24/14)	36(22/14)	SAE:56 ± 17 NE: 54 ± 15	1 d	ELISA	1.81 ± 0.22	Prospective study
Zhang 2016 (32)	29(20/9)	28(13/15)	SAE:55.55 ± 12.72 NE: 56.21 ± 12.85	Within 24 h	ELISA	2.50 ± 0.49	Prospective observational study
Zhao 2016 (44)	56(30/26)	60(32/28)	SAE:47 ± 13.4 NE: 49 ± 13.2	ICU admission	ELISA	0.775 ± 0.356	NA
Zhao 2020 (43)	22 (–) All patients: 100(58/42)	78 (–)	65.3 ± 12.1	1 d	ELISA	0.92 ± 0.11	NA
Zhao 2022 (50)	28(16/12)	32(18/14)	SAE:55.89 ± 16.55 NE: 55.23 ± 16.71	NA	ELISA	0.99 ± 0.28	NA

model was applied. The pooled MD was 0.49 (95% CI = 0.37 ~ 0.60, $P < 0.00001$), suggesting that the serum S100B levels in SAE group were significantly higher than levels observed in NE group. Serum S100B may serve as a blood-based biomarker to assist clinical diagnosis and monitor the progression of SAE contusion, which may provide a simple and effective reference basis for clinical treatment decisions.

3.3.2 Comparison of serum S100B levels between favorable outcomes and unfavorable outcomes

Unfavorable outcome is defined as death or adverse neurological outcome assessment. There were total twelve studies reported serum S100B levels between favorable and unfavorable outcomes, included eight studies (24, 26, 28, 30, 34, 38, 39, 45) reported death as a primary outcome (MD, -0.35 [95% CI (-0.50)-(-0.20), Z =4.69, $P < 0.00001$]), and three studies (29, 42, 48) reported adverse neurological outcome as a primary outcome (MD, -0.34 [95% CI (-0.65)-(- 0. 03), Z =2.12, P =0.03]).The total pooled MD was -0.35 [95% CI (-0.50)-(-0.20), Z =4.60, $P < 0.00001$] which in Figure 5, showed that serum S100B levels in unfavorable outcomes group were significantly higher than in favorable outcomes group, so it may be predictive of poorer prognosis for septic patients to have higher serum levels of S100B. The results developed a new biomarker for predicting clinical status and malignant potential of sepsis that warrants further investigation as a predictive biomarker.

3.4 Subgroup analysis

Subgroup analysis was performed to explore the impact of different serum sample collection times after ICU admission (smaller than or equal to 24 h, greater than 24 h, and unclear time) and different S100B measurement assays (ELISA, CLIA/ECLIA, ICA/FICA, and other assays) which displayed in Figure 6 and Figure 7. The subgroup analysis results suggested that different serum sample collection times (collection time ≤ 24h:I^2 =100%, $P<0.00001$; collection time>24h:I^2 =100%, $P<0.00001$; unclear collection time: I^2 =96%, $P<0.00001$) and measurement assay (ELISA: I^2 =98%, $P<0.00001$; CLIA/ECLIA: I^2 =62%, P=0.02; ICA/FICA: I^2 =0%, P=1.00; Other assays: I^2 =100%, $P<0.00001$) were not sources of heterogeneity. Furthermore, the combined results of subgroup analyses were statistically significant and consistent with the overall combined results, showing serum S100B levels in the SAE group were significantly higher than levels in NE control group whether different serum sample collection time points (MD, 0.49 [95% CI (0.38)-(0.61), Z =8.35, $P < 0.00001$]) or different measure assays (MD, 0.49 [95% CI (0.37)-(0.60), Z =8.29, $P < 0.00001$]) were used. Specific range of serum S100B concentrations in SAE are discussed in the Discussion section.

3.5 Publication bias and sensitivity analysis

We used Egger's and Begg's regression tests and funneled plots to assess the potential publication bias in included studies. When valuated the association between serum S100B levels and SAE, Egger's (t = 1.49, P = 0.1361) and Begg's tests (Z = 2.45, P = 0.0144) of the effective rate indicated publication bias in this included literature. As the association between serum S100B levels and outcomes of septic patients, Egger's test (t = -1.46, P = 0.1444) and Begg's test (Z = -0.55, P = 1.417) of the effective rate also indicated publication bias. Evidence of publication bias was obtained through the visual distribution of funnel plot (Figures 8A, C), and the results of the sensitivity analysis indicated that no individual study dominated the results except Yan 2019, and the findings of this meta-analysis

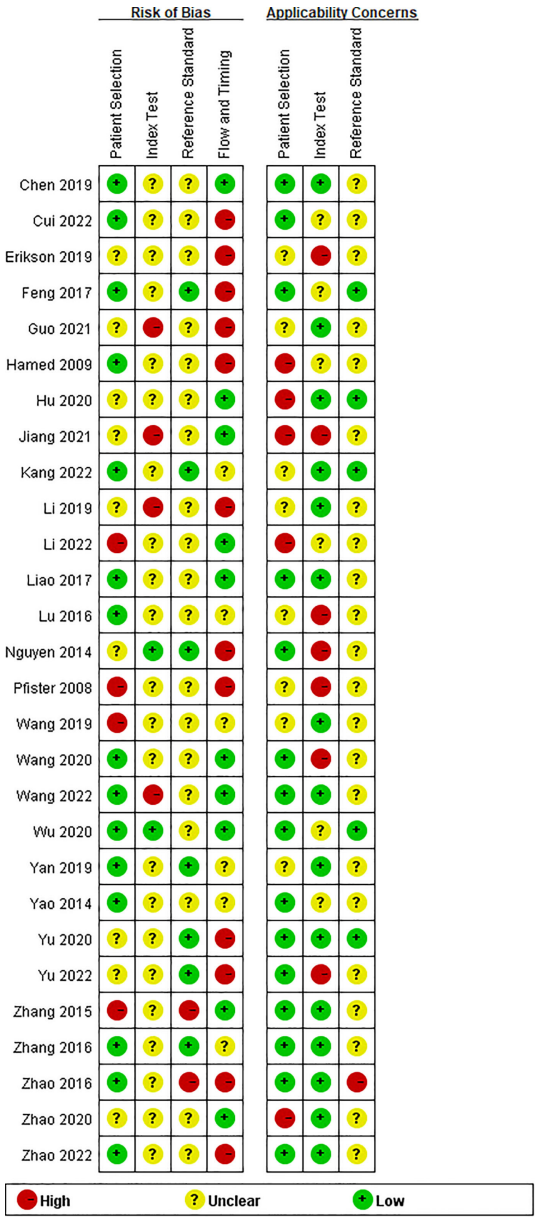

FIGURE 2
Risk of bias and applicability concerns summary: review authors' judgements about each domain for each included study.

were statistically stable (Figures 8B, D), but this had to be interpreted with caution when explain prognostic value of S100B due to Yan 2019 had a stronger impact on the overall effect size which in Figure 8D.

4 Discussion

This meta-analysis aimed to explore the diagnostic and prognostic value of S100B in SAE patients. SAE are frequently encountered in critically ill patients in the ICU and up to 70% of patients with severe systemic infection. Clinically, SAE is characterized by behavioral, cognitive, awakening, and consciousness changes, and a considerable proportion of patients have long-term cognitive dysfunction, which seriously affects daily life and increases the risk of death (51). However, in the absence of an unambiguous definition of SAE and highly accurate diagnostic tools, ICU physicians rely on their own clinical skill set and experience to diagnose SAE.

Our findings demonstrated that serum S100B levels in the SAE group were significantly higher than those observed in the NE group, and serum S100B levels in the favorable outcome group were significantly lower than those in the unfavorable outcome group. The combination of serum S100B and Electroencephalogram (EEG), Computed Tomography (CT), Magnetic resonance imaging (MRI), Transcranial Doppler (TCD) can further confirm the diagnosis and prognosis as well as guide treatment.

A prospective study found that serum S100B is a better biomarker than neuron-specific enolase (NSE) in SAE. GCS scores were related more closely to S100B than NSE, and the area under the curve (AUC) for S100B for diagnosing SAE (*AUC*= 0.824 vs. *AUC*= 0.664) and predicting hospital mortality (*AUC*= 0.730 vs. *AUC*= 0.590) was larger than that for NSE (24). Pfister et al. found a significant association between elevated S100B and sepsis-associated delirium (34); Cohen et al. found S100B can be useful to determine the prognosis for persistent cognitive dysfunction, which defined as the state of altered mentation (AMS) and long-term survival among sepsis patients (52); Calsavara et al. suggested that serum S100B level may associate with anxiety, depression and post-traumatic stress disorder (PTSD) symptoms in sepsis survivors (53). From a clinical perspective, serum S100B provide helpful information for the clinical decision-making and may be a functional biomarker for monitoring clinical conditions for SAE diagnosis and prognosis.

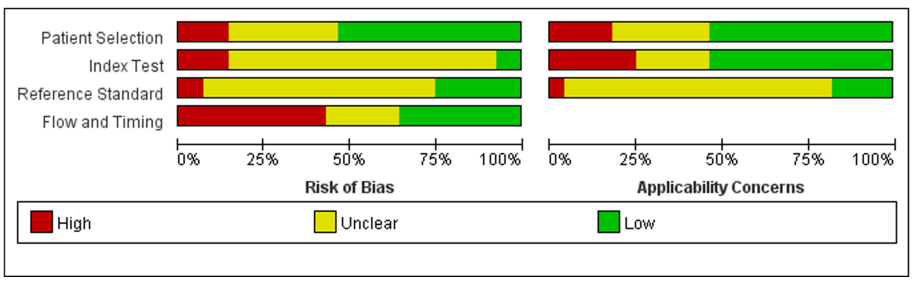

FIGURE 3
Risk of bias and applicability concerns graph: review authors' judgements about each domain presented as percentages across included studies.

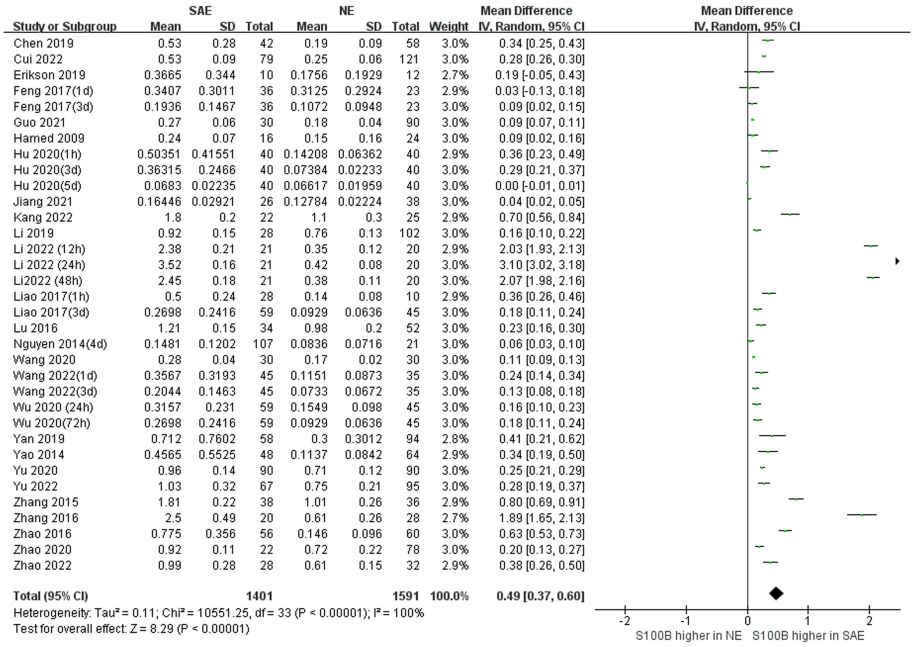

FIGURE 4
Meta-Analysis forest plot: association between serum S100B level and patients with SAE.

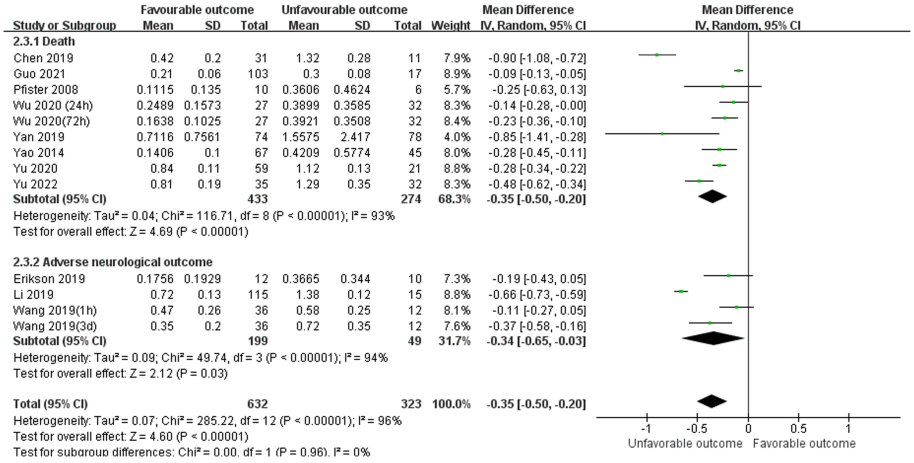

FIGURE 5
Meta-Analysis forest plot: MDs of serum S100B levels between Favorable outcomes and Unfavorable outcomes.

The question from this study should be considered as the range of serum S100B concentrations employed has varied widely across studies, due to differential serum sample collection time or measurement assay or types of patients enrolled in the studies. Serum collection time in our meta-analysis included obscure time points such as ICU admission or within 24 h, and well-defined time points such as days 1, 3, and 7. Subgroup analysis found serum S100B levels which collection time ≤ 24h was higher than > 24h (MD, 0.66 [95% CI (0.41)-(0.91), Z = 5.21, $P < 0.00001$] vs. 0.40 [MD, 95% CI (0.13)-(0.67), Z =2.90, $P < 0.004$]). Thus, S100B may be an early biomarker for SAE which consistent with our previous clinical studies and animal experiments by our group. And patients admitted to the ICU are unpredictable, and emergency and serum collection time may not be sufficiently precise, standardization and generality of its test results remain to be further standardized.

We also explored two special population: Child and burn patients, there are three studies (25, 40, 47) used child participants, and two studies (23, 50) used burn participants. studies from children (MD, 0.28 [95% CI (0.08) -(0.48), Z =2.77, $P = 0.006$]), showing that serum S100B levels in SAE group were significantly higher than those in the NE group whether in adults or children, so there was no age limit for the diagnostic value of serum S100B in SAE (Figure S1). The heterogeneity test depicted significant differences among studies from burn ($Chi^2 = 1547.26$, $I^2 = 100\%$, $P < 0.00001$), so the random-effects model was applied with a pooled (MD, 1.96 [95% CI (0.92) -(2.99), Z =3.71, P =

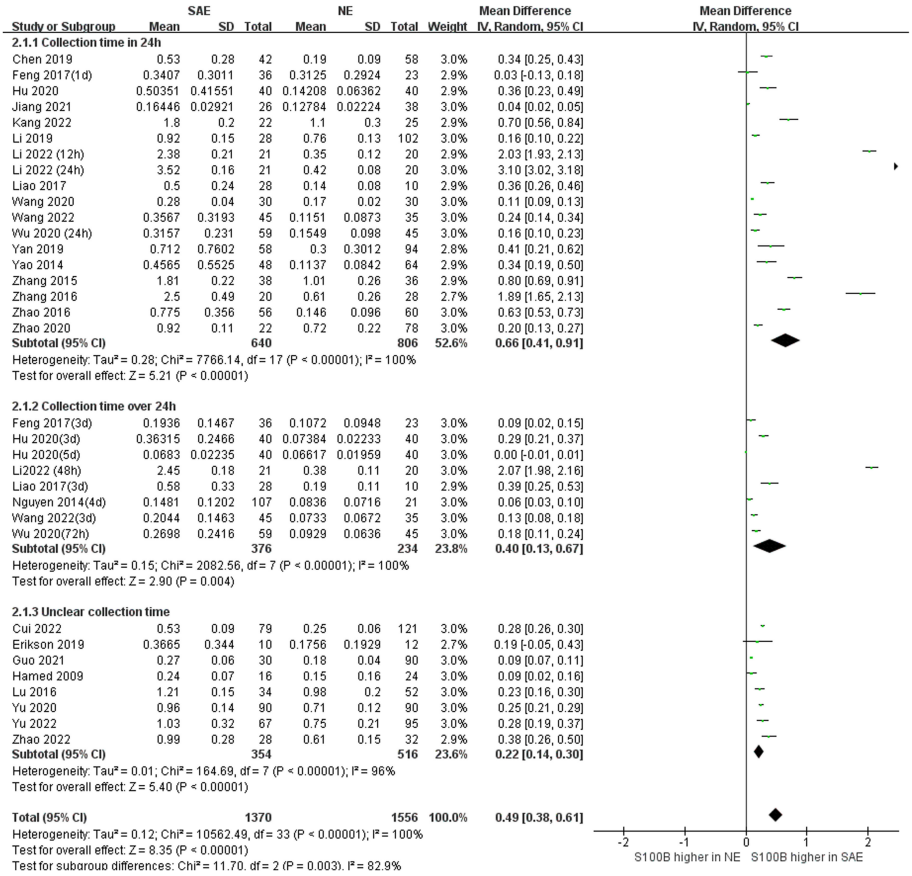

FIGURE 6
Meta-Analysis forest plot: association between serum S100B level and patients with SAE in different serum sample collection time after ICU admission.

0.0002]), showing that serum S100B levels in SAE patients with burn were also higher than those in NE patients with burn (Figure S2), and its levels were significantly above average level (1.96 [95% CI (0.92)-(2.99), Z =3.71, $P < 0.0002$] vs. 0.49 [95% CI (0.37)-(0.60), Z =8.29, $P < 0.0002$]). It is possible that burn sepsis is quite different from mainstream sepsis because of special hypermetabolic reactions and abnormal immune status. Burn stress leads to increased body temperature and heart rate, and immune disorders lead to increased indicators of infection, which is easy to misdiagnose as sepsis. Its pathogenesis is complex, and the interaction of multiple factors may lead to its occurrence (54, 55).

Our results suggest that elevated serum S100B levels are associated with poor prognosis, which also indicates that S100B can be considered an interesting factor for the prevention and treatment of sepsis. Therapies targeting S100B may be promising pharmacological targets to prevent SAE, which may assist in choosing the best combined or primary treatment method. Arundic acid can inhibit the enlargement of brain damage by preventing inflammatory changes caused by the overproduction of S100B protein in astrocytes (56, 57). Moreover, sepsis animal model induced by cecal ligation and perforation (CLP) demonstrated that 10 μg/kg of monoclonal antibody (Anti-S100B) administered intracerebroventricularly could recover habitual memory in the open field task and improve cognitive function (58). The antiprotozoal drug pentamidine can block the S100B/RAGE/NF-κB signaling pathway and reduce neuroinflammation in CLP mouse hippocampus (59), and the mitochondrial division inhibitor Mdivi-1 can inhibit S100B release into plasma in a lipopolysaccharide-induced SAE animal model (60). At present, related antagonistic S100B studies are mostly conducted in animal models and relatively few in clinical applications, and more clinical studies are still needed to prove its therapeutic value for SAE patients in the future.

However, the diagnostic and prognostic role of S100B in SAE is still controversial, and different studies have resulted in large gaps and even opposite conclusions (11, 61), Vuceljic et al. depicted that S100B protein is not a good early predictor of severe sepsis outcomes (62). Weigand et al. suggested no significant difference in serum S100 was observed between sepsis survivors and non-survivors (63). Ehler et al. demonstrated that cerebrospinal fluid S100B levels were not significantly different between sepsis patients and controls (64). Ripper et al. found elevated serum S100B level in patients with delirium but also in septic patients without delirium; this increase was not associated with mortality (65). Considerable variations can be found according to different diagnostic criteria of SAE (66–68), and studies in different eras had different criteria, which may influence the accuracy of the data that we collected. The combination of multiple biomarkers may provide a more objective and reliable guide for the diagnosis and prognosis of SAE, which may be confirmed in further clinical studies.

The specific molecular mechanisms underlying the activity of S100B in SAE have not been elucidated, and it is still unknown whether S100B is the initiating factor or effector of SAE, which means that S100B increased, causing SAE, or SAE causing S100B to increase. Zhang et al. found that S100B regulates mitochondrial dynamics

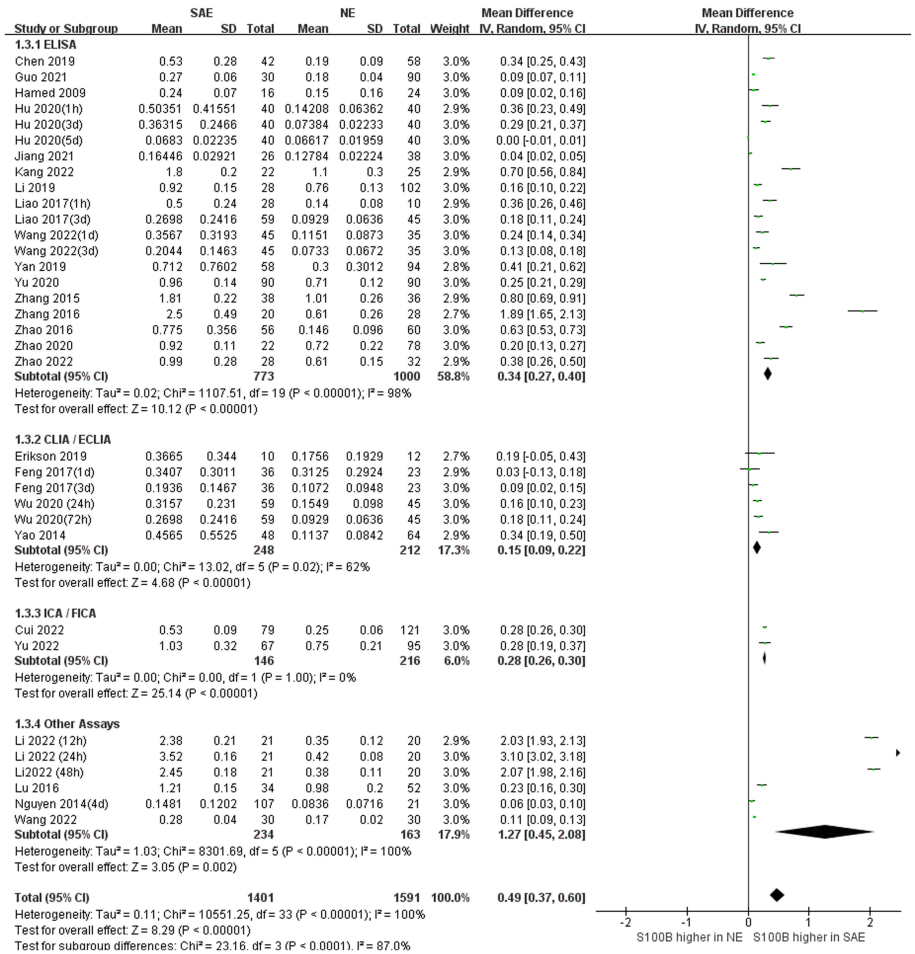

FIGURE 7
Meta-Analysis forest plot: association between serum S100B level and patients with SAE in different measure assay.

through the RAGE/ceramide pathway, as well as acute brain injury and long-term cognitive impairment during SAE (18). Tsoporis et al. suggested that interaction of RAGE and its ligand S100B after myocardial infarction may play a role in myocyte apoptosis by activating ERK1/2 and p53 signaling (14). Therefore, the role of S100B requires further investigation to produce a clear conclusion on the effects of S100B on SAE.

Except for routine serum or plasma S100B testing, using saliva or urine to detect S100B is simpler and faster, bringing hope for the large-scale promotion of S100B screening. S100B can be extracted simultaneously from serum, urine, cerebrospinal fluid and saliva; two studies revealed that measuring salivary (69) or urine (70) S100B could in place of serum S100B in the diagnosis of TBI. This could avoid the risk of infection from blood tests and reduce the time or equipment required to separate blood components. Larger and confirmatory trials are needed to define salivary or urine biomarker kinetics concerning SAE.

In addition to its role in SAE, S100B has been associated with a variety of neurocritical diseases, such as Traumatic Brain Injury (TBI) (71), aneurysmal subarachnoid hemorrhage (72), acute ischemic stroke (73), and neonatal hypoxic-ischemic encephalopathy (74). In the current COVID-19 pandemic era, most SARS-Coronavirus-2-infected patients admitted to the ICU showed common features of sepsis disease, such as the overwhelmed systemic inflammatory response (75, 76), and a recent prospective study demonstrated that serum S100B of Covid patients is correlated with disease severity, and increased serum levels of S100B correlate with the severity of Covid-19 and inflammatory processes (77). Therefore, S100B may serve as an important biomarker for neurocritical care disease detection and longitudinal monitoring in neurocritical care patients. S100B has been described as the brain's CRP (C-reactive protein) due to its potential role as a neurological screening tool or biomarker of CNS injury, analogous to the role of CRP as a marker of systemic inflammation (78).

This meta-analysis has several strengths. First, this is the first systematic review and meta-analysis to evaluate the association between serum S100B levels and the risk of SAE and unfavorable prognosis in septic patients. Additionally, the sensitivity analysis results revealed that the pooled effect model was robust and reliable. There are also a few limitations to this meta-analysis should be taken care. First, our meta-analysis has potential publication bias, which may overstate the diagnosis and prognosis value of S100B. Second, the heterogeneity in our studies is high due to we cannot avoid confounding factors such as age, gender, sedation, hemodynamic status and primary diseases affecting the results. Third, although we aimed to comprehensively search the relevant articles, some studies may not have been published due to negative outcomes, and we do not have

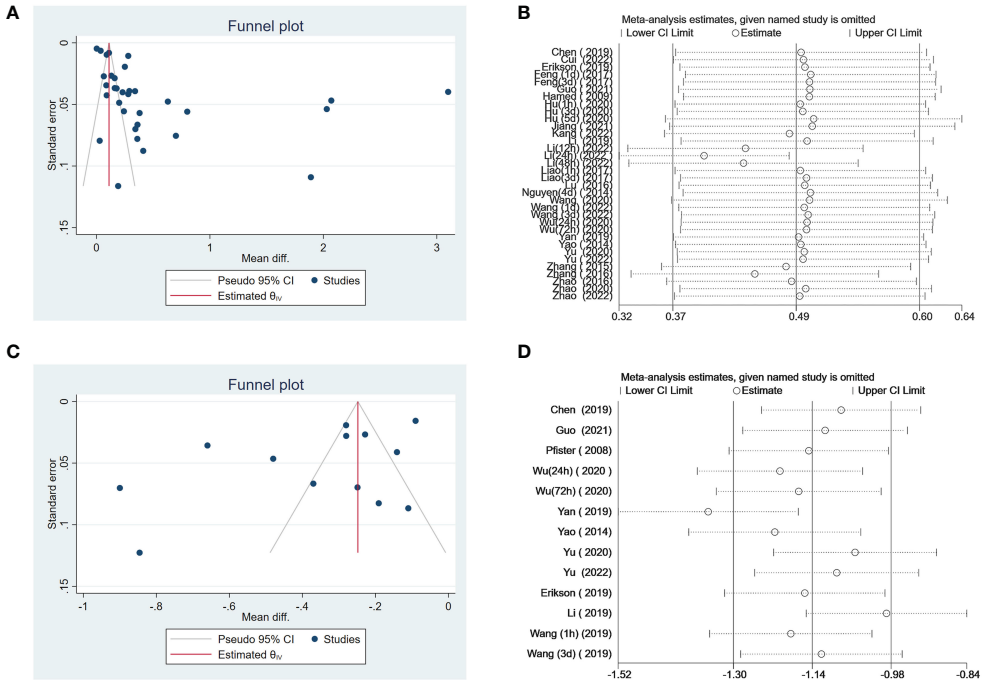

FIGURE 8
Funnel plot showed that it was asymmetry, suggesting potential publication bias may exist in association between serum S100B level and SAE **(A)**, association between serum S100B level and outcomes of septic patients **(C)**. Effect of individual studies on the pooled MD for the effect of association between serum S100B level and SAE **(B)**, and the effect of association between serum S100B level and outcomes of septic patients **(D)**.

access to all the information for proper stratification analysis. In order to obtain better evidence, more high quality, prospective, multicenter randomized controlled studies with large sample sizes are needed.

5 Conclusion

Our Meta-analysis suggests that higher serum S100B level in septic patients is moderately associated with SAE and unfavorable outcomes (The outcomes here mainly refer to the death). Serum S100B may be a potential diagnostic and prognostic biomarker of SAE. Brian is an important target organ during sepsis, and our results provide ICU physicians with the most current information to predict which patients are at risk of SAE and take corresponding intervention measures to reduce morbidity and ameliorate neurological outcomes.

Data availability statement

The original contributions presented in the study are included in the article/Supplementary Material. Further inquiries can be directed to the corresponding author.

Author contributions

JH, SX, WL and LZ contributed to conception and design of the study. JH organized the database. JH and SX assessed the quality of the study. SX and WL performed the statistical analysis. JH wrote the first draft of the manuscript. JH and LZ wrote sections of the manuscript. All authors contributed to manuscript and approved the submitted version.

Funding

This work was supported by the National Natural Science Foundation of China (82172145), the National Natural Science Foundation of China (81873956).

Conflict of interest

The authors declare that the research was conducted in the absence of any commercial or financial relationships that could be construed as a potential conflict of interest.

Publisher's note

Supplementary material

The Supplementary Material for this article can be found online at: https://www.frontiersin.org/articles/10.3389/fimmu.2023.1102126/full#supplementary-material

References

1. Rudd KE, Johnson SC, Agesa KM, Shackelford KA, Tsoi D, Kievlan DR, et al. Global, regional, and national sepsis incidence and mortality, 1990-2017: analysis for the global burden of disease study. *Lancet (London England)* (2020) 395(10219):200–11. doi: 10.1016/S0140-6736(19)32989-7

2. Reinhart K, Daniels R, Kissoon N, Machado FR, Schachter RD, Finfer S. Recognizing sepsis as a global health priority - a WHO resolution. *New Engl J Med* (2017) 377(5):414–7. doi: 10.1056/NEJMp1707170

3. Gofton TE, Young GB. Sepsis-associated encephalopathy. *Nat Rev Neurol* (2012) 8 (10):557–66. doi: 10.1038/nrneurol.2012.183

4. Mosley JD, Feng Q, Wells QS, Van Driest SL, Shaffer CM, Edwards TL, et al. A study paradigm integrating prospective epidemiologic cohorts and electronic health records to identify disease biomarkers. *Nat Commun* (2018) 9(1):3522. doi: 10.1038/s41467-018-05624-4

5. Barichello T, Generoso JS, Singer M, Dal-Pizzol F. Biomarkers for sepsis: more than just fever and leukocytosis-a narrative review. *Crit Care* (2022) 26(1):14. doi: 10.1186/s13054-021-03862-5

6. Osca-Verdegal R, Beltrán-García J, Pallardó FV, García-Giménez JL. Role of microRNAs as biomarkers in sepsis-associated encephalopathy. *Mol Neurobiol* (2021) 58(9):4682–93. doi: 10.1007/s12035-021-02445-3

7. Zhao GJ, Li D, Zhao Q, Lian J, Hu TT, Hong GL, et al. Prognostic value of plasma tight-junction proteins for sepsis in emergency department: An observational study. *Shock* (2016) 45(3):326–32. doi: 10.1097/SHK.0000000000000524

8. Chavan SS, Huerta PT, Robbiati S, Valdes-Ferrer SI, Ochani M, Dancho M, et al. HMGB1 mediates cognitive impairment in sepsis survivors. *Mol Med* (2012) 18(1):930–7. doi: 10.2119/molmed.2012.00195

9. Spapen H, Nguyen DN, Troubleyn J, Huyghens L, Schiettecatte J. Drotrecogin alfa (activated) may attenuate severe sepsis-associated encephalopathy in clinical septic shock. *Crit Care* (2010) 14(2):R54. doi: 10.1186/cc8947

10. Hsu AA, Fenton K, Weinstein S, Carpenter J, Dalton H, Bell MJ. Neurological injury markers in children with septic shock. *Pediatr Crit Care Me* (2008) 9(3):245–51. doi: 10.1097/PCC.0b013e3181727b22

11. Nguyen DN, Spapen H, Su FH, Schiettecatte J, Shi L, Hachimi-Idrissi S, et al. Elevated serum levels of s-1000 protein and neuron-specific enolase are associated with brain injury in patients with severe sepsis and septic shock. *Crit Care Med* (2006) 34 (7):1967–74. doi: 10.1097/01.CCM.0000217218.51381.49

12. Donato R. S100: a multigenic family of calcium-modulated proteins of the EF-hand type with intracellular and extracellular functional roles. *Int J Biochem Cell Biol* (2001) 33 (7):637–68. doi: 10.1016/S1357-2725(01)00046-2

13. Baudier J, Deloulme JC, Shaw GS. The Zn(2+) and Ca(2+) -binding S100B and S100A1 proteins: beyond the myths. *Biol Rev Camb Philos Soc* (2020) 95(3):738–58. doi: 10.1111/brv.12585

14. Tsoporis JN, Izhar S, Leong-Poi H, Desjardins JF, Huttunen HJ, Parker TG. S100B interaction with the receptor for advanced glycation end products (RAGE): a novel receptor-mediated mechanism for myocyte apoptosis postinfarction. *Circ Res* (2010) 106 (1):93–101. doi: 10.1161/CIRCRESAHA.109.195834

15. Langeh U, Singh S. Targeting S100B protein as a surrogate biomarker and its role in various neurological disorders. *Curr Neuropharmacol* (2021) 19(2):265–77. doi: 10.2174/18756190MTA44NjEs3

16. Sathe K, Maetzler W, Lang JD, Mounsey RB, Fleckenstein C, Martin HL, et al. S100B is increased in parkinson's disease and ablation protects against MPTP-induced toxicity through the RAGE and TNF-α pathway. *Brain J Neurol* (2012) 135(Pt 11):3336–47. doi: 10.1093/brain/aws250

17. Lipcsey M, Olovsson M, Larsson E, Einarsson R, Qadhr GA, Sjölin J, et al. The brain is a source of S100B increase during endotoxemia in the pig. *Anesth Analg* (2010) 110(1):174–80. doi: 10.1213/ANE.0b013e3181c0724a

18. Zhang L, Jiang Y, Deng S, Mo Y, Huang Y, Li W, et al. S100B/RAGE/Ceramide signaling pathway is involved in sepsis-associated encephalopathy. *Life Sci* (2021) 277:119490. doi: 10.1016/j.lfs.2021.119490

19. Whiting PF, Rutjes AW, Westwood ME, Mallett S, Deeks JJ, Reitsma JB, et al. QUADAS-2: a revised tool for the quality assessment of diagnostic accuracy studies. *Ann Internal Med* (2011) 155(8):529–36. doi: 10.7326/0003-4819-155-8-201110180-00009

20. Hozo SP, Djulbegovic B, Hozo I. Estimating the mean and variance from the median, range, and the size of a sample. *BMC Med Res methodol* (2005) 5:13. doi: 10.1186/1471-2288-5-13

21. Wan X, Wang W, Liu J, Tong T. Estimating the sample mean and standard deviation from the sample size, median, range and/or interquartile range. *BMC Med Res methodol* (2014) 14:135. doi: 10.1186/1471-2288-14-135

22. Higgins JP, Thompson SG, Deeks JJ, Altman DG. Measuring inconsistency in meta-analyses. *BMJ (Clinical Res ed)* (2003) 327(7414):557–60. doi: 10.1136/bmj.327.7414.557

23. Li XL, Xie JF, Ye XY, Li Y, Li YG, Feng K, et al. [Value of cerebral hypoxic-ischemic injury markers in the early diagnosis of sepsis associated encephalopathy in burn patients with sepsis]. *Zhonghua Shao Shang Za Zhi* (2022) 38(1):21–8. doi: 10.3760/cma.j.cn501120-20211006-00346

24. Yao B, Zhang LN, Ai YH, Liu ZY, Huang L. Serum S100B is a better biomarker than neuron-specific enolase for sepsis-associated encephalopathy and determining its prognosis: a prospective and observational study. *Neurochem Res* (2014) 39(7):1263–9. doi: 10.1007/s11064-014-1308-0

25. Hamed SA, Hamed EA, Abdella MM. Septic encephalopathy: relationship to serum and cerebrospinal fluid levels of adhesion molecules, lipid peroxides and s-100B protein. *Neuropediatrics* (2009) 40(2):66–72. doi: 10.1055/s-0029-1231054

26. Guo W, Li Y, Li Q. Relationship between miR-29a levels in the peripheral blood and sepsis-related encephalopathy. *Am J Trans Res* (2021) 13(7):7715–22.

27. Lu CX, Qiu T, Tong HS, Liu ZF, Su L, Cheng B. Peripheral T-lymphocyte and natural killer cell population imbalance is associated with septic encephalopathy in patients with severe sepsis. *Exp Ther Med* (2016) 11(3):1077–84. doi: 10.3892/etm.2016.3000

28. Yan S, Gao M, Chen H, Jin X, Yang M. [Expression level of glial fibrillary acidic protein and its clinical significance in patients with sepsis-associated encephalopathy]. *Zhong Nan Da Xue Xue Bao Yi Xue Ban* (2019) 44(10):1137–42. doi: 10.11817/j.issn.1672-7347.2019.190180

29. Erikson K, Ala-Kokko TI, Koskenkari J, Liisanantti JH, Kamakura R, Herzig KH, et al. Elevated serum s-100 beta in patients with septic shock is associated with delirium. *Acta Anaesth Scand* (2019) 63(1):69–73. doi: 10.1111/aas.13228

30. Wu L, Feng Q, Ai ML, Deng SY, Liu ZY, Huang L, et al. The dynamic change of serum S100B levels from day 1 to day 3 is more associated with sepsis-associated encephalopathy. *Sci Rep* (2020) 10(1):7718. doi: 10.1038/s41598-020-64200-3

31. Feng Q, Wu L, Ai YH, Deng SY, Ai ML, Huang L, et al. [The diagnostic value of neuron-specific enolase, central nervous system specific protein and interleukin-6 in sepsis-associated encephalopathy]. *Zhonghua Nei Ke Za Zhi* (2017) 56(10):747–51. doi: 10.3760/cma.j.issn,0578-1426,2017.10.008

32. Zhang LN, Wang XH, Wu L, Huang L, Zhao CG, Peng QY, et al. Diagnostic and predictive levels of calcium-binding protein A8 and tumor necrosis factor receptor-associated factor 6 in sepsis-associated encephalopathy: A prospective observational study. *Chin Med J (Engl)* (2016) 129(14):1674–81. doi: 10.4103/0366-6999.185860

33. Nguyen DN, Huyghens L, Zhang H, Schiettecatte J, Smitz J, Vincent JL. Cortisol is an associated-risk factor of brain dysfunction in patients with severe sepsis and septic shock. *BioMed Res Int* (2014) 2014:712742. doi: 10.1155/2014/712742

34. Pfister D, Siegemund M, Dell-Kuster S, Smielewski P, Rüegg S, Strebel SP, et al. Cerebral perfusion in sepsis-associated delirium. *Crit Care* (2008) 12(3):R63. doi: 10.1186/cc6891

35. JIang GQ ZX. The value of NT-proBNP,S100Band 5-HT in predicting sepsis-associated encephalopathy. *Int J Lab Med* (2021) 42(22):2786–90. doi: 10.3969/j.issn.1673-4130.2021.22.021

36. L Z. The value of early stage BIS monitoring in the assessment of sepsis. *Chin J Crit Care Med* (2015) 35(11):982–5. doi: 10.3969/j.issn.1002-1949.2015.11.005

37. GQ L. The relationship between serum and cerebrospinalfluid S100B concentration and electroencephalograph abnorm alities in patients with sepsis encephalopathy. *China Modern Doctor* (2017) 55(08):8–10.

38. Yu DY LX, Ren PX, Liu HF, Li ZX. Study on the value of serum circulating netrin-1 expression level in predicting the risk of brain injury in elderly patients with sepsis. *J Modern Lab Med* (2022) 37(02):76–9+114. doi: 10.3969/j.issn.1671-7414.2022.02.016

39. Yu GL CK, Lou MJ, Liu HF, Li ZX. Serum ghrelin level and severity of brain injury in patients with sepsis-related encephalopathy. *Chin J Nosocomiol* (2020) 30(11):1655–8. doi: 10.11816/cn.ni.2020-191748

40. Song YL, Zhou X, Cao JS, He J, Xiao ZH. The relationship between serum insulin level and prognosis in children with sepsis associated encephalopathy. *J Clin Pediatrics* (2022) 40(03):218–23. doi: 10.12372/jcp.2022.21e1179

41. Wang HY. Observation of serum S100B, NSE and TCD in patients with sepsis-related encephalopathy. *Chin Foreign Med Res* (2020) 18(31):61–3. doi: 10.14033/j.cnki.cfmr.2020.31.024

42. Li K LB, Duan Y, Weng QY. Influence of serum NSE, S100B and IL-6 in the incidence of sepsis related encephalopathy and prognosis of patients with sepsis. *Clin Res Practice* (2019) 4(01):81–2. doi: 10.14033/j.cnki.cfmr.2020.31.024

43. Zhang J, Li YG, Ye XY, Lou JH, Xia CD. Correlation analysis between serum NSE, S100B,; IL-6 and sepsis associated encephalopathy in burn patients. *Chin J Burns Wounds Surface* (2020) 32(06):406–8. doi: 10.3969/j.issn.1001-0726.2020.06.009

44. Zhao LS ZL, Yang GH. Continuous BIS monitoring for patients with sepsis-associated encephalopathy. *China J Modern Med* (2016) 26(06):123–6. doi: 10.3969/j.issn.1005-8982.2016.06.026

45. Wang HJ, Chen CH, Zhuang HY, Wu L. Clinical value of s-100β protein in serum and cerebrospinal fluid in septic encephalopathy in intensive care unit. *J Qiqihar Med Univ* (2019) 40(08):936–8. doi: 10.3969/j.issn.1002-1256.2019.08.005

46. Cui J WJ, Zhao JJ, Yao L. Clinical significance of prognostic serum m ark er exp ression in old er adult patients with sepsis-associated encephalopathy. *Chin J Primary Med Pharmacy* (2022) 29(03):340–5. doi: 10.3760/cma.j.issn.1008-6706.2022.03.005

47. Hu D QG, Liu KX, Zhu XX, Liu XM. Clinical application of GFAP, MBP and S100Bp protein in early identification and severity evaluation of sepsis associated encephalopathy. *J Xuzhou Med University* (2020) 40(09):691–4. doi: 10.3969/j.issn.2096-3882.2020.09.016

48. Wang P LF, Liao GQ. Changes of S100B concentration of serum and its clinical significance in patients with sepsis associated encephalopathy. *Modern Med J China.* (2019) 21(06):22–4. doi: 10.3760/cma.j.issn.1008-6706.2022.03.005

49. JJ W. Changes and significance of serum s-100β, NSE and TCD in patients with sepsis associated encephalopathy. *Med Innovation China.* (2022) 19(05):23–6. doi: 10.3760/cma.j.issn.1008-6706.2022.03.005

50. Zhao CG. Analysis of the risk factors of sepsis-associated encephalopathy in the patients with sepsis. *J Guizhou Med Univ* (2022) 47(03):358–62. doi: 10.19367/j.cnki.2096-8388.2022.03.020

51. Manabe T, Heneka MT. Cerebral dysfunctions caused by sepsis during ageing. *Nat Rev Immunol* (2021) 22(7):444–58. doi: 10.1038/s41577-021-00643-7

52. Cohen SA, Shaw M, Yang Z, Tompkins S, Gul SS, Maldonado NG, et al. 202 neural biomarker panel for sepsis-associated encephalopathy and sepsis outcomes. *Ann Emergency Med* (2019) 74(4):S80. doi: 10.1016/j.annemergmed.2019.08.370

53. Calsavara AJ, Costa PA, Nobre V, Teixeira AL. Prevalence and risk factors for post-traumatic stress, anxiety, and depression in sepsis survivors after ICU discharge. *Braz J Psychiatry* (2021) 43(3):269–76. doi: 10.1590/1516-4446-2020-0986

54. Stanojcic M, Vinaik R, Jeschke MG. Status and challenges of predicting and diagnosing sepsis in burn patients. *Surg infections* (2018) 19(2):168–75. doi: 10.1089/sur.2017.288

55. Greenhalgh DG, Saffle JR, Holmes J, Gamelli RL, Palmieri TL, Horton JW, et al. American Burn association consensus conference to define sepsis and infection in burns. *J burn Care Res* (2007) 28(6):776–90. doi: 10.1097/BCR.0b013e3181599bc9

56. Higashino H, Niwa A, Satou T, Ohta Y, Hashimoto S, Tabuchi M, et al. Immunohistochemical analysis of brain lesions using S100B and glial fibrillary acidic protein antibodies in arundic acid- (ONO-2506) treated stroke-prone spontaneously hypertensive rats. *J Neural Transm (Vienna Austria 1996).* (2009) 116(10):1209–19. doi: 10.1007/s00702-009-0278-x

57. Vizuete AFK, de Lima Cordeiro J, Neves JD, Seady M, Grun LK, Barbé-Tuana FM, et al. Arundic acid (ONO-2526) inhibits stimulated-S100B secretion in inflammatory conditions. *Neurosci Lett* (2021) 751:135776. doi: 10.1016/j.neulet.2021.135776

58. Rocha M, Vieira A, Michels M, Borges H, Goulart A, Fernandes F, et al. Effects of S100B neutralization on the long-term cognitive impairment and neuroinflammatory response in an animal model of sepsis. *Neurochem Int* (2021) 142:104906. doi: 10.1016/j.neuint.2020.104906

59. Huang L, Zhang L, Liu Z, Zhao S, Xu D, Li L, et al. Pentamidine protects mice from cecal ligation and puncture-induced brain damage *via* inhibiting S100B/RAGE/NF-κB. *Biochem Biophys Res Commun* (2019) 517(2):221–6. doi: 10.1016/j.bbrc.2019.07.045

60. Deng S, Ai Y, Gong H, Feng Q, Li X, Chen C, et al. Mitochondrial dynamics and protective effects of a mitochondrial division inhibitor, mdivi-1, in lipopolysaccharide-induced brain damage. *Biochem Biophys Res Commun* (2018) 496(3):865–71. doi: 10.1016/j.bbrc.2018.01.136

61. Piazza O, Russo E, Cotena S, Esposito G, Tufano R. Elevated S100B levels do not correlate with the severity of encephalopathy during sepsis. *Br J Anaesthesia* (2007) 99 (4):518–21. doi: 10.1093/bja/aem201

62. Vuceljic M, Surbatovic M, Vujanic S. S-100 beta PROTEIN IN PATIENTS WITH SEVERE SEPSIS. *J Med Biochem* (2009) 28(1):46–9. doi: 10.2478/v10011-008-0033-0

63. Weigand MA, Volkmann M, Schmidt H, Martin E, Bohrer H, Bardenheuer HJ. Neuron-specific enolase as a marker of fatal outcome in patients with severe sepsis or septic shock. *Anesthesiol* (2000) 92(3):905–7. doi: 10.1097/00000542-200003000-00057

64. Ehler J, Saller T, Wittstock M, Rommer PS, Chappell D, Zwissler B, et al. Diagnostic value of NT-proCNP compared to NSE and S100B in cerebrospinal fluid and plasma of patients with sepsis-associated encephalopathy. *Neurosci Lett* (2019) 692:167–73. doi: 10.1016/j.neulet.2018.11.014

65. Jorge-Ripper C, Alemán MR, Ros R, Aguilera S, González-Reimers E, Espelosín E, et al. Prognostic value of acute delirium recovery in older adults. *Geriatr Gerontol Int* (2017) 17(8):1161–7. doi: 10.1111/ggi.12842

66. Sprung CL, Peduzzi PN, Shatney CH, Schein RM, Wilson MF, Sheagren JN, et al. Impact of encephalopathy on mortality in the sepsis syndrome. The veterans administration systemic sepsis cooperative study group. *Crit Care Med* (1990) 18 (8):801–6. doi: 10.1097/00003246-199008000-00001

67. Eidelman LA, Putterman D, Putterman C, Sprung CL. The spectrum of septic encephalopathy. definitions, etiologies, and mortalities. *Jama* (1996) 275(6):470–3. doi: 10.1001/jama.1996.03530300054040

68. Zauner C, Gendo A, Kramer L, Funk GC, Bauer E, Schenk P, et al. Impaired subcortical and cortical sensory evoked potential pathways in septic patients. *Crit Care Med* (2002) 30(5):1136–9. doi: 10.1097/00003246-200205000-00030

69. Janigro D, Kawata K, Silverman E, Marchi N, Diaz-Arrastia R. Is salivary S100B a biomarker of traumatic brain injury? a pilot study. *Front Neurol* (2020) 11:528. doi: 10.3389/fneur.2020.00528

70. Vedin T, Karlsson M, Edelhamre M, Bergenheim M, Larsson PA. Features of urine S100B and its ability to rule out intracranial hemorrhage in patients with head trauma: a prospective trial. *Eur J Trauma Emerg Surg* (2021) 47(5):1467–75. doi: 10.1007/s00068-019-01201-6

71. Studer M, Goeggel Simonetti B, Heinks T, Steinlin M, Leichtle A, Berger S, et al. Acute S100B in serum is associated with cognitive symptoms and memory performance 4 months after paediatric mild traumatic brain injury. *Brain injury* (2015) 29(13-14):1667–73. doi: 10.3109/02699052.2015.1075250

72. Aineskog H, Johansson C, Nilsson R, Koskinen LD, Lindvall P. Serum S100B correlates with health-related quality of life and functional outcome in patients at 1 year after aneurysmal subarachnoid haemorrhage. *Acta Neurochir (Wien)* (2022) 164(8):2209–18. doi: 10.1007/s00701-022-05272-0

73. Beer C, Blacker D, Bynevelt M, Hankey GJ, Puddey IB. Systemic markers of inflammation are independently associated with S100B concentration: results of an observational study in subjects with acute ischaemic stroke. *J Neuroinflammation* (2010) 7:71. doi: 10.1186/1742-2094-7-71

74. Liu L, Zheng CX, Peng SF, Zhou HY, Su ZY, He L, et al. Evaluation of urinary S100B protein level and lactate/creatinine ratio for early diagnosis and prognostic prediction of neonatal hypoxic-ischemic encephalopathy. *Neonatol* (2010) 97(1):41–4. doi: 10.1159/000227292

75. Li H, Liu L, Zhang D, Xu J, Dai H, Tang N, et al. SARS-CoV-2 and viral sepsis: observations and hypotheses. *Lancet (London England)* (2020) 395(10235):1517–20. doi: 10.1016/S0140-6736(20)30920-X

76. Stasi A, Franzin R, Fiorentino M, Squiccimarro E, Castellano G, Gesualdo L. Multifaced roles of HDL in sepsis and SARS-CoV-2 infection: Renal implications. *Int J Mol Sci* (2021) 22(11):5980. doi: 10.3390/ijms22115980

77. Aceti A, Margarucci LM, Scaramucci E, Orsini M, Salerno G, Di Sante G, et al. Serum S100B protein as a marker of severity in covid-19 patients. *Sci Rep* (2020) 10 (1):18665. doi: 10.1038/s41598-020-75618-0

78. Sen J, Belli A. S100B in neuropathologic states: the CRP of the brain? *J Neurosci Res* (2007) 85(7):1373–80. doi: 10.1002/jnr.21211

frontiers | Frontiers in Immunology

TYPE Original Research
PUBLISHED 30 January 2023
DOI 10.3389/fimmu.2023.1049536

OPEN ACCESS

EDITED BY
Alessandra Stasi,
University of Bari Aldo Moro, Italy

REVIEWED BY
Gianvito Caggiano,
University of Bari Aldo Moro, Italy
Ri Wen,
Sheng Jing Hospital Affiliated to China Medical University, China

*CORRESPONDENCE
Jun Zhou
zhoujun7843@126.com

SPECIALTY SECTION
This article was submitted to Inflammation, a section of the journal Frontiers in Immunology

RECEIVED 20 September 2022
ACCEPTED 13 January 2023
PUBLISHED 30 January 2023

CITATION
Guo C, Fan Y, Cheng J, Deng Y, Zhang X, Chen Y, Jing H, Li W, Liu P, Xie J, Ning W, Chen H and Zhou J (2023) AFM negatively regulates the infiltration of monocytes to mediate sepsis-associated acute kidney injury.
Front. Immunol. 14:1049536.
doi: 10.3389/fimmu.2023.1049536

AFM negatively regulates the infiltration of monocytes to mediate sepsis-associated acute kidney injury

Caiyun Guo[1], Youling Fan[2,3], Jiurong Cheng[1], Yingdong Deng[1], Xiangsheng Zhang[1], Yanna Chen[1], Huan Jing[1], Wenjun Li[1], Pei Liu[1], Jiaqi Xie[1], Wenjun Ning[1], Hongtao Chen[4] and Jun Zhou[1*]

[1]Department of Anesthesiology, The Third Affiliated Hospital, Southern Medical University, Guangzhou, China, [2]Department of Anesthesiology, The First People's Hospital of Kashgar, Xinjiang, China, [3]Department of Anesthesiology, The Second People's Hospital of Panyu, Guangzhou, China, [4]Department of Anesthesiology, Guangzhou Eighth People's Hospital, Guangzhou Medical University, Guangzhou, Guangdong, China

Background: Sepsis is organ dysfunction due to the host's deleterious response to infection, and the kidneys are one of the organs damaged in common sepsis. Sepsis-associated acute kidney injury (SA-AKI) increases the mortality in patients with sepsis. Although a substantial volume of research has improved the prevention and treatment of the disease, SA-SKI is still a significant clinical concern.

Purpose: Aimed to use weighted gene co-expression network analysis (WGCNA) and immunoinfiltration analysis to study SA-AKI-related diagnostic markers and potential therapeutic targets.

Methods: Immunoinfiltration analysis was performed on SA-AKI expression datasets from the Gene Expression Synthesis (GEO) database. A weighted gene co-expression network analysis (WGCNA) analysis was performed on immune invasion scores as trait data, and modules associated with immune cells of interest were identified as hub modules. Screening hub geneset in the hub module using protein-protein interaction (PPI) network analysis. The hub gene was identified as a target by intersecting with significantly different genes screened by differential expression analysis and validated using two external datasets. Finally, the correlation between the target gene, SA-AKI, and immune cells was verified experimentally.

Results: Green modules associated with monocytes were identified using WGCNA and immune infiltration analysis. Differential expression analysis and PPI network analysis identified two hub genes (*AFM* and *GSTA1*). Further validation using additional AKI datasets GSE30718 and GSE44925 showed that *AFM* was significantly downregulated in AKI samples and correlated with the development of AKI. The correlation analysis of hub genes and immune cells showed that *AFM* was significantly associated with monocyte infiltration and hence, selected as a critical gene. In addition, Gene single-enrichment analysis (GSEA) and PPI analyses results showed that *AFM* was significantly related to the occurrence and development of SA-AKI.

10.3389/fimmu.2023.1049536

Conclusions: *AFM* is inversely correlated with the recruitment of monocytes and the release of various inflammatory factors in the kidneys of AKI. *AFM* can be a potential biomarker and therapeutic target for monocyte infiltration in sepsis-related AKI.

KEYWORDS

SA-AKI, AFM, monocyte, WGCNA, immunity

Introduction

Sepsis is an organ dysfunction caused by a dysregulated infection response in a patient (1). The kidney is one of the organs most commonly affected by sepsis, and kidney damage can lead to multiple organ dysfunction through long-term effects (2). In intensive care patients, SA-AKI is a common complication that increases the risk of chronic kidney disease and mortality is extremely high (3). Therefore, understanding the occurrence and development mechanism of SA-AKI is significant for the treatment of sepsis patients and for preventing long-term complications.

It has been suggested that SA-AKI develops and occurs because of a variety of complex mechanisms, inflammatory immune dysregulation plays a crucial role in the occurrence and development of SA-AKI, among other factors (4). AKI often presents a hyperinflammatory state accompanied by elevated systemic cytokine levels, such as IL-6 and TNF-α (5). The damaged kidney in SA-AKI, is a major source of inflammatory chemokines, cytokines, and reactive oxygen species, closely related to the damage of various organs in the system during the progression of sepsis (6). In the early stages of AKI, high levels of these inflammatory factors lead to pro-inflammatory, neutrophil activation, and endothelial dysfunction (7). Previous studies have shown that among immune cells involved in kidney inflammation, neutrophils (recruited during the acute phase), Ly-6C+ (inflammation) monocytes, and resident macrophage populations initiate inflammatory processes that affect acute inflammation or profibrotic changes (8). However, a persistently high inflammatory state inhibits immune system function and clearance of infection, and studies suggest that AKI may attenuate the pro-inflammatory effects of neutrophils and lead to impaired monocyte function (9). In contrast, neutrophil function suppression is more intense in patients with SA-AKI. Therefore, the inflammatory immune response is a crucial entry point for treating SA-AKI. A recent study using single-cell sequencing technology identified inflammatory macrophage subsets as therapeutic targets for alleviating AKI (10). The relationship between SA-AKI and the inflammatory immune response is complex, so we aimed to screen for therapeutic targets by studying the infiltration of immune cells in the SA-AKI-induced kidney damage and provide novel ideas for diagnosing and treating the disease.

Materials and methods

RNA expression data

The research strategy of the study is illustrated in Figure 1.

Three gene expression datasets (GSE139061, GSE30718, and GSE44925) were downloaded from Gene Expression Omnibus (GEO; https://www.ncbi.nlm.nih.gov/geo/).

The GSE139061 dataset includes 39 AKI kidney biopsy samples and 9 nephrectomy samples. The AKI kidney biopsy samples were obtained from patients with confirmed sepsis and pathological diagnosis consistent with AKI. Samples from nephrectomy surgeries were obtained from the University of Michigan's Renal Precision Medicine Program, and Illumina HiSeq 4000 was used for sequencing (11). GSE308718 dataset includes 28 renal biopsy samples from 26 post-transplant AKI patients with an average estimated glomerular filtration rate (eGFR) of 26 mL/min at biopsy and 11 original protocol biopsy samples from stable transplants without histological abnormalities (12). The mean estimated glomerular filtration rate (eGFR) at biopsy was 51.2 mL/min. This dataset was generated using the GPL570 [HG-U133_Plus_2] Affymetrix Human Genome U133 Plus 2.0 Array (Affymetrix, Santa Clara, CA, USA). The GSE44925 dataset was derived from Affymetrix's Mouse Gene 1.0 ST Array [transcript (gene) version] platform based on GPL6246. Finally, five AKI samples (GSM1093979, GSM1093980, GSM1093981, GSM1093982, and GSM1093983) and three normal samples (GSM1093973, GSM1093974, and GSM1093975) were selected from GSE44925 (13).

Gene co-expression network analysis of AKI

The R package of weighted gene co-expression network analysis (WGCNA) was used to construct the weighted co-expression network (14). As a result of these calculations, we were able to cluster the samples and eliminate the outliers based on the average linkage and Pearson's correlation coefficients. Next, an adjacency matrix was built, and a soft threshold β was selected to construct a scale-free network. In addition, a topological overlap matrix (TOM) was derived from the adjacency matrix. Finally, a hierarchical clustering tree was constructed using the dynamic clipping tree algorithm and the network modules were identified.

Evaluation of immune cell infiltration

CIBERSORT is an analytical algorithm that uses gene expression data to estimate the abundance of each cell type in mixed cell

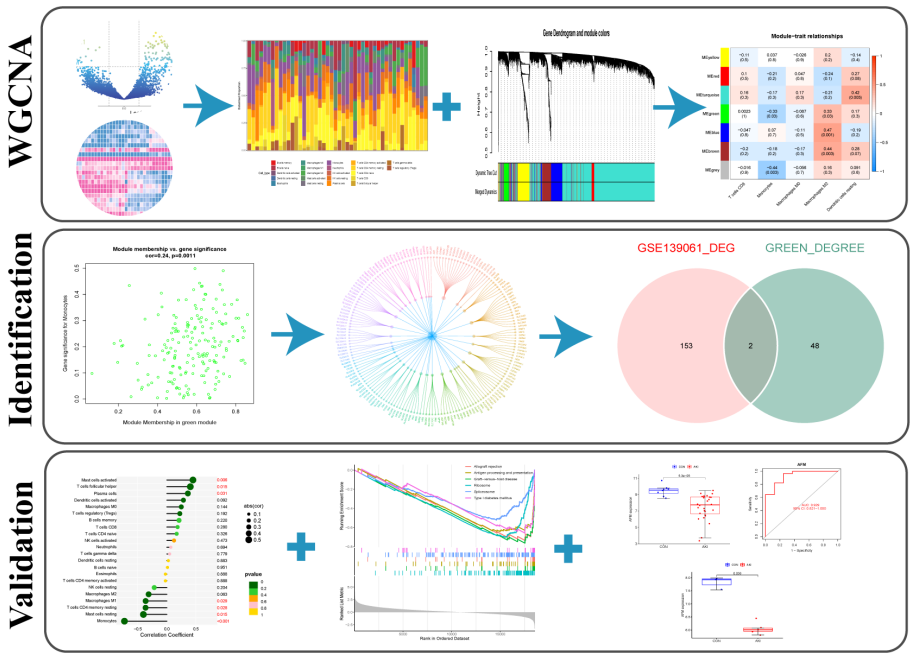

FIGURE 1
The workflow of the study.

populations (15). The infiltration fraction of the leukocyte signature matrix (LM22) was calculated using the R package "CIBERSORT" in this study, and the result was shown as a heatmap. In addition, the results between groups (CON-AKI) were compared, immune cell types with significant differences between groups were screened (P<0.05), and the fraction of immune cells in each sample was used as the trait data for WGCNA.

Identification of hub modules and genes

Among the six modules obtained by WGCNA, those with a high correlation with the immune cells of interest were screened as hub modules by correlation coefficient and significance P value. Then, the protein-protein interactions (PPIs) of hub module genes were analyzed using STRING database (STRING; https://string-db.org/) (16). The PPI network determined the number of protein nodes applied to the central node. Subsequently, these results were combined using Cytoscape (Cytoscape_v3.9.0; https://cytoscape.org/) (17). Differential expression analysis was performed on dataset GSE139061, screened for Adjusted P value (P.adj) <0.05 and |log(Fold Change)| (|logFC|)>1. The 30 genes with the most significant differential multiples in the up-regulated and down-regulated genes among the differential genes were selected to display on the heat map. The differentially expressed genes were intersected with the central node genes to obtain the hub genes.

Validation of hub genes

Datasets GSE30718 and GSE44925 were downloaded from the GEO database to determine the differential expression of hub genes in AKI kidney and healthy kidney tissue from human and mouse species. Reliability of receiver operating characteristic (ROC) curve test for diagnosing AKI central genes using the R package "pROC" (18).

Identification of immune characterization

Using the R package "ggstatsplot" (19), the correlation of hub genes with relevant immune cells was analyzed by scatter plots of hub gene expression and immune cell infiltration levels. P<0.05 indicated statistical significance.

Gene single-enrichment analysis of target genes

GSEA is a computational method to determine whether a fundamentally defined set of genes is statistically significantly different between two biological states (20). According to the median of the target gene expression, the samples were divided into two groups, and the results of GSEA were statistically significant when P.adj<0.05 and q<0.05. Finally, the enrichment pathways were visualized using the R packages "ggplot2" (21) and "clusterProfiler" (22).

Cell culture

Human monocytic leukemia cell line (THP-1) was purchased from the Procell Life Science&Technology Co.,Ltd (Wuhan, China)

and cultured in THP-1 special medium [CM-0233, Procell Life Science&Technology Co.,Ltd (Wuhan, China)] at 37°C in a 5% CO_2 incubator. In all experiments, the cells were cultured in 6-well plates, treated with 1 μg/mL LPS [lipopolysaccharide, Sigma-Aldrich (Shanghai) Trading Co.,Ltd. (Shanghai, China)] for 24 h, and harvested; then, total RNA was extracted.

Animals and treatments

Male wild-type C57BL/6J mice (8–10-weeks-old) were purchased from SiPeiFu Biotechnology Co., Ltd (Beijing, China), housed under standard conditions (12 h light/dark cycle) at constant temperature (22 ± 2°C) and humidity (60%), with given free access to food and water.

After 2 weeks, 12 mice were divided into two groups randomly (n=6): control and LPS. Mice in the LPS group were injected LPS (10 mg/kg) intraperitoneally, while in the control group, mice received an equal volume of saline. The blood and kidney tissues of mice were collected 12 h after LPS treatment.

In the unilateral ischemia-reperfusion (UIRI) model, after a midline abdominal incision, the left renal pedicle was dissected and clamped using microvascular clamps for 45 min at 37 °C. After ischemia, the clamps were released for reperfusion. On day 2 post-UIRI, mice were killed, and the blood and kidneys were collected. The untreated right kidney served as a control group. In addition, the blood of healthy wild-type mice was taken as a control for detecting serum creatinine urea nitrogen in UIRI-induced AKI mice.

The animal experiments were approved by the Animal Protection Committee of the Third Affiliated Hospital of Southern Medical University and conformed to the ethical standards of the Animal Ethics Committee of the Third Affiliated Hospital of Southern Medical University (Guangdong, China).

Assessment of renal function

Mouse whole blood was coagulated at room temperature for 2 h, and serum was collected from the supernatant obtained by centrifugation at 2000 g for 20 min. Blood urea nitrogen (BUN) and serum creatinine (SCr) were determined using a urea detection kit and a Cr detection kit (C013-2-1 and C011-2-1, Nanjing Jiancheng Bioengineering Institute, Nanjing, China).

Kidney injury assessment

Kidney coronal sections were subjected to imaging analysis. The specimens were fixed in 4% paraformaldehyde for at least 24 h before paraffin embedding. Then, hematoxylin-eosin (HE) staining was then performed on the paraffin block in 4-μm sections (23). There were five signs of tubular injury: dilated tubules, atrophy of tubules, formation of tubular casts, shedding of tubular epithelial cells, disappearance of brush borders, and the thickening of the tubular basement membrane. The tubular injury score was calculated semiquantitatively as follows: score 0: no tubular injury; score 1: <10% tubular injury; score 2: 10–24% tubular injury; score 3: 25–49% tubular injury; score 4: 50–74% tubular damage; score 5: damaged tubules ≥75%. Each specimen was randomly examined under 200× magnification in ten fields (24).

RNA extraction and quantitative real time polymerase chain reaction

Total RNA was extracted from whole kidney tissue and monocytes using TRIzol (R0016; Beyotime, Shanghai, China). On a NanoVue (GE Healthcare, USA), absorbance at 260 nm (A260) and 280 nm (A280) were calculated to determine concentration and quality of the extracted RNA. Using a HiScript II Q RT SuperMix for qPCR kit (R222-01, Vazyme Biotech Co., Ltd. China), RNAs whose A260/A280 ratios are 1.8 to 2.0 are suitable for subsequent complementary DNA (cDNA) synthesis. The PCR amplification was performed using the ChamQ Universal SYBR qPCR Master Mix kit (Q711-02, Vazyme Biotech). Each gene was amplified for 40 cycles. We tested all samples three times, and analyzed their melting curves. The target gene mRNA expressions were normalized to that of *GAPDH* using the $2^{-\Delta\Delta Ct}$ method. The PCR primers were synthesized by Tsingke Biotechnology Co., Ltd, and the sequences are listed in Table 1.

Western blot analysis

Mouse kidney tissues and monocyte were dissected and homogenized in radio immune precipitation (RIPA Lysis buffer) lysis buffer (P0013B, Beyotime Biotechnology, China) containing protease inhibitors (FD1001, FUDE Biological Co., Ltd., Hangzhou, China). After centrifugation at 4°C at 12000 rpm for 15 min, the supernatant was collected, and the protein concentration was determined using the BCA Protein Detection Kit (23225, Thermo-Scientific). Bovine serum albumin is the standard. An equal amount of protein lysate is loaded directly on 10 SDS-PAGE and transferred to a polyvinylidene fluoride (PVDF) membrane for western blotting (0.2 μm) (ISEQ00010, MilliporeSigma). Plug the membrane with 5% skim dry milk in Tris-buffered saline and 0.1% Tween-20 (TBS-T) for 1 h at room temperature, followed by overnight incubation with the designated primary antibody at 4°C. After rinsing three times every 5 min with TBS-T, dilute with goat anti-rabbit IgG (1:5000; Signalway Antibody LLC) incubate for 1 h.

Western blotting was visualized using FDbio-Dura Ecl luminescent solution (FD8020, FUDE Biological Co., Ltd., Hangzhou, China) and was visualized under the Tanon-5200 Chemiluminescent Imaging System (Tanon Science and Technology, Beijing, China). Density analysis using ImageJ6.0 software (National Institutes of Health, Bethesda, MD, USA).

10.3389/fimmu.2023.1049536

TABLE 1 Primers for real time-quantitative PCR.

Species	Genes	Primer sequences	
Mouse	AFM	Forward	CCGGACAAGTTCTTTGCTGA
		Reverse	AGAGCTGCCACCATTTCCTT
	CCL2	Forward	TAAAAACCTGGATCGGAACCAAA
		Reverse	GCATTAGCTTCAGATTTACGGGT
	GAPDH	Forward	GGCCTCCAAGGAGTAAGAAA
		Reverse	GCCCCTCCTGTTATTATGG
	NF-κb	Forward	GAGTCACGAAATCCAACGCAG
		Reverse	CCAGCAACATCTTCACATCCC
	IL-18	Forward	GCCATGTCAGAAGACTCTTGCGTC
		Reverse	GTACAGTGAAGTCGGCCAAAGTTGTC
	IL-6	Forward	TAGTCCTTCCTACCCCAATTTCC
		Reverse	TTGGTCCTTAGCCACTCCTTC
	TNF-α	Forward	AGGTTCTGTCCCTTTCACTCACTGG
		Reverse	AGAGAACCTGGGAGTAGACAAGGTA
Human	AFM	Forward	CAGACACCTTCTTTGCGAAGT
		Reverse	GCGTAACGGTAACAACCTGG
	CCL2	Forward	AGCAGCAAGTGTCCCAAAGA
		Reverse	TTGGGTTTGCTTGTCCAGGT
	GAPDH	Forward	GAGAAGGCTGGGGCTCATTT
		Reverse	AGTGATGGCATGGACTGTGG
	NF-κb	Forward	TGCAGCAGACCAAGGAGATG
		Reverse	CCAGTCACACATCCAGCTGTC
	IL-18	Forward	TGCATCAACTTTGTGGCAAT
		Reverse	CAGCTCTGGCTTGTTCCTCA
	IL-6	Forward	CCAGTACCCCCAGGAGAAGA
		Reverse	CAGCTCTGGCTTGTTCCTCA
	TNF-α	Forward	CTGGAAAGGACACCATGAGCA
		Reverse	TCTCTCAGCTCCACGCCATT

Enzyme-linked immunosorbent assay

IL-6, IL-18, and TNF-α levels in kidney tissues were measured using the IL-6 mouse ELISA kit (MM-1011M2, Jiangsu, China), IL-18 mouse ELISA kit (MM-0906M2, Jiangsu, China), and TNF-α mouse ELISA kit (MM-0132M2, Jiangsu, China), respectively.

Statistical analysis

Statistical analysis was performed using GraphPad Prism (GraphPad Prism 9; GraphPad Software, Inc.). The data conformed to a normal distribution. Unpaired Student's t-test was used to analyze the differences between the two groups. $P<0.05$ indicated a statistically significant difference.

Results

Construction of gene co-expression network

A co-expression network of 5000 gene expression values for 46 samples was constructed using the R software package "WGCNA" (14). Consequent to clustering, two outlier samples were removed (Supplementary Figure 1). In this study, we selected the soft threshold β=6 (scale-free R2 = 0.85) to construct a scale-free network and used the dynamic clipping tree algorithm for clustering to construct a

hierarchical clustering tree (Figures 2A, B). Each leaf of the tree represents a gene. Then, the genes of the expression data were combined to form the branches of the tree, representing a gene module; a total of six modules were identified for subsequent analysis (Figure 2C).

Identification of hub modules and genes

The R package "CIBERSORT" was used to calculate the infiltration scores of various immune cells in the gene expression matrix (25). The immune cell infiltration was visualized with a heatmap (Figure 2D). The differences in immune cell infiltration scores between the AKI and normal kidney groups were compared. T cells CD8, monocytes, macrophages M0 and M2, and dendritic cells resting were selected according to P<0.05 (Figure 3A). The five types kinds of immune cells and their infiltration scores in each sample were used as trait data for weighted correlation network analysis. The correlation between the module signature genes and the infiltration of five types of immune cells was displayed on a heat map (Figure 3B). The green modules correlated with both monocytes (R2=-0.33, P=0.03) and M2 macrophages (R2 = 0.33, P=0.03), while the blue (R2 = 0.47, P=0.001) and brown modules (R2 = 0.41, P=0.003) were associated with M2 macrophages. The turquoise-colored module was associated with dendritic cells resting (R2 = 0.42, P=0.005). Herein, we selected the green module as the hub. A scatter plot of the distribution of genes in the hub module is shown in Figure 3C. The hub module genes were analyzed using the STRING database for PPI analysis and were sorted according to the number of nodes. The top 50 genes with the number of nodes were screened as the central node (Figure 3D). These 50 genes intersected with the differential genes of the dataset, and two hub genes, *AFM* and *GSTA1* were obtained.

Screening of differentially expressed genes

The R package "limma" was used to screen the DEGs of AKI and normal kidney samples in GSE139061 (26). According to

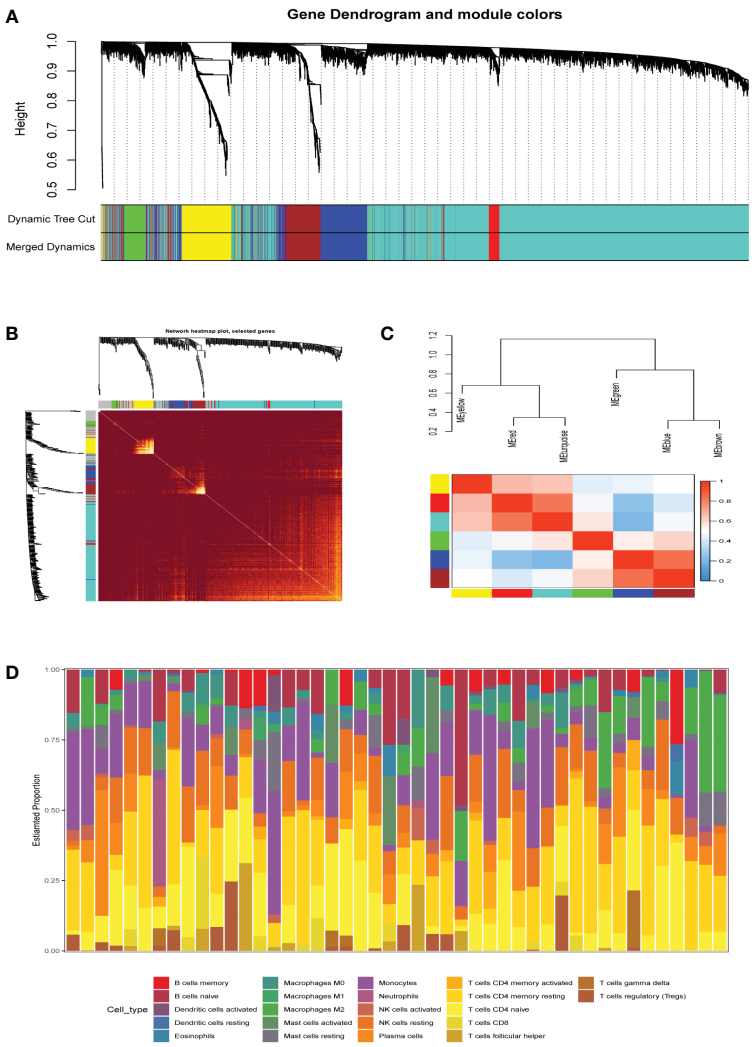

FIGURE 2
(A) Clustering dendrogram of genes, with dissimilarity based on topological overlap, together with assigned merged module colors and the originalmodule colors. **(B)** The heat map depicts the topological overlap matrix (TOM) of all genes in the analysis. Gene dendrograms and module assignmentsare also shown on the left and top. **(C)** Genes are classified into different modules by hierarchical clustering, different colors below the hierarchicalclustering tree represent different modules. **(D)** Correlation heatmap of infiltration of immune cells in normal and AKI renal tissues.

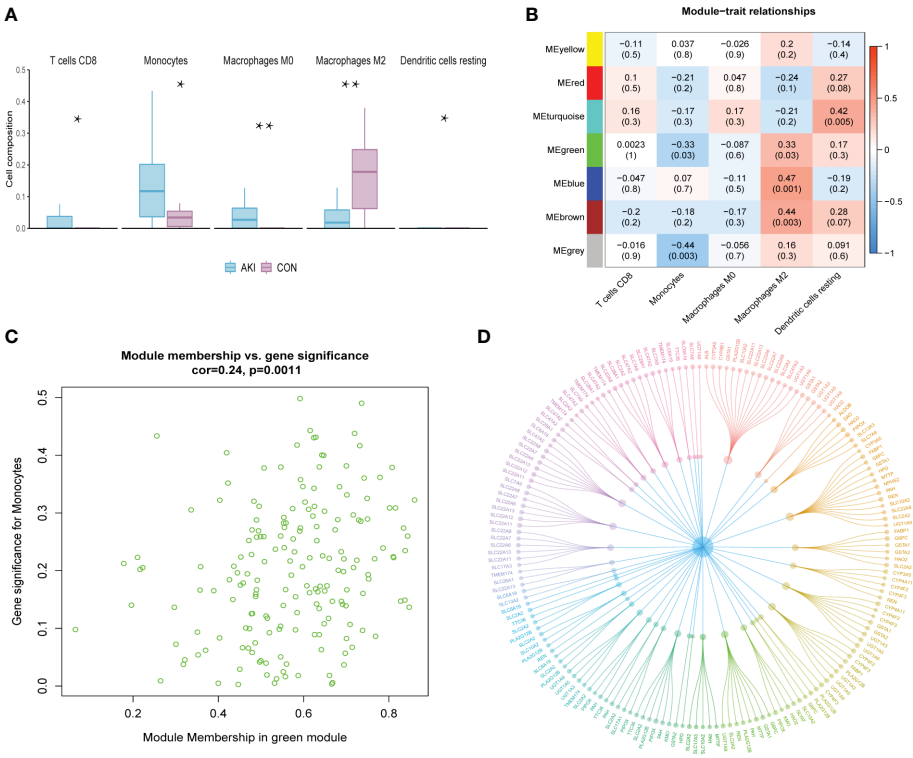

FIGURE 3
(A) The grouped box plot shows immune cells with significantly different immune infiltration scores between the control and experimental groups.**(B)** Heatmap shows the correlation between module eigengenes and immune cells. **(C)** Scatter plot of green module eigengenes. **(D)** PPI network ofgreen module genes. *p < 0.05, **p < 0.01.

P.adj<0.05, |logFC|>1, a total of 155 DEGs were screened, of which 142 were upregulated and 13 were downregulated. The volcano plots were visualized in Figure 4A. The 50 most significant DEGs among the upregulated and downregulated genes were displayed on a heat map (Figure 4C).

Validation of hub genes

The datasets GSE30718 and GSE44925 were downloaded from the GEO database. The volcano plot shows the differential expression of datasets GSE30718 and GSE44925 (Figures 4B, 5C). The expression of two hub genes was downregulated in the AKI group of the dataset GSE30718 (*AFM*: P=5.3e-0.5, *GSTA1*: P=0.0007) (Figure 5A). The ROC curve analysis of the diagnostic value of the two genes for AKI found that the area under the curve (AUC) of the two genes was as follows: *AFM*: 0.929; *GSTA1*: 0.875. The AUC of *AFM* was larger than that of *GSTA1*, suggesting that it had a better diagnostic value (Figure 5B). Moreover, *AFM* was significantly underexpressed in the AKI group in dataset GSE44925 (Figure 5D). Next, we searched the diseases associated with AFM and GSTA1 in The Comparative Toxicogenomics Database (CTD) and found that both genes were associated with AKI (AFM: 67.18; GSTA1: 264.77). We present this result in Table 2. In conclusion, we selected *AFM* as the target gene for our study.

GSEA of the target gene

The samples in the dataset GSE139061 were divided into the high- group and low-expression groups according to the median expression of *AFM*. The pathway enrichment analysis identified 118 significantly enriched pathways (P.adj<0.05, q<0.05). The six enriched pathways with the highest NES in the low-expression group included the immune-related pathways (graft-versus-host disease, allograft rejection, type I diabetes, and antigen processing and presentation), while the high-expression group was not enriched for the immune-related pathways (Figure 6A). The specific information of the six enrichment pathways with the highest NES in the high and low expression groups is shown in Table 3. The enrichment pathways were visualized using the R packages “ggplot2” and “clusterProfiler.”

Significant negative correlation between AFM and monocyte infiltration

To investigate the correlation between *AFM* gene and immune cells, we analyzed the expression data of *AFM* genes in the GSE30718 dataset. The results showed that the expression value of this *AFM* was negatively correlated with the infiltration levels of monocytes, mast cells resting, T cells CD4 memory

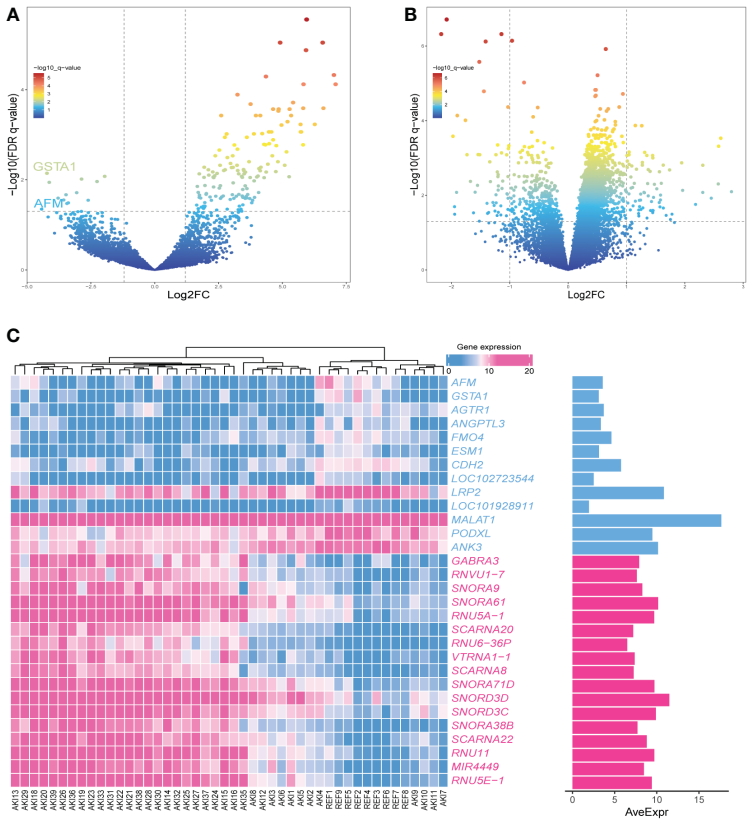

FIGURE 4
(A) The volcano plot showing the differential gene expression (fold change ≥ 1; FDR < 0.05) between control and AKI group in GSEGSE139061 dataset.
(B) The volcano plot showing the differential gene expression (fold change ≥ 1; FDR < 0.05) between control and AKI group in GSE30718 dataset.
(C) Heatmap shows the most significant 30 genes in up- and down-regulation.

resting, and macrophages M1; the highest correlation was with monocytes (R=-0.73) (Figure 5E). The scatter plots of *AFM* expression and monocyte infiltration levels are shown in Figure 5F. Also, the expression of *AFM* in various tissues or cells was queried in the ProteomicsDB database (ProteomicsDB; https://www.proteomicsdb.org/), and it was found to be highly expressed in monocytes (Figure 6B).

AFM is downregulated in mice with AKI

In this study, we constructed two AKI mice models: the LPS-induced SA-AKI and the unilateral ischemia-reperfusion (UIRI) induced AKI.

The serum BUN and creatinine levels were substantial increased in these two AKI models compared to the control group and renal function was significantly decreased (Figure 6C). In addition, HE staining showed deterioration of the histological features of the renal cortex in two AKI models (Figures 6D–G). qRT-PCR and enzyme-linked immunosorbent assay (ELISA) detected the expression of inflammatory factors (IL-6, IL-18, TNF-α) in samples (Figures 7, 8). qRT-PCR detected the expression of AFM. In the AKI renal tissue, *AFM* expression was significantly downregulated, and the *CCL2* and inflammatory indicators (*NF-κB, IL-6, TNF-α, and IL-18*) were significantly upregulated (Figures 7, 8).

LPS inhibits the expression of *AFM* in THP-1 cells

To test whether LPS affects the expression of *AFM* in monocytes, we measured the mRNA and protein expression of *AFM* in LPS-treated THP-1 cells and found that the expression of *AFM* was significantly decreased (Figures 9G, H). *CCL2* is a monocyte chemokine, and the expression level of *CCL2* mRNA increased after LPS stimulation in THP-1 cells. In addition, the LPS treatment increased the mRNA levels of the inflammatory marker, *NF-κB, IL-6, TNF-α, and IL-18* (Figure 9). Based on these findings, we proposed the hypothesis that the decrease expression of *AFM* in monocytes after LPS stimulation may be associated with elevated *CCL2* expression, thereby increasing monocyte infiltration and promoting inflammation.

Discussion

AKI is a clinical disease wherein the glomerular filtration rate decreases suddenly due to various reasons in a short time, resulting in the rapid development of water, electrolyte, acid-base balance, and systemic complications (27, 28). Clinically, the primary causes of AKI include sepsis, renal ischemia-reperfusion, and exposure to nephrotoxin, with sepsis accounting for about half of all AKI cases (29, 30). Sepsis is defined as end-organ dysfunction due to the

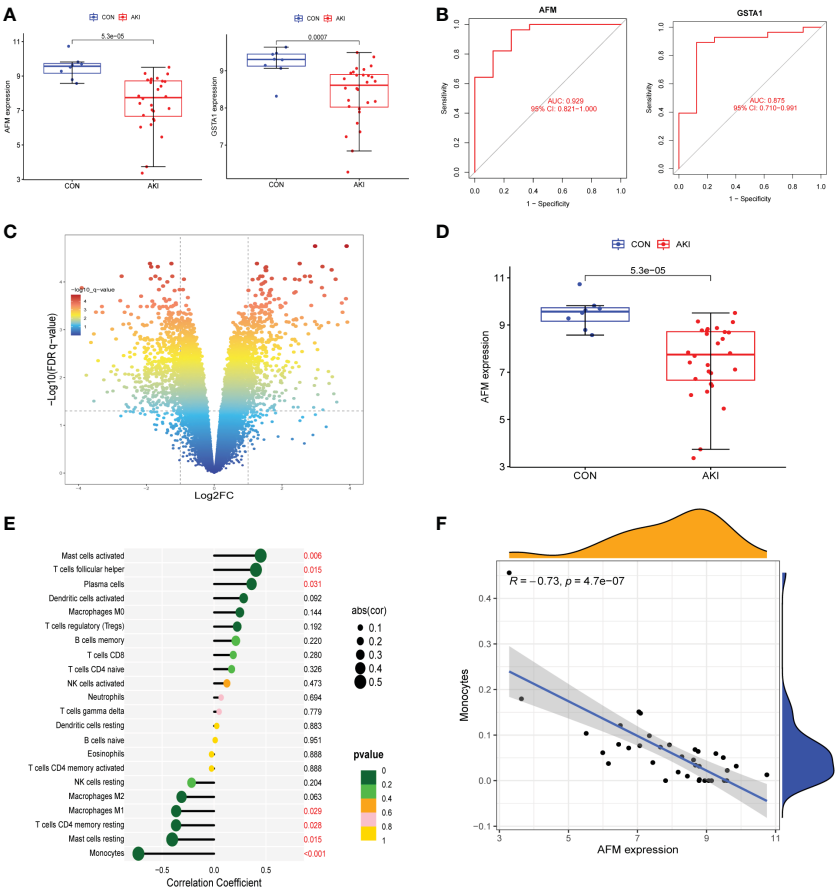

FIGURE 5
(A) The expression of AFM and GSTA1 were high in the AKI group in the GSE30718 dataset. **(B)** ROC curves for AFM, GSTA1. (95% confidence interval (CI), AFM: 0.817-1.000; GSTA1: 0.714-0.996.) **(C)** The volcano plot showing the differential gene expression (fold change ≥ 1; FDR < 0.05) between control and AKI group in GSE44925 dataset. **(D)** The expression of AFM and GSTA1 were high in the AKI group in the GSE44925 dataset. **(E)** The relationship between AFM expression and immune cell infiltration level; P < 0.05 was considered statistically significant. **(F)** Scatter plot of AFM expression versus level of monocyte infiltration.

TABLE 2 Relationship to inflammation and kidney disease to key genes based on the CTD database.

Genes	Disease name	Direct Evidence	Inference score	References
AFM	Inflammation	–	115.82	103
	Fibrosis	–	79.67	62
	Kidney Diseases	–	74.39	387
	Acute Kidney Injury	*	67.18	208
GSTA1	Inflammation	–	291.13	467
	Kidney Diseases	–	264.77	671
	Acute Kidney Injury	*	167.66	627

* A gene that may be a biomarker of a disease.

host's inflammatory response to infection, in which the damaged kidney, a major source of inflammatory chemokines, may have local and remote deleterious effects on the body and increase the risk of mortality in patients with sepsis (3). Several studies have shown that the occurrence and development of SA-AKI are closely related to the infiltration of various immune cells (31). AKI is characterized by inflammatory infiltration within the kidney that induces apoptosis and promotes tubular epithelial cell loss (32). In addition, recent studies have found that the circulation of inflammatory cytokines, such as IL-6 and TNF-α, is associated with an increased risk of death in patients with AKI (33). Three basic mechanisms in the development of SA-AKI include microvascular dysfunction, inflammation, and metabolic reprogramming, in which the recruitment of immune cells and

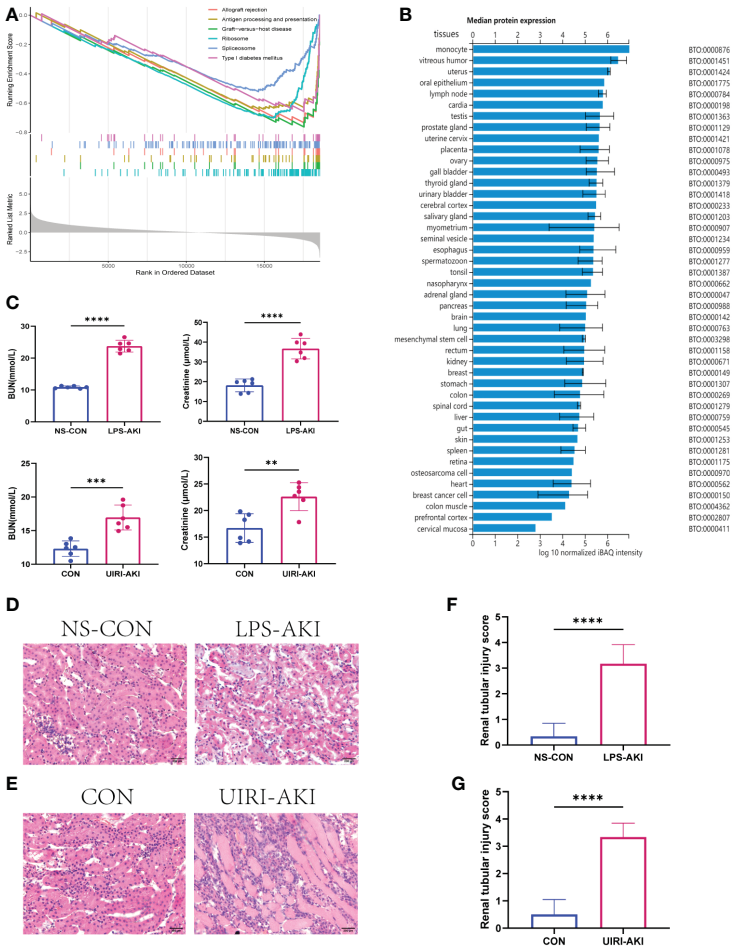

FIGURE 6
(A) GSEA of AFM. The first part shows the enrichment fraction broken line of six pathways, the line in the middle part corresponds to the genes of each diagram, and the third part shows the rank value distribution map of all genes. **(B)** The median protein expression of tissues or cells in the ProteomicsDB. **(C)** BUN and SCr values in two AKI mouse models (LPS-AKI; UIRI-AKI). **(D, E)** HE staining showed deterioration of the histological features of the renal cortex in two AKI models (LPS-AKI; UIRI-AKI). **(F, G)** The renal tubular injury score of two AKI moudules. $^{**}p < 0.01$, $^{***}p < 0.001$, $^{****}p < 0.0001$.

TABLE 3 Single-gene GSEA of AFM.

	ID	setSize	NES	p.adjust
Head	hsa00053	Ascorbate and aldarate metabolism	0.709402	0.000136
	hsa04614	Renin-angiotensin system	0.694034	0.000407
	hsa04977	Vitamin digestion and absorption	0.679851	0.000678
	hsa00982	Drug metabolism - cytochrome P450	0.655219	0.00012
	hsa00591	Linoleic acid metabolism	0.654396	0.000807
	hsa00650	Butanoate metabolism	0.654048	0.000131
Tail	hsa05310	Asthma	-0.64122	0.00078
	hsa04940	Type I diabetes mellitus	-0.65781	0.000463
	hsa05320	Autoimmune thyroid disease	-0.66866	0.00044
	hsa03010	Ribosome	-0.70195	0.001427
	hsa05330	>Allograft rejection	-0.73373	0.000428
	hsa05332	Graft-versus-host disease	-0.76277	0.000428

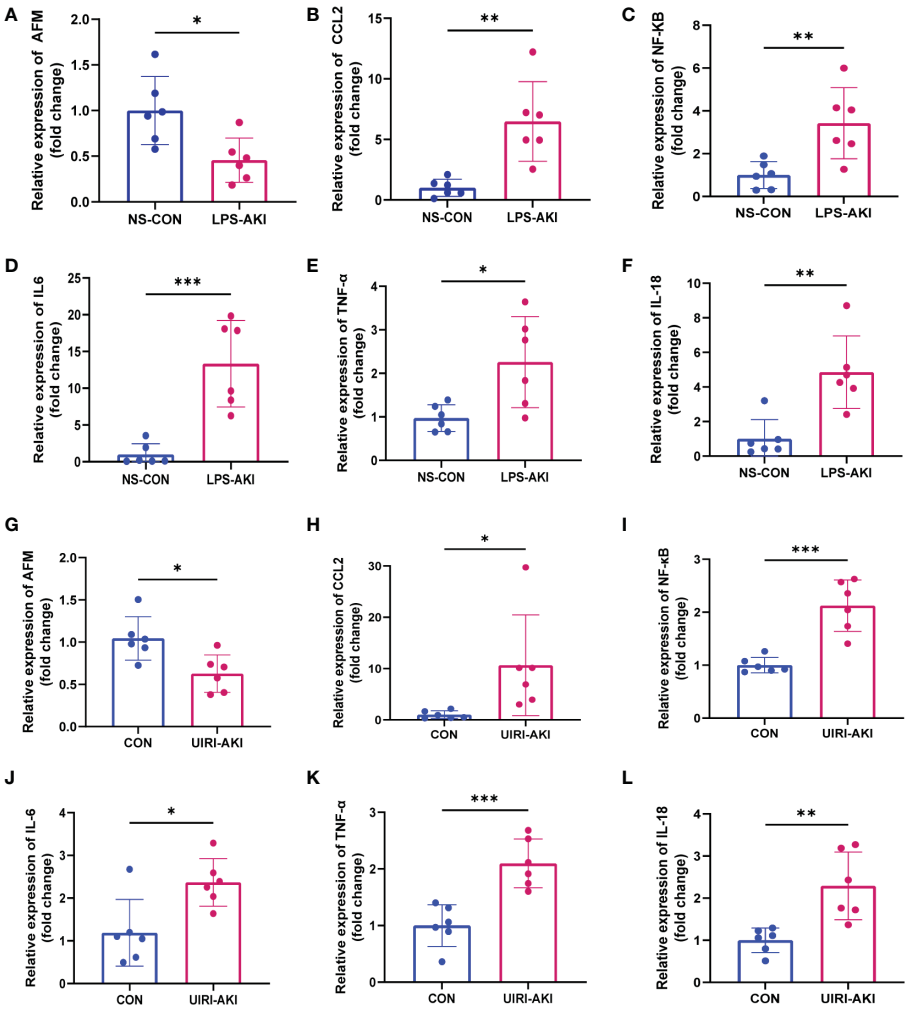

FIGURE 7
(A–F) Relative expression level of AFM, CCL2 and inflammatory indicators mRNA in LPS-AKI mice model. **(G–L)** Relative expression level of AFM, CCL2 and inflammatory indicators mRNA in UIRI-AKI mice model. *p < 0.05, **p < 0.01, ***p < 0.001.

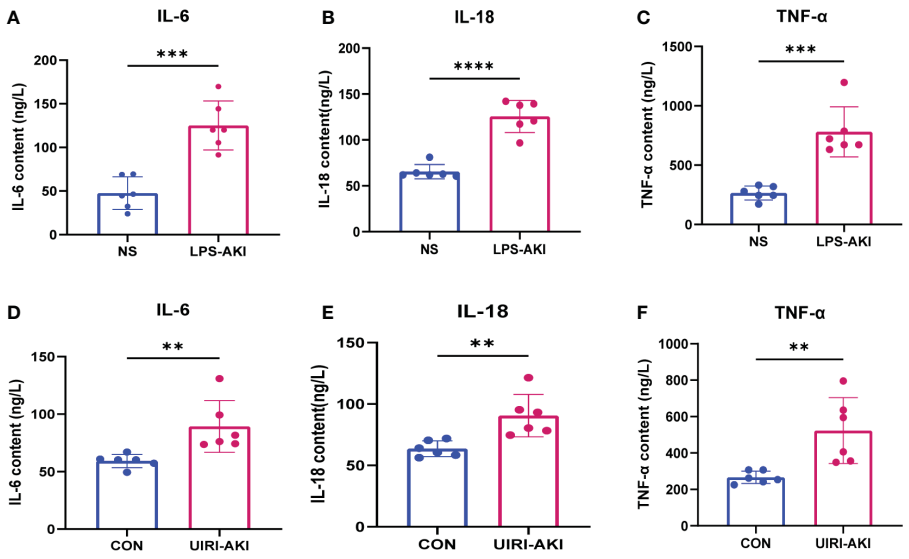

FIGURE 8
(A–F) ELISA analysis of IL-6, IL-18, TNF-α levels in UIRI-AKI and LPS-induced AKI models. Analyze the data using Student's t-test. **p < 0.01, ***p < 0.001, ****p < 0.0001.

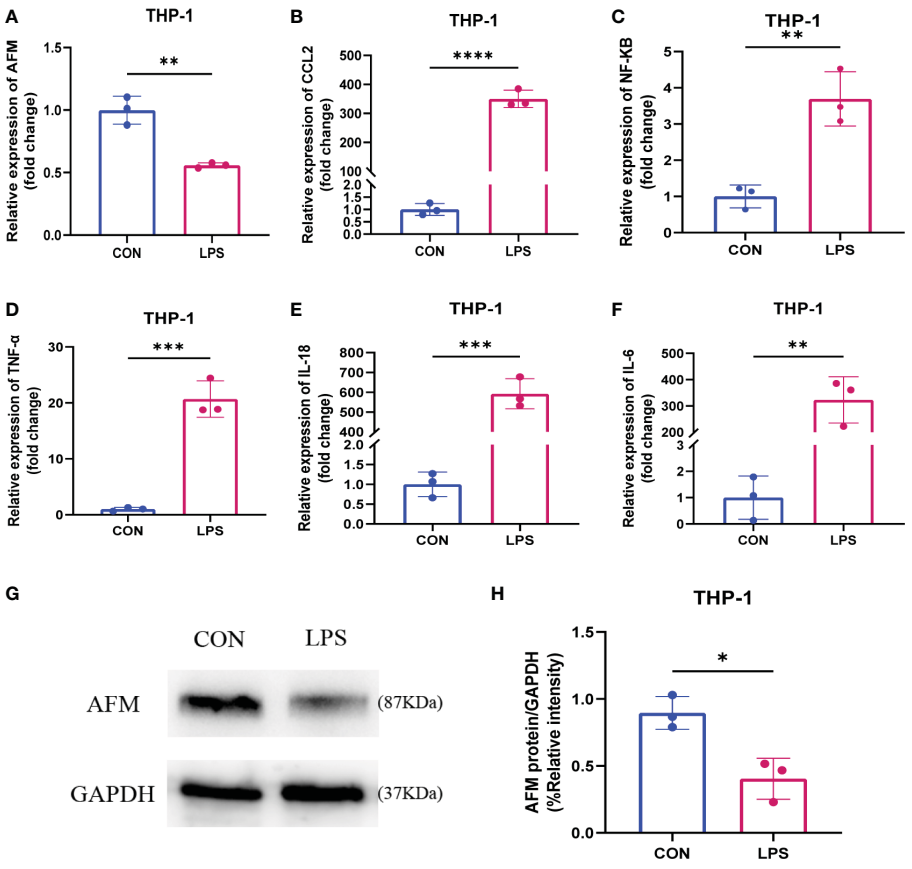

FIGURE 9
(A–F) Relative expression levels of AFM, CCL2 and inflammatory index mRNA in LPS-stimulated monocytes (THP-1). **(G, H)** The immunoblotting **(G)** and quantification grayscale value of AFM in THP-1 cell 24 h post-LPS stimulation **(H)**. *p < 0.05, **p < 0.01, ***p < 0.001, ****p < 0.0001.

the overproduction of pro-inflammatory cytokines play a critical role in developing LPS-induced SA-AKI (3, 34). Although significant efforts have been made to resolve the issues related to treatment, the early diagnosis and treatment of SA-AKI is a significant clinical problem. Therefore, the present study focused on the mechanism of immune infiltration in the development of SA-AKI and the search for new diagnostic markers and therapeutic targets through bioinformatics analysis.

In order to further explore the mechanism of immune cells in sepsis-related AKI and find novel ideas for the diagnosis and treatment, we downloaded the mouse sepsis-related AKI dataset from the GEO database and constructed a network of gene co-expression matrix and immune infiltration analysis. Five types of immune cells with significant differences in immune infiltration scores were screened between the AKI and control groups. Weighted correlation network analysis was performed using the immune infiltration score of each sample as trait data, combining the results of immune infiltration and WGCNA. Based on the analysis, we screened out *AFM* and *GSTA1* as hub genes. We downloaded the human AKI dataset and the mouse rhabdomyolysis-associated AKI dataset as external data to validate these two genes and found that *AFM* was significantly downregulated in the AKI group in both datasets. Next, the *AFM* gene was selected as a potential diagnostic and therapeutic target for SA-AKI based on the results.

AFM, also known as Afamin, is the fourth member of the albumin gene family and is mainly produced by the liver and expressed in the kidney (35). Some studies revealed that *AFM* has multiple binding sites for α- and γ-tocopherol and is a specific binding protein for vitamin E (36, 37). Growing evidence suggests that AFM, as a specific binding protein for vitamin E, may play a role in protecting cells from oxidative damage (38). A clinical trial assessed the strong inverse association between plasma *AFM* and inflammatory disease and biomarkers and hinted it as a potentially harmful acute-phase protein (39). On the other hand, studies on metabolic-related diseases demonstrated that plasma *AFM* significantly correlated with liver lipids, fatty liver index, and liver injury markers (40). Another study in metabolic syndrome and obesity demonstrated that *AFM* may influence the development of obesity-related oxidative stress through *via* insulin resistance (41). In addition, plasma *AFM* levels constitute an independent risk factor for gestational diabetes (42–44). The studies on kidney disease exhibited that urinary *AFM* is closely related to kidney damage and may be a potential marker of kidney damage, which is useful for the early prediction of patients with a high risk of kidney disease in patients with type 2 diabetes (45, 46). Moreover, multiple proteomic analyses have found that urinary AFM is a potential biomarker for various diseases, including membranous nephropathy, lupus nephritis, and osteoarthritis (47–49). To sum up, although several studies have revealed the molecular function of *AFM* and its correlation with various inflammatory diseases, there is still a lack of research on the role

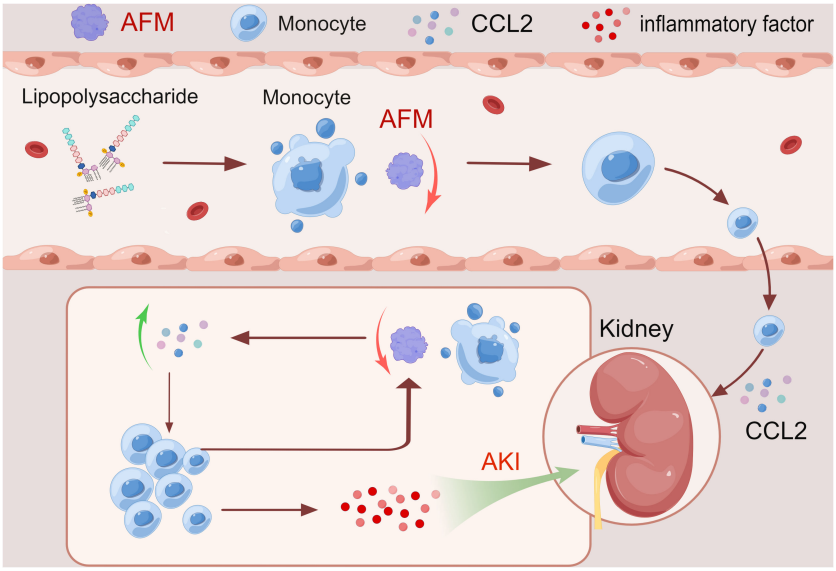

FIGURE 10
Hypothesis map was drawn by Figdraw.

of *AFM* in the development of SA-AKI from the perspective of molecular mechanisms.

Monocyte chemokines regulate monocyte transport, namely CCL2, CCL7, CX3CL1, and various chemokine receptors. CCL2 is a well-known CC chemokine, which is not only one of the critical chemokines in regulating monocytes/macrophage migration and infiltration, but also plays a role in cancer, autoimmune diseases, bacterial and viral infections, and many kidney diseases. In some studies, CCL2 has been recognized as a novel AKI biomarker that plays a vital role in many types of AKI (50). In addition, high CCL2 levels are thought to be positively correlated with renal interstitial fibrosis and tubular atrophy (51, 52). Based on the importance of CCL2 in acute kidney injury, we selected CCL2 as the monocyte chemokine to be detected.

In this study, we used SA-AKI and UIRI models for validation. qPCR detection showed that *AFM* in kidney tissue of SA-AKI mice induced by LPS was significantly decreased, and *CCL2* and inflammatory indexes increased considerably. Furthermore, bioinformatics analysis showed that AFM was negatively correlated with the level of monocyte infiltration. It has been previously reported that AFM can act as a chemokine for pro-osteoblasts and may stimulate osteoclastogenesis and bone resorption through Gi-coupled receptors and the Ca2+/calmodulin-dependent protein kinase (CaMK) pathway (53, 54). It suggests that AFM may be closely related to the monocyte-macrophage system's differentiation and *in vivo* migration. Our experiments indicated that LPS-treated THP-1 decreased *AFM* expression and significantly increased *CCL2* and inflammatory markers compared with controls. Based on the above results, we propose that AFM is a potential biomarker of SA-AKI, and its downregulation may be associated with the recruitment of monocytes to the damaged kidney. Therefore, we hypothesize that AFM is downregulated in monocytes in sepsis-related acute kidney injury, which further increases monocyte recruitment and the release of various inflammatory factors in the injured kidney, thereby aggravating the inflammatory response, thereby promoting the progression of the disease. The hypothesis diagram is shown in Figure 10. In addition, we found that the expression of *AFM* was also significantly downregulated in UIRI-induced AKI, and the changes in *CCL2* and various inflammatory factors were similar to SA-AKI. Therefore, we propose that *AFM* negatively regulates monocyte infiltration in two models of AKI, mediating an inflammatory response that promotes disease progression. However, this study did not perform AFM gene knockout or overexpression to test this conjecture. Therefore, we will further verify this conjecture in subsequent studies. AFM may be a potential diagnostic marker for SA-AKI, and based on this, we hope that the expression of AFM in the hematuria of patients with SA-AKI can be detected in later studies as further to clarify the significance of AFM as a diagnostic marker.

In summary, AFM was significantly reduced in SA-AKI and UIRI-induced AKI and negatively correlated with monocyte infiltration. This finding suggested that AFM may affect the onset of inflammatory responses by negative regulation of monocyte infiltration, thereby regulating SA-AKI progression. These phenomena may provide novel ideas for diagnosing and treating sepsis-related AKI.

Data availability statement

The datasets presented in this study can be found in online repositories. The names of the repository/repositories and accession number(s) can be found in the article/Supplementary Material.

Ethics statement

The animal study was reviewed and approved by The Animal Protection Committee of the Third Affiliated Hospital of Southern Medical University. Written informed consent was obtained from the owners for the participation of their animals in this study.

Author contributions

CG: Conceptualization, Methodology, Validation, Formal Analysis, Writing - Original Draft. JC: Data Curation, Writing - Original Draft. YD: Visualization. XZ: Resources. YC: Validation. HJ: Writing - Review & Editing. WL: Formal Analysis. PL: Visualization. JX: Writing - Review & Editing. WN: Validation. HC: Resources, Supervision. YF: Validation, Writing - Review & Editing, Project Administration, CG and YF contributed equally. JZ: Conceptualization, Funding Acquisition, Resources, Supervision, Writing - Review & Editing. All authors contributed to the article and approved the submitted version.

Funding

This work was supported by the following funds, National Natural Science Foundation of China [Grant No. 82060130, 81860130]; Natural Science Foundation of Guangdong Province [Grant No. 2019A1515011087, 2021A1515012453]; Guangzhou Science and Technology Innovation Committee [Grant No. 202002030038].

Conflict of interest

The authors declare that the research was conducted in the absence of any commercial or financial relationships that could be construed as a potential conflict of interest.

Publisher's note

All claims expressed in this article are solely those of the authors and do not necessarily represent those of their affiliated organizations, or those of the publisher, the editors and the reviewers. Any product that may be evaluated in this article, or claim that may be made by its manufacturer, is not guaranteed or endorsed by the publisher.

Supplementary material

The Supplementary Material for this article can be found online at: https://www.frontiersin.org/articles/10.3389/fimmu.2023.1049536/full#supplementary-material.

References

1. Cecconi M, Evans L, Levy M, Rhodes A. Sepsis and septic shock. *Lancet* (2018) 392 (10141):75–87. doi: 10.1016/S0140-6736(18)30696-2

2. Poston JT, Koyner JL. Sepsis associated acute kidney injury. *Bmj* (2019) 364:k4891. doi: 10.1136/bmj.k4891

3. Peerapornratana S, Manrique-Caballero CL, Gómez H, Kellum JA. Acute kidney injury from sepsis: current concepts, epidemiology, pathophysiology, prevention and treatment. *Kidney Int* (2019) 96(5):1083–99. doi: 10.1016/j.kint.2019.05.026

4. Gómez H, Kellum JA, Ronco C. Metabolic reprogramming and tolerance during sepsis-induced AKI. *Nat Rev Nephrol* (2017) 13(3):143–51. doi: 10.1038/nrneph.2016.186

5. Faubel S, Edelstein CL. Mechanisms and mediators of lung injury after acute kidney injury. *Nat Rev Nephrol* (2016) 12(1):48–60. doi: 10.1038/nrneph.2015.158

6. Lee SA, Cozzi M, Bush EL, Rabb H. Distant organ dysfunction in acute kidney injury: A review. *Am J Kidney Dis* (2018) 72(6):846–56. doi: 10.1053/j.ajkd.2018.03.028

7. Horiguchi H, Loftus TJ, Hawkins RB, Raymond SL, Stortz JA, Hollen MK, et al. Innate immunity in the persistent inflammation, immunosuppression, and catabolism syndrome and its implications for therapy. *Front Immunol* (2018) 9:595. doi: 10.3389/fimmu.2018.00595

8. Lech M, Gröbmayr R, Ryu M, Lorenz G, Hartter I, Mulay SR, et al. Macrophage phenotype controls long-term AKI outcomes–kidney regeneration versus atrophy. *J Am Soc Nephrol* (2014) 25(2):292–304. doi: 10.1681/ASN.2013020152

9. Chang YM, Chou YT, Kan WC, Shiao CC. Sepsis and acute kidney injury: A review focusing on the bidirectional interplay. *Int J Mol Sci* (2022) 23(16):9159. doi: 10.3390/ijms23169159

10. Yao W, Chen Y, Li Z, Ji J, You A, Jin S, et al. Single cell RNA sequencing identifies a unique inflammatory macrophage subset as a druggable target for alleviating acute kidney injury. *Adv Sci (Weinh)* (2022) 9(12):e2103675. doi: 10.1002/advs.202103675

11. Janosevic D, Myslinski J, McCarthy TW, Zollman A, Syed F, Xuei X, et al. The orchestrated cellular and molecular responses of the kidney to endotoxin define a precise sepsis timeline. *Elife* (2021) 10:e62270. doi: 10.7554/eLife.62270

12. Mengel M, Chang J, Kayser D, Gwinner W, Schwarz A, Einecke G, et al. The molecular phenotype of 6-week protocol biopsies from human renal allografts: reflections of prior injury but not future course. *Am J Transplant* (2011) 11(4):708–18. doi: 10.1111/j.1600-6143.2010.03339.x

13. Mathia S, Rudigier LJ, Kasim M, Kirschner KM, Persson PB, Eckardt KU, et al. A dual role of miR-22 in rhabdomyolysis-induced acute kidney injury. *Acta Physiol (Oxf)* (2018) 224(3):e13102. doi: 10.1111/apha.13102

14. Langfelder P, Horvath S. WGCNA: an r package for weighted correlation network analysis. *BMC Bioinf* (2008) 9:559. doi: 10.1186/1471-2105-9-559

15. Newman AM, Liu CL, Green MR, Gentles AJ, Feng W, Xu Y, et al. Robust enumeration of cell subsets from tissue expression profiles. *Nat Methods* (2015) 12 (5):453–7. doi: 10.1038/nmeth.3337.

16. Szklarczyk D, Gable AL, Lyon D, Junge A, Wyder S, Huerta-Cepas J, et al. STRING v11: protein-protein association networks with increased coverage, supporting functional discovery in genome-wide experimental datasets. *Nucleic Acids Res* (2019) 47(D1):D607–d13. doi: 10.1093/nar/gky1131

17. Shannon P, Markiel A, Ozier O, Baliga NS, Wang JT, Ramage D, et al. Cytoscape: A software environment for integrated models of biomolecular interaction networks. *Genome Res* (2003) 13(11):2498–504. doi: 10.1101/gr.1239303

18. Robin X, Turck N, Hainard A, Tiberti N, Lisacek F, Sanchez JC, et al. pROC: an open-source package for r and s+ to analyze and compare ROC curves. *BMC Bioinf* (2011) 12:77. doi: 10.1186/1471-2105-12-77

19. Patil I. Visualizations with statistical details: The'ggstatsplot'approach. *J Open Source Software* (2021) 6(61):3167. doi: 10.21105/joss.03167

20. Subramanian A, Tamayo P, Mootha VK, Mukherjee S, Ebert BL, Gillette MA, et al. Gene set enrichment analysis: a knowledge-based approach for interpreting genome-wide expression profiles. *Proc Natl Acad Sci USA* (2005) 102(43):15545–50. doi: 10.1073/pnas.0506580102

21. Villanueva RAM, Chen ZJ. ggplot2: Elegant Graphics for Data Analysis (2nd ed.). Measurement: Interdisciplinary Research and Perspectives. (2019) 17(3):160:167. doi: 10.1080/15366367.2019.1565254

22. Wu T, Hu E, Xu S, Chen M, Guo P, Dai Z, et al. clusterProfiler 4.0: A universal enrichment tool for interpreting omics data. *Innovation (Camb)* (2021) 2(3):100141. doi: 10.1016/j.xinn.2021.100141

23. Leemans JC, Stokman G, Claessen N, Rouschop KM, Teske GJ, Kirschning CJ, et al. Renal-associated TLR2 mediates ischemia/reperfusion injury in the kidney. *J Clin Invest* (2005) 115(10):2894–903. doi: 10.1172/JCI22832

24. Yang B, Lan S, Dieudé M, Sabo-Vatasescu JP, Karakeussian-Rimbaud A, Turgeon J, et al. Caspase-3 is a pivotal regulator of microvascular rarefaction and renal fibrosis after ischemia-reperfusion injury. *J Am Soc Nephrol* (2018) 29(7):1900–16. doi: 10.1681/ASN.2017050581

25. Ritchie ME, Phipson B, Wu D, Hu Y, Law CW, Shi W, et al. Limma powers differential expression analyses for RNA-sequencing and microarray studies. *Nucleic Acids Res* (2015) 43(7):e47. doi: 10.1093/nar/gkv007

26. Sui S, An X, Xu C, Li Z, Hua Y, Huang G, et al. An immune cell infiltration-based immune score model predicts prognosis and chemotherapy effects in breast cancer. *Theranostics* (2020) 10(26):11938–49. doi: 10.7150/thno.49451

27. Lameire N, Kellum JA. Contrast-induced acute kidney injury and renal support for acute kidney injury: a KDIGO summary (Part 2). *Crit Care* (2013) 17(1):205. doi: 10.1186/cc11455

28. Levey AS, James MT. Acute kidney injury. *Ann Intern Med* (2017) 167(9):Itc66–itc80. doi: 10.7326/AITC201711070

29. Gómez H, Kellum JA. Sepsis-induced acute kidney injury. *Curr Opin Crit Care* (2016) 22(6):546–53. doi: 10.1097/MCC.0000000000000356

30. Liu Z, Yang D, Gao J, Xiang X, Hu X, Li S, et al. Discovery and validation of miR-452 as an effective biomarker for acute kidney injury in sepsis. *Theranostics* (2020) 10 (26):11963–75. doi: 10.7150/thno.50093

31. Zhang M, Wu L, Deng Y, Peng F, Wang T, Zhao Y, et al. Single cell dissection of epithelial-immune cellular interplay in acute kidney injury microenvironment. *Front Immunol* (2022) 13:857025. doi: 10.3389/fimmu.2022.857025

32. Singbartl K, Formeck CL, Kellum JA. Kidney-immune system crosstalk in AKI. *Semin Nephrol* (2019) 39(1):96–106. doi: 10.1016/j.semnephrol.2018.10.007

33. Ren Q, Guo F, Tao S, Huang R, Ma L, Fu P. Flavonoid fisetin alleviates kidney inflammation and apoptosis *via* inhibiting src-mediated NF-κB p65 and MAPK signaling pathways in septic AKI mice. *BioMed Pharmacother* (2020) 122:109772. doi: 10.1016/j.biopha.2019.109772

34. Verma SK, Molitoris BA. Renal endothelial injury and microvascular dysfunction in acute kidney injury. *Semin Nephrol* (2015) 35(1):96–107. doi: 10.1016/j.semnephrol.2015.01.010

35. Dieplinger H, Dieplinger B. Afamin–a pleiotropic glycoprotein involved in various disease states. *Clin Chim Acta* (2015) 446:105–10. doi: 10.1016/j.cca.2015.04.010

36. Voegele AF, Jerković L, Wellenzohn B, Eller P, Kronenberg F, Liedl KR, et al. Characterization of the vitamin e-binding properties of human plasma afamin. *Biochemistry* (2002) 41(49):14532–8. doi: 10.1021/bi026513v

37. Jerkovic L, Voegele AF, Chwatal S, Kronenberg F, Radcliffe CM, Wormald MR, et al. Afamin is a novel human vitamin e-binding glycoprotein characterization and *in vitro* expression. *J Proteome Res* (2005) 4(3):889–99. doi: 10.1021/pr0500105

38. Erol SA, Tanacan A, Anuk AT, Tokalioglu EO, Biriken D, Keskin HL, et al. Evaluation of maternal serum afamin and vitamin e levels in pregnant women with COVID-19 and its association with composite adverse perinatal outcomes. *J Med Virol* (2021) 93(4):2350–8. doi: 10.1002/jmv.26725

39. Dieplinger B, Egger M, Gabriel C, Poelz W, Morandell E, Seeber B, et al. Analytical characterization and clinical evaluation of an enzyme-linked immunosorbent assay for measurement of afamin in human plasma. *Clin Chim Acta* (2013) 425:236–41. doi: 10.1016/j.cca.2013.08.016

40. Kurdiova T, Balaz M, Kovanicova Z, Zemkova E, Kuzma M, Belan V, et al. Serum afamin a novel marker of increased hepatic lipid content. *Front Endocrinol (Lausanne)* (2021) 12:670425. doi: 10.3389/fendo.2021.670425

41. Juhász I, Ujfalusi S, Seres I, Lőrincz H, Varga VE, Paragh GJr., et al. Afamin levels and their correlation with oxidative and lipid parameters in non-diabetic, obese patients. *Biomolecules* (2022) 12(1):116. doi: 10.3390/biom12010116

42. Wang X, Zheng X, Yan J, Xu R, Xu M, Zheng L, et al. The clinical values of afamin, triglyceride and PLR in predicting risk of gestational diabetes during early pregnancy. *Front Endocrinol (Lausanne)* (2021) 12:723650. doi: 10.3389/fendo.2021.723650

43. Köninger A, Iannaccone A, Hajder E, Frank M, Schmidt B, Schleussner E, et al. Afamin predicts gestational diabetes in polycystic ovary syndrome patients preconceptionally. *Endocr Connect* (2019) 8(5):616–24. doi: 10.1530/EC-19-0064

44. Eroğlu H, Örgül G, Tonyalı NV, Biriken D, Polat N, Yücel A, et al. The role of afamin and other trace elements in the prediction of GDM: a tertiary center experience. *Biol Trace Elem Res* (2021) 199(12):4418–22. doi: 10.1007/s12011-020-02559-0

45. Kaburagi Y, Takahashi E, Kajio H, Yamashita S, Yamamoto-Honda R, Shiga T, et al. Urinary afamin levels are associated with the progression of diabetic nephropathy. *Diabetes Res Clin Pract* (2019) 147:37–46. doi: 10.1016/j.diabres.2018.02.034

46. Kollerits B, Lamina C, Huth C, Marques-Vidal P, Kiechl S, Seppälä I, et al. Plasma concentrations of afamin are associated with prevalent and incident type 2 diabetes: A pooled analysis in more than 20,000 individuals. *Diabetes Care* (2017) 40(10):1386–93. doi: 10.2337/dc17-0201

47. Pang L, Li Q, Li Y, Liu Y, Duan N, Li H. Urine proteomics of primary membranous nephropathy using nanoscale liquid chromatography tandem mass spectrometry analysis. *Clin Proteomics* (2018) 15:5. doi: 10.1186/s12014-018-9183-3

48. Anania VG, Yu K, Pingitore F, Li Q, Rose CM, Liu P, et al. Discovery and qualification of candidate urinary biomarkers of disease activity in lupus nephritis. *J Proteome Res* (2019) 18(3):1264–77. doi: 10.1021/acs.jproteome.8b00874

49. Balakrishnan L, Nirujogi RS, Ahmad S, Bhattacharjee M, Manda SS, Renuse S, et al. Proteomic analysis of human osteoarthritis synovial fluid. *Clin Proteomics* (2014) 11(1):6. doi: 10.1186/1559-0275-11-6

50. Nisansala T, Weerasekera M, Ranasinghe N, Marasinghe C, Gamage C, Fernando N, et al. Importance of KIM-1 and MCP-1 in determining the leptospirosis-associated AKI: A Sri Lankan study. *BioMed Res Int* (2021) 2021:1752904. doi: 10.1155/2021/1752904

51. Worawichawong S, Worawichawong S, Radinahamed P, Muntham D, Sathirapongsasuti N, Nongnuch A, et al. Urine epidermal growth factor, monocyte chemoattractant protein-1 or their ratio as biomarkers for interstitial fibrosis and tubular atrophy in primary glomerulonephritis. *Kidney Blood Press Res* (2016) 41(6):997–1007. doi: 10.1159/000452595

52. Menez S, Ju W, Menon R, Moledina DG, Thiessen Philbrook H, McArthur E, et al. Urinary EGF and MCP-1 and risk of CKD after cardiac surgery. *JCI Insight* (2021) 6(11):e147464. doi: 10.1172/jci.insight.147464

53. Kim BJ, Lee YS, Lee SY, Park SY, Dieplinger H, Ryu SH, et al. Afamin secreted from nonresorbing osteoclasts acts as a chemokine for preosteoblasts *via* the akt-signaling pathway. *Bone* (2012) 51(3):431–40. doi: 10.1016/j.bone.2012.06.015

54. Kim BJ, Lee YS, Lee SY, Park SY, Dieplinger H, Yea K, et al. Afamin stimulates osteoclastogenesis and bone resorption *via* gi-coupled receptor and Ca2+/calmodulin-dependent protein kinase (CaMK) pathways. *J Endocrinol Invest* (2013) 36(10):876–82. doi: 10.3275/8975

frontiers | Frontiers in Immunology

TYPE Original Research
PUBLISHED 27 March 2023
DOI 10.3389/fimmu.2023.1122510

OPEN ACCESS

EDITED BY
Alessandra Stasi,
University of Bari Aldo Moro, Italy

REVIEWED BY
Rahul Sharma,
University of Virginia, United States
Gianvito Caggiano,
University of Bari Aldo Moro, Italy

*CORRESPONDENCE
Jwa-Kyung Kim
kjk816@hallym.or.kr
Yong Kyun Kim
amoureuxyk@hallym.or.kr

†These authors have contributed equally to this work

SPECIALTY SECTION
This article was submitted to Inflammation, a section of the journal Frontiers in Immunology

RECEIVED 13 December 2022
ACCEPTED 16 March 2023
PUBLISHED 27 March 2023

CITATION
Kim IS, Kim DH, Lee HW, Kim SG, Kim YK and Kim J-K (2023) Role of increased neutrophil extracellular trap formation on acute kidney injury in COVID-19 patients. *Front. Immunol.* 14:1122510. doi: 10.3389/fimmu.2023.1122510

Role of increased neutrophil extracellular trap formation on acute kidney injury in COVID-19 patients

In Soo Kim[1], Do Hyun Kim[1], Hoi Woul Lee[1], Sung Gyun Kim[1], Yong Kyun Kim[2*†] and Jwa-Kyung Kim[1*†]

[1]Department of Internal Medicine & Kidney Research Institute, Hallym University Sacred Heart Hospital, Anyang, Republic of Korea, [2]Division of Infectious Diseases, Department of Internal Medicine, Hallym University Sacred Heart Hospital, Anyang, Republic of Korea

Background: A strong association between elevated neutrophil extracellular trap (NET) levels and poor clinical outcomes in patients with coronavirus infection 2019 (COVID-19) has been reported. However, while acute kidney injury (AKI) is a common complication of COVID-19, the role of NETs in COVID-19-associated AKI is unclear. We investigated the association between elevated NETs and AKI and the prognostic role of NETs in COVID-19 patients.

Methods: Two representative markers of NETs, circulating nucleosomes and myeloperoxidase-DNA, were measured in 115 hospitalized patients. Serum levels of interleukin [IL]-6, monocyte chemotactic protein-1 [MCP-1], plasma von Willebrand factor (vWF) and urinary biomarkers of renal tubular damage (β2-microglobulin [β2M] and kidney injury molecule 1 [KIM-1]) were measured.

Results: AKI was found in 43 patients (37.4%), and pre-existing chronic kidney disease (CKD) was a strong risk factor for AKI. Higher circulating NET levels were a significant predictor of increased risk of initial ICU admission, in-hospital mortality (adjusted HR 3.21, 95% CI 1.08–9.19) and AKI (OR 3.67, 95% CI 1.30-10.41), independent of age, diabetes, pre-existing CKD and IL-6 levels. There were strong correlations between circulating nucleosome levels and urinary KIM-1/creatinine (r=0.368, p=0.001) and β2M (r=0.218, p=0.049) levels. NETs were also strongly closely associated with serum vWF (r = 0.356, p<0.001), but not with IL-6 or MCP-1 levels.

Conclusions: Elevated NETs were closely associated with AKI, which was a strong predictor of mortality. The close association between NETs and vWF may suggest a role for NETs in COVID-19-associated vasculopathy leading to AKI.

KEYWORDS

neutrophil extracellular traps, acute kidney injury, endothelial, COVID-19, inflammation, mortality

1 Introduction

Neutrophil extracellular traps (NETs) are extracellular webs of DNA, histones, microbicidal proteins, and oxidant enzymes released by activated neutrophils in response to various stimuli, including respiratory viruses and inflammatory cytokines (1). While NETs are thought to have an antimicrobial function in innate immunity, their dysregulation can initiate and propagate inflammation and thrombosis, causing severe tissue injury (2). In patients with influenza A infection, high levels of NETs predict a poor prognosis, and the inhibition of neutrophils and NETs is protective in several models of influenza-associated acute respiratory distress syndrome (ARDS) (3, 4). The presence of NETs in patients with coronavirus infection 2019 (COVID-19), the disease caused by SARS-CoV-2 infection, was first reported in 2020 (5, 6), with subsequent studies showing an association between circulating markers of NETs and clinical outcome (6, 7). In COVID-19, NETs were shown to be a prognostic marker (8).

Acute kidney injury (AKI) is characterized by a rapid decline in the estimated glomerular filtration rate (eGFR), accompanied by reduced renal blood flow, endothelial dysfunction, and tubulointerstitial inflammation (9–12), which together result in a high risk of death in hospitalized patients (13, 14). In COVID-19 patients, the prevalence of AKI ranges from 10% to35%, but is as high as 50% in those with severe disease and those in the intensive care unit (ICU) (15–17). Furthermore, consistent with AKI from other causes, COVID-19 AKI is associated with adverse outcomes, as the risk of all-cause mortality is ≥ 5-fold higher in COVID-19 patients with AKI than in those without (8, 18, 19).

Neutrophil dysregulation and excessive NET formation have been implicated in the development of organ damage. For example, interstitial NETs and NET-associated intravascular thrombi are characteristic features of ARDS in the lungs of patients with lethal COVID-19 (3, 20, 21). Accordingly, a role for NETs in the pathogenesis of COVID-19 AKI is likely to lead to tubular injury, excessive inflammation, and intravascular immune thrombosis (22–26). However, how NETs might induce AKI in COVID-19 is unclear, as are the prognostic implications of NETs in COVID-19 AKI.

In a previous study, we showed that circulating NETs levels are significantly higher in dialysis patients than in the general population and are a strong prognostic marker for mortality (27). In this study, we investigated the association between higher NET levels and AKI in hospitalized patients with COVID-19. We also investigated the relationship between NETs and various inflammatory parameters and the prognostic role of NET-related COVID-19 AKI on in-hospital mortality.

2 Methods

2.1 Study population and blood sampling

The study population consisted of 115 patients with COVID-19 diagnosed between January 2022 and May 2022. Diagnosis was based on reverse transcriptase-polymerase chain reaction detection of viral RNA from nasopharyngeal swabs from patients with clinical symptoms. Patients aged <18 years of age were excluded. Blood and urine samples were collected within 48 h of admission using EDTA tubes (367835, BD, Franklin Lakes, NJ, USA) for plasma and Serum Separator Clot Activator tubes (456073, BD) for serum. Plasma was obtained by centrifugation of blood samples at 1500 g for 10 minutes at 4°C, and serum was obtained by incubation at room temperature for 20-30 minutes followed by centrifugation as described for plasma. Both plasma and serum were aliquoted and stored at -70°C until analysis. This study was approved by our Institutional Ethics Committee (IRB No 2022-02-014). Informed consent was obtained from all study participants or, in the case of incapacity, from their next of kin.

Demographic information, data on comorbidities, and the history of vaccination against COVID-19 at the time of admission were extracted from the patients' medical records. Initial vital signs, information on ICU admission, and the need for mechanical ventilation (MV) were also determined. The cycle threshold value was used to measure viral load. Biochemical parameters, white blood cell (WBC) count, neutrophil count, lymphocyte count, platelet count, albumin levels, the neutrophil/lymphocyte ratio (NLR), and platelet/WBC ratio (PWR), and serum procalcitonin, lactic acid, and brain natriuretic peptide (BNP) levels, were obtained from the patients' medical records.

Inflammatory cytokines were further assessed by measuring serum levels of interleukin (IL)-6, high-sensitivity C-reactive protein (hs-CRP), and monocyte chemotactic protein-1 (MCP-1) levels, using the appropriate kits according to the manufacturer's instructions. The levels of these cytokines were determined using ELISA kits (R&D Systems, Minneapolis, MN, USA).

2.2 Diagnosis of AKI

AKI at the time of admission was diagnosed according to the Kidney Disease: Improving Global Outcomes (KDIGO) consensus definition for AKI, which includes the serum creatinine (SCr) level and urine output. The use of Scr has been reported to be very accurate in predicting COVID-19 AKI (28). The presence of underlying chronic kidney disease (CKD) was determined based on laboratory data obtained in our hospital (n=81) within the previous 2 years. For the 34 patients without previous laboratory data in our hospital, the presence of CKD was determined from their medical history. In addition, SCr level was measured serially during hospitalization, and AKI was diagnosed retrospectively if the SCr level improved and the urine volume increased after intravenous hydration.

Urinary specimens at the time of admission were stored at -80'C until thawed for measurement of biomarkers of renal tubular cell damage. We used two markers, β2-microglobulin (β2M) and kidney injury molecule 1 (KIM-1), which are known to be associated with AKI.

2.3 Measurement of NETs and marker of endothelial damage

In vivo NET levels were quantified by measuring plasma levels of circulating nucleosome (histone-DNA) and MPO-DNA (Cell

Death Detection ELISA Plus Kit; Roche Diagnostics, Basel, Switzerland) levels, as described in our previous paper (27). The degree of endothelial injury or damage was assessed by plasma von Willebrand factor (vWF) levels determined using a commercially available ELISA kit (Ray Biotech, Peachtree Corners, GA, USA).

2.4 Study endpoints

The primary outcome was in-hospital mortality according to baseline NET levels. The duration of hospital stays, ICU admission rates, and COVID-19 AKI occurrence were also compared between higher and lower NET groups.

2.5 Statistical analysis

Variables with normal distributions, confirmed in Kolmogorov-Smirnov tests, were expressed as the mean ± standard deviation (SD). Categorical variables were expressed as percentages and were compared in chi-squared tests. An independent sample t-test was used to identify differences among groups based on continuous values. Pearson's correlation coefficient was calculated for circulating nucleosomes, MPO-DNA, IL-6, BNP, various biochemical factors, and comorbidities. Multiple logistic regression analyses were performed to evaluate the role of increased NET levels as a determinant of AKI. Cumulative survival curves were derived using the Kaplan-Meier method; differences between survival curves were compared using a log-rank test. A Cox proportional hazards model was used to identify independent factors in the development of the study's endpoints. The predictive value was expressed as a hazard ratio (HR) with the corresponding 95% confidence intervals (CIs). A p-value <0.05 was defined as indicating significance. All statistical analyses were performed using SPSS version 24.0 (IBM Corp., Armonk, NY, USA).

3 Results

3.1 Baseline characteristics

The 115 patients included in the analysis had a mean age of 67.6 ± 17.1 years, with ~50% of the patients being older than 70 years. Of the COVID-19 patients, 28 (24.3%) died. Differences in baseline demographic and clinical characteristics according to mortality are described in Table 1. Patients who died during hospitalization were significantly older than survivors and had unstable vital signs on admission (low oxygen saturation, high heart rate, and high respiratory rate). As expected, the rate of ICU admission rate and the need for MV were much higher in these patients. Of all patients, 75 (65.2%) had received a COVID-19 vaccination prior to admission. However, COVID-19 vaccination was not associated with mortality, and the viral load measured at the time of admission did not differ between patients who died and those who survived. However, the time from the last vaccination to infection was significantly longer in the former (152 vs. 111 days, p=0.022). Hypertension (56.5%) and diabetes (40.9%) were the most common comorbidities, but neither was associated with mortality. Pre-existing CKD was present in 35 (30.4%) patients, with a significantly higher prevalence of CKD and pre-existing heart failure (HF) in patients who died than in those who survived (53.6% vs. 23.0% for CKD, and 57.1% vs. 14.9% for HF). Other comorbidities were similar between the two groups.

Baseline biochemical parameters according to mortality are compared in Table 2. In patients who died during hospitalization, the WBC count, neutrophil count, and N/L ratio were significantly higher but the PWR and albumin levels were lower than in surviving patients. In addition, the levels of lactic acid, inflammatory cytokines, IL-6, hs-CRP, MCP-1, and procalcitonin were significantly higher in the patients who died than in those who survived.

3.2 AKI in COVID-19 infection

On admission, 43 patients (37.4%) had AKI, and the prevalence of AKI was significantly higher in patients who died than in those who survived (57.1% vs. 31.0%, p=0.009) (Table 1). Approximately one third of deceased patients required renal replacement therapy. AKI was also common in patients with pre-existing CKD or HF (60.0% in CKD vs. 26.3% in non-CKD, p=0.001, 40.5% with HF vs. 16.4% without HF, p=0.005).

COVID-19 AKI was very strongly associated with poor outcome (Figure 1). Patients with AKI had significantly higher rates of in-hospital mortality (38.1% vs. 16.4%, p=0.009), initial ICU admission (64.3% vs. 37.0%, p=0.004) and MV (33.3% vs. 11.0%, p=0.004) and a significantly longer hospital stay (22.4 ± 19.5 vs. 12.4 ± 10.0 days, p<0.001) than those without AKI (Figures 1A, B). A comparison of COVID-19 AKI and non-AKI patients at baseline showed that WBC (11,000 ± 5,760 vs. 7,900 ± 4,120) and neutrophil (9,280 ± 5,777 vs. 5,980 ± 3,940) counts were significantly higher (p=0.001 and p<0.001) and PWR was significantly lower (20.7 ± 9.0 vs. 31.2 ± 16.2, p<0.001) in the former. In addition, the levels of all inflammatory markers, including serum ln_IL-6 (4.2 ± 1.4 vs. 3.2 ± 1.4, p=0.001), ln_hs-CRP (4.0 ± 1.4 vs. 3.1 ± 1.5, p=0.004), blood lactate (2.6 ± 1.6 vs. 1. 8 ± 1.2, p=0.040), procalcitonin (6.4 ± 11.4 vs. 1.1 ± 2.4, p=0.038) and BNP (792.5 ± 601.4 vs. 207.5 ± 311.4, p=0.001) were significantly higher in patients with AKI than in those without AKI (Figures 1C, D). For urinary biomarkers, urinary KIM-1/creatine (p=0.022) and β2M (p=0.006) levels were significantly higher in patients with AKI compared to non-AKI patients.

3.3 NETs, AKI and mortality in COVID-19 infection

In the COVID-19 patients, we measured two representative markers of NETs, circulating nucleosomes and MPO-DNA, and both were closely associated (Figure 2A). Parameters associated with circulating nucleosome levels were previous coronary artery disease

TABLE 1 Baseline characteristics according to mortality.

Variables	Total (n = 115)	Mortality		p
		Survivor (n = 87)	Death (n = 28)	
Age (years)	67.6 ± 17.1	66.4 ± 16.8	72.6 ± 17.2	0.046
> 70 years	57 (49.6)	38 (43.7)	19 (67.9)	0.022
Gender, Male, n (%)	63 (54.8)	49 (56.3)	14 (50)	0.356
BMI, kg/m^2	23.4 ± 5.7	23.9 ± 5.9	21.9 ± 4.8	0.100
Vital Signs				
SBP, mmHg	131.1 ± 28.8	131.1 ± 2.4.4	130.9 ± 40.0	0.972
DBP, mmHg	76.7 ± 16.9	77.7 ± 14.1	73.6 ± 23.8	0.268
MBP, mmHg	95.5 ± 18.5	95.8 ± 15.3	94.4 ± 26.3	0.730
HR (/min)	92 ± 22	88 ± 20	102 ± 27	0.007
RR (/min)	22 ± 4	21 ± 4	23 ± 4	0.034
Saturation, room air (%)	91.6 ± 10.2	93.8 ± 7.7	84.7 ± 13.5	<0.001
ICU admission, n (%)	54 (47.0)	32 (36.8)	22 (78.6)	<0.001
Mechanical ventilation, n (%)	22 (19.1)	8 (9.2)	14 (50.0)	<0.001
Previous vaccination, n (%)				0.539
None	40 (34.8)	30 (34.5)	10 (35.8)	
1-2	32 (27.8)	23 (26.4)	9 (32.1)	
≥ 3	43 (37.4)	34 (39.5)	9 (32.1)	
Time from last vaccination, day*	120 ± 67	111 ± 57	152 ± 87	0.022
Viral load				
Ct_value_E_gene	23.0 ± 6.0	23.3 ± 6.4	23.6 ± 6.5	0.407
Ct_value_RdRp_gene	23.2 ± 6.1	22.2 ± 4.6	22.2 ± 4.5	0.309
Comorbidities				
Diabetes, n (%)	47 (40.9)	39 (44.8)	8 (28.6)	0.096
Hypertension, n (%)	65 (56.5)	48 (55.2)	17 (60.7)	0.386
Coronary artery disease, n (%)	16 (13.9)	10 (11.5)	6 (21.4)	0.156
Heart failure, n (%)	29 (25.2)	13 (14.9)	16 (57.1)	<0.001
Cerebrovascular disease, n (%)	19 (16.5)	15 (17.2)	4 (14.3)	0.485
Chronic kidney disease, n (%)	35 (30.4)	20 (23.0)	15 (53.6)	0.003
COPD, n (%)	5 (4.3)	3 (3.4)	2 (7.1)	0.353
Liver cirrhosis, n (%)	5 (4.3)	3 (3.4)	2 (7.1)	0.353
Malignancy, n (%)	25 (21.7)	17 (19.5)	8 (28.6)	0183
Dementia, n (%)	19 (16.6)	15 (17.2)	4 (14.3)	0.639
Long-term care facilities, n (%)	13 (11.3)	8 (9.2)	5 (17.8)	0.297
AKI at admission, n (%)	43 (37.4)	27 (31.0)	16 (57.1)	0.009
Total hospital stays, days	16.1 ± 11.4	14.2 ± 12.5	22.0 ± 18.1	0.017

*among 75 patients with vaccination, BMI, body mass index; SBP, systolic BP; DBP, diastolic BP; HR, heart rates; RR, respiratory rates; ICU, intensive care units; Ct-value, the cycle threshold value; COPD, chronic obstructive lung disease; AKI, acute kidney injury.

10.3389/fimmu.2023.1122510

TABLE 2 Biochemical parameters by median NET level and mortality.

Variables	Mortality		p	Nucleosome, median		p
	Survivor (n = 87)	Death (n = 28)		Low (n = 56)	High (n = 59)	
NET markers*						
Nucleosome, OD	0.90 (0.47-1.68)	1.78 (1.19-2.0)	0.010	0.53(0.37-0.82)	1.89 (1.5-2.2)	<0.001
MPO-DNA, OD	0.21(0.13-0.38)	0.33 (0.12-0.5)	0.034	0.18(0.13-0.35)	0.33 (0.1-0.6)	0.003
Biochemical parameters						
WBC,/ul	8397 ± 4642	11216 ± 5475	0.008	7592 ± 3742	10576 ± 5536	0.001
Hemoglobin, g/dL	11.8 ± 2.4	10.9 ± 1.9	0.081	12.0 ± 2.5	11.3 ± 2.2	0.134
Neutrophil,/ul	6470 ± 4515	9418 ± 5595	0.006	5713 ± 3584	8657 ± 4588	0.001
Lymphocyte,/ul	1201 ± 752	940 ± 687	0.112	1148 ± 743	1137 ± 752	0.888
Platelet, $x10^3$/ul	219 ± 97	164 ± 114	0.016	220 ± 101	184 ± 105	0.079
N/L ratio	7.1 ± 5.4	17.4 ± 10.6	<0.001	6.8 ± 5.3	12.3 ± 13.0	0.012
P/W ratio	30.7 ± 14.8	17.2 ± 8.9	<0.001	32.5 ± 16.8	22.6 ± 10.9	<0.001
Albumin, g/dL	3.8 ± 0.5	3.3 ± 0.7	0.003	3.8 ± 0.6	3.4 ± 0.5	0.035
Lactic acid	1.8 ± 1.3	3.0 ± 2.6	0.007	1.8 ± 1.1	2.4 ± 1.8	0.149
BNP, pg/mL	169 ± 330	1202 ± 1523	<0.001	256 ± 678	601 ± 1022	0.032
BUN, mg/dL	23.2 ± 16.2	34.8 ± 22.4	0.004	21.4 ± 17.1	29.7 ± 15.6	0.017
Creatinine, mg/dL	1.7 ± 1.8	2.7 ± 2.0	0.013	1.4 ± 1.0	2.4 ± 2.1	0.025
eGFR, at admission	64.5 ± 31.3	41.9 ± 31.3	0.001	66.8 ± 55.5	52.5 ± 32.8	0.018
<60 mL/min/1.73m^2	35 (40.2)	19 (67.89)	0.010	22 (39.3)	32 (54.2)	0.078
<45 mL/min/1.73m^2	26 (29.9)	17 (60.7)	0.004	16 (28.6)	27 (45.8)	0.040
<30 mL/min/1.73m^2	16 (18.4)	16 (57.1)	<0.001	10 (17.9)	22 (37.3)	0.017
Need for RRT**	10 (11.5)	8 (28.6)	0.036	5 (8.9)	13 (22.0)	0.046
Inflammatory markers						
IL-6, pg/mL***	3.2 ± 1.4	4.6 ± 1.2	<0.001	3.4 ± 1.4	3.7 ± 1.5	0.251
MCP-1, pg/ml	88.3 ± 61.5	128.4 ± 77.9	0.008	89.1 ± 61.4	105.9 ± 72.5	0.204
Procalcitonin, ng/mL***	-1.7 ± 1.9	-0.1 ± 2.0	<0.001	-1.7 ± 1.9	-0.9 ± 2.1	0.027
Endothelial damage marker						
vWF, (μg/mL)	14.2 ± 9.5	15.6 ± 9.2	0.441	11.5 ± 7.8	17.2 ± 9.8	0.002

All data are expressed as mean ± SD except for those with *, which are expressed as median with range. **including both AKI patients with dialysis and CKD patients undergoing chronic dialysis ***log-transformed.

MPO, myeloperoxidase; WBC, white blood cell; N/L, neutrophil/lymphocyte; P/W, platelet/WBC; BNP, B-type natriuretic peptide; BUN, blood urea nitrogen; IL-6. Interleukin-6; MCP-1, monocyte- chemoattractant protein-1; vWF, von-Willebrand Factor.

(r=0.185, p=0.048), HF (r=0.241, p=0.010), WBC count (r=0.258, p<0.001), neutrophil count (r=0.348, p<0.001), PWR (r=−0.347, p<0.001), and eGFR (r=-0.272, p=0.003), (Figures 2B–D). In contrast, the levels of inflammatory markers, including serum IL-6, hs-CRP, and MCP-1, did not correlate with circulating nucleosome levels (Figure 2E). Only procalcitonin levels showed a marginally significant correlation (r=0.173, p=0.072). However, in contrast to inflammatory cytokine levels, higher nucleosome levels had a strong positive correlation with vWF levels (r=0.356, p<0.001), a marker of endothelial damage (Figure 2F). This finding suggests an association between NETs and endothelial damage. There were no significant correlations between vWF and either the IL-6 or MCP-1 levels.

In addition, higher levels of NETs were significantly associated with AKI. As shown in Figure 3A, patients with COVID-19 AKI had significantly higher circulating nucleosomes (p=0.008) and peripheral neutrophil counts (p<0.001) but lower PWR (p<0.001) compared to patients without AKI (Figure 3B). The prevalence of AKI was 50.8% in the high NET group but 21.4% in the low NET group (p=0.001). Supporting these findings, urinary markers of AKI, urinary KIM-1/creatine (r=0.368, p=0.001) and β2M (r=0.218,

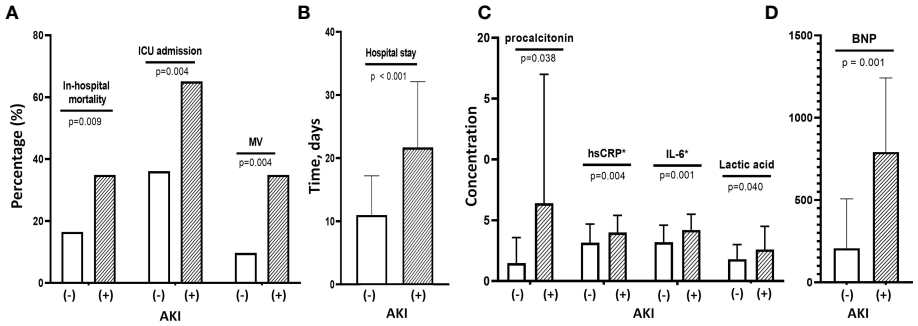

FIGURE 1
Clinical findings and outcomes associated with COVID-19 AKI. **(A)** Patients with COVID-19 AKI had significantly higher rates of in-hospital mortality, initial ICU admission and use of MV compared with patients without AKI. **(B)** These patients with AKI also had longer hospital stays than those without AKI. **(C)** Baseline levels of inflammatory cytokines such as hsCRP, IL-6 and procalcitonin as well as lactic acid levels were significantly higher in patients with AKI than in those without. **(D)** They also had higher baseline BNP levels than those without AKI. MV, mechanical ventilation; AKI, acute kidney injury; hsCRP, high-sensitivity C-reactive protein; IL-6, interleukin-6; BNP, B-type natriuretic peptide.

p=0.049) levels were well-correlated with circulating nucleosome levels (Figure 3C).

We also found that the NET markers, nucleosomes and MPO-DNA, were significantly higher in patients who died than in those who survived (Figure 4A). Similarly, there were significant differences in peripheral neutrophil counts and PWR between the two groups (Figure 4B). When the nucleosome levels were divided into two groups based on the median levels, patients in the higher NET group had significantly worse clinical outcomes than those in the lower NET group (Figures 4C, D). In a Cox regression analysis, higher NET level was independently associated with the risk of in-hospital mortality (unadjusted HR 3.81; 95% CI 1.43–10.16, p=0.007). Even after adjustment for risk factors, higher NET level remained a significant predictor of death (HR 3.21, 95% CI 1.08–9.19, p=0.035) (Table 3).

3.4 Association between higher NET and AKI

Given the strong association between NET and AKI, the risk of COVID-19 AKI associated with higher levels of NET was investigated. In a logistic regression model, significant predictors of AKI in unadjusted analysis, were age >70 years (OR 2.58, 95% CI

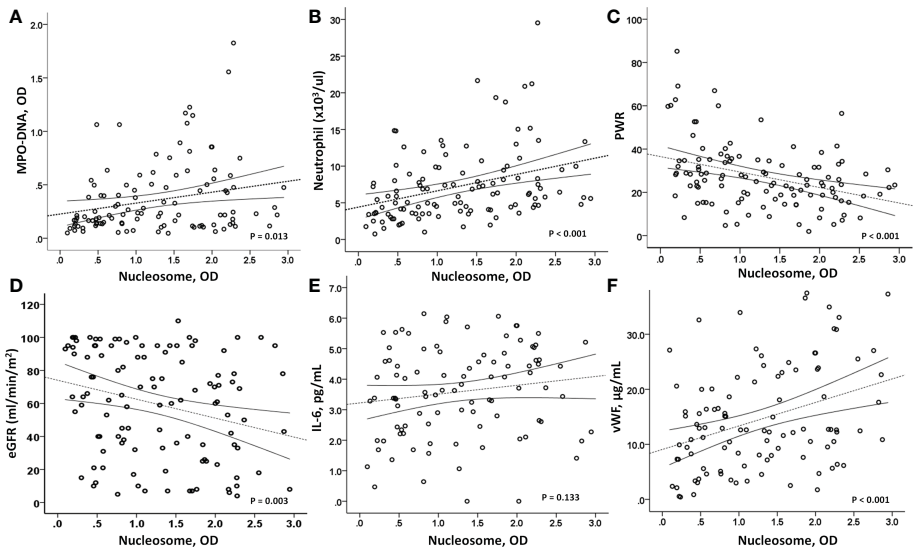

FIGURE 2
Correlation analysis. **(A)** As a marker of NETosis, circulating nucleosome levels were closely associated with MPO-DNA levels (p=0.013). **(B, C)** In addition, a strong correlation between circulating nucleosome levels and peripheral neutrophils (p<0.001) and platelet/WBC ratio (p<0.001) was observed. **(D)** And the nucleosome levels were inversely associated with renal function, eGFR (p=0.003). Interestingly, **(E)** nucleosome levels did not correlate with IL-6 (p=0.133), but **(F)** a strong positive association was observed with vWF levels (p<0.001), suggesting a close relationship between high nucleosome levels and endothelial dysfunction. MPO-DNA, myeloperoxidase-DNA; PWR, platelet/WBC ratio; eGFR, estimated glomerular filtration rate; IL-6, interleukin-6; vWF, von-Willebrand factor.

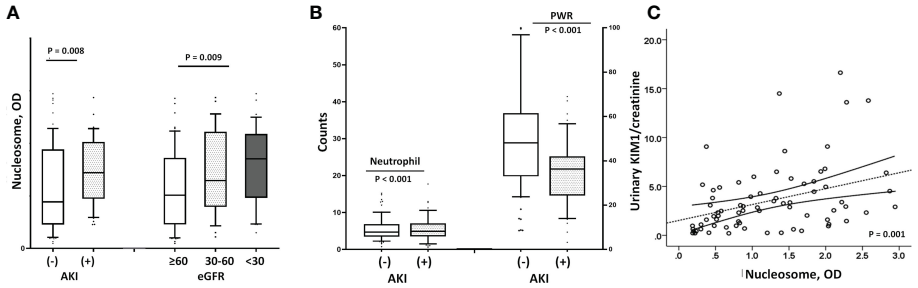

FIGURE 3
Relationship between renal dysfunction and nucleosome levels. **(A)** Patients with AKI had higher nucleosome levels than those without [median with IQR; 1.57 (1.05-1.81) vs. 0.87 (0.45-1.79), p=0.008], and the lower the eGFR, the higher the nucleosome level (p=0.009). **(B)** Similar to the findings with circulating nucleosomes, patients with COVID-19 AKI had significantly higher peripheral neutrophil counts (9288 ± 5777 vs. 5979 ± 3948, p<0.001) and lower PWRs (20.8 ± 9.0 vs. 31.3 ± 16.2, p<0.001) than those without AKI. **(C)** Urinary marker of AKI, the urinary KIM1/creatinine ratio also correlated significantly with higher nucleosome levels (r=0.368, p=0.001). AKI, acute kidney injury; eGFR, estimated glomerular filtration rate; KIM1/creatinine, kidney injury molecule 1/creatinine; BNP, B-type natriuretic peptide.

1.17–5.65, p=0.018), pre-existing CKD (OR 4.21, 95% CI 1.82–9.76, p=0.001), higher IL-6 (OR 1.65, 95% CI 1.19–2.30, p=0.002), higher BNP levels (OR 2.31, 95% CI 1.05–5.04, p=0.036) and higher NET (OR 3.79, 95% CI 1.87–8.58, p=0.001). After model adjustment for age >70 years, sex, diabetes, pre-existing comorbidities, and IL-6 and BNP levels, a higher NET (OR 3.67, 95% CI 1.30–10.41, p=0.014), pre-existing CKD (OR 8.55, 95% CI 2.07–35.38, p=0.010) and increased IL-6 (OR 1.59, 95% CI 1.09-2.32, p=0.016) were significant determinants of COVID-19 AKI (model 3) (Table 4).

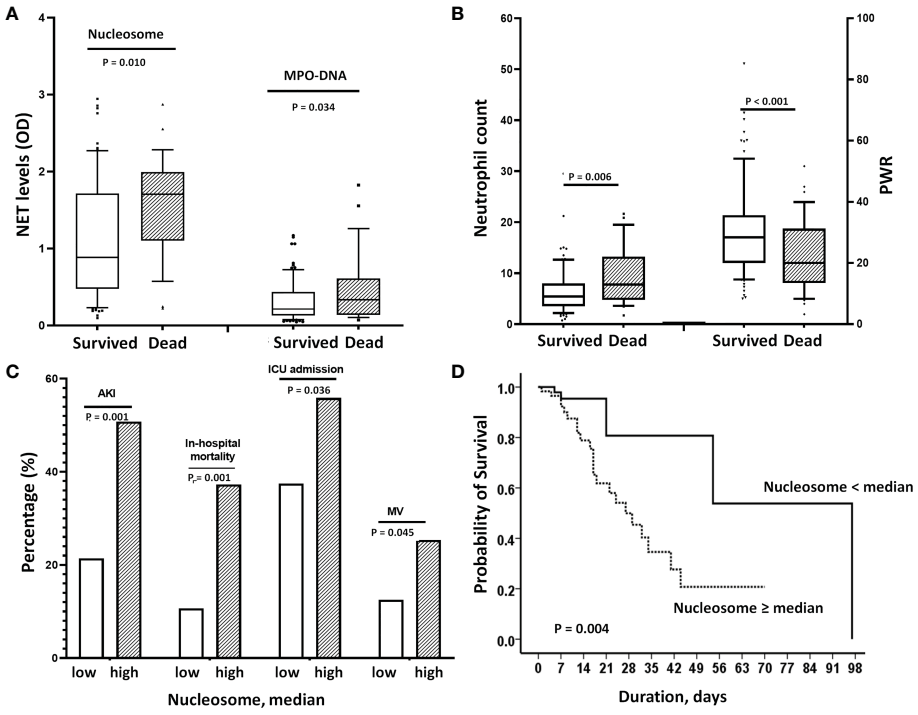

FIGURE 4
Effect of elevated NETs on mortality. **(A)** Nucleosome and MPO-DNA levels were significantly higher in patients who died than in those who survived [nucleosome: 1.78 (1.19-2.0 vs, 0.90 (0.47-1.68), p=0.010, MPO-DNA: 0.33 (0.12-0.5) vs. 0.21(0.13-0.38), p=0.034]. **(B)** Similarly, deceased patients had higher neutrophil counts (p=0.006) and lower PWRs (p<0.001) than survivors. **(C)** When nucleosome levels were divided into 2 groups according to median levels, patients in the high nucleosome group had worse clinical outcomes; significantly higher rates of AKI, in-hospital mortality, initial ICU admission and use of MV. **(D)** Kaplan-Meier analysis showed that higher nucleosome levels (>median) were associated with increased in-hospital mortality. In the adjusted Cox's proportional hazards regression model, it significantly increased the risk by 3.2-fold. NET, neutrophil extracellular trap; PWR, platelet/WBC ratio; AKI, acute kidney injury; ICU, intensive care unit; BNP, MV, mechanical ventilation.

TABLE 3 Clinical Factors Influencing In-Hospital Mortality in COVID-19 Patients.

	Unadjusted		Adjusted	
Mortality	HR (95% CI)	P	HR (95% CI)	P
Age, year	1.02 (1.01-1.08)	0.030	0.98 (0.94-1.01)	0.208
Sex, male	1.10 (0.75-1.59)	0.619	–	–
SBP <90 mmHg	2.85 (1.08-7.51)	0.034	1.84 (0.56-5.95)	0.309
AKI at admission	2.52 (1.19-5.33)	0.015	1.11 (0.42-2.92)	0.835
NET > median	3.81 (1.43–10.16)	0.004	3.21 (1.08-9.19)	0.035
PWR	0.92 (0.88-0.96)	0.001	0.95 (0.89-1.00)	0.050
IL-6*	2.00 (1.35-2.95)	0.004	1.46 (0.93-2.30)	0.098
BNP > median	10.24 (3.10-33.95)	<0.001	5.92 (1.50-23.26)	0.011

*log transformed, AKI, acute kidney injury; PWR, platelet/WBC ratio; IL-6. Interleukin-6; BNP, B-type natriuretic peptide.
"-" this variable is not included in the adjusted analysis.

3.5 Comparison of nucleosome levels, neutrophil count and PWR for predicting prognosis

As the neutrophil count or the PWR at the time of admission was found to be as good as the nucleosome level in predicting clinical outcome, the sensitivity and specificity of these variables in predicting prognosis were compared using ROC analysis. We found that the AUCs of circulating nucleosome, peripheral neutrophil count, and P/W ratio were very similar; 0.678, 0.640, and 0.761 for mortality prediction and 0.681, 0.666, and 0.717 for AKI prediction, respectively. Pairwise comparisons showed that the difference between AUCs was not statistically significant, suggesting the usefulness of peripheral neutrophil count and PWR in predicting outcomes (Supplementary Figure 1).

4 Discussion

Our study provides evidence that elevated levels of NETs in patients with COVID-19 are closely associated with AKI, and that higher NET-related AKI is a strong predictor of higher mortality. We measured two markers of NETs, circulating nucleosomes and MPO-DNA, and found that both were significantly higher in patients with AKI than in those without AKI at admission. The urinary KIM/creatinine ratio and β2M were also significantly increased in patients with higher nucleosome levels than in those without, suggesting a role for NETs in renal injury. The increased risk of AKI with higher NET levels was independent of age, pre-existing CKD or inflammatory cytokine levels.

It was first proposed in 2004 that NETosis contributes to the first line of host defense against invading microorganisms (29). Although NETs have a protective role against pathogens, these complexes have been implicated in several thrombo-inflammatory conditions, including sepsis, thrombosis, and respiratory failure (1). Support for the pathogenic role of NETs comes from studies showing that the inhibition of neutrophils and NETs is protective in models of influenza-associated ARDS. This observation sparked interest in the role and clinical features of NETs in COVID-19 infections. The first detection of NETs in the plasma of SARS-CoV-2-infected patients was followed by reports of a significant role of NETs in COVID-19 (6). Elevated levels of blood neutrophils and NETs are an early indicator of SARS-CoV-2 infection, predicting severe respiratory disease and worse outcomes (6, 7, 30). In addition, neutrophils exposed to live SARS-CoV-2 develop NETs to a greater extent than other neutrophils, suggesting that SARS-

TABLE 4 Risk of AKI in association with high NET level.

	Unadjusted		Model 1		Model 2		Model 3	
AKI, at admission	OR (95% CI)	P	OR (95% CI)	P	OR (95% CI)	P	OR (95% CI)	P
NET > median	3.79 (1.87-8.58)	0.001	3.91 (1.70-9.01)	0.001	2.83(1.16-6.61)	0.023	3.67 (1.30-10.41)	0.014
Age >70 years	2.58 (1.17-5.65)	0.018	2.43 (1.05-5.66)	0.039	2.46 (1.02-5.95)	0.044	2.03 (0.62-4.54)	0.401
diabetes	1.13 (0.53-2.45)	0.435	1.22 (0.58-2.83)	0.632	1.10 (0.60-2.00)	0.580	0.90 (0.17-1.90)	0.555
Pre-existing CKD	4.21 (1.82-9.76)	0.001	–		3.84 (1.37-10.72)	0.010	8.55 (2.07-35.38)	0.010
IL-6	1.65 (1.19-2.30)	0.002	–		–		1.59 (1.09-2.32)	0.016
BNP > median	2.31 (1.05-5.04)	0.036	–		–		0.64 (0.40-1.02)	0.631

Model 1, adjusted with age>70, sex, and diabetes Model 2, model 1 + adjustment for pre-existing CKD, Model 3: model 4 + adjustment for BNP and ln_IL-6.
CKD, chronic kidney disease; IL-6. Interleukin-6; BNP, B-type natriuretic peptide.
"-" this variable is not included in the adjusted analysis.

CoV-2 infection is a pro-NETosis state (20). The virus itself as well as damaged epithelial cells, activated platelets, activated endothelial cells, and inflammatory cytokines are thought to trigger NETosis in COVID-19 (3, 8, 31).

As with the pulmonary complications of COVID-19, renal complications associated with COVID-19 have recently been reported. In particular, AKI is common, especially in ICU patients (32). In our patients, the prevalence of AKI at the time of admission was 36.5% and as high as 55% in patients admitted to the ICU (33). Consistent with other data (8, 18, 19), our study shows that COVID-19 AKI is associated with significantly higher rates of ICU admission, a greater need for MV, increased in-hospital mortality, and longer hospital stays. Recently, the 25th Consensus Conference of the Acute Disease Quality Initiative proposed that endothelial dysfunction, coagulopathy, tubular damage, and complement activation are key mechanisms of COVID-19 AKI (33–35). Intravascular NETs may also contribute to COVID-19 AKI by inducing microvascular inflammation and thrombosis (26). Indeed, endothelial dysfunction associated with microvascular damage and pro-thrombotic conditions leading to thrombotic occlusion of the renal microvasculature may be a key feature of NET-associated AKI (36, 37). In support of this, our data show that nucleosome levels correlate very strongly with a higher serum vWF levels, a marker of endothelial activation and damage. And the nucleosome and vWF levels were significantly higher in those with AKI than in those without.

We also found that patients with high nucleosome levels had significantly lower PWR than those with low nucleosome levels, and that low PWR predicted AKI and mortality as well as nucleosome levels. Like neutrophils, platelets also play an important role in the intravascular immune response. In COVID-19 patients, platelets coordinate with neutrophils to release NETs, which can induce platelet-neutrophil aggregates with thrombocytopenia (38, 39). These can activate the procoagulant cascade, which is associated with the prognosis of septic death and microvascular thrombosis and subsequent organ dysfunction (40, 41). Consistent with our findings, a recent study from Thailand found that PWR can be an accurate predictor of in-hospital mortality in patients with severe COVID-19 pneumonia (42). These findings suggest the importance and utility of neutrophil count and PWR in predicting clinical outcomes in COVID-19.

One of the hallmarks of COVID-19 infection is systemic inflammation leading to a cytokine storm (43, 44), which in turn has been implicated in severe multi-organ failure during acute viral infection (45, 46). High levels of pro-inflammatory cytokines are associated with more severe respiratory disease. Our study also shows significantly higher serum levels of IL-6, MCP-1, and procalcitonin in COVID-19 patients who died than in those who survived, but surprisingly, plasma nucleosome levels were not associated with IL-6 and MCP-1 levels. In contrast to our findings, Zuo et al. reported that cell-free DNA is strongly associated with CRP levels in patients with severe COVID-19 infection (6, 26). The difference in results may be due to the fact that cell-free DNA is a less specific marker of NETs and therefore may correlate with the overall level of inflammation, rather than being specific to neutrophil activation. Another possible explanation for the difference is that serum IL-6 or MCP-1 levels may not fully represent the overall immune activation status in COVID-19 infections. In fact, circulating levels of IL-6 are significantly lower in patients with COVID-19 than in patients with sepsis (47). This suggests that cytokines are only moderately elevated in COVID-19 and are therefore unlikely to have a significant relationship with NET levels in these patients (33). Another alternative explanation is that NETs are more closely associated with endothelial damage and coagulation dysfunction rather than representing a cytokine storm, although the latter may be involved in significant crosstalk with NETs (21). It is also possible that the close association between NETs and the hyperinflammatory response is only seen in severe cases. Further research is needed to fully understand their interactions, as well as the role of systemic inflammation and NET formation in COVID-19 AKI.

This study had several limitations. First, blood samples were taken at the time of admission, but the duration of the disease from the onset of symptoms will have varied greatly given the differences in the severity of symptoms between patients. In addition, some patients were transferred from another hospital during their treatment. Second, it was not possible to adjust for the effect of antiviral therapy in predicting prognosis because the dose and duration of antiviral agents used depended on the patient's clinical situation. Third, NETs may have been partially degraded over time, which would have affected their measurement. Fourth, it would be helpful to compare circulating nucleosome levels between non-hospitalized and hospitalized COVID-19 patients to show the prognostic significance of high nucleosome levels. However, it was practically difficult to collect blood and urine samples from non-hospitalized COVID-19 patients, most of whom are in quarantine. Fifth, the diagnostic or prognostic cut-off value of circulating nucleosomes has not yet been established. Therefore, we arbitrarily divided the patients into 2 groups according to the median value. Finally, a causal relationship between COVID-19 AKI and NETs could not be established in this study, nor could we evaluate the long-term effects of NETs or AKI on mortality after patient discharge. Furthermore, the relationship between NETs and COVID-19 vaccination and the prognostic role of NETs in COVID-19 patients with different vaccination histories is uncertain. Future studies should investigate the predictive power of circulating NETs and NET-related AKI in well-characterized longitudinal cohorts with different vaccination histories.

In conclusion, elevated levels of NETs in patients with COVID-19 can predict in-hospital mortality. In addition, higher NETs were significant determinants of COVID-19 AKI, independent of age, pre-existing CKD, and inflammatory cytokine levels. Circulating nucleosome levels were strongly associated with higher vWF, but not with inflammatory cytokine levels, suggesting a role for NETs in endothelial injury or coagulopathy in the development of COVID-19 AKI. Our results suggest a role for NET-related AKI in NET-related mortality, mediated by vascular injury and inflammation. However, a causal relationship between NETs and AKI or poor outcomes remains to be established.

Data availability statement

The raw data supporting the conclusions of this article will be made available by the authors, without undue reservation.

Ethics statement

The studies involving human participants were reviewed and approved by HALLYM 2022-02-014-001. The patients/participants provided their written informed consent to participate in this study.

Author contributions

J-KK and YK: Study design, set-up, data analysis and interpretation. J-KK, IK and HL: acquisition of experimental data and writing-up. DK: patient recruitment and clinical data acquisition. SK: Data analysis and statistical advisory. All authors contributed to the article and approved the submitted version.

Funding

This research was supported by Hallym university Research Fund (HURF-2022-02).

Conflict of interest

The authors declare that the research was conducted in the absence of any commercial or financial relationships that could be construed as a potential conflict of interest.

Publisher's note

Supplementary material

The Supplementary Material for this article can be found online at: https://www.frontiersin.org/articles/10.3389/fimmu.2023.1122510/full#supplementary-material

References

1. Mantovani A, Cassatella MA, Costantini C, Jaillon S. Neutrophils in the activation and regulation of innate and adaptive immunity. *Nat Rev Immunol* (2011) 11:519–31. doi: 10.1038/nri3024

2. Mcdonald B, Davis RP, Kim SJ, Tse M, Esmon CT, Kolaczkowska E, et al. Platelets and neutrophil extracellular traps collaborate to promote intravascular coagulation during sepsis in mice. *Blood* (2017) 129:1357–67. doi: 10.1182/blood-2016-09-741298

3. Cortjens B, De Boer OJ, De Jong R, Antonis AF, Sabogal Piñeros YS, Lutter R, et al. Neutrophil extracellular traps cause airway obstruction during respiratory syncytial virus disease. *J Pathol* (2016) 238:401–11. doi: 10.1002/path.4660

4. Twaddell SH, Baines KJ, Grainge C, Gibson PG. The emerging role of neutrophil extracellular traps in respiratory disease. *Chest* (2019) 156:774–82. doi: 10.1016/j.chest.2019.06.012

5. Guan WJ, Ni ZY, Hu Y, Liang WH, Ou CQ, He JX, et al. Clinical characteristics of coronavirus disease 2019 in China. *N Engl J Med* (2020) 382:1708–20. doi: 10.1056/NEJMoa2002032

6. Zuo Y, Yalavarthi S, Shi H, Gockman K, Zuo M, Madison JA, et al. Neutrophil extracellular traps in COVID-19. *JCI Insight* (2020) 5(11):e138999. doi: 10.1172/jci.insight.138999

7. Masso-Silva JA, Moshensky A, Lam MTY, Odish MF, Patel A, Xu L, et al. Increased peripheral blood neutrophil activation phenotypes and neutrophil extracellular trap formation in critically ill coronavirus disease 2019 (COVID-19) patients: A case series and review of the literature. *Clin Infect Dis* (2022) 74:479–89. doi: 10.1093/cid/ciab437

8. Ng JH, Hirsch JS, Hazzan A, Wanchoo R, Shah HH, Malieckal DA, et al. Outcomes among patients hospitalized with COVID-19 and acute kidney injury. *Am J Kidney Dis* (2021) 77:204–215.e201. doi: 10.1053/j.ajkd.2020.09.002

9. Sawhney S, Fraser SD. Epidemiology of AKI: Utilizing Large databases to determine the burden of AKI. *Adv Chronic Kidney Dis* (2017) 24:194–204. doi: 10.1053/j.ackd.2017.05.001

10. Golmai P, Larsen CP, Devita MV, Wahl SJ, Weins A, Rennke HG, et al. Histopathologic and ultrastructural findings in postmortem kidney biopsy material in 12 patients with AKI and COVID-19. *J Am Soc Nephrol* (2020) 31:1944–7. doi: 10.1681/ASN.2020050683

11. Sharma P, Uppal NN, Wanchoo R, Shah HH, Yang Y, Parikh R, et al. COVID-19-Associated kidney injury: A case series of kidney biopsy findings. *J Am Soc Nephrol* (2020) 31:1948–58. doi: 10.1681/ASN.2020050699

12. Werion A, Belkhir L, Perrot M, Schmit G, Aydin S, Chen Z, et al. SARS-CoV-2 causes a specific dysfunction of the kidney proximal tubule. *Kidney Int* (2020) 98:1296–307. doi: 10.1016/j.kint.2020.07.019

13. Fu EL, Janse RJ, De Jong Y, van der Endt VHW, Milders J, van der Willik EM, et al. Acute kidney injury and kidney replacement therapy in COVID-19: A systematic review and meta-analysis. *Clin Kidney J* (2020) 13:550–63. doi: 10.1093/ckj/sfaa160

14. Chan L, Chaudhary K, Saha A, Chauhan K, Vaid A, Zhao S, et al. AKI in hospitalized patients with COVID-19. *J Am Soc Nephrol* (2021) 32:151–60. doi: 10.1681/ASN.2020050615

15. Peng S, Wang HY, Sun X, Li P, Ye Z, Li Q, et al. Early versus late acute kidney injury among patients with COVID-19-a multicenter study from wuhan, China. *Nephrol Dial Transplant* (2020) 35:2095–102. doi: 10.1093/ndt/gfaa288

16. Portolés J, Marques M, López-Sánchez P, De Valdenebro M, Muñez E, Serrano ML, et al. Chronic kidney disease and acute kidney injury in the COVID-19 Spanish outbreak. *Nephrol Dial Transplant* (2020) 35:1353–61. doi: 10.1093/ndt/gfaa189

17. Russo E, Esposito P, Taramasso L, Magnasco L, Saio M, Briano F, et al. Kidney disease and all-cause mortality in patients with COVID-19 hospitalized in Genoa, northern Italy. *J Nephrol* (2021) 34:173–83. doi: 10.1007/s40620-020-00875-1

18. Cheng Y, Luo R, Wang K, Zhang M, Wang Z, Dong L, et al. Kidney disease is associated with in-hospital death of patients with COVID-19. *Kidney Int* (2020) 97:829–38. doi: 10.1016/j.kint.2020.03.005

19. Gupta S, Coca SG, Chan L, Melamed ML, Brenner SK, Hayek SS, et al. AKI treated with renal replacement therapy in critically ill patients with COVID-19. *J Am Soc Nephrol* (2021) 32:161–76. doi: 10.1681/ASN.2020060897

20. Veras FP, Pontelli MC, Silva CM, Toller-Kawahisa JE, De Lima M, Nascimento DC, et al. SARS-CoV-2-triggered neutrophil extracellular traps mediate COVID-19 pathology. *J Exp Med* (2020) 217(12):e20201129. doi: 10.1084/jem.20201129

21. Zhou Z, Ren L, Zhang L, Zhong J, Xiao Y, Jia Z, et al. Heightened innate immune responses in the respiratory tract of COVID-19 patients. *Cell Host Microbe* (2020) 27:883–90.e882. doi: 10.1016/j.chom.2020.04.017

22. Mulay SR, Linkermann A, Anders HJ. Necroinflammation in kidney disease. *J Am Soc Nephrol* (2016) 27:27–39. doi: 10.1681/ASN.2015040405

23. Jansen MP, Emal D, Teske GJ, Dessing MC, Florquin S, Roelofs JJ. Release of extracellular DNA influences renal ischemia reperfusion injury by platelet activation and formation of neutrophil extracellular traps. *Kidney Int* (2017) 91:352–64. doi: 10.1016/j.kint.2016.08.006

24. Nakazawa D, Kumar SV, Marschner J, Desai J, Holderied A, Rath L, et al. Histones and neutrophil extracellular traps enhance tubular necrosis and remote organ injury in ischemic AKI. *J Am Soc Nephrol* (2017) 28:1753–68. doi: 10.1681/ASN.2016080925

25. Jewell PD, Bramham K, Galloway J, Post F, Norton S, Teo J, et al. COVID-19-related acute kidney injury; incidence, risk factors and outcomes in a large UK cohort. *BMC Nephrol* (2021) 22:359. doi: 10.1186/s12882-021-02557-x

26. Henry BM, De Oliveira MHS, Cheruiyot I, Benoit J, Rose J, Favaloro EJ, et al. Cell-free DNA, neutrophil extracellular traps (NETs), and endothelial injury in coronavirus disease 2019- (COVID-19-) associated acute kidney injury. *Mediators Inflamm* (2022) 2022:9339411. doi: 10.1155/2022/9339411

27. Kim JK, Lee HW, Joo N, Lee HS, Song YR, Kim HJ, et al. Prognostic role of circulating neutrophil extracellular traps levels for long-term mortality in new end-stage renal disease patients. *Clin Immunol* (2020) 210:108263. doi: 10.1016/j.clim.2019.108263

28. Pode Shakked N, De Oliveira MHS, Cheruiyot I, Benoit JL, Plebani M, Lippi G, et al. Early prediction of COVID-19-associated acute kidney injury: Are serum NGAL and serum cystatin c levels better than serum creatinine? *Clin Biochem* (2022) 102:1–8. doi: 10.1016/j.clinbiochem.2022.01.006

29. Brinkmann V, Reichard U, Goosmann C, Fauler B, Uhlemann Y, Weiss DS, et al. Neutrophil extracellular traps kill bacteria. *Science* (2004) 303:1532–5. doi: 10.1126/science.1092385

30. Zhang B, Zhou X, Zhu C, Song Y, Feng F, Qiu Y, et al. Immune phenotyping based on the neutrophil-to-Lymphocyte ratio and IgG level predicts disease severity and outcome for patients with COVID-19. *Front Mol Biosci* (2020) 7:157. doi: 10.3389/fmolb.2020.00157

31. Sil P, Wicklum H, Surell C, Rada B. Macrophage-derived IL-1β enhances monosodium urate crystal-triggered NET formation. *Inflammation Res* (2017) 66:227–37. doi: 10.1007/s00011-016-1008-0

32. Legrand M, Bell S, Forni L, Joannidis M, Koyner JL, Liu K, et al. Pathophysiology of COVID-19-associated acute kidney injury. *Nat Rev Nephrol* (2021) 17:751–64. doi: 10.1038/s41581-021-00452-0

33. Nadim MK, Forni LG, Mehta RL, Connor MJJr., Liu KD, Ostermann M, et al. COVID-19-associated acute kidney injury: consensus report of the 25th acute disease quality initiative (ADQI) workgroup. *Nat Rev Nephrol* (2020) 16:747–64. doi: 10.1038/s41581-020-00356-5

34. Noris M, Benigni A, Remuzzi G. The case of complement activation in COVID-19 multiorgan impact. *Kidney Int* (2020) 98:314–22. doi: 10.1016/j.kint.2020.05.013

35. Su H, Yang M, Wan C, Yi LX, Tang F, Zhu HY, et al. Renal histopathological analysis of 26 postmortem findings of patients with COVID-19 in China. *Kidney Int* (2020) 98:219–27. doi: 10.1016/j.kint.2020.04.003

36. Fuchs TA, Brill A, Duerschmied D, Schatzberg D, Monestier M, Myers DD Jr., et al. Extracellular DNA traps promote thrombosis. *Proc Natl Acad Sci USA* (2010) 107:15880–5. doi: 10.1073/pnas.1005743107

37. Salazar-Gonzalez H, Zepeda-Hernandez A, Melo Z, Saavedra-Mayorga DE, Echavarria R. Neutrophil extracellular traps in the establishment and progression of renal diseases. *Medicina (Kaunas)* (2019) 55(8):431. doi: 10.3390/medicina55080431

38. Liu Y, Sun W, Guo Y, Chen L, Zhang L, Zhao S, et al. Association between platelet parameters and mortality in coronavirus disease 2019: Retrospective cohort study. *Platelets* (2020) 31:490–6. doi: 10.1080/09537104.2020.1754383

39. Middleton EA, He XY, Denorme F, Campbell RA, Ng D, Salvatore SP, et al. Neutrophil extracellular traps contribute to immunothrombosis in COVID-19 acute respiratory distress syndrome. *Blood* (2020) 136:1169–79. doi: 10.1182/blood.2020007008

40. Layios N, Delierneux C, Hego A, Huart J, Gosset C, Lecut C, et al. Sepsis prediction in critically ill patients by platelet activation markers on ICU admission: A prospective pilot study. *Intensive Care Med Exp* (2017) 5:32. doi: 10.1186/s40635-017-0145-2

41. Wang D, Wang S, Wu H, Gao J, Huang K, Xu D, et al. Association between platelet levels and 28-day mortality in patients with sepsis: A retrospective analysis of a Large clinical database MIMIC-IV. *Front Med (Lausanne)* (2022) 9:833996. doi: 10.3389/fmed.2022.833996

42. Thungthienthong M, Vattanavanit V. Platelet-to-White blood cell ratio as a predictor of mortality in patients with severe COVID-19 pneumonia: A retrospective cohort study. *Infect Drug Resist* (2023) 16:445–55. doi: 10.2147/IDR.S398731

43. Mehta P, Mcauley DF, Brown M, Sanchez E, Tattersall RS, Manson JJ. COVID-19: consider cytokine storm syndromes and immunosuppression. *Lancet* (2020) 395:1033–4. doi: 10.1016/S0140-6736(20)30628-0

44. Liuzzo G, Patrono C. COVID 19: in the eye of the cytokine storm. *Eur Heart J* (2021) 42:150–1. doi: 10.1093/eurheartj/ehaa1005

45. Chu KH, Tsang WK, Tang CS, Lam MF, Lai FM, To KF, et al. Acute renal impairment in coronavirus-associated severe acute respiratory syndrome. *Kidney Int* (2005) 67:698–705. doi: 10.1111/j.1523-1755.2005.67130.x

46. Tisoncik JR, Korth MJ, Simmons CP, Farrar J, Martin TR, Katze MG. Into the eye of the cytokine storm. *Microbiol Mol Biol Rev* (2012) 76:16–32. doi: 10.1128/MMBR.05015-11

47. Spittler A, Razenberger M, Kupper H, Kaul M, Hackl W, Boltz-Nitulescu G, et al. Relationship between interleukin-6 plasma concentration in patients with sepsis, monocyte phenotype, monocyte phagocytic properties, and cytokine production. *Clin Infect Dis* (2000) 31:1338–42. doi: 10.1086/317499

frontiers | Frontiers in Medicine

TYPE Case Report
PUBLISHED 10 May 2023
DOI 10.3389/fmed.2023.1158582

OPEN ACCESS

EDITED BY
Patrick Honore,
CHU UCL Namur Site Godinne, Belgium

REVIEWED BY
Bojan Joksimović,
Medical Faculty Foča, Bosnia and Herzegovina
Mauro Giuffrè,
University of Trieste, Italy

*CORRESPONDENCE
Jianchun Wang
✉ wangjianchun@medmail.com.cn

RECEIVED 04 February 2023
ACCEPTED 20 April 2023
PUBLISHED 10 May 2023

CITATION
Zhao Y, Feng D, Wang X, Sun Y, Liu J, Li X, Zhou N and Wang J (2023) Case report: Concurrent pylephlebitis and subarachnoid hemorrhage in an octogenarian patient with *Escherichia coli* sepsis. *Front. Med.* 10:1158582. doi: 10.3389/fmed.2023.1158582

Case report: Concurrent pylephlebitis and subarachnoid hemorrhage in an octogenarian patient with *Escherichia coli* sepsis

Yong Zhao[1,2], Dandan Feng[1,2], Xinyu Wang[1,3], Yuanyuan Sun[1,2], Junni Liu[1,2], Xiaodong Li[1,2], Nannan Zhou[1,2] and Jianchun Wang[1,2]*

[1]Department of Geriatrics, Shandong Provincial Hospital Affiliated to Shandong First Medical University, Jinan, Shandong, China, [2]Department of Geriatric Cardiology, Shandong Provincial Hospital Affiliated to Shandong First Medical University, Jinan, Shandong, China, [3]Department of Geriatric Neurology, Shandong Provincial Hospital Affiliated to Shandong First Medical University, Jinan, Shandong, China

Background: Pylephlebitis refers to an infective suppurative thrombosis that occurs in the portal vein and its branches. Concurrent pylephlebitis and subarachnoid hemorrhage (SAH) are rare but fatal for patients with sepsis. This scenario drives the clinicians into a dilemma of how to deal with coagulation and bleeding simultaneously.

Case summary: An 86-year-old man was admitted to hospital for chills and fever. After admission, he developed headache and abdominal distension. Neck stiffness, Kernig's and Brudzinski's sign were present. Laboratory tests discovered decreased platelet count, elevated inflammatory parameters, aggravated transaminitis, and acute kidney injury. *Escherichia coli* (*E. coli*) were identified in blood culture. Computed tomography (CT) revealed thrombosis in the superior mesenteric vein and portal veins. Lumbar puncture and Brain CT indicated SAH. The patient had eaten cooked oysters prior to illness. It was speculated that the debris from oyster shell might have injured his intestinal mucosa and resulted in bacterial embolus and secondary thrombosis in portal veins. The patient was treated with effective antibiotics, fluid resuscitation, and anticoagulation. The dose titration of low molecular weight heparin (LMWH) under close monitoring attributed to diminution of the thrombosis and absorption of SAH. He recovered and was discharged after 33-day treatment. One-year follow-up indicated that the post-discharge course was uneventful.

Conclusion: This report describes a case of an octogenarian with *E. coli* septicemia who survived from concurrent pylephlebitis and SAH along with multiple organ dysfunction syndrome. For such patients with life-threatening complications, even in the acute stage of SAH, decisive employment of LMWH is essential to resolve thrombosis and confers a favorable prognosis.

KEYWORDS

sepsis, pylephlebitis, subarachnoid hemorrhage, octogenarian, disseminated intravascular coagulation, anticoagulation

Introduction

Pylephlebitis is a common complication of intra-abdominal infections. The incidence is 0.37–2.7 cases per 100,000 person-years. Most patients (70%) are male with a median age of 50 years. The most common pathogen is *Escherichia coli (E. coli)*, and the mortality rangs from 8.7 to 19%. Sepsis is prevalent in nearly 60% of the patients with pylephlebitis and is a potent risk factor for mortality (1, 2). Sepsis is defined as life-threatening organ dysfunction due to a dysregulated host response to infection (3). The mortality of sepsis is 66.7/100,000 in China, and increases dramatically with age. It is 71.3/100,000 in the elderly aged 60–64 and 3136.5/100,000 in those ≥85 (4). The mortality could conceivably be more horrendous in septic patients who develop disseminated intravascular coagulation (DIC). Here we report a very elderly patient who successfully survived from *E. coli* septicemia complicating DIC, pylephlebitis, subarachnoid hemorrhage (SAH), and reactive arthritis.

Case description

An 86-year-old man was admitted to our hospital on Feb. 13, 2020 with the chief complaint of chills and fever during the past 13 h. His body temperature had been at the peak of 39.0°C. Apart from fatigue and weakness, he vomited bile-stained fluid. Medical history included well-controlled essential hypertension, stable coronary artery disease, and asymptomatic cholelithiasis. On admission, physical examination did not reveal any remarkable signs. His body temperature was 35.0°C, pulse rate 87 beats per minute, respiratory rate 21 breaths per minute, blood pressure 102/62 mmHg, and oxygen saturation 96%. Electrocardiogram showed sinus rhythm and normal ST segments. Laboratory tests demonstrated that the serum amylase, lipase, and urinary amylase were all within the reference ranges, but the inflammatory parameters increased and the platelet count decreased ($102\times10^3/\mu L$). In addition, mild transaminitis and acute kidney injury were present (Table 1). Conventional chest CT, which covered part of the epigastrium, reported not only chronic inflammation in both lungs, but intrahepatic gas and cholecystolithiasis. The gas was perplexing, because it was hard to tell whether it was in the intrahepatic bile ducts or in the portal venous system. Anyway, all the rapid changes indicated a severe infection.

The patient was managed empirically with intravenous moxifloxacin, a fluoroquinolone antibiotic, but his condition deteriorated 8 h after admission. Fever recurred with chills. The temperature increased to 38.8°C. Venous blood was drawn immediately for germiculture and antibiotic susceptibility test. Then, he started to show unbearable headache and abdominal distension, neck stiffness, and Kernig's and Brudzinski's sign. No tenderness was detected in the abdomen. The platelets dropped abruptly to $46\times10^3/\mu L$ in 24 h and to $27\times10^3/\mu L$ in 48 h. D-dimer was >20 mg/L. Blood culture for 12 h was astonishingly positive for Gram-negative bacilli, and then E. coli was identified. Contrast-enhanced abdomen CT (Figures 1A1, A2) was conducted on hospital day 2. The image of thrombosis with diffuse gas was demonstrated in the superior mesenteric and portal veins, which suggested a hypercoagulable state of DIC caused by *E. coli* bacteremia. Abdominal ultrasonography revealed a normal gallbladder wall and common bile duct, but a mural thrombus in the main portal vein. A trace-back inquiry revealed that the patient had eaten cooked oysters and spat out debris of the shells prior to becoming ill. It was speculated that the debris from oyster shell might have injured his intestinal mucosa and resulted in systemic inflammation and bacterial embolus.

However, the most worrying point was what actually caused the neurological anomaly: purulent meningitis or cerebral hemorrhage? For the time being, the patient was in the hypercoagulable state of DIC, which was manifested as diffuse venous thrombosis. Meanwhile, he got caught in a consumed hypocoagulable stage with an apparent drop of platelets. Hence, intracranial hemorrhage was strongly suspected. Unfractionated heparin was intended to be attempted but was abandoned because of the uncertainty of cerebral condition. Nevertheless, antibiotic regimen was switched to cefoperazone/sulbactam and then imipenem/cilastatin upon results of pathogenic culture and susceptibility test, which showed that the strains of E. coli were most susceptible to these antibiotic agents. Levornidazole was added later to reinforce the antimicrobial therapy. Human immunoglobulin, fresh plasma, recombinant human thrombopoietin, and platelets were administered as well. However, the headache was getting even worse. It was urgent to identify the cause of the encephalopathy. On hospital day 5, a stratification of cerebrospinal fluid (CSF) in the lateral ventricles was suspected on brain magnetic resonance imaging. The substratum had the feature of high signal on T1WI, which implied SAH. Lumbar puncture yielded bloody CSF with an opening pressure of 200 mmH_2O. Hemophagocytosis was observed, but CSF culture was negative for any bacteria. These results ruled out purulent meningitis and confirmed the presence of SAH. Corticosteroids, diuretics, and mannitol were used to lower the elevated intracranial pressure and prevent cerebral edema. On the very night, the patient experienced a grand mal epilepsy lasting for about 10 min. Phenobarbital sodium was injected intramuscularly, and valproate sodium and levetiracetam were taken orally. The temperature began to drop since the adjustment of antibiotics based on culture result, and the inflammatory parameters declined as well. Although persistent, the headache did not aggravate. Neither chills nor epileptic seizure happened again.

It looked like the patient was on the mend, but 10 days after admission, his abdominal discomfort became the dominant symptom. He was anorexic, and complained of abdominal distension. He defecated only once on hospital day 3, and passed less flatus since then. Therefore, adynamic ileus was considered. Meanwhile, the laboratory parameters got worse again. WBC was $14.08\times10^3/\mu L$ with 88.6% neutrophilia. Among the hepatic biomarkers, bilirubins were moderately compromised, and gamma-glutamyl transferase (GGT) increased to 398 U/L. Abdominal ultrasonography discovered extension of thrombus from the main portal vein to its branches. Contrast-enhanced abdomen CT was repeated. It showed that the thrombosis in superior mesenteric and portal veins enlarged distinctly, and the left branch of portal vein was completely obstructed, which was speculated to be responsible for above symptoms and aberrant

TABLE 1 Laboratory results.

			Hospitalization														Follow-up			
			Year 2020														Year 2020			Year 2021
	Biomarkers	Reference	Feb. 13 Day 1	Feb. 14 Day 2	Feb. 15 Day 3	Feb. 16 Day 4	Feb. 17 Day 5	Feb. 18 Day 6	Feb. 20 Day 8	Feb. 24 Day 12	Feb. 26 Day 14	Feb. 29 Day 17	Mar. 2 Day 19	Mar. 5 Day 22	Mar. 9 Day 26	Mar. 15 Day 32	Apr. 7	May. 22	Dec. 11	Feb. 20
Inflammation	WBCs ($\times 10^3/\mu L$)	3.5–9.5	5.37	11.56	8.08	7.94	8.56	7.4	11.53	14.08	7.06	7.71	5.29	4.24	5.38	6.81	5.64	6.59	–	5.74
	Neutrophils (%)	40–75	89.7	92.5	85.4	84.3	80	81.4	77.3	88.6	78.6	77.6	68.6	63	64.9	68.3	52.3	49.8	–	48.3
	CRP (mg/L)	0–8	66.16	136.8	138.9	116.8	99.7	60.37	18.55	29.71	24.47	44.3	42.27	24.97	–	5.3	2.14	–	–	–
	PCT (ng/ml)	0–0.05	5.22	10.8	10.99	3.64	1.81	1.25	0.49	0.26	–	0.16	0.14	0.29	0.1	0.06	–	–	–	–
Coagulation	Platelets ($\times 10^3/\mu L$)	125–350	102	46	27	60	55	74	179	321	322	311	267	242	234	217	188	182	–	–
	D-dimers (mg/L)	0–0.5	–	>20	>20	7.05	4.41	4.6	6.73	4.35	2.97	2.19	–	1.38	1.2	0.75	0.58	–	–	–
	FDPs (μg/ml)	0–5	–	–	–	–	–	10.67	13.69	8.69	5.95	5.3	–	3.21	3	1.79	2.70	–	–	–
	PT (sec)	9.4–12.5	–	18.5	16	16.7	15.1	12.4	12	12.1	12.4	13.4	–	12.1	12.7	11.8	13.4	12.1	–	–
	Fibrinogen (g/L)	2.38–4.98	–	3.42	3.73	4.04	4.18	3.68	3.02	3.83	3.38	4.09	–	4.14	3.52	3.17	3.31	2.84	–	–
Heart	HS-TnT (pg/ml)	0–14	32.23	112	–	–	22.8	15.48	12.2	10.7	–	–	–	–	–	–	–	–	–	–
	CK-MB (ng/ml)	0.1—4.94	1.16	3.92	–	–	1.07	0.89	0.56	1.17	–	–	–	–	–	–	–	–	–	–
	NT-proBNP (pg/ml)	<1,800	246.9	–	–	4132	5006	6270	1269	478	–	–	–	–	–	–	–	–	–	–
Liver	AST (U/L)	15–40	71	77	54	39	–	20	61	57	89	68	46	35	23	24	45	35	41	31
	ALT (U/L)	9–50	44	43	33	30	–	19	43	74	103	100	75	51	27	25	49	25	29	23
	GGT (U/L)	10–60	59	84	70	91	–	131	236	398	393	478	432	342	281	189	114	119	107	78
	Total BIL (μmol/L)	3.5–23.5	44.53	52.3	27.97	21.93	–	18.5	14.06	31.61	22.19	26.34	23.08	11.99	13.04	12.23	19.56	25.26	20.35	22.61
	Direct BIL (μmol/L)	0.5–6.5	17.92	20.36	9.56	7.31	–	5.27	3.96	9.35	6.09	7.39	6.41	3.64	3.57	2.75	3.28	4.34	3.48	3.44
	Indirect BIL (μmol/L)	1–17	26.61	31.94	18.41	14.62	–	12.23	10.1	22.26	16.1	18.95	16.67	8.35	9.47	9.48	16.28	20.92	16.87	19.17
	Albumin (g/L)	40–55	42	36	29.7	29.8	–	33.8	32	38.9	32	33	32.1	30.7	33.3	35.3	42.3	40.9	46.3	44.5
Kidneys	BUN (mmol/L)	2.8–7.14	8.7	7.7	11	4.7	3.8	6	9.4	4.3	4.1	3.8	3.4	4.6	4	4.1	5.3	4.2	5.1	5.0
	Creatinine (μmol/L)	0–135	139.4	101.1	107.9	87.9	72.5	74.4	65.7	49.8	49.9	57.5	61.1	58.8	62.7	56.8	73.8	82.6	91.0	81.4
	Cystatin C (mg/L)	0.63–1.25	1.31	1.12	1.22	0.92	0.95	1.08	1.31	0.95	0.99	1.06	0.94	1.07	1.14	1.22	1.24	–	1.26	–
	eGFR (ml/min/1.73m^2)	>90	44	60	54	75	79	72	64	86	83	77	83	76	72	70	84	–	66	–

ALT, indicates alanine aminotransferase; AST, aspartate aminotransferase; BIL, bilirubin; BUN, blood urea nitrogen; CK-MB, creatine kinase-MB; CRP, C-reactive protein. eGFR, estimated glomerular filtration rate; FDPs, fibrinogen degradation products; GGT, gamma-glutamyl transferase; HS-TnT, high-sensitivity troponin T; NT-proBNP, N-terminal B-type natriuretic peptide; PCT, Procalcitonin; PT, prothrombin time; WBCs, white blood cells.

10.3389/fmed.2023.1158582

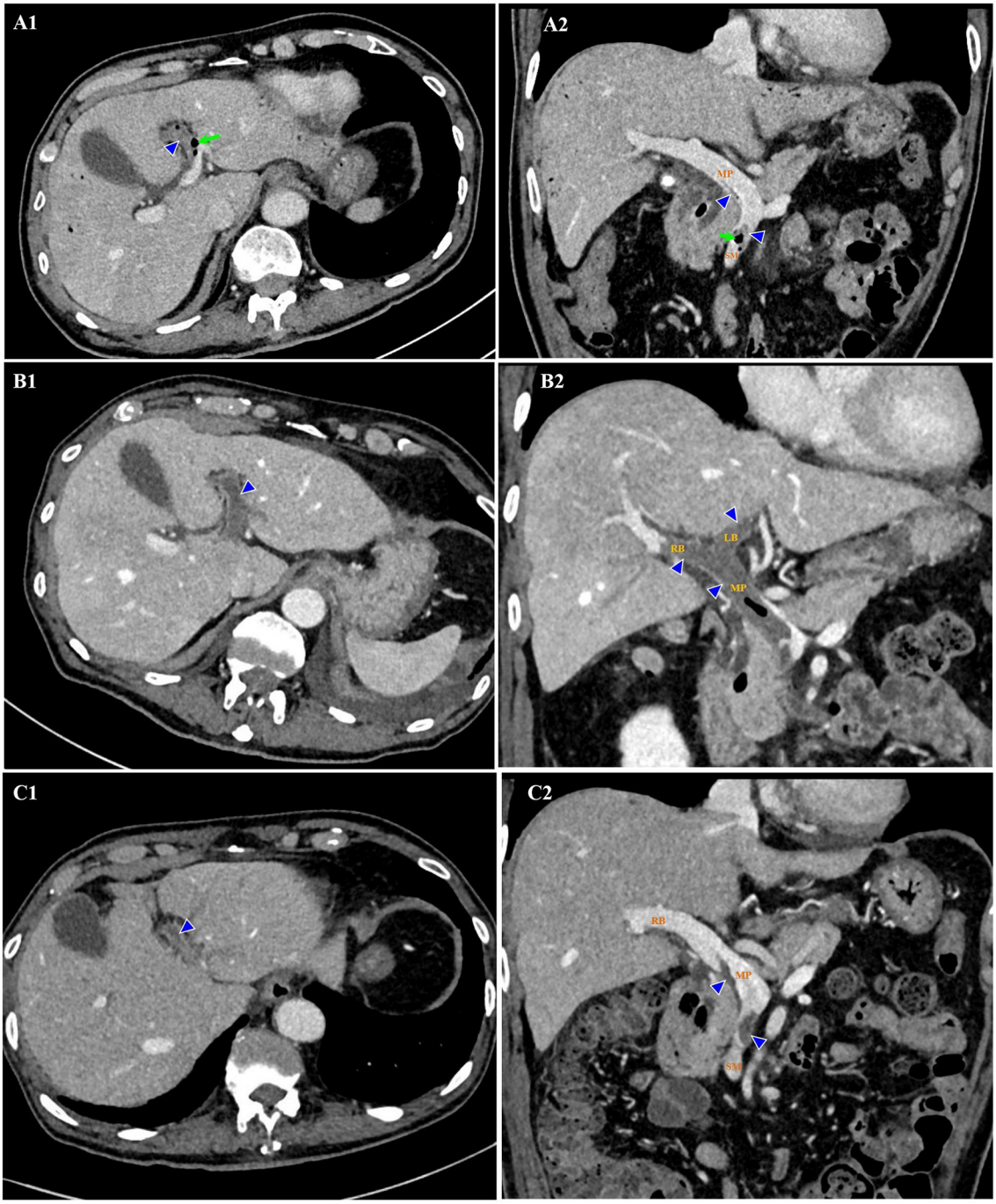

FIGURE 1
Thrombosis (triangles) and gas (arrows) in the superior mesenteric and portal veins on contrast-enhanced CT. Hospital day 2 (February 14, 2020). Thrombosis and gas in the LB of portal vein on axial view **(A1)**. Thrombosis in the SM and MP, and gas in the SM on coronal view **(A2)**. Hospital day 12 (February 24, 2020). Thrombosis enlarged in the extended LB of portal vein on axial view **(B1)**. Thrombosis enlarged in the MP, LB, and RB of portal vein, with gas in the MP on coronal view **(B2)**. Hospital day 23 (March 6, 2020). Thrombosis shrank in the LB of portal vein on axial view **(C1)**. Thrombosis shrank in the SM, MP, and RB of portal vein on coronal view **(C2)**. No gas was detected. CT indicates computed tomography; LB, left branch (of portal vein); MP, main portal vein; RB, right branch (of portal vein); SM, superior mesenteric vein.

laboratory findings (Figures 1B1, B2). Brain CT demonstrated SAH in the right and left parietal and occipital lobes (Figure 2A).

The patient was caught between Scylla and Charybdis. If the thrombosis had not been treated, liver failure and intestinal necrosis would have been resulted from persistent ischemia. But if anticoagulants had been delivered, SAH might have been exacerbated and threatened his life. We weighted the dilemma carefully. Because the SAH was thought to be diffuse oozing of blood resulting from thrombocytopenia, and the platelet count had recovered to 321 $\times$ $10^3/\mu L$ by now, we decided to try low molecular

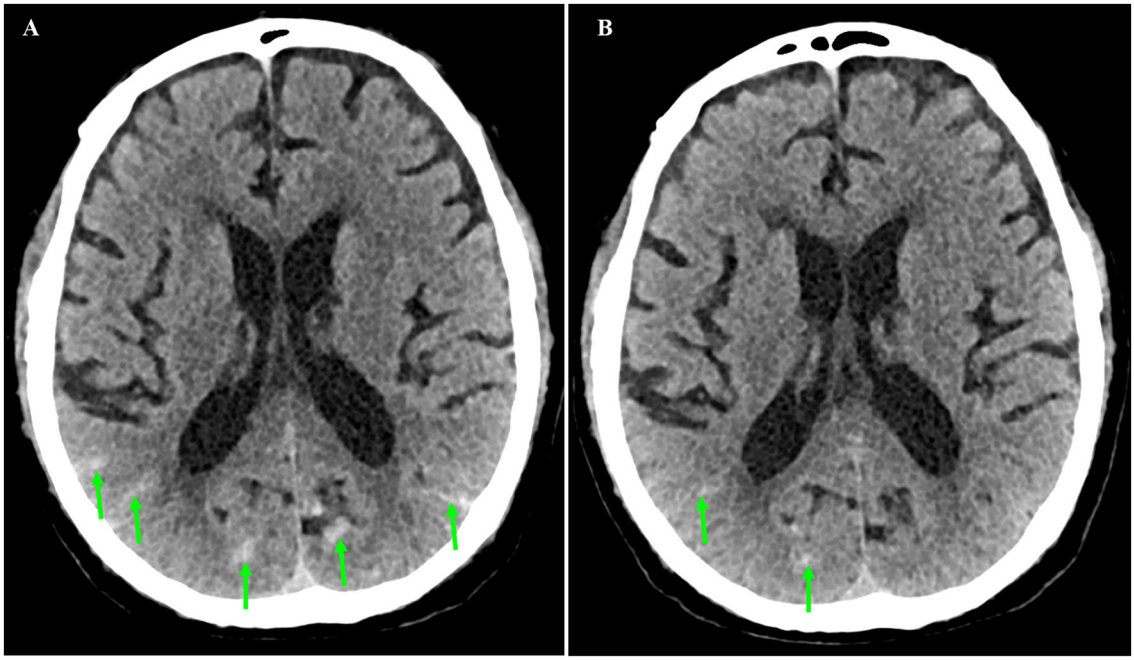

FIGURE 2
Axial sections of non-contrast brain computed tomography. **(A)** Subarachnoid hemorrhage was present in the right and left parietal and occipital lobes (arrow) on hospital day 12 (February 24, 2020). **(B)** Subarachnoid hemorrhage was almost absorbed on hospital day 23 (March 6, 2020).

weight heparin (LMWH) under close monitoring. Enoxaparin was started subcutaneously from a daily small dose of 2000 u. To our surprise, the symptoms and signs of adynamic ileus began to subside on the next day. Enoxaparin was supposed to bring about the improvement. Then it was up-titrated gradually to 3000 u on the 4th day and to 6,000 u on the 6th day. Abdominal ultrasonography detected blood flow in main portal vein, but not in the sagittal part of left portal vein. CT was repeated after 10 days of anticoagulation. In comparison with previous findings, not only thrombosis in the superior mesenteric and portal veins diminished (Figures 1C1, C2), but SAH in both sides was absorbed (Figure 2B). Enoxaparin had been kept in use for 18 days, and then was replaced by oral rivaroxaban.

It seemed that the patient's condition was getting better, however, the adventure was not over yet. When he woke up in the morning of hospital day 19, he felt pain in both wrists, and then fell into a sudden onset of chills with the temperature rising to 38.7°C. Physical examination detected symmetrical redness, swelling, and heat on his wrists. It was considered as reactive arthritis, although his human leukocyte antigen (HLA)-B27 allele was negative. Methylprednisolone and celecoxib were prescribed. This syndrome took a favorable turn on the next day.

After 33-day hospitalization, the patient's condition was greatly improved. Most laboratory abnormalities were normalized (Table 1). He was discharged on March 16, 2020. Table 2 shows the timeline for events and interventions during hospital stay. During the hospitalization, the patient's body weight reduced from 65 to 57 kg. He did not experience a septic shock or fluid depletion. His lowest mean arterial pressure was 72 mmHg, 24-h fluid input was 3,000–4,000 ml, and the urine output was 0.91–3.11 ml/kg/h. Renal function was assessed by estimated glomerular filtration rate (eGFR), which was calculated according to Creatinine-Cystatin C Equation (CKD-EPI 2012) (5). It was improved from 44 ml/min/1.73 m^2 at admission to 70 ml/min/1.73 m^2 at discharge.

Follow-up

Follow-up was performed via face-to-face interview. The post-discharge course was uneventful. Rivaroxaban had been taken orally for 3 months and then was stopped. The patient had no recurrence of pylephlebitis, and engaged in daily activities of life comfortably. He was very grateful to the medical workers for their professional help. Laboratory findings from April, 2020 to February, 2021 indicated that most of the biomarkers in inflammation, coagulation, and hepatic function were within the normal range except for a mildly elevated D-dimers and GGT (Table 1). Abdominal ultrasonography on March 17, 2021 showed that the superior mesenteric vein and the main portal vein were both patent without any thrombosis, but no blood flow was detected in the sagittal part of the left branch of portal vein.

Discussion

The present case reflects the diagnostic and therapeutic challenge in the elderly with sepsis. Identification of the pathogen and source is quite necessary for the management. Current guidelines recommend that broad-spectrum antibiotics should be administered intravenously within the 1st hour once the diagnosis of sepsis is confirmed (6). In this case, blood culture and antibiotic

10.3389/fmed.2023.1158582

TABLE 2 Timeline.

Date (Year 2020)	Hospital day	Events	Interventions
Feb. 13	1	• Admission to hospital. • Conventional chest CT demonstrated chronic inflammation in both lungs and gas in dilated intrahepatic bile ducts.	• Empiric therapy with intravenous antibiotic: Moxifloxacin.
Feb. 14	2	• Detection of Gram-negative bacilli in blood sample.	• Combination therapy with broad-spectrum antibiotics: Sulperazone and Imipenem. • Administration of intravenous immunoglobulin.
		• Platelet count 46,000/μL.	• Subcutaneous injection of recombinant human thrombopoietin.
		• Contrast-enhanced abdominal CT detected thrombus in the sagittal part of left portal vein and superior mesenteric vein. Gas was found in the main portal vein and its left and right branches, and superior mesenteric vein. But the gas in the left lobe of liver was decreased in comparison with that of last day.	• Supplement with fresh plasma.
Feb. 15	3	• Identification of E. Coli from blood culture.	• Dual antibiotics: Imipenem and Levornidazole.
		• Platelet count 27,000/μL.	• Platelet transfusion.
		• Abdominal ultrasonography revealed mural thrombus in the main portal vein.	• Intravenous infusion of unfractionated heparin.
Feb. 16	4	• Abdominal ultrasonography revealed extension of thrombus from the main portal vein to its sagittal part and superior mesenteric vein.	
Feb. 17	5	• Transient loss of consciousness and epileptic attack. • Subarachnoid hemorrhage confirmed by brain MRI and lumbar puncture.	• Low dose of Enoxaparin, a LMWH, had been tried for once, but then was suspended for fear of major bleeding. • Intracranial pressure was reduced with intravenous Mannitol for 9 days. • Anti-elilepsy was started with oral Depakine for 1 day, and then intramuscular Phenobarbital for 8 days and oral Levetiracetam up to discharge. • Alleviation of cerebral edema with intravenous methylprednisolone for once and then dexamethasone for 6 days. • Prevention of cerebral vasospasm with intravenous Nimodipine for 10 days and then oral Nimodipine up to discharge.
			• Deescalation of antibiotics from combination therapy to a broad-spectrum agent: Meropenem.
Feb. 18	6	• Abdominal ultrasonography detected blood flow in main portal vein, but not in the sagittal part.	
Feb. 20	8	• Blood sample was drawn for the 2nd bacterial culture.	
Feb. 24	12	• Contrast-enhanced abdominal CT demonstrated that the thrombus increased in the portal veins and superior mesenteric vein. The left branch of portal vein was completely obstructed. A small amount of gas was detected in the main portal vein and the lower part of common bile duct.	• Subcutaneous Enoxaparin was administered daily at low dose and then was titrated cautiously.
		• Brain CT confirmed subarachnoid hemorrhage in the parietal, occipital, and temporal lobes of both cerebral hemispheres.	
Feb. 25	13	• No bacteria was isolated in the 2nd blood culture.	• Escalation of antibiotics: Daptomycin was added to Meropenem.
Feb. 26	14	• Abdominal ultrasonography detected blood flow in main portal vein and mesenteric vein, but not in the sagittal part of left portal vein.	
Feb. 28	16	• Blood sample was drawn for the 3rd bacterial culture.	
Mar. 2	19	• Blood sample was drawn for the 4th bacterial culture.	• Deescalation of antibiotic to an effective narrow-spectrum agent: Sulperazone.
		• Reactive arthritis.	• Intravenous Methylprednisolone and oral Celebrex were administered for 4 days, then methylprednisolone was taken orally up to discharge.
Mar. 5	22	• No bacteria was isolated in the 3rd blood culture.	
		• Abdominal ultrasonography detected blood flow in main portal vein, but not in the sagittal part of left portal vein.	

(Continued)

TABLE 2 (Continued)

Date (Year 2020)	Hospital day	Events	Interventions
Mar. 6	23	• Contrast-enhanced abdominal CT demonstrated that the thrombus decreased in the portal veins and superior mesenteric vein. But the left branch of portal vein was still completely obstructed. No gas was detected in the main portal vein.	
		• Brain CT demonstrated improvement of subarachnoid hemorrhage.	
Mar. 8	25	• No bacteria was isolated in the 4th blood culture.	
Mar. 13	30		• LMWH and antimicrobial therapy were stopped. Rivaroxaban, a NOAC, was administered.
Mar. 16	33	• Discharge from hospital.	

CT, indicates tomography; LMWH, low molecular weight heparin; MRI, magnetic resonance imaging; NOAC, non-vitamin K antagonist oral anticoagulant.

susceptibility test were performed in time, which was crucial for the subsequent treatment. But it was hard to tell whether the invasive *E. Coli* was from injured intestinal mucosa or chologenic infection. The patient did have cholecystolithiasis, but he vomited bilious contents at the early onset of sepsis, which suggested no obstruction in the biliary tracts. In addition, the gallbladder was not hypertonic, and the location of stones in it was not fixed. It seemed that the chologenic infection was not likely the culprit. On the other hand, the patient came across some debris of shells when he was eating oysters. Thrombosis in the superior mesenteric and portal veins was detected on imaging study, which was probably in part due to bacterial embolus. It was reasonable to think that the injury to intestinal mucosa was the source of sepsis. A review reported that the most common site of thrombosis in patients with pylephlebitis was right portal vein (33%), followed by main portal vein (32%), superior mesenteric vein (31%), left portal vein (24%), splenic vein (18%), and inferior mesenteric vein (8%) (7). For this patient, main portal vein, left portal vein, right portal vein and superior mesenteric vein were all involved. Even anticoagulants were administrated for a long time, thrombosis in the sagittal part of left portal vein was resistant to resolve.

Although pylephlebitis was diagnosed by the fever, bacteremia, and radiological findings of portal and mesenteric vein thrombosis in the patient, it should be differentiated from other causes of acute abdomen presentation with systemic inflammatory response, such as acute suppurative cholecystitis, bacterial hepatic abscess, and acute pancreatitis. In this case, there was no history of chronic hepatic or pancreatic diseases. Physical examination did not find a palpable gallbladder with tenderness in the right upper quadrant of abdomen. Laboratory results showed normal amylase and lipase. Imaging tests did not revealed any signs of emphysematous cholecystitis, hypodense rounded contours in the liver, and enlargement of gallbladder or pancreas. Thus, pylephlebitis was considered as the principal diagnosis for this patient.

In terms of the primary complications of pylephlebites, pyogenic liver abscesses are present in 37% of cases. Other complications include intestinal ischaemia and portal hypertension (1). Multiple organ dysfunction syndrome (MODS) is common in septic patients. Sepsis-associated encephalopathy may result directly from the infection in central nervous system, but more often it is attributable to a variety of sterile neurologic disorders including stroke (8). A post mortem analysis showed that the prevalence of cerebral hemorrhage was 26% in patients who had died from septic shock (9). Lumbar puncture was critical for the differential diagnosis of SAH from purulent meningitis in this patient, and dictated the subsequent strategy of treatment. SAH was attributable to impaired synthesis of coagulation factors by hepatocytes and decreased platelet count because of excessive consumption. Sepsis-associated hepatic dysfunction may result from infection, overactive inflammatory response, or microvascular thrombosis. It is manifested as impaired clearance of bilirubin, decreased synthesis of proteins, disturbance of coagulation, and cholestasis (10). In this case, primary bacterial embolism and secondary thrombosis in the portal veins were responsible for the liver injury. Moreover, the patient had gone through an experience of cardiac and kidney injury. He got a decreased eGFR and elevated cardiac biomarkers (Table 1). Fortunately, these impairments were transient and reversible. He recovered with timely diagnosis and proper treatment.

Sepsis and coagulaopathy are entangled with each other. Thrombocytopenia below $50 \times 10^3/\mu L$ strongly suggests an unfavorable prognosis for patients with sepsis (11). International Society on Thrombosis and Haemostasis (ISTH) has devised a composite scoring system for the diagnosis of DIC, and a score equal or more than 5 was adopted as the cutoff value of criteria for overt DIC (12). As for the scoring algorithm criteria established by the Japanese Association for Acute Medicine (JAAM), a total score of 4 was accepted as the cutoff points to diagnose DIC, because it was validated as an early and sensitive predictor of organ dysfunction and poor outcomes in Logistic regression analysis (13). A multicenter retrospective observational study demonstrated that according to ISTH and JAAM criteria, the prevalence of DIC in patients with sepsis on intensive care unit admission was 29% and 61%, respectively (14). However, there is no consensus on the use of anticoagulants in pylephlebitis. It is generally believed that anticoagulation should be delivered to the patients with thrombosis progression. In a retrospective cohort study, 3 points or more according to both the ISTH overt and the JAAM DIC scoring systems was used as the optimal cutoff for initiation of anticoagulant therapy in septic patients with DIC. Results

showed that it was associated with a minimal all-cause in-hospital mortality and an acceptable incidence of bleeding complications (15). In addition, for patients with pylephlebitis, those treated with anticoagulants had a higher resolution rate of portal vein thrombosis than non-anticoagulated ones, without significant risk of major bleeding (16). In this case, sepsis-associated coagulopathy was much more complicated. The score was ≥5 points for DIC according to ISTH and JAAM criteria. Widespread thrombosis in the superior mesenteric and portal veins as well as SAH developed successively in only a couple of hours after the onset of sepsis, which was a fatal threat to an 86-year elderly patient. Scrupulous administration of enoxaparin at the right time was of crucial importance for saving his life. The situation did begin to take a change for the better thereafter. All the facts confirmed the benefits of early anticoagulation in septic patients with DIC.

The mortliaty of pylephlebitis ranges from 8.7% to 19%. However, it has been significantly reduced in recent decades due to improvement in the identification and treatment of this disease. The overall mortality was reported to be <10% in patients with pylephlebitis who were diagnosed after 2010 (1). An observational retrospective study from a tertiary hospital in Spain indicated that survivors usually had a good prognosis without recurrence of pylephlebitis, and anticoagulation was associated with a lower mortality (17).

Looking back at this case, we learned that the proper timing for this intervention might be as follows. First, there was no sign of active bleeding, even it was still at the acute stage of SAH. Second, platelet count had recovered to the normal range. Third, bacteremia had been under control. Anticoagulant therapy with LMWH should be started from a small dosage, and then be up-titrated gradually to a larger one under close monitoring.

Conclusion

We presented herein a rare case of an octogenarian patient with sepsis, who experienced pylephlebitis, SAH, MODS, and reactive arthritis. The pathogen was verified as *E. coli*. This patient had eaten cooked oysters prior to becoming ill. It was speculated that the debris from oyster shell might have injured his intestinal mucosa and resulted in bacterial embolus, which led to a secondary thrombosis in portal veins. Immediate microorganism culture is important for the verification of pathogen and subsequent treatment with optimal antibiotics. With the concurrent hemorrhage and thrombosis, the timing of anticoagulation is supremely important. Even in the acute stage of SAH, decisive employment of LMWH is essential to resolve thrombosis without aggravating bleeding and confers a favorable prognosis.

Data availability statement

The raw data supporting the conclusions of this article will be made available by the authors, without undue reservation.

Ethics statement

The studies involving human participants were reviewed and approved by Ethics Committee of Shandong Provincial Hospital Affiliated to Shandong First Medical University. The patients/participants provided their written informed consent to participate in this study. Written informed consent was obtained from the individual(s) for the publication of any potentially identifiable images or data included in this article.

Author contributions

YZ and JW were responsible for the conception, drafting, and critical revision of the manuscript. DF and XW contributed to the retrieval and review of relevant literature. YS and JL collected and assembled clinical information. NZ analyzed and interpreted the data. XL conducted the follow-up. All authors have read the manuscript and approved it for publication.

Funding

This work was supported by grants from China National Center for Biotechnology Development, Ministry of Science and Technology of the People's Republic of China (National Key R&D Program of China 2020YFC2008900).

Acknowledgments

We thank the patient for granting permission to publish his information. We are most grateful to the clinicians, nurses, pharmacists, and technicians in Shandong Provincial Hospital Affiliated to Shandong First Medical University for their remarkable contributions to the management of a life-threatening sepsis with concurrent pylephlebitis and subarachnoid hemorrhage in the octogenarian patient.

Conflict of interest

The authors declare that the research was conducted in the absence of any commercial or financial relationships that could be construed as a potential conflict of interest.

Publisher's note

References

1. Fusaro L, Di Bella S, Martingano P, Crocè LS, Giuffrè M. Pylephlebitis: a systematic review on etiology, diagnosis, and treatment of infective portal vein thrombosis. *Diagnostics*. (2023) 13:429. doi: 10.3390/diagnostics13030429

2. Jevtic D, Gavrancic T, Pantic I, Nordin T, Nordstrom CW, Antic M, et al. Suppurative thrombosis of the portal vein (Pylephlebits): a systematic review of literature. *J Clin Med.* (2022) 11:4992. doi: 10.3390/jcm11174992

3. Seymour CW, Liu VX, Iwashyna TJ, Brunkhorst FM, Rea TD, Scherag A, et al. Assessment of clinical criteria for sepsis: for the third international consensus definitions for sepsis and septic shock. *JAMA*. (2016) 315:762–74. doi: 10.1001/jama.2016.0288

4. Weng L, Zeng XY, Yin P, Wang LJ, Wang CY, Jiang W, et al. China critical care clinical trials group (CCCCTG). Sepsis-related mortality in China: a descriptive analysis. *Intensive Care Med.* (2018) 44:1071–80. doi: 10.1007/s00134-018-5203-z

5. Inker LA, Schmid CH, Tighiouart H, Eckfeldt JH, Feldman HI, Greene T, et al. CKD-EPI Investigators. Estimating glomerular filtration rate from serum creatinine and cystatin. *CN Engl J Med.* (2012) 367:20–9. doi: 10.1056/NEJMoa1114248

6. Rhodes A, Evans LE, Alhazzani W, Levy MM, Antonelli M, Ferrer R, et al. Surviving sepsis campaign: international guidelines for management of sepsis and septic shock: 2016. *Intensive Care Med.* (2017) 43:304–77. doi: 10.1007/s00134-017-4683-6

7. Choudhry AJ, Baghdadi YM, Amr MA, Alzghari MJ, Jenkins DH, Zielinski MD. Pylephlebitis: a review of 95 cases. *J Gastrointest Surg.* (2016) 20:656–61. doi: 10.1007/s11605-015-2875-3

8. Gotts JE, Matthay MA. Sepsis: pathophysiology and clinical management. *BMJ.* (2016) 353:i1585. doi: 10.1136/bmj.i1585

9. Sharshar T, Annane D, de la Grandmaison GL, Brouland JP, Hopkinson NS, Françoise G. The neuropathology of septic shock. *Brain Pathol.* (2004) 14:21–33. doi: 10.1111/j.1750-3639.2004.tb00494.x

10. Woznica EA, Inglot M, Woznica RK, Łysenko L. Liver dysfunction in sepsis. *Adv Clin Exp Med.* (2018) 27:547–51. doi: 10.17219/acem/68363

11. Greco E, Lupia E, Bosco O, Vizio B, Montrucchio G. Platelets and multi-organ failure in sepsis. *Int J Mol Sci.* (2017) 18:2200. doi: 10.3390/ijms18102200

12. Taylor FB Jr, Toh CH, Hoots WK, Wada H, Levi M. Scientific subcommittee on disseminated intravascular coagulation (DIC) of the international society on thrombosis and haemostasis (ISTH). Towards definition, clinical and laboratory criteria, and a scoring system for disseminated intravascular coagulation. *Thromb Haemost.* (2001) 86:1327–30. doi: 10.1055/s-0037-1616068

13. Gando S, Iba T, Eguchi Y, Ohtomo Y, Okamoto K, Koseki K, et al. A multicenter, prospective validation of disseminated intravascular coagulation diagnostic criteria for critically ill patients: comparing current criteria. *Crit Care Med.* (2006) 34:625–31. doi: 10.1097/01.CCM.0000202209.42491.38

14. Saito S, Uchino S, Hayakawa M, Yamakawa K, Kudo D, Iizuka Y, et al. Japan septic disseminated intravascular coagulation (JSEPTIC DIC) study group. Epidemiology of disseminated intravascular coagulation in sepsis and validation of scoring systems. *J Crit Care.* (2019) 50:23–30. doi: 10.1016/j.jcrc.2018.11.009

15. Yamakawa K, Umemura Y, Murao S, Hayakawa M, Fujimi S. Optimal timing and early intervention with anticoagulant therapy for sepsis-induced disseminated intravascular coagulation. *Clin Appl Thromb Hemost.* (2019) 25:1076029619835055. doi: 10.1177/1076029619835055

16. Naymagon L, Tremblay D, Schiano T, Mascarenhas J. The role of anticoagulation in pylephlebitis: a retrospective examination of characteristics and outcomes. *J Thromb Thrombolysis.* (2020) 49:325–31. doi: 10.1007/s11239-019-01949-z

17. Belhassen-García M, Gomez-Munuera M, Pardo-Lledias J, Velasco-Tirado V, Perez-Persona E, Galindo-Perez I, et al. Pylephlebitis: incidence and prognosis in a tertiary hospital. *Enferm Infecc Microbiol Clin.* (2014) 32:350–4. doi: 10.1016/j.eimc.2013.09.002

frontiers | Frontiers in Immunology

TYPE Original Research
PUBLISHED 28 June 2023
DOI 10.3389/fimmu.2023.1087691

OPEN ACCESS

EDITED BY
Alessandra Stasi,
University of Bari Aldo Moro, Italy

REVIEWED BY
Guoyun Chen,
University of Tennessee Health Science Center (UTHSC), United States
Jing Liu,
University of Illinois Chicago, United States

*CORRESPONDENCE
Jianqiang Mei
mjq1000000@sina.com
Fenqiao Chen
chenfenqiao@126.com

†These authors have contributed equally to this work

RECEIVED 02 March 2023
ACCEPTED 12 June 2023
PUBLISHED 28 June 2023

CITATION
Wang Q, Wang C, Zhang W, Tao Y, Guo J, Liu Y, Liu Z, Liu D, Mei J and Chen F (2023) Identification of biomarkers related to sepsis diagnosis based on bioinformatics and machine learning and experimental verification.
Front. Immunol. 14:1087691.
doi: 10.3389/fimmu.2023.1087691

Identification of biomarkers related to sepsis diagnosis based on bioinformatics and machine learning and experimental verification

Qianfei Wang[1,2†], Chenxi Wang[1†], Weichao Zhang[1,2], Yulei Tao[1,2], Junli Guo[1,2], Yuan Liu[1,2], Zhiliang Liu[1,2], Dong Liu[1,2], Jianqiang Mei[2*] and Fenqiao Chen[2*]

[1]Hebei University of Chinese Medicine, Shijiazhuang, China, [2]The First Affiliated Hospital ,Hebei University of Chinese Medicine, Shijiazhuang, China

Sepsis is a systemic inflammatory response syndrome caused by bacteria and other pathogenic microorganisms. Every year, approximately 31.5 million patients are diagnosed with sepsis, and approximately 5.3 million patients succumb to the disease. In this study, we identified biomarkers for diagnosing sepsis analyzed the relationships between genes and Immune cells that were differentially expressed in specimens from patients with sepsis compared to normal controls. Finally, We verified its effectiveness through animal experiments. Specifically, we analyzed datasets from four microarrays(GSE11755、GSE12624、GSE28750、GSE48080) that included 106 blood specimens from patients with sepsis and 69 normal human blood samples. SVM-RFE analysis and LASSO regression model were carried out to screen possible markers. The composition of 22 immune cell components in patients with sepsis were also determined using CIBERSORT. The expression level of the biomarkers in Sepsis was examined by the use of qRT-PCR and Western Blot (WB). We identified 50 differentially expressed genes between the cohorts, including 2 significantly upregulated and 48 significantly downregulated genes, and KEGG pathway analysis identified Salmonella infection, human T cell leukemia virus 1 infection, Epstein–Barr virus infection, hepatitis B, lysosome and other pathways that were significantly enriched in blood from patients with sepsis. Ultimately, we identified COMMD9, CSF3R, and NUB1 as genes that could potentially be used as biomarkers to predict sepsis, which we confirmed by ROC analysis. Further, we identified a correlation between the expression of these three genes and immune infiltrate composition. Immune cell infiltration analysis revealed that COMMD9 was correlated with T cells regulatory (Tregs), T cells follicular helper, T cells CD8, et al. CSF3R was correlated with T cells regulatory (Tregs), T cells follicular helper, T cells CD8, et al. NUB1 was correlated with T cells regulatory (Tregs), T cells gamma delta, T cells follicular helper, et al. Taken together, our findings identify potential new diagnostic markers for sepsis that shed light on novel mechanisms of disease pathogenesis and, therefore, may offer opportunities for therapeutic intervention.

KEYWORDS

sepsis, gene, pathways, RNA, immune infiltration

1 Introduction

Sepsis occurs when pathogenic microorganisms and their toxins invade the blood circulatory system (1, 2). The resulting immune system hyperactivation produces a variety of inflammatory cytokines and inflammatory mediators that cause systemic inflammatory response syndrome, and this can lead to multiple organ failure and shock (3). Worldwide, approximately 31.5 million people develop sepsis each year, and the disease is fatal for approximately 5.3 million of them (4). Unfortunately, the number of sepsis cases and related deaths continues to increase each year.

The pathogenesis of sepsis is complex, and it is generally believed to be related to dysregulation of the pro-inflammatory/anti-inflammatory responses, coagulation disorders, bacterial and endotoxin translocation, and gene polymorphisms. The uncontrolled inflammatory response plays a particularly important role in the rapid disease progression that is characteristic of sepsis. However, although this is well established and disease biomarkers such as PCT, white blood cell (WBC) count, and C-reactive protein (CRP) are used to inform on the disease state (5), the currently available approaches are often insufficient for clinicians to predict, monitor, and respond to changes in the condition of patients in a timely manner and with sufficient data to improve clinical outcomes. Therefore, the development of improved diagnostic biomarkers reflecting inflammation to improve clinical treatment of patients with sepsis is an urgent unmet medical need.

Several recent studies have identified specific genes that are involved in the pathogenesis and progression of sepsis (6–8). However, to date, the diagnostic value of many genes in sepsis has not been investigated. Currently, few studies have reported on target genes and immune cells in the blood or tissues of patients with sepsis. In this study, four microarrays(GSE11755, GSE12624, GSE28750, GSE48080) were merged into one comprehensive dataset to identify genes that are differentially expressed in patients with sepsis. We identified three genes, COMMD9, CSF3R, and NUB1, that were differentially expressed in sepsis compared to non-pathological specimens, and we correlated the differential expression of these genes with the immune cell composition of immune infiltrate. These findings identify novel genes that may be relevant for the pathogenesis of sepsis and that may be useful as diagnostic or predictive biomarkers for early disease detection.

2 Methods

2.1 Animals specimens

This study used nine healthy, six-week-old male Sprague Dawley (SD) rats with body weight 200 ± 20 g obtained from the Beijing Weitong Lihua Laboratory Animal Technology Co., Ltd. The animals were reared in three separate cages (3 per cage) in the animal husbandry center with standard sterile feed and drinking water supply ad libitim, natural light, at room temperature 22-26°C, in humidity 45-65% and with bedding changed twice weekly to ensure the rats lived in a well-regulated, quiet, and clean environment. After 7 days of adaptive rearing, the formal experiment was carried out. Eating, drinking, activity level, and defecation were monitored daily. After all rats were confirmed to be healthy, they were assigned to either the control group (n = 3) 、LPS sepsis model group (n = 3)、Cecal ligation perforation model (CLP) sepsis model group (n = 3) into three groups using a random number table. Rats were intragastrically administered 2 mL of saline once a day for 7 consecutive days. One hour after the last administration, the control group was given intraperitoneal injection of 5ml/kg saline, LPS group was given intraperitoneal injection of endotoxin (LPS 2 mg/ml) 10 mg/kg (9), CLP (10)group was given cecal ligation and puncture. After 24 hours, samples were collected and weighed. The ileum tissue and serum were taken and stored at -80°C. The study was approved by the Ethics Committee of Hebei University of Chinese Medicine (Number:DWL2019023).

2.2 Quantitative Real-Time PCR assay

Ileum tissue or serum was processed to extract total RNA. Next, 2 ug of total RNA was denatured to use as template RNA for qRT-PCR (BIO-RAD, model CFX96) in a mixture containing Oligo dT Primer and random primers at 70°C for 5 min and then immediately cooled on ice. The processed RNA was then added to the reverse transcription reaction solution containing reaction buffer, MgCl2, PCR nucleotide mix, ribonuclease inhibitor, reverse transcriptase and nuclease-free water to bring the volume of the reaction solution to 20 μl. The reaction was mixed slowly, briefly centrifuged, and placed in the PCR machine using the following cycle: 25°C for 5 min (annealing), 42°C for 60 min (extension), 70°C for 15 min (inactivation), for cycles. Then the reaction was cooled on ice and stored at -20° C for later use. The Cq values of each target gene and the internal reference gene β-actin were obtained. The Q value of each target gene/the Q value of the first sample, that is, RQ==2-ΔΔCq, represents the relative quantitative value of the expression of each target gene, and the RQ value was used for statistical analysis. The primers were as follows: COMMD9:forward (5′- CATCAGAGCATTTCGTGGCG -3′) and reverse (5′-AAGGGCTGAACTGGAGAAGC -3′); CSF3R: for-ward (5′-TGAGGGAAACAGAAAGGCCC -3′) and reverse (5′-AGACCTAGGGGTGTAGCCTG -3′); NUB1: for-ward (5′-GAATGAAAACAAACGGCGGC -3′) and reverse (5′-TCTGCGCCATCCTTGAAAGT -3′); and beta-actin forward (5′-GCAGGAGTACGATGAGTCCG -3′) and reverse (5′-ACGCAGCTCAGTAACAGTCC -3′).

2.3 Western blot

Western blot was used to detect the expression levels of COMMD9, CSF3R, and NUB1 proteins in rat ileum tissue. The ileum tissue was taken and placed in a centrifuge tube, and the protein in the ileum tissue was extracted using RIPA lysate. The supernatant was centrifuged and the protein concentration was measured using BCA method. We added the protein solution in a 4:1 ratio to 5×Loading buffer, denatured it in a boiling water bath for 25 minutes, performed 10% SDS-PAGE electrophoresis, and

transferred the PVDF membrane for 30 minutes. The membrane was placed in a TBST incubation tank, shaken at room temperature with skim milk, and sealed for 2 hours. We added the diluted first antibody and incubated it at 4 °C on a shaker overnight. We used TBST to elute 3 times, each time for 5 minutes. The secondary antibody was diluted with TBST in a ratio of 1:5000, incubated at room temperature for 2 hours, and colored using ECL method. Finally, we used Image J software to analyze the grayscale values of the bands, and the relative expression level of the target protein=the grayscale value of the target protein/β- Action grayscale value.

2.4 Microarray data

Human microarrays were obtained from the NCBI Gene Expression Omnibus (GEO; https://www.ncbi.nlm.nih.gov/geo/). GSE11755 including 31 specimens from patients with sepsis and 10 healthy control specimens, was on the foundation of the GPL570 [HG-U133_Plus_2] Affymetrix Human Genome U133 Plus 2.0 Array; GSE28750 including 21 specimens from patients with sepsis and 20 healthy controls, was on the foundation of the GPL570[HG-U133_Plus_2] Affymetrix Human Genome U133 Plus 2.0 Array; GSE48080 including 20 specimens from patients with sepsis and 3 healthy controls, was on the foundation of the GPL4133 Agilent-014850 Whole Human Genome Microarray 4x44K G4112F (Feature Number version); and GSE12624 including 34 specimens from patients with sepsis and 36 healthy controls, was on the foundation of the GPL4204 GE Healthcare/ Amersham Biosciences CodeLink UniSet Human I Bioarray. We combined the four datasets using the SVA package functionality of the R program, removing batch effects.

2.5 DEGs and identification of differentially expressed genes

In this study, the limma package of R software was used to identify DEGs from the processed microarray data. The filter conditions were: |log2 Fold change (FC)| > 2, FDR < 0.05. Genes that met these criteria were identified as DEGs.

2.6 Functional enrichment analyses

Gene Ontology (GO) analysis and Kyoto Encyclopedia of Genes and Genomes (KEGG) analysis were completed based on the classification of high- and low-risk patients using the "cluster Profiler" R package of R software in this study, and $p < 0.05$ was considered statistically significant.

2.7 Candidate diagnosis marker selection

We applied two machine learning algorithms, LASSO and Support vector machine (SVM), to predict sepsis status. LASSO is a compressed estimate that retains the advantages of subset shrinkage. It is a biased estimate for processing data with complex collinearity. LASSO determines whether the discrimination between sepsis samples and normal samples is significant through the "glmnet" package in R software.

SVM is a class of generalized linear classifiers that perform binary classification on data in a supervised learning manner. The RFE algorithm was used to screen the optimal genes from the metadata cohort, and SVM-RFE was used to screen suitable features to identify strong gene sets.

2.8 CIBERSORT analysis

To determine the relationship between immune cell populations and sepsis, we determined the responses of 22 immune cell populations using the CIBERSORT method and assessed the association between these immune cells and the expression of key genes in normal samples and in samples from patients with sepsis.

2.9 Statistical analysis

Gene expression differences between specimens from patients with sepsis and normal specimens were compared using Student's t-test. The ROC curve and AUC were calculated using the R package "proc" to test the classification effect of key genes in specimens from patients with sepsis and normal specimens. Statistical analysis was performed using R software (version 4.2.1) and GraphPad Prism (version 9.0.0) software, ∗ indicates p<0:05, ∗∗ indicates p<0:01.

3 Results

3.1 Determination of DEGs in sepsis

In this study, four microarrays GSE11755, GSE12624, GSE28750, and GSE48080 were retrospectively analyzed that together included 106 specimens from patients with sepsis and 69 specimens from healthy subjects. After removing batch effects, the LIMMA software package was used to identify DEGS from metadata. A total of 50 DEGs were identified: 2 genes were significantly up-regulated and 48 genes were significantly down-regulated in samples from patients with sepsis compared to normal controls (Figure 1).

3.2 Functional enrichment analyses

We used the ClusterProfile R software package to perform GO analysis and KEGG analysis on the 50 DEGs. The results showed that the DEGS were mainly involved in proteasomal protein catabolism process, proteasomal protein catabolic process, viral process, proteasome–mediated ubiquitin–dependent protein

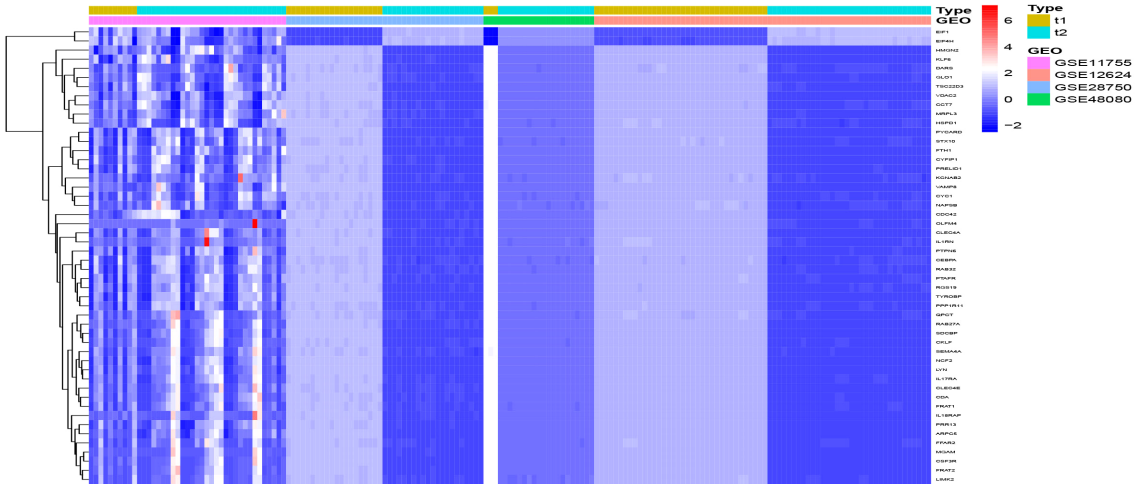

FIGURE 1
DEGs between Sepsis and control specimens, t1=normal, t2=sepsis.

catabolic process, lymphocyte differentiation, focal adhesion, vesicle lumen, vesicle lumen, secretory granule lumen, transcription coregulator activity, transcription coregulator activity (Figure 2A). In addition, KEGG analysis showed some signaling pathways, including the Salmonella infection pathway, Human T−cell leukemia virus 1 infection, Epstein−Barr virus infection, were also significantly different between the two cohorts (Figure 2B).

3.3 Determination and verification of diagnosis markers

We used the LASSO regression algorithm to interrogate the 50 DEGs for diagnostic markers of sepsis, which uncovered 44 potentially diagnostically relevant genes (Figure 3A). We also analyzed the 50 DEGs using the SVM-RFE algorithm, which identified eight feature subsets (Figure 3B). Only three genes were identified by both of the approaches: COMMD9, CSF3R, and NUB1 (Figure 3C), suggesting these genes may be involved in sepsis diagnose.

3.4 The expression and diagnosis significance of COMMD9, CSF3R, NUB1 in sepsis

We found that, compared with normal samples, the expression levels of COMMD9 and CSF3R were all significantly down-regulated in samples from patients with sepsis compared to control samples (Figures 4A, B). NUB1 was significantly up-regulated in the samples (Figure 4C). We next performed ROC analysis of COMMD9, CSF3R, NUB1, and the results showed that COMMD9 (Figure 4D, AUC=0.841), CSF3R (Figure 4E, AUC=0.907), NUB1 (Figure 4F, AUC=0.719).

3.5 COMMD9, CSF3R, NUB1 are related to immunocyte infiltration levels

Infiltration of immunocytes in the tissue microenvironment is an independent prognostic indicator of overall survival. We

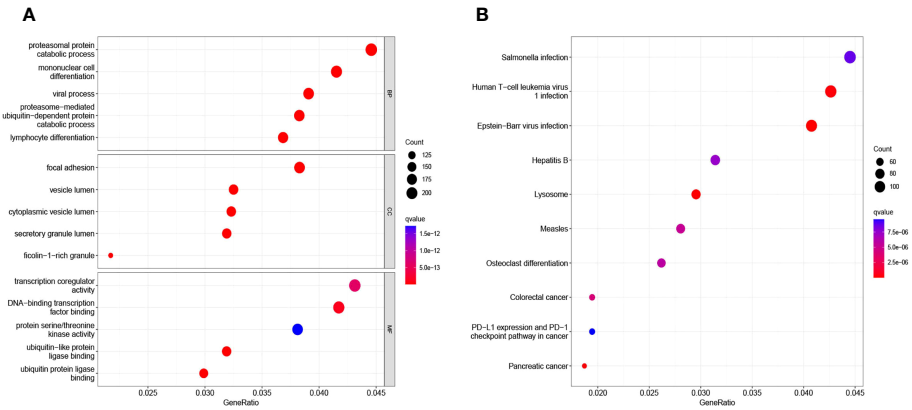

FIGURE 2
GO analysis **(A)** and KEGG analysis **(B)** of 50 DEGs via the ClusterProfile.

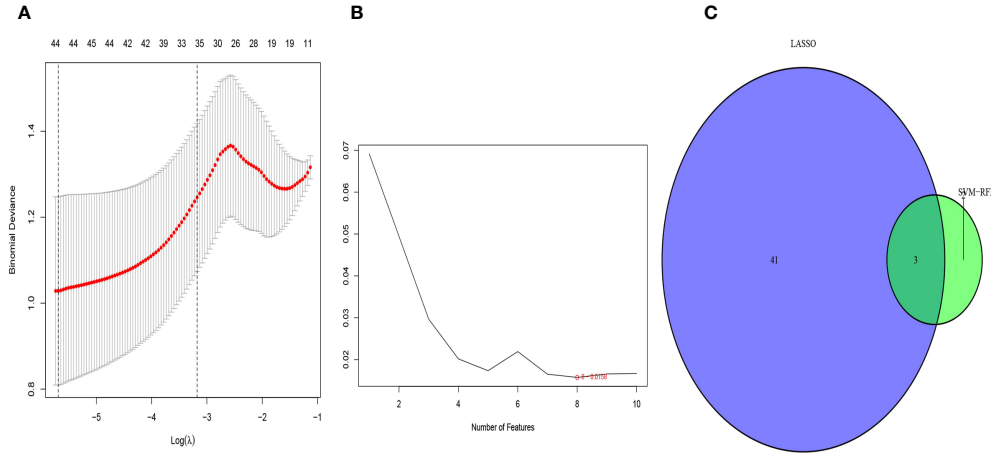

FIGURE 3
Selection of diagnosis marker candidates for sepsis: **(A)** tuning feature screening in the LASSO model; **(B)** a plot of biological marker screening via the SVM-RFE arithmetic; **(C)** Venn graph displaying 3 diagnosis biomarkers shared by LASSO and SVM-RFE.

therefore investigated the relationship between COMMD9, CSF3R, and NUB1 expression and the infiltration of immune cells in specimens from patients with sepsis and healthy controls. CIBERSORT was used to characterize the immune cell composition of the two cohorts (Figures 5A, B). And we also found some statistically significant differences in B cells memory, Plasma cells, T cells CD8, T cells CD4 native, T cells CD4 memory resting, T cells follicular helper, T cells regulatory, T cells gamma delta, NK cells activated, Monocytes, Macrophages M0, Dendritic cells resting, Dendritic cells activated, Mast cells resting, Mast cells activated, Eosinophils, Neutrophils (Figure 5C).This demonstrated that there is a correlation between lower expression of COMMD9, CSF3R and NUB1 and increased immune cell infiltration (Figures 6A–C). These data suggest that COMMD9, CSF3R, and NUB1 may regulate immune cells in patients with sepsis.

3.6 The identification of the expression of three diagnostic genes in our cohort

The PCR results in rat ileum tissue show that,compared with control group samples, the expression levels of COMMD9 and CSF3R were significantly decreased from rats with two sepsis model (LPS group=model1, CLP group=model2) (Figures 7A, B), and the expression level of NUB1 was significantly increased (Figure 7C).

The PCR results in rat serum show that, compared with control group samples, the expression levels of COMMD9 and CSF3R were significantly decreased from rats with two sepsis model (LPS group=model1, CLP group=model2) (Figures 7D, E), and the expression level of NUB1 was significantly increased (Figure 7F).

The WB results show in rat ileum tissue that (Figure 7G), compared with control group samples, the expression levels of

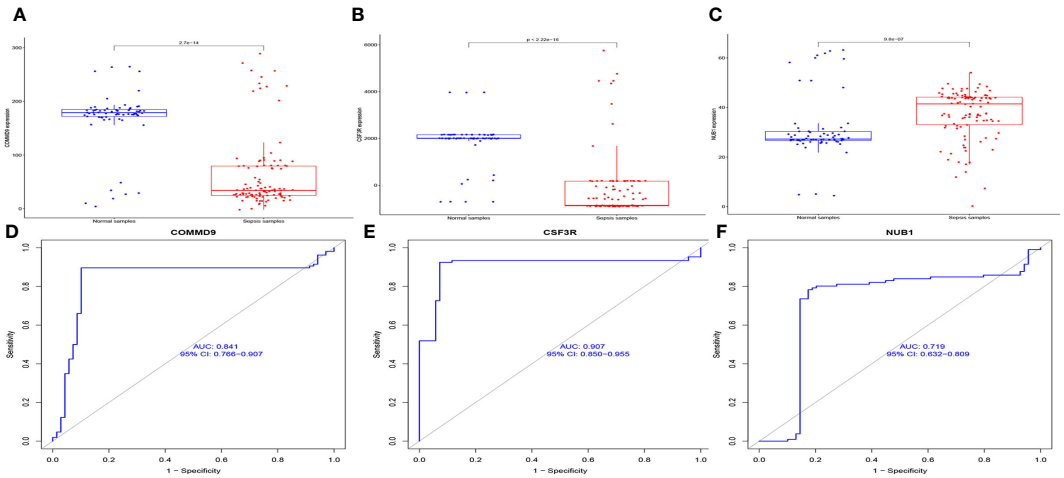

FIGURE 4
The expression and diagnosis significance of COMMD9、CSF3R、NUB1 in Sepsis: **(A)** COMMD9 expression was distinctly downregulated in Sepsis samples; **(B)** CSF3R expression was distinctly downregulated in Sepsis samples; **(C)** NUB1 expression was distinctly upregulated in Sepsis samples; **(D–F)** ROC assays for COMMD9, CSF3R, NUB1 in Sepsis.

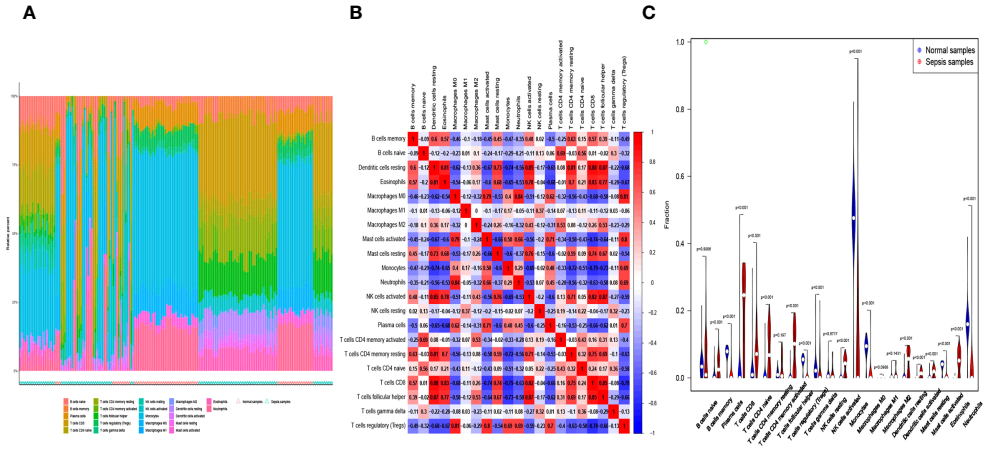

FIGURE 5
(A, B) The percentage of the 22 immunocytes identified via the CIBERSORT arithmetic. **(C)** The diversities in the architecture of immunocytes between Normal and Sepsis samples.

COMMD9 and CSF3R were significantly decreased from rats with two sepsis model (LPS group=model1, CLP group=model2) (Figures 7H, I), and the expression level of NUB1 was significantly increased (Figure 7J).

4 Discussion

Sepsis is a systemic inflammatory response syndrome caused by bacteria and other pathogenic microorganisms infiltrating the blood. It often occurs secondary to other critical illness and severe infection of organs or tissues. There are currently no reliable biomarkers for early detection and diagnosis of sepsis and, because sepsis can quickly lead to death, there is an urgent need for new approaches to identify the disease as early as possible. To this end, in this study, we evaluated datasets from four microarrays of patients with sepsis and healthy subjects to identify DEGs that may have diagnostic value. GO analysis results show that 50 DEGS mainly involve in the processing of proteomic protein catabolic, proteasomal protein catabolic process, viral process, proteasome–mediated ubiquitin–dependent protein catabolic process, lymphocyte differentiation, focal adhesion, vesicle lumen, vesicle lumen, secretory granule lumen, transcription coregulator activity, transcription coregulator activity. And KEGG analysis showed some signaling pathways, including the Salmonella infection pathway, Human T–cell leukemia virus 1 infection, Epstein–Barr virus infection. We uncovered 50 DEGs between the cohorts that we further analyzed, resulting in prioritization of COMMD9, CSF3R, and NUB1 as potential biomarkers to diagnose sepsis.

This study is the first to propose and verify differential expression of COMMD9, CSF3R, and NUB1 in patients with

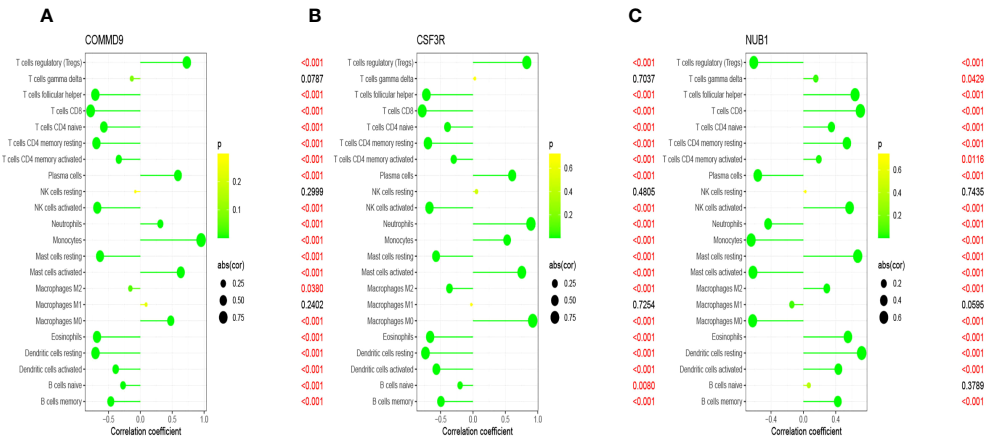

FIGURE 6
Correlation between key genes and infiltrating immune cells in sepsis and normal samples. **(A)** COMMD9 and infiltrating immune cells; **(B)** CSF3R and infiltrating immune cells; **(C)** NUB1 and infiltrating immune cells.s

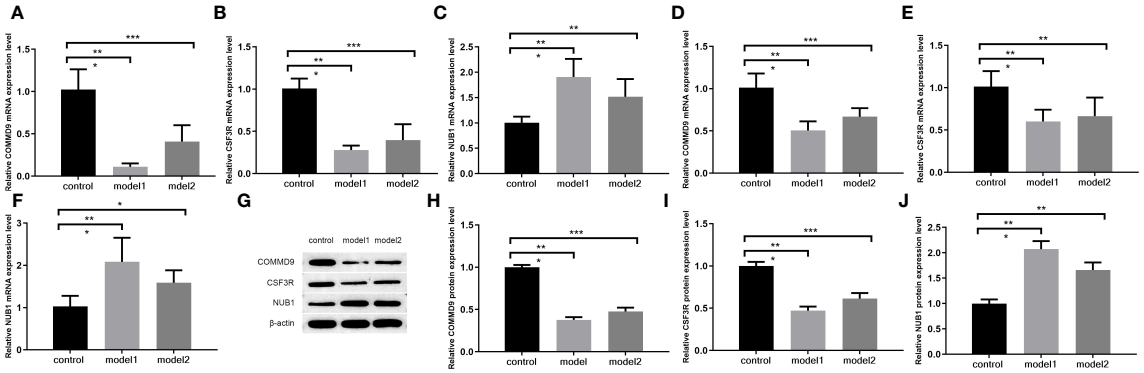

FIGURE 7
The qRT-PCR **(A–F)** and WB **(G–J)** for the levels of key genes. **(A–C)** The mRNA level of COMMD9, CSF3R, NUB1 in ileum tissue; **(D–F)**_The mRNA level of COMMD9 , CSF3R, NUB1 in serum; **(G–J)** The protein level of COMMD9、CSF3R、NUB1 in ileum tissue (*p<0.05、**p<0.01、***p<0.001).

sepsis, and ROC analysis confirmed that they may be useful as diagnostic biomarkers. The Copper Metabolism Murr1 Domain (COMMD) protein family plays an important role in the regulation of nuclear factor-κB (nf-κB) activity, copper ion metabolism, and sodium ion problems, and mutations in this gene have been associated with related biological phenotypes (11–13). The nf-κB signaling pathway is one of the most important signaling pathways in sepsis. Therefore, we speculate that COMMD9 plays a role in the nf-κB signaling pathway, and we will investigate whether it is related in the future. Colony-Stimulating Factor-3 Receptor (CSF3R) is a protein-coding gene located in the p34 region of chromosome 1 that regulates the generation, differentiation, and signal transduction of granulocytes (14). At present, CSF3R research is mainly focused on its role in blood diseases, especially in the blood of patients with chronic neutrophilic leukemia (15, 16). CSF3R is also involved in cancer progression (17). However, the expression and role of CSF3R in patients with sepsis are not known. NEDD8 Ultimate Buster-1 (NUB1) is an interferon-inducible gene whose overexpression inhibits cell growth. It is known to play an important role in cancer and cell physiology (18–20), but its role in sepsis is not clear.

Sepsis primarily manifests as a severe inflammatory response. In addition to inflammatory cells, a large number of B cells, T cells and other immune cells are observed in the tissue infiltrate, and they each play different roles. Indeed, immune cell infiltration is one of the critical mechanisms that induces sepsis (21, 22). CD4+ T cells are thought to be the most prone to cell death during sepsis, thereby inducing an immune paralysis state (23, 24).After activation of CD4 + T cells in the intestinal mucosa, T regulatory cells decrease, which in turn hyperactivates the immune response, eventually damaging the intestinal epithelial cells (25). Studies have found that recurrent sepsis can deplete human CD4+ T cells, thereby changing the prognosis of patients (26). Other immune cells have different pathogenic or protective effects. Therefore, identifying new immunotherapeutic targets by characterizing immune cell infiltration is a priority. In this study, we found that COMMD9, CSF3R, and NUB1 regulate immune cell infiltrate during sepsis, and we speculate that the activity of these genes may influence the development of sepsis. Future pre-clinical and clinical studies are needed to verify their effectiveness and interrelationships.

We recognize some limitations of this study. First, our study was based on a bioinformatics analysis of microarray data made available by others and validated with only one small animal study. Larger-scale experiments and mechanistic evaluation are needed to validate the potential role of DEGs in sepsis. Second, the four microarrays varied from one another with regard to patient country, race, and gender. Third, the correlation we identified between three DEGs and immune cell infiltrate is reported here as a phenomenon, and rigorous studies to determine how those genes influence immune cell behavior in the context of sepsis—and whether this differs from their role in a non-pathological context—are required.Due to insufficient funding, we were unable to verify the relationship between key genes and immune cells.

We identified COMMD9, CSF3R, and NUB1 as potentially biologically relevant genes and diagnostic markers for sepsis. Our findings prompt additional studies of these three genes to understand how they may contribute to the pathological mechanisms of sepsis onset and progression and to identify novel opportunities to treat sepsis by targeting aberrant immune cell behaviors.

Data availability statement

The datasets presented in this study can be found in online repositories. The names of the repository/repositories and accession number(s) can be found below: https://www.ncbi.nlm.nih.gov/, GSE1175, https://www.ncbi.nlm.nih.gov/, GSE28750, https://www.ncbi.nlm.nih.gov/, GSE48080, https://www.ncbi.nlm.nih.gov/, GSE12624.

Ethics statement

The animal study was reviewed and approved by Ethics Committee of Hebei University of Traditional Chinese Medicine (Number: DWL2019023).

Author contributions

QW and CW: manuscript preparation, data analysis, and the research conception. JM, FC: manuscript revision. YL, ZL, DL: conception and design. WZ, YT, JG: data analysis. All authors contributed to the article and approved the submitted version.

Funding

This work was supported by the Hebei Natural Science Foundation (No.H2022423369) and the Hebei Provincial Government Funding the Training of Excellent Clinical Medical Talents and Basic Research Projects (No.2016034829).

Conflict of interest

The authors declare that the research was conducted in the absence of any commercial or financial relationships that could be construed as a potential conflict of interest.

Publisher's note

References

1. Evans L, Rhodes A, Alhazzani W, Antonelli M, Coopersmith CM, French C, et al. Surviving sepsis campaign: international guidelines for management of sepsis and septic shock 2021. *Intensive Care Med* (2021) 47:1181–247. doi: 10.1007/s00134-021-06506-y

2. Purcarea A, Sovaila S. Sepsis, a 2020 review for the internist. *Rom J Intern Med* (2020) 58(3):129–37. doi: 10.2478/rjim-2020-0012

3. Thompson K, Venkatesh B, Finfer S. Sepsis and septic shock: current approaches to management. *Intern Med J* (2019) 49(2):160–70. doi: 10.1111/imj.14199

4. Fleischmann C, Scherag A, Adhikari NK, Hartog CS, Tsaganos T, Schlattmann P, et al. Assessment of global incidence and mortality of hospital-treated sepsis. current estimates and limitations. *Am J Respir Crit Care Med* (2016) 193:259–72. doi: 10.1164/rccm.201504-0781OC

5. Gauer R, Forbes D, Boyer N. Sepsis: diagnosis and management. *Am Fam Physician.* (2020) 101(7):409–18.

6. Jia X, Peng Y, Ma X, Liu X, Yu K, Wang C. Analysis of metabolic disturbances attributable to sepsis-induced myocardial dysfunction using metabolomics and transcriptomics techniques. *Front Mol Biosci* (2022) 9:967397. doi: 10.3389/fmolb.2022.967397

7. Maiese A, Scatena A, Costantino A, Chiti E, Occhipinti C, La Russa R, et al. Expression of MicroRNAs in sepsis-related organ dysfunction: a systematic review. *Int J Mol Sci* (2022) 23(16):9354. doi: 10.3390/ijms23169354

8. Lai Y, Lin C, Lin X, Wu L, Zhao Y, Shao T, et al. Comprehensive analysis of molecular subtypes and hub genes of sepsis by gene expression profiles. *Front Genet* (2022) 13:884762. doi: 10.3389/fgene.2022.884762

9. El-Awady MS, Nader MA, Sharawy MH. The inhibition of inducible nitric oxide synthase and oxidative stress by agmatine attenuates vascular dysfunction in rat acute endotoxemic model. *Environ Toxicol Pharmacol* (2017) 55:74–80. doi: 10.1016/j.etap.2017.08.009

10. Rittirsch D, Huber-Lang MS, Flierl MA, Ward PA. Immunodesign of experimental sepsis by cecal ligation and puncture. *Nat Protoc* (2009) 4(1):31–6. doi: 10.1038/nprot.2008.214

11. Zhan W, Wang W, Han T, Xie C, Zhang T, Gan M, et al. COMMD9 promotes TFDP1/E2F1 transcriptional activity via interaction with TFDP1 in non-small cell lung cancer. *Cell Signal* (2017) 30:59–66. doi: 10.1016/j.cellsig.2016.11.016

12. Liu YF, Swart M, Ke Y, Ly K, MnDonald FJ, et al. Functional interaction of COMMD3 and COMMD9 with the epithelial sodium channel. *Am J Physiol Renal Physiol* (2013) 305:F80–9. doi: 10.1152/ajprenal.00158.2013

13. Singla A, Chen Q, Suzuki K, Song G, Fedoseienko A, Wijers M, et al. Regulation of murine copper homeostasis by members of the COMMD protein family. *Dis Model Mech* (2021) 14. doi: 10.1242/dmm.045963

14. Sheng G, Zhang J, Zeng Z, Pan J, Wang Q, Wen L, et al. Identification of a novel CSF3R-SPTAN1 fusion gene in an atypical chronic myeloid leukemia patient with t (1;9)(p34;q34) by RNA-seq. *Cancer Genet* (2017) 216-217:16–9. doi: 10.1016/j.cancergen.2017.05.002

15. Sapra A, Jaksik R, Mehta H, Biesiadny S, Kimmel M, Corey SJ, et al. Effect of the unfolded protein response and oxidative stress on mutagenesis in CSF3R: a model for evolution of severe congenital neutropenia to myelodysplastic syndrome/acute myeloid leukemia. *Mutagenesis* (2020) 35:381–9. doi: 10.1093/mutage/geaa027

16. Trottier AM, Druhan LJ, Kraft IL, Lance A, Feurstein S, Helgeson M, et al. Heterozygous germ line CSF3R variants as risk alleles for development of hematologic malignancies. *Blood Adv* (2020) 4:5269–84. doi: 10.1182/bloodadvances.2020002013

17. Fujiyoshi S, Honda S, Minato M, Ara M, Suzuki H, Hiyama E, et al. Hypermethylation of CSF3R is a novel cisplatin resistance marker and predictor of response to postoperative chemotherapy in hepatoblastoma. *Hepatol Res* (2020) 50:598–606. doi: 10.1111/hepr.13479

18. Tanji K, Tanaka TMori F, Kito K, Takahashi H, Wakabayashi K. NUB1 suppresses the formation of lewy body-like inclusions by proteasomal degradation of synphilin-1. *Am J Pathol* (2006) 169:553–65. doi: 10.2353/ajpath.2006.051067

19. Zhang D, Wu P, Zhang Z, An W, Zhang C, Pan S, et al. Overexpression of negative regulator of ubiquitin-like proteins 1 (NUB1) inhibits proliferation and invasion of gastric cancer cells through upregulation of p27Kip1 and inhibition of epithelial-mesenchymal transition. *Pathol Res Pract* (2020) 216:153002. doi: 10.1016/j.prp.2020.153002

20. Arshad M, Abdul Hamid N, Chan MC, Ismail F, Tan GC, Pezzella F, et al. NUB1 and FAT10 proteins as potential novel biomarkers in cancer: a translational perspective. *Cells* (2021) 10(9):2176. doi: 10.3390/cells10092176

21. Duan S, Jiao Y, Wang J, Tang D, Xu S, Wang R, et al. Impaired b-cell maturation contributes to reduced b cell numbers and poor prognosis in sepsis. *Shock* (2020) 54:70–7. doi: 10.1097/SHK.0000000000001478

22. Lee KA, Gong MN. Pre-b-cell colony-enhancing factor and its clinical correlates with acute lung injury and sepsis. *Chest* (2011) 140(2):382–90. doi: 10.1378/chest.10-3100

23. Martin Matthew D, Badovinac VP, Griffith Thomas S. CD4 T cell responses and the sepsis-induced immunoparalysis state. *Front Immunol* (2020) 11:1364. doi: 10.3389/fimmu.2020.01364

24. Brady J, Horie S, Laffey JG. Role of the adaptive immune response in sepsis. *Intensive Care Med Exp* (2020) 8:20. doi: 10.1186/s40635-020-00309-z

25. Assimakopoulos Stelios F, Eleftheriotis G, Lagadinou M, Karamouzos V, Dousdampanis P, Siakallis G, et al. SARS CoV-2-Induced viral sepsis: the role of gut barrier dysfunction. *Microorganisms* (2022) 10(5):1050. doi: 10.3390/microorganisms10051050

26. He W, Xiao K, Xu J, Guan W, Xie S, Wang K, et al. Recurrent sepsis exacerbates CD4 T cell exhaustion and decreases antiviral immune responses. *Front Immunol* (2021) 12:627435. doi: 10.3389/fimmu.2021.627435

frontiers | Frontiers in Immunology

TYPE Review
PUBLISHED 11 September 2023
DOI 10.3389/fimmu.2023.1242640

OPEN ACCESS

EDITED BY
Alessandra Stasi,
University of Bari Aldo Moro, Italy

REVIEWED BY
Yuxiang Fei,
China Pharmaceutical University, China
Wei Zhu,
Huazhong University of Science and Technology, China

*CORRESPONDENCE
Yi Guo
guoyi_168@163.com
Xiaowei Lin
linxiaoweiwqhz@163.com

†These authors have contributed equally to this work

RECEIVED 19 June 2023
ACCEPTED 15 August 2023
PUBLISHED 11 September 2023

CITATION
Yang L, Zhou D, Cao J, Shi F, Zeng J, Zhang S, Yan G, Chen Z, Chen B, Guo Y and Lin X (2023) Revealing the biological mechanism of acupuncture in alleviating excessive inflammatory responses and organ damage in sepsis: a systematic review. *Front. Immunol.* 14:1242640. doi: 10.3389/fimmu.2023.1242640

Revealing the biological mechanism of acupuncture in alleviating excessive inflammatory responses and organ damage in sepsis: a systematic review

Lin Yang[1†], Dan Zhou[1,2†], Jiaojiao Cao[1], Fangyuan Shi[1], Jiaming Zeng[1], Siqi Zhang[3], Guorui Yan[4], Zhihan Chen[1], Bo Chen[1,2], Yi Guo[2,5*] and Xiaowei Lin[2,5,6*]

[1]School of Acupuncture-Moxibustion and Tuina, Tianjin University of Traditional Chinese Medicine, Tianjin, China, [2]Research Center of Experimental Acupuncture Science, Tianjin University of Traditional Chinese Medicine, Tianjin, China, [3]Ministry of Education, State Key Laboratory of Component-Based Chinese Medicine, Tianjin University of Traditional Chinese Medicine, Tianjin, China, [4]The First Teaching Hospital of Tianjin University of Traditional Chinese Medicine, Pharmacy Department, Tianjin, China, [5]Tianjin Key Laboratory of Modern Chinese Medicine Theory of Innovation and Application, Tianjin University of Traditional Chinese Medicine, Tianjin, China, [6]School of Traditional Chinese Medicine, Tianjin University of Traditional Chinese Medicine, Tianjin, China

Sepsis is a systemic inflammation caused by a maladjusted host response to infection. In severe cases, it can cause multiple organ dysfunction syndrome (MODS) and even endanger life. Acupuncture is widely accepted and applied in the treatment of sepsis, and breakthroughs have been made regarding its mechanism of action in recent years. In this review, we systematically discuss the current clinical applications of acupuncture in the treatment of sepsis and focus on the mechanisms of acupuncture in animal models of systemic inflammation. In clinical research, acupuncture can not only effectively inhibit excessive inflammatory reactions but also improve the immunosuppressive state of patients with sepsis, thus maintaining immune homeostasis. Mechanistically, a change in the acupoint microenvironment is the initial response link for acupuncture to take effect, whereas PROKR2 neurons, high-threshold thin nerve fibres, cannabinoid CB2 receptor (CB2R) activation, and Ca^{2+} influx are the key material bases. The cholinergic anti-inflammatory pathway of the vagus nervous system, the adrenal dopamine anti-inflammatory pathway, and the sympathetic nervous system are key to the transmission of acupuncture information and the inhibition of systemic inflammation. In MODS, acupuncture protects against septic organ damage by inhibiting excessive inflammatory reactions, resisting oxidative stress, protecting mitochondrial function, and reducing apoptosis and tissue or organ damage.

KEYWORDS

sepsis, acupuncture, anti-inflammation, autonomic nerve, mechanism research

10.3389/fimmu.2023.1242640

1 Introduction

The definition of sepsis has evolved, deepened, and improved with the development of medical practices. In Sepsis 3.0, sepsis is defined as life-threatening organ dysfunction due to an imbalance in the host inflammatory response caused by infection (1); reducing inflammation and correcting organ dysfunction are the core strategies for treating sepsis. Sepsis is a critical disease with high incidence and rapid development. It is a prominent problem and a key disease in contemporary medicine. The latest data from the *Lancet* in 2020 show that in 2017, there were approximately 48.9 million cases of sepsis worldwide and approximately 11 million sepsis-related deaths, accounting for 19.7% of the total deaths worldwide (2). More importantly, these figures may be further exacerbated by the global COVID-19 pandemic and high medical costs associated with sepsis. Modern research has shown that early intervention in patients with possible sepsis, extensive cooperation in the medical field, and optimisation and improvement of treatment plans are effective ways to reduce the occurrence of sepsis.

Currently, the treatment strategies for sepsis include anti-infection and organ support strategies. Acupuncture has been used to treat inflammatory diseases for thousands of years (3, 4). Modern evidence has shown the significant anti-inflammatory effects of acupuncture on sepsis. Acupuncture may be a promising complementary strategy for early prevention and treatment of septic inflammation, improvement of survival rates, and protection of organs. Therefore, we summarised the pathological process of sepsis, current status of the clinical application of acupuncture in treating sepsis, commonly used animal models for the study of the mechanism of acupuncture in treating sepsis, and acupuncture intervention parameters, focusing on the research progress of the mechanism of acupuncture prevention and treatment of sepsis from the perspectives of the acupoint microenvironment, autonomic neurobiological mechanisms, and target organ effects.

2 Pathological mechanism of sepsis

2.1 Hyperinflammatory response

Sepsis is a gradual sequential reaction. Starting with an inflammatory reaction, the body can exhibit three states when stimulated by pathogens. First, when inflammatory cells are overactivated, causing an imbalance between proinflammatory and anti-inflammatory effects, an uncontrolled inflammatory cascade reaction is initiated. Uncontrolled inflammatory reactions in the body are considered an important basis for multiple organ dysfunction caused by sepsis, which is mainly characterized by the release of a large number of proinflammatory mediators. Second, if sepsis cannot be controlled for a short time, a mixed immune state (i.e., an immune disorder) can occur. Finally, as the disease progresses, the immune state gradually transforms into immunosuppression/immune paralysis, causing repeated infections (Figure 1). In the early stage of sepsis, the first death peak is caused by multiple organ failure caused by uncontrolled inflammation storms, whereas the second death peak of sepsis patients is often caused by secondary severe infection as a result of immunosuppression.

The cytokine storm stage is a period with a high incidence of death in patients with sepsis. During uncontrolled inflammation, excessive activation of inflammatory cells and the release of a large number of inflammatory factors are important mechanisms of multiple organ dysfunction in sepsis. Pathogen-associated molecular patterns (PAMPs) and damage-associated molecular patterns (DAMPs) are recognized and activated by pattern recognition receptors (PRRs) on immune cell surfaces. When the number of pathogens is limited, local inflammatory reactions are sufficient to remove them. For example, macrophages engulf bacteria and produce a series of inflammatory cytokines that activate the innate immune system to fight pathogenic invasion. However, when a large number of pathogens invade, immune cells are overactivated, resulting in the release of numerous inflammatory factors, such as tumor necrosis factor-α (TNF-α), interleukin-1beta (IL-1beta), IL-6, and IL-17, which form a storm of inflammatory factors and initiate a sepsis-like network reaction. During sepsis development, the body is not constantly in a state of immune activation. Anti-inflammatory and proinflammatory responses occur almost simultaneously, and anti-inflammatory cytokines limit persistent or excessive inflammatory responses. The negative feedback regulation mechanism of the body's immune system can promote the secretion of anti-inflammatory cytokines, such as IL-4, IL-10, and transforming growth factor beta (TGF-beta), thereby inhibiting the production and release of proinflammatory mediators, such as TNF-α, IL-1β, and IL-6. However, the amount of proinflammatory cytokines and anti-inflammatory cytokines in patients with sepsis is often unbalanced. When anti-inflammatory cytokines are insufficient, the body experiences immune dysfunction, which aggravates the progression of sepsis. TNF-α is the earliest inflammatory factor synthesized during the occurrence and development of sepsis, and also one of the initiating factors of sepsis (5). Recent research has shown that the gene polypeptide at the promoter-308 site is closely related to the susceptibility and outcome of sepsis and septic shock (6). It was found that the G/A gene polymorphism of TNF-α-308 is

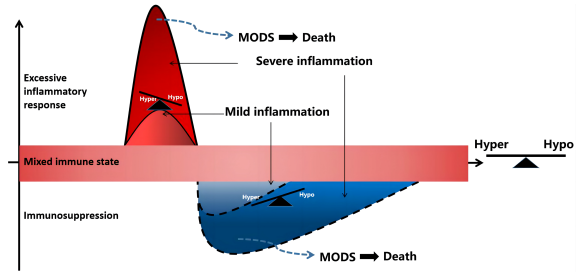

FIGURE 1
Sepsis is a process of inflammatory imbalance. multiple organ dysfunction syndrome (MODS), multiple organ dysfunction syndrome; Hyper, hyper-inflammatory; hypo-inflammatory.

significantly positively associated with a higher incidence of sepsis and increased expression of cytokines such as TNF-α, IL-6, and IL-8 in patients (7). In addition, the study found that subjects with IL-10-1082 AA and IL-6-174 CC genotypes had a higher risk of sepsis and increased mRNA levels. Overproduction of IL-10 can lead to a compensatory anti-inflammatory response and inhibit the inflammatory defense system in patients with sepsis. IL-6 is the main mediator of systemic inflammatory response syndromes. Excess IL-6 activates the coagulation system and increases vascular permeability, providing conditions for rapid diffusion of inflammation. Therefore, these genetic variants could be used as therapeutic targets in patients with sepsis (8).

2.2 Immunosuppression

If sepsis is not controlled within a short time, a mixed immune state, namely an immune disorder, can occur. During the period of mixed immunity, the cytokine cascade amplification reaction in the high inflammatory response state of the body begins to decrease, and the compensatory anti-inflammatory reaction initiated by the inflammatory reaction continues. In the late stage of mixed immunity, there are usually three outcome trends (1): the immune state of the body gradually returns to balance and the disease improves; (2) mixed immune state: the inflammatory and anti-inflammatory mechanisms of the body are not reconciled, and the clinical manifestations are complex; (3) immune suppression: there is severe immune damage caused by strong pathogenic factors or deterioration due to the disease, and the immune state gradually transforms into immunosuppression or loss of immune ability, also known as immune paralysis.

Immunosuppression in the late stages of sepsis is the main cause of long-term complications and death from sepsis. Currently, immunosuppression is believed to be mainly related to anti-inflammatory mediators and apoptosis. Immunosuppression involves abundant lymphocyte apoptosis accompanied by a decrease in their proliferative capacity, leading to a decrease or no reaction of T cells, presenting an immune response dominated by type 2 helper T (Th2) cells, a decrease in the number of CD4+ antigen-presenting cells, apoptosis or incompetence, and an inability to present antigens and produce effectors (9). Specifically, the anti-inflammatory factors produced by monocytes significantly increased, such as IL-10 and TGF-β, and proinflammatory factors (such as TNF-α and IL-1β) decreased, presenting immunosuppression. In addition, the production of Th2 type cytokines (IL-4, IL-10) is increased and Th1 type cytokines (IL-12 and IFN-γ) is decreased, which affects the differentiation of T lymphocytes and causes the body to present a Th2-based immune response and damage the cellular immune function (10). In the immunosuppressive stage, a large number of B lymphocytes, CD4 +T lymphocytes, dendritic cells, and other antigen-presenting cells undergo apoptosis, resulting in reduced antibody production and human leukocyte antigen-DR (HLA-DR) capacity (11–14). However, the number of inhibitory receptors, such as programmed cell death protein 1, regulatory T cells, and myeloid-derived suppressor cells (MDSCs), is significantly increased, leading to the development of severe immunosuppression in later stages (15). Simultaneously, neutrophils differentiate into subsets with immunosuppressive effects and produce numerous cytokines that inhibit immune response, such as IL-10 (16). In addition, inherent immune natural killer (NK) cell subsets (CD56 Hi and CD56 Low) are significantly reduced, and the degree of reduction is closely related to mortality (17).

2.3 Oxidative stress, mitochondrial damage, and apoptosis lead to sepsis organ damage and coagulation dysfunction

In the course of sepsis, mitochondria, which are important energy and material metabolism centers, are most vulnerable to oxidative stress damage, which is also key to organ dysfunction (18). The release of several inflammatory mediators can affect the coupling process of the normal oxidative respiratory chain in mitochondria, resulting in an increase in ROS production. The large increase in ROS damages the activity of functional enzymes and leads to the destruction of mitochondrial membrane lipids, which severely reduce the energy supply required by cells (19). This process is the main mechanism underlying oxidative stress injury caused by sepsis. Lipopolysaccharide (LPS) can increase ROS production by increasing the expression of nitric oxide synthase (NOS) and nicotinamide adenine dinucleotide phosphate (NADPH) oxidase 4 (NOX4) (20), causing oxidative stress. The accumulation of a large amount of ROS leads to insufficient ATP production in the mitochondria, and mitochondrial autophagy is a self-adaptive change in the body during inflammatory reactions. Mitochondrial autophagy can clear mitochondria with impaired function and reduce the cell damage caused by ROS during aerobic glycolysis (21). During sepsis, inflammatory reactions, oxidative stress, and mitochondrial membrane depolarization can activate a large amount of mitochondrial autophagy. Excessive mitochondrial autophagy induces apoptosis. However, when the function of phagocytes declines, apoptotic cells cannot be cleared in time, and abundant content is released, which aggravates organ damage. During sepsis, the apoptosis of intestinal epithelial cells, respiratory epithelial cells, myocardial cells, and lymphocytes increases significantly (22). Impairment of autophagy in hepatocytes in a sepsis mouse model can aggravate mitochondrial dysfunction and induce liver damage (23). Therefore, reducing ROS production, resisting oxidative stress, and reducing mitochondrial function damage and cell apoptosis are key to the treatment of multiple organ function damage in sepsis (24, 25).

Coagulation dysfunction is the main pathological manifestation of the late stages of sepsis. In mild cases, the coagulation indicators are disordered, whereas in severe cases, disseminated intravascular coagulation (DIC) may occur. The main pathological mechanisms of coagulation dysfunction caused by sepsis include activation of the coagulation system, impairment of the anticoagulation system, and inhibition of the fibrinolysis pathway. First, the stimulation of endotoxins and inflammatory mediators can damage the vascular wall, leading to the release of tissue factors (TFs) from vascular

endothelial cells, neutrophils, mononuclear phagocytes, and platelets. After TFs enter the blood, they successively activate exogenous and endogenous coagulation pathways and cause extensive microvascular thrombosis through a positive feedback mechanism (26). Simultaneously, the antithrombotic microenvironment in the vascular lumen is impaired by the damage to the vascular endothelium (27). The main manifestations of anticoagulation system damage are a reduction in antithrombin level (28), damage to the protein C (PC) system (protein C, protein C inhibitor, protein S, and thrombomodulin), and damage to the tissue factor pathway inhibitor (TFPI). Clinical observations showed that a decrease in AT levels was closely related to high mortality. The PC system is the most effective physiological anticoagulant system for regulating inflammatory reactions and is mainly secreted by the liver. It inhibits the transformation of prothrombin to thrombin via negative feedback. TFPI is a natural anticoagulant and is an important exogenous inhibitor of the coagulation pathway *in vivo*. The inhibition of the fibrinolysis pathway is mainly manifested in the biphasic reaction of the fibrinolysis system, which is first activated and then inhibited. First, the tissue-type plasminogen activator (t-PA), an important physiological activator of the fibrinolysis system, can convert plasminogen into plasmin and degrade and eliminate fibrin clots. In early sepsis, TNF-α causes t-PA to be released from endothelial cells and activates the fibrinolytic system. Second, with the development of sepsis, the level of plasminogen activator inhibitor-1 (PAI-1) in the plasma continues to rise, and fibrinolytic activity is inhibited, leading to an increase in blood coagulation, and a large amount of fibrin cannot be degraded in time, leading to thrombosis (29, 30). Additionally, PAMPs and DAMPs can activate neutrophil extracellular traps (NETs), leading to platelet thrombosis and accelerated blood coagulation (31, 32). Recent research has shown that NETs can promote thrombosis by interacting with NET-carrying EVs (33).

3 Clinical application of acupuncture in the prevention and treatment of sepsis

Clinical evidence has accumulated regarding the extensive application of acupuncture in sepsis (Table 1). In clinical practice, acupuncture intervention is usually combined with conventional clinical therapies such as anti-infection, nutritional support, fluid management, and mechanical ventilation, which can significantly reduce the systemic inflammatory response and organ damage as well as improve the function of immune cells in patients with sepsis (34, 36, 38–43, 45, 46). For example, 4 Hz continuous wave electroacupuncture (EA) at the Zusanli (ST36) and Shangjuxu (ST37) acupoints combined with conventional treatment can significantly reduce plasma procalcitonin (PCT), TNF-α, intestinal fatty acid binding protein (I-FABP), and D-lactic acid levels in patients with sepsis-induced intestinal dysfunction and intestinal obstruction syndrome, and plays a protective role in intestinal function (42). The curative effect of acupuncture combined with conventional Western medicine is better than that of Western medicine alone, and can reduce inflammatory response indices and improve gastrointestinal function (40). Studies have shown that electroacupuncture or transcutaneous electrical acupoint stimulation (TEAS) combined with conventional treatment has a protective effect on intestinal function in patients with sepsis, which can effectively reduce the excretion rate of the lactulose-to-mannitol ratio (L: M) in urine and the level of serum D-lactate, and improve intestinal permeability in patients with sepsis (36, 37). Some clinical studies have shown that acupuncture combined with conventional treatment for one week can effectively reduce the levels of C-reactive protein (CRP), IL-6, and neuron-specific enolase (NSE) and improve brain damage in patients with sepsis-associated encephalopathy (SAE) (41). In addition, patients with sepsis may gradually develop rapid muscle atrophy in the intensive care unit, a phenomenon known as septic myopathy. A clinical study on the results of acupuncture treatment of sepsis-induced myopathy is underway (47). The results of this study may contribute to a new understanding of early muscle atrophy and the therapeutic effects of acupuncture in patients with sepsis-induced myopathy. These findings may provide new guidance for these patients. In conclusion, acupuncture combined with conventional treatment can significantly inhibit the excessive secretion of serum inflammatory cytokines in the early stages of sepsis, improve intestinal permeability, protect normal intestinal function, and prevent brain damage in patients with sepsis.

Acupuncture not only inhibits sepsis inflammation and plays an organ-protective role but also improves the immune cell function of the body in the later stages of sepsis. Clinical studies have shown that acupuncture combined with conventional therapy can significantly reduce mortality and Acute Physiologic and Chronic Health Evaluation (APACHE) II scores in patients with sepsis. The white blood cell count, PCT, TNF-α, and IL-6 levels in blood were reduced, and CD3+, CD4+, and monocytes of HLA-DR were improved at day 7 after treatment compared with routine therapy alone (46), and the levels of T cell subsets and immunoglobulin (IgA and IgM) in the blood of sepsis patients were significantly increased (38). Human leukocyte antigen (HLA)-DR is a key effector molecule in the process of cell phagocytosis. Its reduced expression is an important indicator of immunosuppression in sepsis patients. Based on conventional treatment, EA ST36, Guanyuan (CV4) can significantly promote the expression of HLA-DR. After EA treatment, the expression of T lymphocyte subsets CD3+, and the CD4/CD8+ ratio significantly increased, thus regulating cellular immune function (43).

In summary, acupuncture therapy has a two-way benign adjustment effect on the immune system of patients with sepsis. In the stage of excessive immune response in patients with sepsis, acupuncture can achieve organ protection by inhibiting excessive activation of the immune system and the systemic inflammatory response. Acupuncture therapy can significantly improve immune function in patients with immunosuppressed sepsis. The duration of the acupuncture intervention is generally 20-60 min, and the treatment cycle is generally 3-10 days.

TABLE 1 Clinical study on acupuncture treatment of sepsis.

Sepsis model	sample size	Intervention methods	Acupoints	Parameter of acupuncture	outcome indicator	Refs.
Intestinal dysfunction	82	EA	ST36, ST37	20min, twice a day, 5 d	TNF-α↓, IL-1β↓, IAP↓	Meng. (2018) (34)
Gastrointestinal dysfunction	40	MA	EX-B2	30 min, once a day, 10 d	APACHE II scores↓, intra-abdominal pressure↓, intragastric residual volume↓	Li. (2019) (35)
AGI	49	TEAS	ST25, ST37, ST41, SP8, ST36, CV12, SP15	dilatational wave, 2 Hz/10 Hz, twice a day, 30 min	MI↑, the time of the standard of enteral nutrition and hospitalization time↓	Liu. (2020) (36)
Sepsis	50	EA	ST36, ST25, ST37, ST39	Continuous wave, 4 Hz, twice a day, 60 min, 3 d	L/M↓, serum D-lactic acid level↓	Wu. (2013) (37)
Sepsis	90	MA	ST36, GB34, PC6, RN4	the twirling reinforcing method, 30 min, once per day, 6 d	CD3+↑, CD4+↑, CD8+↑, Ig G↑, Ig A↑, Ig M↑, ICU hospitalization length↓, the hospital readmission rate and the 28-day mortality↓	Xiao. (2015) (38)
SAE	64	MA	Main acupoints: GV20, GV26, GV16, GV24, GV14, GV11	>200 r/min, 40 min, once daily, 10 d	MoCA↑, IL-6↓, CRP↓, Lac↓	Lin. (2019) (39)
Gastrointestinal dysfunction	118	MA	EX-b2, T6-T12	30 min, once a day, 10 d	WBC↓, hs-CRP↓,PCT↓, the gastrointestinal dysfunction scores↓, feeding dose↑	Li. (2019) (40)
SAE	70	EA	GV20,GV26	1 mA, 2 Hz/15 Hz, dilatational wave, 30 min every 12 hours, 7 d	CRP↓, IL-6↓, NSE↓, MoCA↑, GCS↑	Zheng. (2020) (41)
Intestinal dysfunction	71	EA	ST36,ST37	continuous wave, 4Hz, 20 min, twice a day, 5 d	PCT↓, TNF-α↓, I-FABP↓, D-lactate↓, citrulline↑	Meng. (2018) (42)
Sepsis	60	EA	ST36, RN4	continuous wave, 30 min, twice a day, 7 d	APACHE-II score↓, CD3+↑, CD4+↑, CD8+↑, CD4+/CD8+↑, HLA-DR↑	Yang. (2016) (43)
Septic shock	58	early acupoint electrical stimulation	GB30, ST32, ST36, GB39, LR3,	discontinuous wave, 2 Hz, 5 mA, 2 times daily, 7 d	MRC↑, bilateral quadriceps thickness and gastrocnemius pinnate angle↑	Wang. (2020) (44)
Sepsis	60	EA	ST36, CV4, CV6	4/20Hz, twice per day, 30 min, 5 d	sPD-1↓, CD3+T lymphocytes↑, CD4+T lymphocytes↑, NK cells↑, the percentage of lymphocytes↑, INF-γ↑, WBC↓, percentage and count of neutrophils↓, ratio of neutrophils to lymphocytes↓, CRP↓, TNF-α↓	Yang. (2022) (45)

↑, upregulated by acupuncture; ↓, downregulated by acupuncture.
EA, electroacupuncture; ST36, Zusanli; ST37, Shangjuxu; TNF-α, tumor necrosis factor-alpha; IL-1β, interleukin-1beta; IAP, intraabdominal pressure; MA, manual acupuncture; EX-B2, Jiaji; APACHE:acute physiologic and chronic health evaluation; AGI, acute gastrointestinal injury; TEAS, transcutaneous electrical acupoint stimulation; ST25, Tianshu; ST41:Jiexi; SP8:Diji; CV12, Zhongwan; SP15, Daheng; MI, antral motility index; ST39, Xiajuxu; L/M, ratio of lactulose to mannitol; GB34, Yanglingquan; PC6, Neiguan; RN4, Guanyuan; SAE, sepsis-associated encephalopathy; GV20, Baihui; GV26, Shuigou; GV16, Fengfu; GV24, Shenting; GV14, Dazhui; GV11, Shendao; MoCA, Montreal Cognitive Assessment; IL-6, interleukin 6; CRP, C-reactive protein; Lac, lactic acid; WBC, white blood cell; hs-CRP, hypersensitive C-reactive protein; PCT, procalcitonin; NSE, neuron-specific enolase; MoCA, Montreal Cognitive Assessment; GCS, Glasgow Coma Scale; I-FABP, intestinal fatty acid-binding proteins; HLA-DR, human leukocyte antigen-DR; GB30, Huantiao; ST32, Futu; GB39, Xuanzhong; LR3, Taichong; MRC, medical research council; CV4, Guanyuan; CV6, Qihai; sPD-1, soluble programmed death protein 1; INF-γ, interferon-γ.

4 Animal models and acupuncture intervention parameters for the basic study of sepsis

4.1 Animal models of sepsis in the study of acupuncture mechanism

Currently, animal models used to study the mechanism of sepsis include the exogenous toxin model, exogenous live bacteria model, intraperitoneal infection model, and extraperitoneal sepsis model, with rats and rabbits as the main model animals. The exogenous toxin model involves systemic inflammation induced by intravenous or intraperitoneal injection of an endotoxin or LPS. The LPS model exhibits strong controllability and consistent animal reactivity. Exogenous live bacteria, such as *Escherichia coli*, can cause systemic inflammation through intraperitoneal or intravenous injection. The intraperitoneal infection model refers to a sepsis model that causes excessive inflammation through caecal ligation and puncture (CLP) (48) or colon ascendens stent peritonitis (CASP) (49). Necrotic tissue can be a source of inflammatory reactions. The CLP model (50) simulates a mixed bacterial infection caused by human appendicitis or diverticulitis. The characteristics of the CLP model are that the increase in cytokine levels is relatively gentle and lasts for a long time. The length of caecal ligation is a major factor affecting the mortality of the CLP model mice when the needle size and puncture times are controlled (51, 52). The CASP model involves the implantation of a stent with a fixed diameter into the ascending colon so that the intestinal contents continue to leak into the abdominal cavity, causing acute multi-bacterial sepsis peritonitis. The severity of sepsis can be adjusted by changing the stent diameter, or removing the stent during the second surgery and suturing the intestinal perforation (53, 54). The extraperitoneal sepsis model can induce lung infection by injecting bacteria into the trachea or nasal cavity, and can be used to study the local pathology of sepsis. This model is characterised by simple operation and high repeatability; however, its course is affected by the selected strains, dose, and antibiotics, which have certain limitations (55). The exogenous toxin and intraperitoneal infection models are commonly used to study the pathological mechanisms of sepsis. The CLP model was improved by Wichterman et al. and has been gradually standardised for more than 30 years (56, 57). As its pathological process is similar to the clinical symptoms, the CLP model is considered the gold standard for sepsis research (52, 58).

4.2 Rule of acupoint selection and acupuncture parameters in the study of acupuncture mechanism

We reviewed 54 basic studies on the acupuncture treatment of sepsis (Table 2) and found that 21 studies used ST36 alone as acupuncture intervention acupoints, three used ST36 and Feishu (BL13), three used ST36 and Neiguan (PC6), four used ST36 and Baihui (GV20/DU20), and six studies used ST36 combined with Tianshu (ST25), DU20, Quchi (LI11), Neiguan (PC6), and other acupoints. ST36 is the most commonly used acupuncture point in studies of sepsis mechanisms. Acupuncture at ST36 and BL13 improved sepsis-induced lung injury. Acupuncture with ST36 combined with GV20/DU20 improved brain injury in sepsis. In the fever and sepsis model (63, 90, 96, 99), acupoints Dazhui, LI11, and Yongquan were selected for acupuncture.

In research on the mechanism of acupuncture treatment for sepsis, EA (45 studies) was the most commonly used acupuncture intervention. Generally, the duration of the EA treatment was 30 min, the depth of acupuncture was mostly 1.5–5 mm, and the range of stimulation intensity was mainly between 1 and 4 mA. Low-frequency (1, 2, and 10 Hz) and variable-frequency (2/14 Hz, 2/15 Hz, and 2/100 Hz) stimulations are commonly used. Strong and weak electrical stimulation can activate different anti-inflammatory signalling pathways. High-intensity (3 mA) EA at ST36 or ST25 activates neuropeptide Y (NPY) splenic sympathetic reflex through the spinal sympathetic axis to play an anti-inflammatory role. Low-intensity (0.5 mA) EA at ST36 can activate the vagus–adrenal axis to play an anti-inflammatory role, whereas ST25 low-intensity (0.5 mA) stimulation cannot activate this pathway (60). This shows a correlation between the intensity of EA intervention and its efficacy. In the comparison of waveforms, research has shown that dilation waves, intermittent waves, or continuous waves can inhibit the activation of microglia and reduce inflammation, oxidative stress, and apoptosis to reduce sepsis-induced brain damage; however, the effect of dilation waves is the most significant, followed by intermittent waves, while the phase contrast of continuous waves is poor (69, 99). This suggests that dilated wave preconditioning may be a promising therapeutic strategy for alleviating sepsis-induced brain injury. Additionally, before the sepsis model was established, high-intensity (3 mA) EA at ST36 or ST25 played an anti-inflammatory role by activating the NPY splenic sympathetic nerve reflex through the spinal sympathetic axis. The same intervention showed a proinflammatory effect after the sepsis model was established (60). This indicates that the pathological state of sepsis at the time of acupuncture affects the therapeutic effects of acupuncture.

In addition to EA, seven studies used manual acupuncture (MA) intervention in animal models of sepsis. Some studies have compared the efficacy of MA and EA and found that MA more effectively reduced the production of proinflammatory cytokines in the spleens of septic mice, whereas EA more effectively induced c-Fos expression than MA (59). However, whether this is associated with the parameters of the MA and EA interventions remains unclear. Therefore, the anti-inflammatory effects of EA and MA require further investigation. Acupuncture manipulation is closely related to curative effects. In the rabbit model of fever induced by endotoxin, it was found that 'Shaoshanhuo' (heat-producing needling) and 'Toutianliang' (cool-producing needling) both reduced rectal temperature and serum endotoxin levels, while the effect of a cold needle in reducing endotoxin content was relatively good (97).

TABLE 2 Mechanism of acupuncture in preventing and treating sepsis.

Sepsis model	Species	Model induction method	Intervention methods	Acupoints	Parameter of acupuncture	Acupuncture Pretreatment or post-treatment	Test site Site + Mechanism	Refs.
Endotoxemia	Mice	LPS (ip)	MA, EA	ST36	MAC: 30 min; EAC: 1v, 1 Hz, 30 min	post-treatment	Plasma/spleen: TNF-α↓; DVC: c-Fos↑	Lim (2016) (59)
Endotoxemia	Mice	LPS (ip)	EA	ST36, ST25	10 Hz, 0-3.0 mA, 15 min	Pretreatment and post-treatment	Serum: TNF-α↓, IL-1β↓, IL-6↓; Serum catecholamine: NA↑, A↑, DA↑; spinal intermediolateral nuclei/ suprarenal ganglia/DMV: c-Fos↑	Liu (2021) (60)
ALI	Rabbit	LPS (iv)	EA	ST36, BL13	2 Hz/15 Hz, ≤1 mA, 15 min	Pretreatment	Lung: W/D↓, HO-1↑, Nrf2↑, SOD↑, MDA↓; serum: CAT↑, GPx↑; Plasma: TNF-α↓, IL-6↓	Yu (2014) (61)
Endotoxic shock	Rabbit	LPS (iv)	EA	ST36, BL13	10 Hz, disperse-dense wave, 15 min	Pretreatment	Lung: W/D↓, HO-1↑, SOD↑, MDA↓, EB↓; Plasma: CO↑	Yu (2013) (62)
Fever	Rabbit	Bacterial endotoxin	MA	LI11	Lifting and propulsion; Amplitude: 2 mm, 60 cycles/min	post-treatment	serum: TNF-α↓, IL-1β↓, IL-4↑	Wang (2017) (63)
Myocardial Injury in Septic	Rat	CLP	EA	ST36	2-100 Hz, 2 mA, 1 hour	post-treatment	Plasma: CK-MB↓; cardiac muscle: TNF-α↓, NO↓, MPO↓	Zhang (2018) (64)
Endotoxemia	Rat	LPS (iv)	EA	ST36	2-100 Hz, 2 mA, 1.5 hour	post-treatment	Plasma: TNF-α↓, ALT↓, CK-MB↓, DAO↓, Cr↓	Song (2014) (65)
Sepsis	Mice	CLP	EA	ST36, GV20	2 Hz, 1 mA, 30 min, 2 times per day	post-treatment	Hippocampus: NO↑, p-eNOS↑, Aβ↓	Jun (2022) (66)
cognitive impairment	Mice	LPS (ip)	EA	GV20	2/100 Hz, 4 mA, dilatational wave	Pretreatment	Hippocampus: MDA↓, H2O2↓, GSH↑, CAT↑, IL-1β↓, IL-6↓, TNF-α↓, α7nAChR↑, ACh↑, ChAT↑, AChE↓	Han (2018) (67)
SAE	Mice	LPS (ip)	EA	ST36, DU20	1 mA, 30 min	post-treatment	Hippocampus: PICK1-TLR4↑, TLR4↓, p-ERK/JNK/ P38↓; Plasma: IL-1β↓, IL-6↓, TNF-α↓	Mo (2021) (68)
Sepsis	Rat	CLP	EA	ST36, GV20	2-15 Hz, 2 mA, continuous wave, dilatational wave, intermittent wave, 5 days, 30 min	Pretreatment	serum and hippocampus: TNF-α↓, IL-6↓, MDA↓, SOD↑, CAT↑; hippocampus: TLR-4↓, NF-κB↓, Iba 1↓	Chen (2016) (69)
Endotoxemia	Rat	LPS (ip)	EA	LI4, PC6	2 Hz/100 Hz, 4 mA, 45 min	Pretreatment	Serum: TNF-α↓, IL-1β↓, IL-6↓	Song (2012) (70)
ABI	Rat	CLP	EA	ST36	2-100 Hz, 3 mA	post-treatment	Serum : TNF-α↓, HMGB1↓, ghrelin↑; bowel: MPO↓, DAO↑, GSH-R↑, ghrelin↑, HMGB1↓	Wu (2017) (71)
Sepsis	Rat	CLP	EA	ST36	2-100 Hz, 2 mA, 30 min	Pretreatment and post-treatment	Plasma: D-Lactose↓; Intestinal Mucosa: SIgA↑; CD3+T↑, γ/δ↑, CD4+ T↑, ratio of CD4+/CD8+ T cells↑	Zhu (2015) (72)
Hippocampal injury	Mice	LPS (ip)	EA	ST36, DU20	2/15 Hz, <1.5 mA, disperse-dense waves, 30 min	Pretreatment and post-treatment	Hippocampus: ROS↓, SOD↑, MDA↓, ATP↑	Mu (2022) (73)

(Continued)

10.3389/fimmu.2023.1242640

TABLE 2 Continued

Sepsis model	Species	Model induction method	Intervention methods	Acupoints	Parameter of acupuncture	Acupuncture Pretreatment or post-treatment	Test site Site + Mechanism	Refs.
ALI	Mice	LPS	EA	ST36	2 Hz, 1 mA, continuous wave, 10 min	Pretreatment	Serum/BALF: TNF-α↓, IL-1β↓, IL-6↓, IL-4↑, IL-10↑; lung: W/D↓, Sirt1↑, NF-κB↓, ac-NF-κB↓, ACE2↑	Luo (2022) (74)
SAE	Rat	CLP	EA	ST36, DU20, LI11	2 Hz/15 Hz, <1.5 mA, disperse-dense wave, 30 min	Pretreatment and post-treatment	Hippocampus: PSD-95↑, synaptophysin↑, MDA↓, SOD↑, Nrf2↑, HO-1↑	Li (2020) (75)
AKI	Rabbit	LPS (iv)	EA	ST36, PC6	2Hz/15 Hz, 1 mA, disperse-dense wave, 15 min	Pretreatment	Renal tissues: MDA↓, SOD↑, P-Akt↑, HO-1↑, Nrf2↑; Plasma : BUN↓, TNF-α↓, IL-10↑, Cr↓; Urine: NAG↓	Yu (2015) (76)
ALI/ARDS	Mice	LPS (ip)	EA	ST36	4/20 Hz, 0.5 mA, 20 min	post-treatment	Lung: W/D↓, MDA↓, GSH↑, ROS↓, GPX4↑, SLC7A11↑, FTH1↑, TNF-a↓, IL-1β↓, a7nAchR↑	Zhang (2022) (77)
Endotoxemia	Rat	LPS	EA	PC6	50 Hz, 1-3 mA(increased gradually), 4 v, 10 min	post-treatment	Plasma : ALT↓, AST↓, LDH↓	Liu (2011) (78)
Sepsis	Rat	CLP	EA	ST36	30 Hz, 40 mA, 20 min	post-treatment	Serum: TNF-a↓, IL-6↓, HMGB1↓, nitrite↓	Villegas (2014) (79)
AKI	Rat	LPS (iv)	EA	ST36, PC6	2 Hz, ≤1 mA, 30 min	Pretreatment	Renal tissue: iNOS↓, NF-kB↓; Plasma: TNF-a↓, IL-1β↓, IL-10↑, nitrite↓; BUN↓, Cr↓	Gu (2011) (80)
Sepsis	Rat	CLP	MA	ST36, GV01, B25, GV03, GV14, Liv02, Er Jien, LI11	/	post-treatment	Peritoneal lavage fluid: bacterial counts↓, neutrophil migration↑	Scognamillo (2004) (48)
Sepsis	Rat	CLP	EA	ST36	4/50 Hz, 3 mA, 30 min	post-treatment	Ileum: occludin↑; serum: D-lactate↓	Zhang (2018) (81)
Sepsis	Rat	CLP	EA	ST36, LI11, ST25	3 Hz, 2V, 15 min	post-treatment	Serum: TNF-α↓, IL-10↓, D-LA↓, DAO↓	Xie (2020) (82)
AKI	Rat	Eschericia coli ATCC (ip)	EA	ST36	2 Hz, 30 min	Pretreatment	Plasma: urea↓, creatinine↓	Harpin (2020) (84)
Injured lung induced by endotoxic shock	Rabbit	LPS (iv)	EA	ST36, BL13	2 or 100 Hz, disperse-dense wave, 30 min	Pretreatment	Lung: W/D↓, MDA↓, SOD↑, HO-1↑, p-ERK1/2↑; Serum: TNF-a↓	Zhang (2014) (83)
Endotoxemia	mice	LPS (ip); CLP	EA	ST36	40 mA, 4V, 15 min	Pretreatment and post-treatment	Serum: TNF-α↓, IL-6↓, MCP-1↓, INF-γ↓, DA↑, NE↑, E↑	Torres (2014) (85)
Sepsis	Rat	LPS (ip)	MA	ST36	twirled and twisted (>360°), 60 turns/min for 1 min, 30 min	Pretreatment and post-treatment	Plasma: BUN↓, Cr↓; kidney: PMN↓, MPO↓, iNOS↓, NO ↓	Huang (2007) (86)
ALI	Rat	LPS (ip)	MA	ST36	30 min	Pretreatment	Lung: NO↓, iNOS↓, MPO↓	Huang (2006) (87)

(Continued)

10.3389/fimmu.2023.1242640

TABLE 2 Continued

Sepsis model	Species	Model induction method	Intervention methods	Acupoints	Parameter of acupuncture	Acupuncture Pretreatment or post-treatment	Test site Site + Mechanism	Refs.
Sepsis	Mice	LPS (ip)	EA	ST36, ST25, BL56, LI10	10 Hz, 0.5/1.0/3.0 mA, 15 min	Pretreatment	Serum: TNF-α↓, IL-6↓, Catecholamine: NA↑, A↑, DA↑; DMV/vagal efferent neurons: Fos+↑	Liu (2021) (88)
Endotoxic shock	Rat	E.CoLi (iv)	EA	ST36, DU26	15 min	post-treatment	adrenal gland: SDH↑, ALP↑, Glycogen↑	Wang (1996) (89)
Fever	Rabbit	Escherichia coli endotoxin (iv)	MA, EA	GV14, LI11(left)	5 Hz, continuous bimodal pulse wave, 16 min	post-treatment	/	Kuang (1992) (90)
Endotoxin induced liver injury	Rat	LPS(iv)	EA	ST36	2-100 Hz, 2 mA, 1.5 hour	post-treatment	Liver: TNF-α↓; Plasma: ALT↓	Shi (2008) (91)
Endotoxemia	Rat	LPS (ip)	EA	BL32	30 Hz, 30 min	Pretreatment and post-treatment	Serum: TNF-α↓, IL-6↓, IL-1β↓	Wu (2021) (92)
Endotoxin shock	Rat	LPS (iv)	EA	PC6	2/14 Hz, 1 mA, Density wave	post-treatment	Plasma: TNF-α↓, NO↓	Li (2003) (93)
Endotoxin shock	Rat	E.CoLi (iv)	EA	ST36, DU26	15 min	post-treatment	Liver: G-6-Pase↑, SDH↑, 5′-Nase↑, Mg++-ATPase↑, liver glycogen↑	Huang (1995) (94)
ALI	Rat	CLP	EA	ST36, PC6	2-14 Hz, l mA, Density wave, 30 min	post-treatment	Lung: W/D↓, TNF-α↓, IL-6↓, P-JAK1↓, P-STAT3↓, Caspase-3↓, Bax↓	Xie (2020) (95)
Fever	Rabbit	ET (iv)	EA	KI1	8 Hz, 4.5 V/25 V, continuous square wave pulse, 4 cycles for 1 hour.	post-treatment	PO-AH: HSN↑	Dong (2008) (96)
Heat syndrome rabbits	Rabbit	ET	MA	LI11	/	post-treatment	Serum : ET↓; rectal temperature↓	Zhou (2012) (97)
Sepsis	Rat	CLP	EA	ST36	2/100 Hz, 2 mA, 1 hour	post-treatment	HBF↑; Plasma: ALT↓; liver: MDA↓, XOD↓	Shi (2010) (98)
Endotoxin induced fever model	Rabbit	ET (iv)	EA	CV14, LI11	12 Hz, 0.6-2 V, 10 min	post-treatment	Plasma/CSF: AVP↑; rectal temperature↓	Yang (1994) (99)
SE	Rat	CLP	EA	ST36	2-100 Hz, 2-3 mA, 30 min	post-treatment	Cerebral tissue: TNF-α↓, IL-6↓; Plasma: NSE↓	Wang (2013) (100)
Endotoxemia	Rat	LPS (iv)	EA	ST36, The auricular concha	10 Hz, 1 mA, 1 ms, 20 min	post-treatment	Serum: TNF-α↓, IL-6↓; Lung: NF-κB p65↓	Zhao (2011) (101)
Sepsis	Rat	CLP	EA	ST36	2-100 Hz, 2 mA, 30 min	post-treatment	Serum: HMGB1↓, Ghrelin↑; Jejunum tissue: HMGB1↓, Ghrelin↑	Wu (2014) (102)

(Continued)

10.3389/fimmu.2023.1242640

TABLE 2 Continued

Sepsis model	Species	Model induction method	Intervention methods	Acupoints	Parameter of acupuncture	Acupuncture Pretreatment or post-treatment	Test site Site + Mechanism	Refs.
ALI	Rat	LPS	MA	ST36	5 min, 4 days	Pretreatment	Blood/BALF: count of total leukocytes↓, count of total neutrophils↓	Ferreira (2009) (103)
Endotoxemia	Rat	LPS (ip)	EA	ST36	2 Hz, 1 mA, 5 min; 2 Hz, 1.5 mA, 5 min; 2 Hz, 2 mA, 20 min; continuous wave	Pretreatment	Serum: TNF-α↓, IL-1β↓, IL-6↓; Zusanli Acupoint/ Serum: Ca^{2+}↓; Spleen: CB2R↑, TLR4↓, NF-κB p65↓	Chen (2019) (104)
Peritonitis	Rat	LPS (ip)	MA	SP6	10 min	Pretreatment	Peritoneal fluid: MPO↓, TNF-α↓, IL-6↓, IL-10↑, leukocytes and neutrophil counts↓; brainstem: TNF-α↓, IL-6↓	Ramires (2021) (50)
Sepsis	Mice	LPS (ip)	EA	ST36	10 Hz, 0.1 mA, continuous wave, 30 min	Pretreatment	Serum: TNF-α↓, IL-1β↓, IL-5↓, IL-6↓, IL-10↓, IL-17A↓, eotaxin↓, IFN-γ↓, MIP-1β↓, KC↓	Lv (2022) (105)
Sepsis	Rat	CLP	EA	ST36	2 Hz, 2mA, 30 min	post-treatment	Small intestinal tissue: Bcl-2↑, Bax↓, IL-4↑; small intestinal mucus: sIgA↑	Lou (2022) (106)
septic cardiomyopathy model	Mice	LPS (ip)	EA	PC6, ST36	0.3 mA, 2 Hz, 30 min, once a day for 7 days	Pretreatment	Cardiac function: EF↑, FS↑, E/A↑; Serum and heart tissue: TNF-α↓, IL-1β↓; BAX\Bcl2↓; cardiomyocyte apoptosis↓; calpain-2↓; p-STAT3↓	Li (2022) (107)
Sepsis	Rat	LPS (ip)	EA	ST25	15 Hz, a pulse width of 1 ms, 3 mA, 20 min	post-treatment	Blood: NE↑, IL-10↑, IL-6↓, IL-1β↓	Zhang (2022) (108)
Sepsis	Rat	CLP	EA	PC6	2/15 Hz, 2 mA, 20 min	post-treatment	LF/HF↓, pH↑, BE↑, lactate levels↓, MAP↑; plasma: BNP↓, cTnI↓, TNF-α↓, IL-1β↓; cardiac tissue: α7nAChR↑; percent survival↑	Wu (2023) (109)
Endotoxemia	Mice	LPS (ip)	EA	ST36, LI4	2 Hz/15 Hz, 1 mA	Pretreatment	Intestine mucosa: ATP↑,DAO↑, ROS↓, OCR↓, HO-1↑, PINK1↑, Mfn1↑, Mfn2↑, OPA-1↑, Drp1↓, Fis1↓, caspase-1↓, IL-1β↓	Zhang (2023) (110)

↑, upregulated by acupuncture; ↓, downregulated by acupuncture.

LPS, lipopolysaccharide; ip, intraperitoneal Injections; MA, manual acupuncture; EA, electroacupuncture; ST36, Zusanli; MAC, manual acupuncture; EAC, electroacupuncture; TNF-α, tumor necrosis factor-alpha; DVC, the dorsal vagal complex; ST25, Tianshu; IL-1beta, interleukin-1beta; IL-6, interleukin 6; NA, noradrenaline; A,adrenaline; DA, dopamine; DMV, dorsal motor nucleus of the vagus nerve; IV,intravenous injection; BL13, Feishu; W/D, wet/dry; HO-1, heme oxygenase-1; Nrf2,nuclear factor erythroid-2 related factor-2; SOD, superoxide dismutase; MDA, malondialdehyde; CAT, catalase; ALI, acute lung injury; GPx, glutathione peroxidase; EB, evans blue; CK-MB, creatine kinase MB; NO, nitric oxide; MPO, myeloperoxidase; ALT, alanine aminotransferase; DAO, diamine oxidase; Cr, creatinine; GV20/DU20, Baihui; eNOS, endothelial nitric oxide; Aβ,β–peptide; H2O2, hydrogen peroxide; GSH, glutathione; α7nAChR, α7 nicotinic acetylcholine receptors; ACh, acetylcholine; ChAT, choline acetyltransferase; AChE, acetylcholinesterase;PICK1, protein Kinase C; TLR4, toll-like receptor 4; ERK1/2, extracellular signal regulated kinases1/2; JNK, the c-Jun N-terminal kinases; Iba 1, ionized calcium binding adaptor molecule 1; PC-6, Neiguan; HMGB1, high mobility group box-1; SAE, sepsis-associated encephalopathy; ABI, acute bowel injury; GSH-R, ghrelin receptor; ATP, adenosine triphosphate; BALF, bronchoalveolar lavage fluid; ACE2, angiotensin-converting enzyme 2; LI11, Quchi; PSD-95, postsynaptic density protein-95; AKI, acute kidney injury; BUN, blood urea nitrogen; Cr, creatinine; NAG, N-acetyl-glucosaminidase; ARDS, acute respiratory distress syndrome; ROS, reactive oxygen species; GPX4, glutathione peroxidase 4; SLC7A11, solute carrier family 7 member 11; FTH1, ferritin heavy chain 1; AST, aspartate aminotransferase; LDH, lactate dehydrogenase; iNOS, nitric oxide synthase; GV14, Dazhui; GV01, Changqiang; GV03, Yaoyangguan; D-LA, D-lactic acidosis; MCP-1, monocyte chemotactic protein-1; INF-γ, interferon-γ; NE, norepinephrine; E, epinephrine; DA, dopamine; PMN, polymorphonuclear neutrophil; NA, noradrenaline; DU26, Renzhong; SDH, succinate dehydrogenase; ALP, alkaline phosphatase; BL32, Ciliao; G-6-Pase, glucose-6-phosphatase; 5' -Nase,5 '- Nucleotidase; NK, the c-Jun N-terminal kinases; STAT3, signal transducer and activator of transcription 3; Caspase-3, cysteine aspastic acid-specific protease 3; Bax, BCL-2-associated X protein; PO-AH, preoptic region and anterior hypothalamus; HSN, the heat sensitive neurons; ET, endotoxin; HBF, hepatic blood flow; CV14,juque; CSF, cerebrospinal fluid; AVP, arginine vasopressin; SE, septic encephalopathy; NSE, neuron-specific enolase; CB2R, cannabinoid CB2 receptor; SP6, sanyinjiao; KC, keratinocyte-derived chemokine; MIP-1β, macrophage inflammatory protein-1β; sIgA,secretory IgA; Bcl-2, B-cell lymphoma-2; EF, ejection fraction; FS, fractional shortening; E, A, early diastolic mitral annular velocity and late diastolic mitral annular velocity; CV6, Qihai; LF, low-frequency; HF, high frequency; pH, potential of hydrogen; BE, base excess; MAP, mean arterial pressure; BNP, brain natriuretic peptide; cTnI,cardiac troponin I; OCR, oxygen consumption rate; PINK1, PTEN-induced putative kinase 1; Mfn1/2, mitofusin 1 and 2; OPA-1, optic atrophy 1; Drp1, dynamin-related protein 1; Fis1, mitochondrial division protein 1.

10.3389/fimmu.2023.1242640

5 Acupoint initiation mechanism of acupuncture for anti-inflammatory effects

Acupuncture stimulates the local acupoints to produce curative effects. Local mechanical stimulation at acupoints is converted into chemical signals that activate the body's neuroendocrine-immune system and initiate the acupuncture effect (111, 112). The study found that collagen fibres (fascicular or reticular arrangement) in the LI11 acupoint may be the first material basis for the acupoint to perceive the acupuncture mechanical force. Acupuncture stimulation can cause deformation of collagen fibres in the extracellular matrix of the local acupoint and transmit mechanical signals to the surrounding connective tissue cells (63), producing cascade reactions. A research report published in *Nature* showed that the PROKR2 sensory neuron at the ST36 acupoint may be the anatomical basis for EA to drive the vagus adrenal axis in mice and play a role in inhibiting sepsis inflammation (88). These neurons control the deep fascia of the hind limb (such as the periosteum), which is crucial for driving the vagal-adrenal axis. In 2014, Ulloa et al. found that EA further activated aromatic l-amino acid decarboxylase to control systemic inflammation and improve the survival rate of septic mice by activating the sciatic nerve to induce the vagus nerve (85). Dong found that EA stimulation of acupoint KI1 antagonises the electrical activity of heat-sensitive neurons (HSN) in the preoptic area and hypothalamus induced by endotoxic heat, which may be caused by the activation of high-threshold thin nerve fibres at local acupoints (96). In addition, studies have shown that the change in Ca^{2+} influx in the ST36 acupoint area of endotoxic rats may serve as a bridge between local EA stimulation and systemic effects. Its potential mechanism may be that EA pretreatment reduces Ca^{2+} influx by activating the cannabinoid CB2 receptor (CB2R) at the ST36 local acupoint, thereby inhibiting the inflammatory response in endotoxic rats (104).

The above evidence shows that acupuncture may act on local fascicular or reticular collagen fibres through mechanical stimulation, causing local tissue deformation, further transmitting acupuncture signals to connective tissue cells, or activating sensory nerve fibres (PROKR2 neurons, high threshold thin nerve fibres, sciatic nerve) in the acupoint area, and at the same time, it may cause the release of bioactive chemicals (CB2R activation, Ca^{2+} influx) in the acupoint area, causing cascade reactions, thus playing a role in acupuncture.

6 Autonomic neurobiological mechanism of acupuncture in inhibiting sepsis inflammation

The interaction between the sympathetic and parasympathetic nerves of the autonomic nervous system and immune system affects inflammation. The vagus nerve is the main parasympathetic nerve responsible for the physiological regulation of most internal organs. The regulation by sympathetic nerves of the inflammatory response is affected by receptor subtypes expressed by neurotransmitters and immune cells, which have proinflammatory and anti-inflammatory effects. Both the sympathetic and parasympathetic nervous systems are involved in the acupuncture inhibition of systemic inflammation in sepsis, including the vagal cholinergic anti-inflammatory pathway, vagal adrenal medulla dopamine pathway, and sympathetic pathway.

6.1 Vagal cholinergic anti-inflammatory pathway

The cholinergic anti-inflammatory pathway (CAP) was first proposed by Borovikova et al. in the early 20th century (113). The vagus nerve CAP is a neuroimmune anti-inflammatory pathway that is mainly composed of nicotinic acetylcholine receptors (α7nAChR) containing α7 subunits on immune cells, and acetylcholine (ACh) released by the vagus nerve and its terminals. Compared with the humoral anti-inflammatory pathway, the cholinergic anti-inflammatory pathway has a very short reaction time. It rapidly and efficiently regulates systemic inflammatory responses and reduces mortality rates. Studies have shown that electroacupuncture can increase the activity of the vagus nerve, promote the expression of α7nAChR in macrophages in the myocardial tissue, prevent the occurrence of hyperlactatemia, alleviate the decline in left ventricular ejection fraction, inhibit the systemic and cardiac inflammatory response, and alleviate the histopathological manifestations of the heart (109). In the rat CLP model, EA ST36 can reduce the plasma activity of creatine kinase MB (CK-MB) and TNF-α in the myocardium and reduce the expression of nitric oxide (NO) and myeloperoxidase (MPO). When the bilateral abdominal vagus nerves are cut off, the effect of acupuncture on inhibiting the level of inflammatory factors in sepsis rats decreases significantly, suggesting that the cholinergic anti-inflammatory pathway is one of the main mechanisms of EA's anti-inflammatory and myocardial protective effects (64). The auricular concha is distributed along the branches of the auricular vagus nerve. Both EA of the auricular concha and vagus nerve can increase serum TNF-α and IL-6 levels, and downregulate pulmonary NF-κB p65 expression levels in endotoxemia, with similar cholinergic anti-inflammatory mechanisms (101). Iron death has been shown to occur in alveolar epithelial cells of mice with sepsis. The inhibition of ferroptosis can reduce lung injury (114). Zhang et al. found that EA at the ST36 acupoint can activate α7nAchR on the surface of alveolar epithelial cells of lung tissue, inhibit LPS-induced iron death of alveolar epithelial cells, and reduce the lung inflammatory response (77). Parasympathetic branches of the sacral plexus near the Ciliao (BL32) acupoint. Studies have found that EA at BL32 can start the anti-inflammatory effect of the parasympathetic nervous system, improve the survival rate of rats with lethal endotoxaemia, and reduce the inflammatory cytokines TNF-α, IL-6, and IL-1β with its systemic anti-inflammatory effect. Pelvic nerve resection significantly reduces the effect of EA on BL32. The pelvic nerve-mediated parasympathetic pathway of the sacral plexus may have a

more rapid effect than the cervical vagus nerve-mediated anti-inflammatory pathway (92). In addition, pretreatment of acupoint Hegu (LI4) with EA can significantly reduce the release of serum proinflammatory factors, such as TNF-α, IL-1β, and IL-6; therefore, it can reduce the systemic inflammatory reaction, significantly improve the survival rate of rats with fatal endotoxemia, and EA at LI 4 has a stronger protective effect than at PC6 acupoint, while electrical stimulation of non-acupoints is ineffective. The protective effects of EA can be eliminated when the vagus nerve is cut off, the spleen is excised, or the central muscarine receptor and surrounding nicotine receptors are inhibited (70). Lim et al. found that acupuncture signals were transmitted to the dorsal vagal complex (DVC) and activated the splenic nerve through vagal activity, inducing an anti-inflammatory response in splenic macrophages (59). Organ failure due to excessive inflammation is the main cause of early mortality in patients with acute pancreatitis (AP). Zhang confirmed through experiments that EA can inhibit the infiltration of macrophages in the pancreas, reduce plasma amylase and TNF-α, IL-1β, and IL-6 expression, and inhibit systemic inflammation, and that cervical vagotomy or blocking α7nAChR can inhibit the protective effect of EA on the pancreas (115). The above research shows that the vagus cholinergic anti-inflammatory pathway can regulate the immune response and production of proinflammatory cytokines, which is an important acupuncture anti-inflammatory mechanism.

6.2 Vagus adrenal medulla dopamine pathway

In 2014, Ulloa et al. found that in mice with sepsis, EA increased the serum levels of three catecholamines, mainly dopamine and norepinephrine, and inhibited serum TNF, MCP-1, IL-6, and INF through the sciatic nerve activating the vagus adrenal medulla dopamine pathway-γ; therefore, reducing the systemic inflammatory reaction can improve the survival rate. EA with a wooden stopcock or stimulation with a non-acupuncture acupoint did not inhibit inflammatory levels. Capsaicin agonists, reserpine, sciatic nerve or neck, subphrenic vagotomy, and adrenalectomy can eliminate the anti-inflammatory effects of EA (85). In a rat model of CLP-induced sepsis, the effect of EA on reducing the levels of serum inflammatory factors depended on the integrity of the vagus nerve and catecholamine production (79). These studies have shown that EA can inhibit the systemic inflammatory reaction in mice with sepsis and improve the survival rate by activating the vagus nerve-adrenal medulla dopamine pathway through the sciatic nerve. In 2020, Professor Ma Qiufu of Harvard Medical School found that EA stimulation drives sympathetic pathways in somatotopy- and intensity-dependent manners. Low-intensity EA stimulation of ST36 (0.5 mA, 10 Hz) can activate the vagus adrenal axis anti-inflammatory pathway; however, low-intensity EA stimulation of ST25 does not affect the vagus nervous system or sympathetic nerves. In 2021, it further revealed the specific neuroanatomical basis of EA stimulation and found that low-intensity EA stimulation of ST36 acupoints in mice drove the vagal-adrenal anti-inflammatory axis to achieve an anti-inflammatory effect mediated by neurons expressing Prokr2 at the ST36 acupoint (88). Therefore, low-intensity EA stimulation may inhibit inflammation by activating the vagus nerve of the parasympathetic nervous system.

6.3 Sympathetic nerves

The sympathetic nervous system plays a dual role in regulating inflammatory responses and mediates both proinflammatory and anti-inflammatory effects. A previous study found that stimulating the homosegmental acupoint ST25 with 3 mA EA can drive the release of peripheral NE from the sympathoadrenal medullary axis (108). Unlike low-intensity EA, high-intensity EA activates the sympathetic nervous system and inhibits sepsis-induced inflammation. Before LPS-induced systemic inflammation, 3 mA high-intensity EA stimulation of ST25 on the abdomen can activate peripheral NPY+sympathetic neurons projecting to immune organs such as the spleen and play a role in β2-norepinephrine receptor-mediated anti-inflammatory effects. However, after LPS-induced inflammation, the application of the same abdominal acupoints and stimulation intensity showed obvious proinflammatory effects, mainly because LPS can induce and promote inflammation and increase the expression of α2-adrenergic receptors. High-intensity EA at ST36 can activate the 'spinal sympathetic' reflex, thus playing an anti-inflammatory role. Similar to the ST25 acupoint, high-intensity EA stimulation of the ST36 acupoint after LPS-induced inflammation has an inflammatory effect (60). This shows that high-intensity EA stimulation (3 mA) of ST36 or abdominal ST25 acupoints can activate the spinal cord and peripheral sympathetic reflexes, respectively. Moreover, the inflammatory regulatory effect of EA stimulation is bidirectional and related to the inflammatory state of the body during the acupuncture intervention.

The above results reveal that acupuncture at body surface acupoints can induce multiple somatosensory autonomic nerve target organ reflex pathways and regulate immune inflammation. This regulatory effect is related to acupoint location, stimulus intensity, and body state and has the characteristics of acupoint specificity, intensity dependence, and bidirectionality. These studies enrich the modern scientific connotation of body surface therapies, such as acupuncture and moxibustion, and provide an important scientific basis for the clinical optimisation of acupuncture parameters, inducing different autonomic nerve reflexes, and thus treating specific diseases (such as sepsis).

7 Acupuncture prevents sepsis organ dysfunction by inhibiting inflammation, antioxidative stress and reducing apoptosis

The regulation of acupuncture in the body is characterised by multiple systems, pathways, and targets. The response of the target organs is the key link for acupuncture to take effect. Acupuncture regulates the nerve endocrine immune system (NEI) of the body through the activation of the 'acupoint network', through

integrating nerve conduction, and has a therapeutic effect through the 'effect network'. Multiple-organ dysfunction syndrome (MODS) is the primary cause of death in sepsis. In sepsis, excessive inflammation, oxidative stress, and apoptosis are the main mechanisms that lead to multiple organ dysfunction. Acupuncture can reduce the levels of proinflammatory cytokines, increase the levels of anti-inflammatory cytokines, regulate the balance of prinflammatory and anti-inflammatory factors in two directions, reduce oxidative stress, improve cell energy metabolism, maintain mitochondrial function, and regulate cell apoptosis to prevent the progressive aggravation of sepsis, leading to MODS.

7.1 Lung

The lungs are the earliest organs damaged in sepsis with MODS (116–118). Acute lung injury (ALI) is an independent risk factor for organ dysfunction and death in sepsis patients (119). Acupuncture has a significant effect on relieving acute lung injury (103). During the development of ALI induced by endotoxins, the content of the oxidative stress products malondialdehyde (MDA), myeloperoxidase (MPO), and NO increased significantly, while that of superoxide dismutase (SOD) decreased significantly, leading to increased apoptosis (120). Heme oxygenase-1 (HO-1) is a rate-limiting enzyme in the process of heme catabolism and is a strong negative regulator of oxidative stress in the endotoxins of ALI and pneumonia. Its metabolites, bilirubin, carbon monoxide, and iron have the effects of antioxidative damage (121). Several studies have shown that HO-1 mediates the ability of acupuncture to relieve sepsis-induced lung injury. EA pretreatment at ST36 and BL13 acupoints for 5 days significantly increased the plasma CO content, reduced MDA and MPO, the number of apoptotic cells in the lung, and wet/dry (W/D) lung weight ratio, and reduced ALI caused by endotoxic shock, whereas acupuncture at non-acupoints showed no significant effect. Further research showed that EA preconditioning for 5 days promoted the expression of HO-1 mRNA and protein levels in ALI lung tissue, and the protective effect of EA preconditioning on septic lung injury disappeared after tail vein injection of the HO-1 inhibitor ZnPP IX, indicating that acupuncture protects the lungs by promoting the expression of HO-1 (62). In another report, acupuncture at ST36 significantly reduced the expression of lung-induced nitric oxide synthase (iNOS) and NO biosynthesis, and reduced LPS-induced acute lung injury in rats (87). Nuclear factor erythroid-2 related factor-2 (Nrf2) is a cap n-collar alkaline leucine zipper transcription factor that promotes the transcription of HO-1 by combining with the antioxidant response element (ARE). The Nrf-2/HO-1 signalling pathway is considered an antioxidant and protective pathway, especially in inflammatory diseases, including sepsis (122). The study found that pretreatment of bilateral ST36 and BL13 acupoints with EA promotes the expression of Nrf2 and HO-1 in ALI rabbit lung tissue and reduces the inflammatory factors TNF-α and IL-6 (61). This suggests that the promotion of HO-1 expression by EA pre-conditioning may be related to the Nrf2/ARE signalling pathway. In addition, Zhang found that EA stimulation of ST36 and BL13 upregulates HO-1 in the lungs of endotoxic shock rabbits, and the potential mechanism of reducing lung injury may be related to the upregulation of signal transduction of the extracellular signal-regulated kinases1/2 (ERK1/2) pathway (83). NAD-dependent deacetylase sirtuin 1 (SIRT1) can inhibit NF-κB signal activation, reducing oxidative stress and apoptosis, which is important role organ protection (123). Angiotensin-converting enzyme 2 (ACE2) is a single carboxyl peptidase that is important in maintaining the renin-angiotensin system (RAS). RAS can weaken immunity, inflammation, and other physiological activities (124), and ACE2 can prevent inflammatory damage in alveolar type II (AT II) cells by activating SIRT1-related pathways (125). The study found that EA pretreatment of ST36 acupoint for 7 days can more effectively improve LPS-induced acute lung injury than for 1 day, and promote the expression of ACE2 and SIRT1 in lung tissue, thereby reducing the acetylation modification of NF-κB. Reducing the inflammatory cytokines TNF-α, IL-1β, and IL-6 alleviated ALI (74). The JAK1/STAT3 signalling pathway is one of the key pathways that inhibits the polarisation of M2 macrophages with an inflammatory response (126). EA at ST36 can inhibit the release of TNF-α and IL-6, reduce apoptosis, and reduce lung injury in septic rats by activating the JAK1/STAT3 pathway (95). Therefore, acupuncture may alleviate acute lung injury caused by sepsis by inhibiting oxidative stress and inflammatory reactions. In this process, HO-1 is the key molecule for acupuncture to inhibit oxidative stress, SIRT1/NF-κB and JAK1/STAT3 signal pathways are involved in the process of acupuncture inhibiting inflammatory reaction.

7.2 Brain

Sepsis-associated encephalopathy (SAE) is a common complication of severe sepsis and is associated with high mortality rates in the intensive care unit. Generally, sepsis survivors have obvious cognitive deficits that may lead to poor quality of life (127). The degree of hippocampal injury induced by inflammatory reactions and oxidative stress positively correlates with cognitive dysfunction in sepsis (128). Several studies have shown that acupuncture alleviates sepsis-induced cognitive dysfunction by inhibiting neuroinflammation and oxidative stress.

ACh is a neurotransmitter necessary for maintaining normal cognition and memory, and its expression is positively correlated with cognitive ability (129). Choline acetyltransferase (ChAT) catalyzes ACh synthesis, while acetylcholinesterase (AChE) catalyzes ACh hydrolysis and degradation (130). In the SAE mouse model, EA significantly reduces AChE activity in the hippocampus, increases ChAT activity and ACh content, and enhances α7nAChR protein expression, reducing IL-1β, IL-6, and TNF-α levels to reduce neuroinflammation. This indicates that acupuncture can inhibit inflammation in the hippocampus of SAE mice through a cholinergic anti-inflammatory pathway (67). PICK1 is an important regulatory protein involved in brain-related diseases and plays a protective role in sepsis. PICK1 can bind to the TLR4 receptor on microglia and remain in the cytoplasm, preventing TLR4 from reaching the cell membrane and mediating inflammation. Mo et al. found that EA significantly increased the formation of the PICK1-TLR4 complex, thereby inhibiting the

expression of proinflammatory cytokines (68). Neuron-specific enolase (NSE) is a clinical index used to assess the degree of central nervous system injury and prognosis. In the rat model of CLP-induced sepsis, EA at ST36 significantly reduced the plasma NSE level and the expression of proinflammatory cytokines in brain tissue, such as TNF-α and IL-6, reducing brain damage (100).

Endothelial nitric oxide (eNOS) is a calcium-dependent protease that exists in vascular endothelial cells and can synthesise trace amounts of NO, keeping the endothelium smooth and intact, maintaining vascular tension, and preventing thrombosis. β-peptide (Aβ) is formed by β-Amyloid precursor protein produced and released into the extracellular space. Under normal conditions, Aβ is swallowed up by microglia in the brain. However, when the Aβ concentration is too high, large plaques will form that damage neurons, and they will also enter the synaptic space to prevent memory formation. p-eNOS reduction and Aβ deposition are closely related to long-term cognitive deficits. Previous studies have shown that EA intervention can prevent and treat long-term cognitive dysfunction after sepsis-induced brain injury. The ST36 and GV20/DU20 acupoints are the most effective combination for improving cognitive function (131). The latest research confirms that EA GV20 and ST36 acupoints can increase the level of NO and p-eNOS and reduce Aβ in the hippocampus of sepsis-surviving mice and improve the long-term cognitive impairment caused by sepsis. However, intraperitoneal injection of the eNOS inhibitor L-NAME weakened the efficacy of EA therapy (66). Improving mitochondrial dysfunction is the key to preventing oxidative stress in the brain during sepsis. HO-1 is an endogenous protective substance essential for maintaining mitochondrial function (132). Mu et al. found that EA pretreatment of acupoints DU20 and ST36 significantly increased the activities of mitochondrial respiratory chain complexes I, II, III, and IV, as well as the levels of SOD and ATP, and reduced the levels of the oxidative stress products, ROS and MDA, in the hippocampi of septic mice. This suggests that EA prevents LPS-induced oxidative damage and mitochondrial respiratory defects. Interestingly, HO-1 knockout increases ROS and MDA levels and decreases SOD and ATP levels. HO-1 deficiency aggravates mitochondrial swelling, crest relaxation, and vacuole degeneration, indicating the key role of HO-1 in maintaining mitochondrial energy production and resisting oxidative damage in the hippocampus (73). In an SAE rat model, Li et al. found that EA DU20, ST36, and LI11 acupoints upregulated the expression of Nrf-2 mRNA and HO-1 protein, increased the SOD level, reduced the MDA level in the hippocampus, reduced the loss of neurons in the hippocampal CA1 area, and increased the 14-day survival rate (75). In addition, acupuncture reduced the levels of MAD and hydrogen peroxide (H2O2), increased the levels of catalase (CAT) and glutathione (GSH) in the hippocampus, and inhibited oxidative stress (67). This suggests that EA may exert antioxidant and protective effects against SAE by activating the Nrf-2/HO-1 pathway.

Acupuncture may increase PICK1-TLR4 complex formation, reduce plasma NSE levels and inhibit inflammatory reactions through the acetylcholine pathway, protect mitochondrial function by activating the Nrf-2/HO-1 pathway, increase p-eNOS, and reduce Aβ deposition, thus alleviating hippocampus damage during sepsis.

7.3 Intestines

Systemic hyperinflammation can lead to intestinal ischaemia, oedema, increased intestinal mucosal permeability, and translocation of intestinal bacteria and toxins, subsequently causing heterogeneous sepsis and MODS. It is important to effectively inhibit the production of proinflammatory factors in the early stages and protect the intestinal mucosal barrier for the prevention and treatment of sepsis.

Studies have shown that acupuncture significantly improves sepsis-associated intestinal hyperinflammation. Ghrelin is a brain-gut peptide secreted by endocrine cells of the gastrointestinal tract, which can inhibit the proinflammatory factors HMGB1 and TNF-α. Wu et al. found that the ST36 acupoint in EA sepsis model rats increased the expression rate of ghrelin-immunopositive cells in the intestine and reduced the serum and intestinal content of HMGB1. Correlation analysis revealed that HMGB1 levels decreased with increased ghrelin expression. However, ghrelin receptor blockers can block the inhibition of the inflammatory mediator HMGB1, proving that ghrelin mediates EA to inhibit intestinal inflammation (71, 102). HO-1 catalyses the breakdown of heme into free iron, carbon monoxide, and biliverdin, thereby regulating mitochondrial homeostasis and preventing oxidative cell damage (133, 134). TEN-induced putative kinase 1 (PINK1), the only kinase located mainly in the mitochondrial intima, has been found to exert a protective effect on the mitochondria during cellular stress. Studies have shown that EA induces the translocation of HO-1 to the mitochondrial inner membrane; activates PINK1; increases ATP production, DAO activity, and OCR; regulates mitochondrial fusion/division balance; reduces ROS content and OCR; and protects intestinal barrier function (110).

Increased intestinal mucosal permeability is a pathological mechanism underlying heterogeneous sepsis. The intestinal tight junction (TJ) barrier is an important component of the intestinal mucosal barrier. Intestinal epithelial cell tight junction (occludin) is an important protein in the intestinal epithelial cell TJ, and is negatively related to the permeability of the cell gap (135, 136). Monitoring blood D-lactate levels can also reflect changes in intestinal permeability and the degree of damage (137). Zhang et al. found that EA stimulation of ST36 increased the expression of occludin in rats with sepsis, reduced the level of serum D-lactate, and maintained the intestinal mucosal barrier (81). The immune barrier, composed of lymphocytes and secretory immunoglobulin A (sIgA) from humoral immunity, is crucial for maintaining the intestinal mucosal immune function and inhibiting intestinal bacterial translocation (138, 139). In the blood of septic mice, the concentration of D-lactose, a biomarker of intestinal permeability produced by intestinal bacteria, increased significantly (140). Zhu et al. found that EA pretreatment of ST36 significantly reduced the level of serum D-lactose, increase the concentration of sIgA in the intestinal mucosa, increase CD3+, γ/δ, CD4+T cell percentage, and

CD4+/CD8+T cell ratio, reduce the permeability of CLP rats, and improve intestinal injury (72). Xie et al. also found that EA at ST36 and LI11 can restore intestinal T cell immune function to normal and significantly reduce TNF-α and IL-10 in the serum of CLP model rats. When the spleen is removed, EA ST36 cannot reduce blood TNF-α, IL-10, and D-LA levels; however, it can improve intestinal immune function by balancing the proportion of T lymphocytes (CD3+CD4+/CD3+CD8+cells and Treg/Th17 cells). Therefore, the spleen may be necessary for EA at ST36 to improve systemic inflammation, but regulation of the intestinal barrier and immune defence is not essential (82).

The above studies show that EA can inhibit intestinal hyperinflammation in sepsis, protect the intestinal mucosal barrier by regulating the immune function of intestinal lymphocytes, prevent intestinal bacterial translocation, and improve intestinal injury.

7.4 Kidney

Sepsis-associated acute kidney injury (SAKI) seriously affects the prognosis of patients with sepsis and increases mortality (141). EA has a significant inhibitory effect on oxidative stress and excessive inflammatory reactions in patients with SAKI. For example, Harpin et al. found that EA pretreatment at the ST36 acupoint significantly reduced urea and creatinine levels in SAKI rat models and protected renal function (84). Endotoxic shock results in an abnormal adrenal glucose metabolism and decreased adrenal glycogen levels. Succinate dehydrogenase (SDH), located in the mitochondria, is a key enzyme involved in the oxidative phosphorylation of glucose metabolism. The main function of alkaline phosphatase (ALP) is to increase phosphate metabolism, plasma membrane permeability, and the transport function of cells (142). In a rat model of endotoxic shock, EA at Renzhong (DU26) or ST36 prevented the loss of glycogen in the adrenal gland, enhanced the activities of SDH and ALP, and enhanced adrenal cortex function in endotoxic shock rats (89). The phosphoinositide 3-kinase (PI3K)/Akt signalling pathway controls the activation of Nrf2 and participates in the induction of HO-1 (143–145). In a rabbit model of acute renal injury, EA stimulation of the ST36 and PC6 acupoints significantly inhibited the LPS-induced increase in the AKI biochemical indicators, blood urea nitrogen (BUN), creatinine (Cr), and N-acetyl-glucosaminidase (NAG). EA at these acupoints also increases the PI3K/Akt/Nrf2 pathway and HO-1 protein expression, increases SOD and IL-10 levels, reduces MDA and TNF-α levels, and reduces apoptosis of renal tubular cells, thereby reducing renal injury. Intravenous injection of wortmannin, a PI3K/Akt pathway inhibitor, weakened the partial protective effect of EA. This indicated that the PI3K/Akt/Nrf2/HO-1 pathway mediates the protective effects of acupuncture (76). During sepsis, overactivation of the NF-κB signalling pathway induced the expression of iNOS and excessive production of NO level, which affected renal hemodynamics (146–149). Research has shown that acupuncture pretreatment at ST36 significantly reduces the overexpression of iNOS and the resulting NO in SAKI rats. However, acupuncture after sepsis onset had no obvious protective effects against renal injury (86). Another report demonstrated that EA at ST36 and PC6 acupoints inhibits NF-κB activity in renal tissue of SAKI rats, reduces iNOS expression in the kidney and plasma BUN and Cr levels, inhibits the release of TNF-α and IL-1β, and increases the release of anti-inflammatory factor IL-10 to reduce renal injury induced by endotoxaemia (80). These studies indicate that EA may pass through the PI3K/Akt/Nrf2/HO-1 and NF-κB signalling pathways and inhibit renal hyperinflammation and oxidative stress.

7.5 Liver

Liver injury is a manifestation of sepsis and multiple organ dysfunction syndrome. Liver injury can occur at all stages of sepsis and is an independent risk factor for MODS and death. An increasing number of studies have confirmed that early acupuncture intervention can improve the prognosis of patients with sepsis and liver injury. Various liver enzymes, including alanine aminotransferase (ALT), aspartate aminotransferase (AST), and lactate dehydrogenase (LDH), enter the blood circulation after liver cell injury in sepsis, and their activities can reflect the degree of liver injury. EA at PC6 significantly reduced the biochemical indicators ALT, AST, and LDH in rats with septic liver injury and reduced the deterioration of liver dysfunction in rats with endotoxic shock (78). In addition to enzyme system disorders, endotoxic shock is often accompanied by abnormal glucose metabolism and impaired cell membrane transport. In the early stages of shock, hyperglycaemia commonly causes hypoglycaemia as the shock deepens and blood glucose drops. Glucose-6-phosphatase (G-6-Pase) is a marker enzyme in the endoplasmic reticulum and a key enzyme in glucose metabolism. Glucose 6-phosphate is hydrolyzed into glucose into blood circulation through G-6-Pase, which is an indicator of the degree of liver cell damage and recovery; 5′-Nucleotidase (5′-Nase) and magnesium-activated adenosine triphosphate (Mg++- ATPase) are plasma membrane marker enzymes related to membrane transport function and also reflect the early damage of liver cells. Research has shown that EA at acupoints DU26 and ST36 increases the expression of G-6-Pase, SDH, 5′-Nase, and Mg++-ATPase, improve glucose metabolism, increase energy production, activate liver cell function, and improve the transport function of the liver cell membrane in septic rats (94). TNF-α is a multifunctional proinflammatory cytokine that induces an inflammatory storm, and most of it is synthesised in the liver, leading to sepsis and liver damage. Studies show that EA at ST36 can reduce TNF-α content in the liver tissue of rats with endotoxin-induced liver injury and plasma ALT activity to protect liver tissue (91). During sepsis, the liver is prone to ischaemia-reperfusion and oxygen-free radical damage. Increasing the blood flow to the liver tissue reduces tissue lipid peroxidation and oedema and improving liver damage. In a rat model of sepsis, EA ST36 reduced the MDA content in liver tissue, the activity of xanthine oxidase (XOD), and the expression of plasma ALT, improved tissue dysfunction, reduced liver oedema, and increased liver blood flow to improve ischaemia (98).

7.6 Heart

Myocardial injury is a common complication of septic shock and is an important reason for the poor prognosis of sepsis. Effective prevention and treatment of myocardial injury are important aspects of sepsis treatment. STAT3, a protein that promotes survival and inflammation in the heart, is closely associated with calpain in cardiomyocytes. Studies have shown that EA pretreatment can downregulate the expression of calpain-2, thereby inhibiting STAT3 phosphorylation and improving cardiac inflammation and dysfunction (107). In sepsis or MODS, NO loses control and aggravates organ damage. NO is an endothelium-derived vasodilator that relaxes the blood vessels. NO is a substrate of MPO. MPO is a peroxidase secreted by neutrophils, monocytes, and macrophages, and is involved in myocardial reperfusion injury. When myocardial ischaemia/reperfusion occurs, neutrophil infiltration can produce a large number of lysosomal enzymes, such as MPO, which not only reflects the number of neutrophils infiltrating the myocardium, but also the degree of activation. It can be used as a marker of neutrophil infiltration during myocardial injury. MPO reduces NO bioavailability and inhibits NOS activity. iNOS is expressed only after cells are stimulated by lipopolysaccharides, cytokines, and other factors. Lipopolysaccharide-activated iNOS can produce NO and inhibit myocardial contractility, and myocardial injury can be accompanied by an increase in the levels of the myocardial enzyme CK-MB. In a rat CLP model, EA reduced the levels of CK-MB in the plasma and TNF-α in the myocardium, and the activity of NO and MPO reduced the oedema of heart tissue and protected the myocardium (64). Song also found that EA at the ST36 acupoint reduced CK-MB and TNF in plasma-α horizontal when the α7 subunit of cholinergic N receptor was antagonised by α-BGT. Bilateral cervical vagotomy can also aggravate organ dysfunction and weaken the protective effect of EA on the myocardium. In addition, EA can reduce the levels of ALT, Cr, and DAO in the plasma, indicating that EA has protective effects in multiple organs in endotoxemic rats (65).

The above research shows that EA has a protective effect on the lungs, brain, intestines, kidneys, liver, and heart. Acupuncture can resist oxidative stress, inhibit excessive inflammation, improve cell energy metabolism, maintain mitochondrial function, regulate cell apoptosis, prevent multiple organ damage, and maintain and improve the integrity of body tissues, cell morphology, and function. In addition, EA significantly reduced the T lymphocyte apoptosis or pyroptosis in septic mice (105, 106). Electro-acupuncture expresses an anti-endotoxin shock effect by repressing the plasmic NO and TNFalpha concentrations smoothly and retrieving the blood pressure stably (93). In future medical research, it will be necessary to carry out multi-level comprehensive exploration at the whole-body, organ, cell, molecule, gene, and other levels, accurately understand the key links and regulatory pathways of network effects between major cells or inflammatory mediators, and deeply understand and clarify the pathogenesis of sepsis to effectively improve the treatment of sepsis and MODS.

8 Conclusion

The degree of imbalance in immune homeostasis is the core event in the disease process and determines the severity of sepsis. We systematically reviewed the animal model and acupuncture intervention parameters for the basic study of sepsis and the key molecular mechanisms underlying its anti-inflammatory effects (Table 2). In clinical studies, acupuncture has been shown to bidirectionally regulate the body's immune system, inhibit systemic inflammatory responses, and improve the immunosuppressive state of patients with sepsis to improve or delay the pathological process of sepsis. In preclinical studies, exogenous toxin models, represented by intraperitoneal or intravenous injections of lipopolysaccharide (LPS), and intraperitoneal infection models of CLP are commonly used to study the pathological mechanism of sepsis. Acupuncture intervention is usually performed using a single acupoint or a multi-acupoint combination, among which ST36 is the most commonly used. The intervention methods and parameters of acupuncture, such as MA, EA, intensity, duration, depth, and waveform, are closely related to its effects. At a local acupoint, the initial mechanism of action of acupuncture is closely related to the release of collagen fibres and a number of biochemical substances in the acupoint microenvironment. PROKR2 neurons, high-threshold thin nerve fibres, CB2R activation, and Ca^{2+} influx are the key material bases for the transmission of acupuncture information from the acupoint area to the central nervous system. Different stages of acupuncture intervention can produce opposite effects. High-intensity EA at ST36 and ST25 had anti-inflammatory effects if applied before modelling, but promoted inflammatory responses if applied after modelling. Acupuncture can exert anti-inflammatory effects through the vagus-adrenal medullary-dopamine, vagus-adrenal axis/spinal sympathetic, vagus-spleen cholinergic, or transcutaneous auricular vagus-cholinergic anti-inflammatory pathways. Acupuncture at acupoints on the body surface can induce various somatosensory-autonomic nervous target organ reflex pathways that play a role in the regulation of immune inflammation in the body. However, this regulatory effect of acupuncture is related to the location of acupoints, stimulation intensity, and body state, and has the characteristics of acupoint specificity, intensity dependence, and bidirectionality. Specifically, low-intensity EA at ST36 can activate the vagus-adrenal axis or vagus-cholinergic pathway of the parasympathetic nervous system to inhibit systemic inflammation in sepsis. Acupuncture intervention before and after modelling has an anti-inflammatory effect, but low-intensity EA at ST25 has no anti-inflammatory effect. High-intensity EA stimulation can activate the spinal cord or the peripheral sympathetic nervous system to play an anti-inflammatory role. High-intensity EA at ST36 can activate the spinal sympathetic reflex to inhibit systemic inflammation in sepsis, whereas high-intensity EA at ST25 can activate NPY peripheral sympathetic neurons to exert anti-inflammatory effects. Acupuncture protects multiple organs from damage during sepsis. Acupuncture can regulate the function of immune cells (such as macrophages and T lymphocytes), inhibit the excessive

inflammatory response in sepsis and anti-oxidative stress, protect mitochondrial function, reduce cell apoptosis, and reduce tissue or organ damage. Among these, the Nrf-2/HO-1, PI3K/Akt/Nrf2/HO-1, JAK1/STAT3, SIRT1/NF-κB, HO-1/PINK1, calpain-2/STAT3, and PICK1-TLR4 signalling pathways may be involved in the effects of acupuncture on the inhibition of the inflammatory response, reduction of oxidative stress, and protection of mitochondrial damage in the target organs of sepsis (Figure 2).

9 Discussion

This article reviews the existing evidence on the use of acupuncture and moxibustion in the prevention and treatment of sepsis. First, mechanistic research has focused on target organs, and the upstream pathway, especially the central integration mechanism, has been less studied. Second, a large number of existing studies on the protective effects of acupuncture on septic organs are related to anti-inflammation, and there are few basic studies on acupuncture and immunosuppression, which cannot clearly explain the improvement and potential mechanism of acupuncture and moxibustion in immunosuppression. Third, clinical sepsis is usually treated after the disease onset. Animal studies have shown that both pre- and post-treatment with acupuncture can treat sepsis, but whether the signal transduction mechanisms involved are similar or different remains unknown. Currently, there are few research reports in this area, and they are fragmented; therefore, the principles cannot be systematically revealed. Fourth, it is difficult to fully replicate the complexity of human sepsis, which is affected and restricted by many factors, in clinical practice. Most patients with clinical sepsis are over 50 years old, whereas the general age of experimental rats is 2-3 months, which is equivalent to 10 years in humans, Turnbull et al. (150) confirmed the correlation between age and mortality in the CLP model. Presently, research mostly uses young and healthy animals without complications for modelling, which is difficult to match with the actual situation in which clinical patients are often old and have multiple complications. In addition, there is a big difference between clinical practice and the fact that no other supportive treatment measures are provided in modelling research. Deitch believed that the selection of models depends on the main objectives of the proposed research and the clinical situation to be modelled (151, 152). Therefore, it is necessary to improve animal models and conduct clinical studies to explore the efficacy of EA in sepsis.

While focusing on the advantages of acupuncture in the prevention and treatment of sepsis, its adverse effects cannot be ignored. The increase in adverse events associated with acupuncture is closely related to the vigorous development of acupuncture and moxibustion. Adverse reactions and accidents associated with acupuncture mainly include dizziness, broken needles, bent needles, stuck needles, infection, and organ injury (35, 44). Adverse reactions to acupuncture are mainly caused by dizziness,

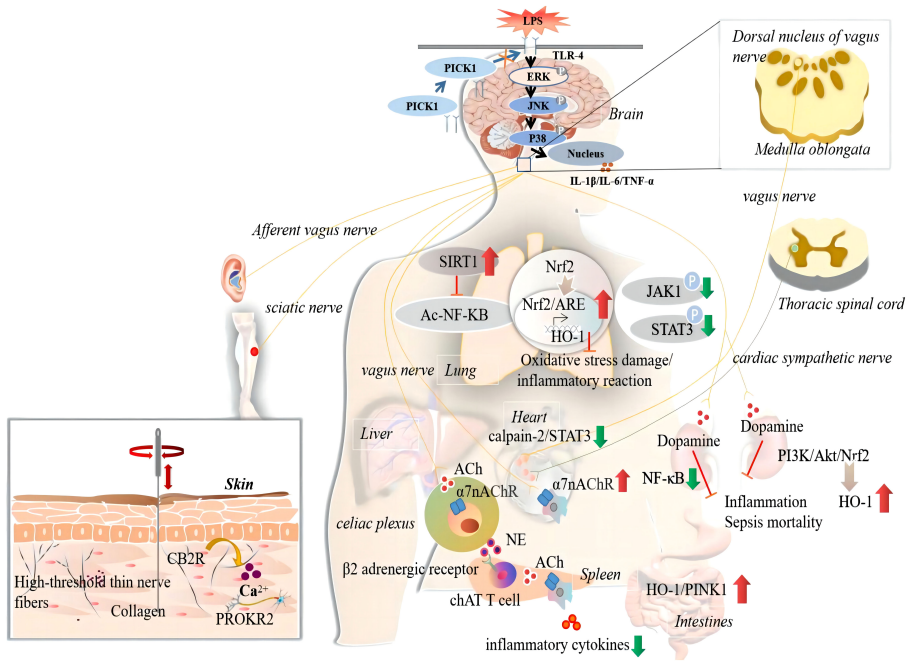

FIGURE 2
The anti-inflammatory actions and mechanisms of acupuncture in sepsis. The '↑' represents upregulated by acupuncture; The '↓' represents downregulated by acupuncture. CB2R, cannabinoid CB2 receptor; PICK1, protein Kinase C; ERK, extracellular signal-regulated kinase; JNK, the c-Jun N-terminal kinases; IL-1beta, interleukin-1beta; IL-6, interleukin 6; TNF-α, tumor necrosis factor-alpha; SIRT1, sirtuin 1; Ac, acetylation; NF-kB, the nuclear factor-kappa B; TLR4, toll-like receptor 4; Nrf2, nuclear factor erythroid-2 related factor-2; ARE, antioxidant response element; HO-1, heme oxygenase-1; JAK1, janus kinase 1; STAT3, signal transducer and activator of transcription 3; ACh, acetylcholine; α7nAChR, α7 nicotinic acetylcholine receptors; NE, norepinephrine; ChAT, choline acetyltransferase; P13K, phosphatidylinositol 3 kinase; Akt, protein kinase B; PINK1, PTEN-induced putative kinase 1.

unknown allergy history, emotional instability, physical differences, and other reasons. There are also many reasons leading to acupuncture accidents, including a lack of strict disinfection, improper acupuncture operation, improper treatment after acupuncture, bending needles, and folding needles. Differences in the methods of the acupuncturists will cause significant differences in the odds of adverse acupuncture events. For example, some acupuncturists prefer deep stimulation, strong stimulation, or application of needles in dangerous areas to maximise efficacy, which may lead to an increased incidence of adverse acupuncture events. Therefore, acupuncture adverse events can only indicate the safety level of the corresponding acupuncture operator and cannot be used to evaluate the safety of acupuncture therapy as a whole.

A comprehensive understanding of the mechanisms of action of acupuncture and moxibustion in the prevention and treatment of sepsis is important for future animal and clinical studies. Presently, to prevent COVID-19 patients from becoming septic, those who are qualified for asymptomatic infection can undergo EA at Guanyuan, ST36, and other acupoints according to their conditions at home and during rest time to adjust their autoimmunity. The early use of acupuncture and other supplementary anti-inflammatory therapies can effectively prevent the risk of sepsis caused by 'cytokine storms' resulting from excessive release of proinflammatory cytokines, and reduce the use of hormones. However, acupuncture has not been widely used for the prevention and treatment of COVID-19, which may be due to a lack of extensive understanding of the anti-inflammatory mechanism of acupuncture. After discharge, some cured cases are accompanied by coughing, poor food intake, fatigue, or abnormal mood, and different degrees of tissue or organ function damage. During this period, the patient's immunity was low. If they were reinfected with bacteria or viruses, the damage would exacerbate. Therefore, prevention of disease recurrence is necessary. In summary, this article showed that acupuncture can improve the immune function of patients, reduce possible multiple organ dysfunction problems, and further improve the symptoms of discharged patients through targeted acupoint selection. In short, acupuncture may have beneficial effects that can prevent diseases before they occur, worsening of diseases, and their recurrence after rehabilitation.

This review provides strong evidence for the effectiveness of acupuncture and moxibustion in the prevention and treatment of sepsis. Clarification of the existing evidence on acupuncture and moxibustion in the prevention and treatment of sepsis will provide various opportunities for acupuncture, moxibustion, and these two therapies combined with drugs for the prevention and treatment of sepsis. Simultaneously, with interdisciplinary cooperation and the combination of modern science, technology, and equipment, more in-depth and comprehensive research on the roles of acupuncture and moxibustion in preventing sepsis and protecting organs will be promoted. In the future, acupuncture and moxibustion could accurately drive different neural pathways to treat specific diseases. Therefore, it is extremely important to continue research on this subject.

Author contributions

LY and XL: concept design and manuscript writing. JC, FS and JZ: data collection and analysis. ZC, SZ, and BC made language modifications and reviewed the manuscript. DZ and YG: Concept design and manuscript review. All the authors contributed to the manuscript and approved the submitted version.

Funding

This study was financially supported by the National Natural Science Foundation of China (NSFC) (Nos. 82105024 and 82030125), the National Natural Science Foundation of Tianjin (No. 20JCQNJC00280), and the Tianjin Health Commission (No. 2021056).

Conflict of interest

The authors declare that this study was conducted in the absence of any commercial or financial relationships that could be construed as potential conflicts of interest.

Publisher's note

References

1. Singer M, Deutschman CS, Seymour CW, Shankar-Hari M, Annane D, Bauer M, et al. The third international consensus definitions for sepsis and septic shock (Sepsis-3). *JAMA* (2016) 315(8):775–87. doi: 10.1001/jama.2016.0287

2. Rudd KE, Johnson SC, Agesa KM, Shackelford KA, Tsoi D, Kievlan DR, et al. Global, regional, and national sepsis incidence and mortality, 1990-2017: analysis for the Global Burden of Disease Study. *Lancet* (2020) 395(10219):200–11. doi: 10.1016/S0140-6736(19)32989-7

3. NIH Consensus Conference. Acupuncture. *JAMA* (1998) 280(17):1518–24.

4. Zhang Q, Sharan A, Espinosa SA, Gallego-Perez D, Weeks J. The path toward integration of traditional and complementary medicine into health systems globally: The world health organization report on the implementation of the 2014-2023 strategy. *J Altern Complement Med* (2019) 25(9):869–71. doi: 10.1089/acm.2019.29077.jjw

5. Westbrook AM, Wei B, Hacke K, Xia M, Braun J, Schiestl RH. The role of tumour necrosis factor-α and tumour necrosis factor receptor signalling in inflammation-associated systemic genotoxicity. *Mutagenesis* (2012) 27(1):77–86. doi: 10.1093/mutage/ger063

6. Kothari N, Bogra J, Abbas H, Kohli M, Malik A, Kothari D, et al. Tumor necrosis factor gene polymorphism results in high TNF level in sepsis and septic shock. *Cytokine* (2013) 61(2):676–81. doi: 10.1016/j.cyto.2012.11.016

7. Baghel K, Srivastava RN, Chandra A, Goel SK, Agrawal J, Kazmi HR, et al. TNF-α, IL-6, and IL-8 cytokines and their association with TNF-α-308 G/A polymorphism and

postoperative sepsis. *J Gastrointest Surg* (2014) 18(8):1486–94. doi: 10.1007/s11605-014-2574-5

8. Mao ZR, Zhang SL, Feng B. Association of IL-10 (-819T/C, -592A/C and -1082A/G) and IL-6 -174G/C gene polymorphism and the risk of pneumonia-induced sepsis. *Biomarkers* (2017) 22(2):106–12. doi: 10.1080/1354750X.2016.1210677

9. Gentile LF, Cuenca AG, Efron PA, Ang D, Bihorac A, McKinley BA, et al. Persistent inflammation and immunosuppression: a common syndrome and new horizon for surgical intensive care. *J Trauma Acute Care Surg* (2012) 72(6):1491–501. doi: 10.1097/TA.0b013e318256e000

10. Schwacha MG. Macrophages and post-burn immune dysfunction. *Burns* (2003) 29(1):1–14. doi: 10.1016/S0305-4179(02)00187-0

11. Hotchkiss RS, Swanson PE, Freeman BD, Tinsley KW, Cobb JP, Matuschak GM, et al. Apoptotic cell death in patients with sepsis, shock, and multiple organ dysfunction. *Crit Care Med* (1999) 27(7):1230–51. doi: 10.1097/00003246-199907000-00002

12. Felmet KA, Hall MW, Clark RS, Jaffe R, Carcillo JA. Prolonged lymphopenia, lymphoid depletion, and hypoprolactinemia in children with nosocomial sepsis and multiple organ failure. *J Immunol* (2005) 174(6):3765–72. doi: 10.4049/jimmunol.174.6.3765

13. Pastille E, Didovic S, Brauckmann D, Rani M, Agrawal H, Schade FU, et al. Modulation of dendritic cell differentiation in the bone marrow mediates sustained immunosuppression after polymicrobial sepsis. *J Immunol* (2011) 186(2):977–86. doi: 10.4049/jimmunol.1001147

14. Grimaldi D, Llitjos JF, Pène F. Post-infectious immune suppression: a new paradigm of severe infections. *Med Mal Infect* (2014) 44(10):455–63. doi: 10.1016/j.medmal.2014.07.017

15. Boomer JS, To K, Chang KC, Takasu O, Osborne DF, Walton AH, et al. Immunosuppression in patients who die of sepsis and multiple organ failure. *JAMA* (2011) 306(23):2594–605. doi: 10.1001/jama.2011.1829

16. Pillay J, Kamp VM, van Hoffen E, Visser T, Tak T, Lammers JW, et al. A subset of neutrophils in human systemic inflammation inhibits T cell responses through Mac-1. *J Clin Invest* (2012) 122(1):327–36. doi: 10.1172/JCI57990

17. Ushiki T, Huntington ND, Glaser SP, Kiu H, Georgiou A, Zhang JG, et al. Rapid inflammation in mice lacking both SOCS1 and SOCS3 in hematopoietic cells. *PloS One* (2016) 11(9):e0162111. doi: 10.1371/journal.pone.0162111

18. Coletta C, Módis K, Oláh G, Brunyánszki A, Herzig DS, Sherwood ER, et al. Endothelial dysfunction is a potential contributor to multiple organ failure and mortality in aged mice subjected to septic shock: preclinical studies in a murine model of cecal ligation and puncture. *Crit Care* (2014) 18(5):511. doi: 10.1186/s13054-014-0511-3

19. Arulkumaran N, Deutschman CS, Pinsky MR, Zuckerbraun B, Schumacker PT, Gomez H, et al. Mitochondrial function in sepsis. *Shock* (2016) 45(3):271–81. doi: 10.1097/SHK.0000000000000463

20. Quoilin C, Mouithys-Mickalad A, Lécart S, Fontaine-Aupart MP, Hoebeke M. Evidence of oxidative stress and mitochondrial respiratory chain dysfunction in an *in vitro* model of sepsis-induced kidney injury. *Biochim Biophys Acta* (2014) 1837(10):1790–800. doi: 10.1016/j.bbabio.2014.07.005

21. Gómez H, Kellum JA, Ronco C. Metabolic reprogramming and tolerance during sepsis-induced AKI. *Nat Rev Nephrol* (2017) 13(3):143–51. doi: 10.1038/nrneph.2016.186

22. Hotchkiss RS, Monneret G, Payen D. Sepsis-induced immunosuppression: from cellular dysfunctions to immunotherapy. *Nat Rev Immunol* (2013) 13(12):862–74. doi: 10.1038/nri3552

23. Thiessen SE, Derese I, Derde S, Dufour T, Pauwels L, Bekhuis , et al. The role of autophagy in critical illness-induced liver damage. *Sci Rep* (2017) 7(1):14150. doi: 10.1038/s41598-017-14405-w

24. Permpikul C, Cheranakhorn C. The temporal changes of tissue oxygen saturation (StO2) and central venous oxygen saturation (ScvO2) during sepsis/septic shock resuscitation. *J Med Assoc Thai* (2014) 97 Suppl 3:S168–175. doi: mdl-23590047

25. Arulkumaran N, Pollen S, Greco E, Courtneidge H, Hall AM, Duchen MR, et al. Renal tubular cell mitochondrial dysfunction occurs despite preserved renal oxygen delivery in experimental septic acute kidney injury. *Crit Care Med* (2018) 46(4):e318–25. doi: 10.1097/CCM.0000000000002937

26. Iba T, Gando S, Thachil J. Anticoagulant therapy for sepsis-associated disseminated intravascular coagulation: the view from Japan. *J Thromb Haemost* (2014) 12(7):1010–9. doi: 10.1111/jth.12596

27. Iba T, Levy JH, Raj A, Warkentin TE. Advance in the management of sepsis-induced coagulopathy and disseminated intravascular coagulation. *J Clin Med* (2019) 8(5):728. doi: 10.3390/jcm8050728

28. Chappell D, Brettner F, Doerfler N, Jacob M, Rehm M, Bruegger D, et al. Protection of glycocalyx decreases platelet adhesion after ischaemia/reperfusion: an animal study. *Eur J Anaesthesiol* (2014) 31(9):474–81. doi: 10.1097/EJA.0000000000000085

29. Muth H, Maus U, Wygrecka M, Jacob M, Rehm M, Bruegger D, et al. Pro- and antifibrinolytic properties of human pulmonary microvascular versus artery endothelial cells: impact of endotoxin and tumor necrosis factor-alpha. *Crit Care Med* (2004) 32(1):217–26. doi: 10.1097/01.CCM.0000104941.89570.5F

30. Iba T, Levy JH. Inflammation and thrombosis: roles of neutrophils, platelets and endothelial cells and their interactions in thrombus formation during sepsis. *J Thromb Haemost* (2018) 16(2):231–41. doi: 10.1111/jth.13911

31. Iba T, Miki T, Hashiguchi N, Tabe Y, Nagaoka I. Is the neutrophil a 'prima donna' in the procoagulant process during sepsis? *Crit Care* (2014) 18(4):230. doi: 10.1186/cc13983

32. Liaw PC, Ito T, Iba T, Thachil J, Zeerleder S. DAMP and DIC: The role of extracellular DNA and DNA-binding proteins in the pathogenesis of DIC. *Blood Rev* (2016) 30(4):257–61. doi: 10.1016/j.blre.2015.12.004

33. Wang Y, Luo L, Braun OÖ, Westman J, Madhi R, Herwald H, et al. Neutrophil extracellular trap-microparticle complexes enhance thrombin generation via the intrinsic pathway of coagulation in mice. *Sci Rep* (2018) 8(1):4020. doi: 10.1038/s41598-018-22156-5

34. Meng JB, Jiao YN, Xu XJ, Lai ZZ, Zhang G, Ji CL, et al. Electro-acupuncture attenuates inflammatory responses and intraabdominal pressure in septic patients: A randomized controlled trial. *Med (Baltimore)* (2018) 97(17):e0555. doi: 10.1097/MD.0000000000010555

35. Li HF, Hu GQ, Liu WW. [Clinical trials of acupuncture of Jiaji (EX-B2) for treatment of gastrointestinal dysfunction in sepsis patients]. *Zhen Ci Yan Jiu* (2019) 44(1):43–6. doi: 10.13702/j.1000-0607.170579

36. Liu H, Zhu J, Ni HB, Hu XX. [Transcutaneous electrical acupoint stimulation for early enteral nutrition tolerance in patients with sepsis of gastrointestinal dysfunction: a multi-center randomized controlled trial]. *Zhongguo Zhen Jiu* (2020) 40(3):229–33. doi: 10.13703/j.0255-2930.20190426-0003

37. Wu JN, Zhu MF, Lei S, Wang LC. [Impacts of electroacupuncture on intestinal permeability in sepsis patients]. *Zhongguo Zhen Jiu* (2013) 33(3):203–6. doi: 10.13703/j.0255-2930.2013.03.006

38. Xiao QS, Ma MY, Zhang XS, Deng MH, Yang Yan Z. [Effect of acupuncture on prognosis and immune function of sepsis patients]. *Zhongguo Zhong Xi Yi Jie He Za Zhi* (2015) 35(7):783–6. doi: 10.7661/CJIM.2015. 07.0783

39. Lin W, Yang F, Zhang Y, Chen XM, Ye BC, Zhou BZ. [Effect of "Tongdu Tiaoshen" needling on cognitive dysfunction in patients with sepsis asso-ciated encephalopathy and its mechanism]. *Zhen Ci Yan Jiu* (2019) 44(12):888–92. doi: 10.13702/j.1000-0607.190411

40. Li HF, Hu GQ, Liu WW, Chen W. [Clinical observation on the inflammatory indexes in septic gastrointestinal dysfunction treated with acupuncture at Jiaji (EX-B 2)]. *Zhongguo Zhen Jiu* (2019) 39(10):1055–8. doi: 10.13703/j.0255-2930.2019.10.006

41. Zheng SM, Zhao FL, Luo YY, Lin XF, Wen MY. [Clinical effect of electroacupuncture at Baihui and Shuigou points in treatment of brain injury in patients with sepsis-associated encephalopathy]. *Zhen Ci Yan Jiu* (2020) 45(5):402–6. doi: 10.13702/j.1000-0607.190781

42. Meng JB, Jiao YN, Zhang G, Xu XJ, Ji CL, Hu MH, et al. Electroacupuncture improves intestinal dysfunction in septic patients: A randomised controlled trial. *BioMed Res Int* (2018) 2018:8293594. doi: 10.1155/2018/8293594

43. Yang G, Hu RY, Deng AJ, Huang Y, Li J. Effects of Electro-Acupuncture at Zusanli, Guanyuan for Sepsis Patients and Its Mechanism through Immune Regulation. *Chin J Integr Med* (2016) 22(3):219–24. doi: 10.1007/s11655-016-2462-9

44. Wang SL, Zhu J, Zhao ZG, Liu H, Ni HB, Hu XX. Effect of early acupoint electrical stimulation on lower limb muscle strength in patients with septic shock. *Zhongguo Zhen Jiu* (2020) 40(11):1173–7. doi: 10.13703/j.0255-2930.20191022-0005

45. Yang G, Zheng B, Yu Y, Huang J, Zhu H, Deng D, et al. Electroacupuncture at Zusanli (ST36), Guanyuan (CV4), and Qihai (CV6) Acupoints Regulates Immune Function in Patients with Sepsis via the PD-1 Pathway. *BioMed Res Int* (2022) 2022:7037497. doi: 10.1155/2022/7037497

46. Xian J, Wang L, Zhang C, Wang J, Zhu Y, Yu H, et al. Efficacy and safety of acupuncture as a complementary therapy for sepsis: a systematic review and meta-analysis. *Acupunct Med* (2023) 41(1):3–15. doi: 10.1177/09645284221086288

47. Chen WT, Sun C, Zhou YB, Liu DH, Peng ZL, Chen J, et al. Evaluation on the effect of acupuncture on patients with sepsis-induced myopathy (ACU-SIM pilot study): A single center, propensity-score stratified, assessor-blinded, prospective pragmatic controlled trial. *Med (Baltimore)* (2020) 99(21):e20233. doi: 10.1097/MD.0000000000020233

48. Scognamillo-Szabó MV, Bechara GH, Ferreira SH, Cunha FQ. Effect of various acupuncture treatment protocols upon sepsis in Wistar rats. *Ann N Y Acad Sci* (2004) 1026:251-6. doi: 10.1196/annals.1307.039

49. Carpenter KC, Hakenjos JM, Fry CD, Nemzek JA. The influence of pain and analgesia in rodent models of sepsis. *Comp Med* (2019) 69(6):546–54. doi: 10.30802/AALAS-CM-19-000004

50. Ramires CC, Balbinot DT, Cidral-Filho FJ, Dias DV, da Silva MD. Acupuncture reduces peripheral and brainstem cytokines in rats subjected to lipopolysaccharide-induced inflammation. *Acupunct Med* (2021) 39(4):376-84. doi: 10.1177/0964528420938379

51. Singleton KD, Wischmeyer PE. Distance of cecum ligated influences mortality, tumor necrosis factor-alpha and interleukin-6 expression following cecal ligation and puncture in the rat. *Eur Surg Res* (2003) 35(6):486–91. doi: 10.1159/000073387

52. Ruiz S, Vardon-Bounes F, Merlet-Dupuy V, Conil JM, Buléon M, Fourcade O, et al. Sepsis modeling in mice: ligation length is a major severity factor in cecal ligation and puncture. *Intensive Care Med Exp* (2016) 4(1):22. doi: 10.1186/s40635-016-0096-z

53. Murando F, Peloso A, Cobianchi L. Experimental abdominal sepsis: Sticking to an awkward but still useful translational model. *Mediators Inflammation* (2019) 2019:8971036. doi: 10.1155/2019/8971036

54. Nicolai O, Pötschke C, Schmoeckel K, Darisipudi MN, van der Linde J, Raafat D, et al. Antibody production in murine polymicrobial sepsis-kinetics and key players. *Front Immunol* (2020) 11:828. doi: 10.3389/fimmu.2020.00828

55. Korneev KV. [Mouse models of sepsis and septic shock]. *Mol Biol (Mosk)* (2019) 53(5):799–814. doi: 10.1134/S0026893319050108

56. Wichterman KA, Baue AE, Chaudry IH. Sepsis and septic shock–a review of laboratory models and a proposal. *J Surg Res* (1980) 29(2):189–201. doi: 10.1016/0022-4804(80)90037-2

57. Rittirsch D, Huber-Lang MS, Flierl MA, Ward PA. Immunodesign of experimental sepsis by cecal ligation and puncture. *Nat Protoc* (2009) 4(1):31–6. doi: 10.1038/nprot.2008.214

58. Lekkou A, Karakantza M, Mouzaki A, Kalfarentzos F, Gogos CA. Cytokine production and monocyte HLA-DR expression as predictors of outcome for patients with community-acquired severe infections. *Clin Diagn Lab Immunol* (2004) 11 (1):161–7. doi: 10.1128/CDLI.11.1.161-167.2004

59. Lim HD, Kim MH, Lee CY, Namgung U. Anti-inflammatory effects of acupuncture stimulation via the vagus nerve. *PloS One* (2016) 11(3):e0151882. doi: 10.1371/journal.pone.0151882

60. Liu S, Wang ZF, Su YS, Ray RS, Jing XH, Wang YQ, et al. Somatotopic organization and intensity dependence in driving distinct NPY-expressing sympathetic pathways by electroacupuncture. *Neuron* (2020) 108(3):436–50.e7. doi: 10.1016/j.neuron.2020.07.015

61. Yu JB, Shi J, Gong LR, Dong SA, Xu Y, Zhang Y, et al. Role of Nrf2/ARE pathway in protective effect of electroacupuncture against endotoxic shock-induced acute lung injury in rabbits. *PloS One* (2014) 9(8):e104924. doi: 10.1371/journal.pone.0104924

62. Yu JB, Dong SA, Luo XQ, Gong LR, Zhang Y, Wang M, et al. Role of HO-1 in protective effect of electro-acupuncture against endotoxin shock-induced acute lung injury in rabbits. *Exp Biol Med (Maywood)* (2013) 238(6):705–12. doi: 10.1177/1535370213489487

63. Wang F, Cui GW, Kuai L, Xu JM, Zhang TT, Cheng HJ, et al. Role of acupoint area collagen fibers in anti-inflammation of acupuncture lifting and thrusting manipulation. *Evid Based Complement Alternat Med* (2017) 2017:2813437. doi: 10.1155/2017/2813437

64. Zhang L, Huang Z, Shi X, et al. Protective effect of electroacupuncture at zusanli on myocardial injury in septic rats. *Evid Based Complement Alternat Med* (2018) 2018:6509650. doi: 10.1155/2018/6509650

65. Song Q, Hu S, Wang H, Jin S, Zhu C, Shen Y, et al. Electroacupuncturing at Zusanli point (ST36) attenuates pro-inflammatory cytokine release and organ dysfunction by activating cholinergic anti-inflammatory pathway in rat with endotoxin challenge. *Afr J Tradit Complement Altern Med* (2014) 11(2):469–74. doi: 10.4314/ajtcam.v11i2.35

66. Jun G, Yong Y, Lu L, Lv Y, Shi X, Sheng Z, et al. Electroacupuncture treatment ameliorated the long-term cognitive impairment via activating eNOS/NO pathway and related Aβ downregulation in sepsis-survivor mice. *Physiol Behav* (2022) 243:113646. doi: 10.1016/j.physbeh.2021.113646

67. Han YG, Qin X, Zhang T, Lei M, Sun FY, Sun JJ, et al. Electroacupuncture prevents cognitive impairment induced by lipopolysaccharide via inhibition of oxidative stress and neuroinflammation. *Neurosci Lett* (2018) 683:190–5. doi: 10.1016/j.neulet.2018.06.003

68. Mo Y, Wang L, Ren M, Xie W, Ye X, Zhou B, et al. Electroacupuncture prevents LPS- induced neuroinflammation via upregulation of PICK-TLR4 complexes in the microglia of hippocampus. *Brain Res Bull* (2021) 177:295–304. doi: 10.1016/j.brainresbull.2021.10.010

69. Chen Y, Lei Y, Mo LQ, Li J, Wang MH, Wei JC, et al. Electroacupuncture pretreatment with different waveforms prevents brain injury in rats subjected to cecal ligation and puncture via inhibiting microglial activation, and attenuating inflammation, oxidative stress and apoptosis. *Brain Res Bull* (2016) 127:248–59. doi: 10.1016/j.brainresbull.2016.10.009

70. Song JG, Li HH, Cao YF, Lv X, Zhang P, Li YS, et al. Electroacupuncture improves survival in rats with lethal endotoxemia via the autonomic nervous system. *Anesthesiology* (2012) 116(2):406–14. doi: 10.1097/ALN.0b013e3182426ebd

71. Wu J, Lyu B, Gan T, Wang L, Zhu M. Electroacupuncture improves acute bowel injury recovery in rat models. *Exp Ther Med* (2017) 14(5):4655–62. doi: 10.3892/etm.2017.5159

72. Zhu MF, Xing X, Lei S, Wu JN, Wang LC, Huang LQ, et al. Electroacupuncture at bilateral zusanli points (ST36) protects intestinal mucosal immune barrier in sepsis. *Evid Based Complement Alternat Med* (2015) 2015:639412. doi: 10.1155/2015/639412

73. Mu R, Li N, Yu JB, Gong LR, Dong SA, Shi J, et al. Electroacupuncture relieves hippocampal injury by heme oxygenase-1 to improve mitochondrial function. *J Surg Res* (2022) 273:15–23. doi: 10.1016/j.jss.2021.12.013

74. Luo D, Liu L, Zhang HM, Zhou YD, Zhou MF, Li JX, et al. Electroacupuncture pretreatment exhibits lung protective and anti-inflammation effects in lipopolysaccharide-induced acute lung injury via SIRT1-dependent pathways. *Evid Based Complement Alternat Med* (2022) 2022:2252218. doi: 10.1155/2022/2252218

75. Li C, Yu TY, Zhang Y, Wei LP, Dong SA, Shi J, et al. Electroacupuncture improves cognition in rats with sepsis-associated encephalopathy. *J Surg Res* (2020) 256:258–66. doi: 10.1016/j.jss.2020.06.056

76. Yu JB, Shi J, Zhang Y, Gong LR, Dong SA, Cao XS, et al. Electroacupuncture Ameliorates Acute Renal Injury in Lipopolysaccharide-Stimulated Rabbits via Induction of HO-1 through the PI3K/Akt/Nrf2 Pathways. *PloS One* (2015) 10(11): e0141622. doi: 10.1371/journal.pone.0141622

77. Zhang Y, Zheng L, Deng H, Feng D, Hu S, Zhu L, et al. Electroacupuncture alleviates LPS-induced ARDS through α7 nicotinic acetylcholine receptor-mediated inhibition of ferroptosis. *Front Immunol* (2022) 13:832432. doi: 10.3389/fimmu.2022.832432

78. Liu HW, Liu MC, Tsao CM, Liao MH, Wu CC. Electro-acupuncture at 'Neiguan' (PC6) attenuates liver injury in endotoxaemic rats. *Acupunct Med* (2011) 29(4):284–8. doi: 10.1136/aim.2010.003525

79. Villegas-Bastida A, Torres-Rosas R, Arriaga-Pizano LA, Flores-Estrada J, Gustavo-Acosta A, Moreno-Eutimio MA. Electrical Stimulation at the ST36 Acupoint Protects against Sepsis Lethality and Reduces Serum TNF Levels through Vagus Nerve- and Catecholamine-Dependent Mechanisms. *Evid Based Complement Alternat Med* (2014) 2014:451674. doi: 10.1155/2014/451674

80. Gu G, Zhang Z, Wang G, Han F, Han L, Wang K, et al. Effects of electroacupuncture pretreatment on inflammatory response and acute kidney injury in endotoxaemic rats. *J Int Med Res* (2011) 39(5):1783–97. doi: 10.1177/147323001103900521

81. Zhang Z, Shi Y, Cai D, Jin S, Zhu C, Shen Y, et al. Effect of electroacupuncture at ST36 on the intestinal mucosal mechanical barrier and expression of occludin in a rat model of sepsis. *Acupunct Med* (2018) 36(5):333–8. doi: 10.1136/acupmed-2016-011187

82. Xie DP, Zhou GB, Chen RL, Qin XL, Du JD, Zhang Y, et al. Effect of electroacupuncture at zusanli (ST36) on sepsis induced by cecal ligation puncture and its relevance to spleen. *Evid Based Complement Alternat Med* (2020) 2020:1914031. doi: 10.1155/2020/1914031

83. Zhang Y, Yu JB, Luo XQ, Gong LR, Wang M, Cao XS, et al. Effect of ERK1/2 signaling pathway in electro-acupuncture mediated up-regulation of heme oxygenase-1 in lungs of rabbits with endotoxic shock. *Med Sci Monit* (2014) 20:1452–60. doi: 10.12659/MSM.890736

84. Harpin D, Simadibrata CL, Mihardja H, Barasila AC. Effect of electroacupuncture on urea and creatinine levels in the wistar sepsis model. *Med Acupunct* (2020) 32(1):29–37. doi: 10.1089/acu.2019.1369

85. Torres-Rosas R, Yehia G, Peña G, Mishra P, del Rocio Thompson-Bonilla M, Moreno-Eutimio MA, et al. Dopamine mediates vagal modulation of the immune system by electroacupuncture. *Nat Med* (2014) 20(3):291–5. doi: 10.1038/nm.3479

86. Huang CL, Tsai PS, Wang TY, Yan LP, Xu HZ, Huang CJ. Acupuncture stimulation of ST36 (Zusanli) attenuates acute renal but not hepatic injury in lipopolysaccharide-stimulated rats. *Anesth Analg* (2007) 104(3):646–54. doi: 10.1213/01.ane.0000255288.68199.eb

87. Huang CL, Huang CJ, Tsai PS, Yan LP, Xu HZ. Acupuncture stimulation of ST-36 (Zusanli) significantly mitigates acute lung injury in lipopolysaccharide-stimulated rats. *Acta Anaesthesiol Scand* (2006) 50(6):722–30. doi: 10.1111/j.1399-6576.2006.01029.x

88. Liu S, Wang Z, Su Y, Qi L, Yang W, Fu M, et al. A neuroanatomical basis for electroacupuncture to drive the vagal-adrenal axis. *Nature* (2021) 598(7882):641–5. doi: 10.1038/s41586-021-04001-4

89. Wang Z, Huang W, Xu Q, Huang K, Cai H, Zhang X. [The effect of electro-acupuncture on the adrenal gland of endotoxic shocked rats]. *Zhen Ci Yan Jiu* (1996) 21(1):73–5. doi: 10.13702/j.1000-0607.1996.01.01

90. Kuang X, Liang C, Liang Z, Lu C, Zhong G. [The effect of acupuncture on rabbits with fever caused by endotoxin]. *Zhen Ci Yan Jiu* (1992) 17(3):212-6. doi: 10.13702/j.1000-0607.1992.03.015

91. Shi X, Song Q, Hu S, Li ZF, Liu Q, Wang L. [Study on protective action of electroacupuncture on endotoxin-induced hepatic injury in rats]. *Zhongguo Zhen Jiu* (2008) 28(4):290–2. doi: 10.13703/j.0255-2930.2008.04.020

92. Wu YR, Pan YH, Zhan Z, Yang S, Jiang JF. [Parasympathetic innervation contributes to the increase of survival rate and anti-inflammatory effect of electroacupuncture at "Ciliao"(BL32) in rats with lethal endotoxemia]. *Zhen Ci Yan Jiu* (2021) 46(11):942–7. doi: 10.13702/j.1000-0607.201080

93. Li H, Li C, Du SH, Li YW, Chen DF. [Influence of electro-acupuncture of Neiguan on plasmic concentrations of NO and TNFalpha in endotoxin shock rats]. *Zhong Xi Yi Jie He Xue Bao* (2003) 1(4):281-4. doi: 10.3736/jcim20030415

94. Huang W, Huang K, Xu Q, Wang Z, Sun Y, Cai H, et al. [Histochemical observation of the effect of electroacupuncture on the livers of rats with endotoxic shock]. *Zhen Ci Yan Jiu* (1995) 20(3):36–9. doi: 10.1074/jbc.273.32.20021

95. Xie C, Wu S, Li Z, Huang B, Zeng W. [Electroacupuncture protects septic rats from acute lung injury through the JAK1/STAT3 pathway]. *Nan Fang Yi Ke Da Xue Bao* (2020) 40(11):1662–7. doi: 10.12122/j.issn.1673-4254.2020.11.20

96. Dong QS, Dong XM, Zhang XQ. [Effects of strong and weak electroacupuncture on endotoxin-induced changes of electrical activities of heat-sensitive neurons in preoptic area and anterior hypothalamus in rabbits]. *Zhen Ci Yan Jiu* (2008) 33 (2):124–30. doi: 10.13702/j.1000-0607.2008.02.003

97. Zhou HY, Yang J, Feng Y, Yang SQ. [Effects of heat and cool-producing needling manipulations on rectal temperature and serum endotoxin content in endotoxin-induced heat syndrome rabbits]. *Zhen Ci Yan Jiu* (2012) 37(4):277–80. doi: 10.13702/j.1000-0607.2012.04.005

98. Shi X, Zhang LJ, Bai HY, Bao CM, Hu S, Guan L. [Effects of electroacupuncture on hepatic blood flow and lipid peroxidation in septic rats]. *Zhongguo Zhen Jiu* (2010) 30(5):397–400. doi: 10.13703/j.0255-2930.2010.05.013

99. Yang Y, Zhi D. [Effects of acupuncture hypothermia and its relationship to changes of AVP contents in the plasma and CSF in the rabbits]. *Zhen Ci Yan Jiu* (1994) 19(2):56–9. doi: 10.13702/j.1000-0607.1994. 02. 017

100. Wang H, Du MH, Shi X. [Effects of acupuncture at "Zusanli" (ST 36) on cerebral proinflammatory cytokine and plasma neuron specific enolase in septic rats]. *Zhongguo Zhen Jiu* (2013) 33(12):1105–7. doi: 10.13703/j.0255-2930.2013.12.018

101. Zhao YX, He W, Gao XY, Rong PJ, Zhu B. [Effect of electroacupuncture of auricular concha on inflammatory reaction in endotoxaemia rats]. *Zhen Ci Yan Jiu* (2011) 36(3):187–92. doi: 10.13702/J.1000-0607.2011.03.006

102. Wu JN, Wu W, Jiang RL, Zhu MF, Lei S, Lu B. [Effect of electro-acupuncture at zusanli (ST36) on the expression of ghrelin and HMGB1 in the small intestine of sepsis rats]. *Zhongguo Zhong Xi Yi Jie He Za Zhi* (2014) 34(9):1113–7. doi: 10.7661/CJIM.2014.09.1113

103. Ferreira Ade S, Lima JG, Ferreira TP, Lopes CM, Meyer R. Prophylactic effects of short-term acupuncture on Zusanli (ST36) in Wistar rats with lipopolysaccharide-induced acute lung injury. *Zhong Xi Yi Jie He Xue Bao* (2009) 7(10):969–75. doi: 10.3736/jcim20091011

104. Chen T, Xiong Y, Long M, Zheng D, Ke H, Xie J. Electro-acupuncture pretreatment at zusanli (ST36) acupoint attenuates lipopolysaccharide-induced inflammation in rats by inhibiting ca(2+) influx associated with cannabinoid CB2 receptors. *Inflammation* (2019) 42(1):211–20. doi: 10.1007/s10753-018-0885-5

105. Lv ZY, Shi YL, Bassi GS, Chen YJ, Yin LM, Wang Y, et al. Electroacupuncture at ST36 (Zusanli) Prevents T-Cell Lymphopenia and Improves Survival in Septic Mice. *J Inflamm Res* (2022) 15:2819-33. doi: 10.2147/JIR.S361466

106. Lou Y, Zhu ZQ, Xie LL, Feng YR. [Electroacupuncture at "Zusanli"(ST36) protects intestinal mucosal immune barrier by suppre-ssing apoptosis of intestinal lymphocytes and regulating expression of Bcl-2 and Bax in sepsis rats]. *Zhen Ci Yan Jiu* (2022) 47(5):386-92. doi: 10.13702/j.1000-0607.20210580

107. Li X, Wang L, Ying X, Zheng Y, Tan Q, Yu X, et al. Electroacupuncture pre-treatment alleviates sepsis-induced cardiac inflammation and dysfunction by inhibiting the calpain-2/STAT3 pathway. *Front Physiol* (2022) 13:961909. doi: 10.3389/fphys.2022.961909

108. Zhang Z, Cui X, Liu K, Gao X, Zhou Q, Xi H, et al. Adrenal sympathetic nerve mediated the anti-inflammatory effect of electroacupuncture at ST25 acupoint in a rat model of sepsis. *Anat Rec (Hoboken)* (2022). doi: 10.1101/2022.07.14.499985

109. Wu Z, Xia Y, Wang C, Lu W, Zuo H, Wu D, et al. Electroacupuncture at Neiguan (PC6) attenuates cardiac dysfunction caused by cecal ligation and puncture via the vagus nerve. *BioMed Pharmacother* (2023) 162:114600. doi: 10.1016/j.biopha.2023.114600

110. Zhang Y, Meng Z, Wu L, Liu X, Guo C, Yu J, et al. Protective effect of electroacupuncture on the barrier function of intestinal injury in endotoxemia through HO-1/PINK1 pathway-mediated mitochondrial dynamics regulation. *Oxid Med Cell Longev* (2023) 2023:1464853. doi: 10.1155/2023/1464853

111. Wu SY, Chen WH, Hsieh CL, Lin YW. Abundant expression and functional participation of TRPV1 at Zusanli acupoint (ST36) in mice: mechanosensitive TRPV1 as an "acupuncture-responding channel". *BMC Complement Altern Med* (2014) 14:96. doi: 10.1186/1472-6882-14-96

112. Mingfu L, Xiaotong D, Xiaojing S, Jin J, Jinling Z, Ying H. Study on the dynamic compound structure composed of mast cells, blood vessels, and nerves in rat acupoint. *Evid Based Complement Alternat Med* (2013) 2013:160651. doi: 10.1155/2013/160651

113. Borovikova LV, Ivanova S, Zhang M, Yang H, Botchkina GI, Watkins LR, et al. Vagus nerve stimulation attenuates the systemic inflammatory response to endotoxin. *Nature* (2000) 405(6785):458–62. doi: 10.1038/35013070

114. Xu B, Wang H, Chen Z. Puerarin inhibits ferroptosis and inflammation of lung injury caused by sepsis in LPS induced lung epithelial cells. *Front Pediatr* (2021) 9:706327. doi: 10.3389/fped.2021.706327

115. Zhang L, Wu Z, Zhou J, Lu S, Wang C, Xia Y, et al. Electroacupuncture ameliorates acute pancreatitis: A role for the vagus nerve-mediated cholinergic anti-inflammatory pathway. *Front Mol Biosci* (2021) 8:647647. doi: 10.3389/fmolb.2021.647647

116. Fan E, Fan J. Regulation of alveolar macrophage death in acute lung inflammation. *Respir Res* (2018) 19(1):50. doi: 10.1186/s12931-018-0756-5

117. Park I, Kim M, Choe K, Song E, Seo H, Hwang Y, et al. Neutrophils disturb pulmonary microcirculation in sepsis-induced acute lung injury. *Eur Respir J* (2019) 53 (3):1800786. doi: 10.1183/13993003.00786-2018

118. Kumar V. Pulmonary innate immune response determines the outcome of inflammation during pneumonia and sepsis-associated acute lung injury. *Front Immunol* (2020) 11:1722. doi: 10.3389/fimmu.2020.01722

119. Li W, Li D, Chen Y, Abudou H, Wang H, Cai J, et al. Classic signaling pathways in alveolar injury and repair involved in sepsis-induced ALI/ARDS: New research progress and prospect. *Dis Markers* (2022) 2022:6362344. doi: 10.1155/2022/6362344

120. Yazar E, Er A, Uney K, Bulbul A, Avci GE, Elmas M, et al. Effects of drugs used in endotoxic shock on oxidative stress and organ damage markers. *Free Radic Res* (2010) 44(4):397–402. doi: 10.3109/10715760903513025

121. Ryter SW, Choi AM. Heme oxygenase-1/carbon monoxide: novel therapeutic strategies in critical care medicine. *Curr Drug Targets* (2010) 11(12):1485–94. doi: 10.2174/1389450111009011485

122. Cherry AD, Piantadosi CA. Regulation of mitochondrial biogenesis and its intersection with inflammatory responses. *Antioxid Redox Signal* (2015) 22(12):965–76. doi: 10.1089/ars.2014.6200

123. Liu FJ, Gu TJ, Wei DY. Emodin alleviates sepsis-mediated lung injury via inhibition and reduction of NF-kB and HMGB1 pathways mediated by SIRT1. *Kaohsiung J Med Sci* (2022) 38(3):253–60. doi: 10.1002/kjm2.12476

124. Ye R, Liu Z. ACE2 exhibits protective effects against LPS-induced acute lung injury in mice by inhibiting the LPS-TLR4 pathway. *Exp Mol Pathol* (2020) 113:104350. doi: 10.1016/j.yexmp.2019.104350

125. Xu H, Xiao J. ACE2 promotes the synthesis of pulmonary surfactant to improve AT II cell injury via SIRT1/eNOS pathway. *Comput Math Methods Med* (2021) 2021:7710129. doi: 10.1155/2021/7710129

126. Pang QM, Yang R, Zhang M, Zou WH, Qian NN, Xu QJ, et al. Peripheral blood-derived mesenchymal stem cells modulate macrophage plasticity through the IL-10/STAT3 pathway. *Stem Cells Int* (2022) 2022:5181241. doi: 10.1155/2022/5181241

127. Iwashyna TJ, Ely EW, Smith DM, Smith DM, Langa KM. Long-term cognitive impairment and functional disability among survivors of severe sepsis. *JAMA* (2010) 304(16):1787–94. doi: 10.1001/jama.2010.1553

128. Rajendrakumar SK, Revuri V, Samidurai M, Mohapatra A, Lee JH, Ganesan P, et al. Peroxidase-mimicking nanoassembly mitigates lipopolysaccharide-induced endotoxemia and cognitive damage in the brain by impeding inflammatory signaling in macrophages. *Nano Lett* (2018) 18(10):6417–26. doi: 10.1021/acs.nanolett.8b02785

129. Micheau J, Marighetto A. Acetylcholine and memory: a long, complex and chaotic but still living relationship. *Behav Brain Res* (2011) 221(2):424–9. doi: 10.1016/j.bbr.2010.11.052

130. Prado MA, Reis RA, Prado VF, de Mello MC, Gomez MV, de Mello FG. Regulation of acetylcholine synthesis and storage. *Neurochem Int* (2002) 41(5):291–9. doi: 10.1016/S0197-0186(02)00044-X

131. Ye Y, Li H, Yang JW, Wang XR, Shi GX, Yan CQ, et al. Acupuncture attenuated vascular dementia-induced hippocampal long-term potentiation impairments via activation of D1/D5 receptors. *Stroke* (2017) 48(4):1044–51. doi: 10.1161/STROKEAHA.116.014696

132. Shi J, Yu T, Song K, Du S, He S, Hu X, et al. Dexmedetomidine ameliorates endotoxin-induced acute lung injury *in vivo* and *in vitro* by preserving mitochondrial dynamic equilibrium through the HIF-1a/HO-1 signaling pathway. *Redox Biol* (2021) 41:101954. doi: 10.1016/j.redox.2021.101954

133. Bindu S, Pal C, Dey S, Goyal M, Alam A, Iqbal MS, et al. Translocation of heme oxygenase-1 to mitochondria is a novel cytoprotective mechanism against non-steroidal anti-inflammatory drug-induced mitochondrial oxidative stress, apoptosis, and gastric mucosal injury. *J Biol Chem* (2011) 286(45):39387–402. doi: 10.1074/jbc.M111.279893

134. Agarwal A, Bolisetty S. Adaptive responses to tissue injury: role of heme oxygenase-1. *Trans Am Clin Climatol Assoc* (2013) 124:111–22.

135. Hirase T, Staddon JM, Saitou M, Ando-Akatsuka Y, Itoh M, Furuse M, et al. Occludin as a possible determinant of tight junction permeability in endothelial cells. *J Cell Sci* (1997) 110(Pt 14):1603–13. doi: 10.1242/jcs.110.14.1603

136. Balda MS, Flores-Maldonado C, Cereijido M, Matter K. Multiple domains of occludin are involved in the regulation of paracellular permeability. *J Cell Biochem* (2000) 78(1):85–96. doi: 10.1002/(SICI)1097-4644(20000701)78:1<85::AID-JCB8>3.0.CO;2-F

137. Wu QJ, Zhou YM, Wu YN, Zhang LL, Wang T. The effects of natural and modified clinoptilolite on intestinal barrier function and immune response to LPS in broiler chickens. *Vet Immunol Immunopathol* (2013) 153(1-2):70–6. doi: 10.1016/j.vetimm.2013.02.006

138. Maxson RT, Johnson DD, Jackson RJ, Smith SD. The protective role of enteral IgA supplementation in neonatal gut-origin sepsis. *Ann N Y Acad Sci* (1996) 778:405–7. doi: 10.1111/j.1749-6632.1996.tb21157.x

139. Mauser M, Kruger D, Pather S, Plani F. Trauma results in immune cell-induced intestinal epithelial damage with subsequently increased sepsis rate. *J Trauma Acute Care Surg* (2021) 90(3):565–73. doi: 10.1097/TA.0000000000003043

140. Welch M. D-lactate as an early marker of intestinal ischaemia after ruptured abdominal aortic aneurysm repair. *Br J Surg* (1999) 86(5):712. doi: 10.1046/j.1365-2168.1999.1104a.x

141. Mehta RL, Bouchard J, Soroko SB, Ikizler TA, Paganini EP, Chertow GM, et al. Sepsis as a cause and consequence of acute kidney injury: Program to Improve Care in Acute Renal Disease. *Intensive Care Med* (2011) 37(2):241–8. doi: 10.1007/s00134-010-2089-9

142. Peters E, Heemskerk S, Masereeuw R, Pickkers P. Alkaline phosphatase: a possible treatment for sepsis-associated acute kidney injury in critically ill patients. *Am J Kidney Dis* (2014) 63(6):1038–48. doi: 10.1053/j.ajkd.2013.11.027

143. Kang KW, Lee SJ, Park JW, Kim SG. Phosphatidylinositol 3-kinase regulates nuclear translocation of NF-E2-related factor 2 through actin rearrangement in

response to oxidative stress. *Mol Pharmacol* (2002) 62(5):1001–10. doi: 10.1124/mol.62.5.1001

144. Tsai PS, Chen CC, Tsai PS, Yang LC, Huang WY, Huang CJ. Heme oxygenase 1, nuclear factor E2-related factor 2, and nuclear factor kappaB are involved in hemin inhibition of type 2 cationic amino acid transporter expression and L-Arginine transport in stimulated macrophages. *Anesthesiology* (2006) 105(6):1201–1210; discussion 5A. doi: 10.1097/00000542-200612000-00020

145. Kuwana H, Terada Y, Kobayashi T, Okado T, Penninger JM, Irie-Sasaki J, et al. The phosphoinositide-3 kinase gamma-Akt pathway mediates renal tubular injury in cisplatin nephrotoxicity. *Kidney Int* (2008) 73(4):430–45. doi: 10.1038/sj.ki.5002702

146. Szabó C, Thiemermann C. Regulation of the expression of the inducible isoform of nitric oxide synthase. *Adv Pharmacol* (1995) 34:113–53. doi: 10.1016/S1054-3589(08)61083-2

147. Taylor BS, Alarcon LH, Billiar TR. Inducible nitric oxide synthase in the liver: regulation and function. *Biochem (Mosc)* (1998) 63(7):766–81.

148. Chu LC, Tsai PS, Lee JJ, Yen CH, Huang CJ. NF-kappaB inhibitors significantly attenuate the transcription of high affinity type-2 cationic amino acid transporter in LPS-stimulated rat kidney. *Acta Anaesthesiol Taiwan* (2005) 43(1):23–32.

149. Yao YM, Xu CL, Yao FH, Yu Y, Sheng ZY. [The pattern of nuclear factor-kappaB activation in rats with endotoxin shock and its role in biopterin-mediated nitric oxide induction]. *Zhonghua Shao Shang Za Zhi* (2006) 22(6):405–10. doi: 10.1631/jzus.2006.B0099

150. Turnbull IR, Clark AT, Stromberg PE, Dixon DJ, Woolsey CA, Davis CG, et al. Effects of aging on the immunopathologic response to sepsis. *Crit Care Med* (2009) 37(3):1018–23. doi: 10.1097/CCM.0b013e3181968f3a

151. Deitch EA. Rodent models of intra-abdominal infection. *Shock* (2005) 24 Suppl 1:19–23. doi: 10.1097/01.shk.0000191386.18818.0a

152. Doi K. How to replicate the complexity of human sepsis: development of a new animal model of sepsis. *Crit Care Med* (2012) 40(9):2722–3. doi: 10.1097/CCM.0b013e31825bc83f

10.3389/fimmu.2023.1242640

Glossary

MODS	multiple organ dysfunction syndrome
PAMP	pathogen-associated molecular pattern
DAMP	damage-associated molecular pattern
PRR	pattern recognition receptor
TGF-beta	transforming growth factor beta
TNF-α	tumor necrosis factor-α
IL-1beta	interleukin-1beta
Th2	type 2 helper T
HLA-DR	human leukocyte antigen-DR
MDSCs	myeloid-derived suppressor cells
NK	natural killer
LPS	lipopolysaccharide
NOS	nitric oxide synthase
NADPH	nicotinamide adenine dinucleotide phosphate
NOX4	NADPH oxidase 4
PC	protein C
DIC	disseminated intravascular coagulation
TF	tissue factor
TFPI	tissue factor pathway inhibitor
t-PA	tissue-type plasminogenactivator
PAI-1	plasminogen activator inhibitor-1
NETs	neutrophil extracellular traps
EA	electroacupuncture
ST36	Zusanli
ST37	Shangjuxu
PCT	procalcitonin
IFABP	intestinal fatty acid binding protein
TEAS	transcutaneous electrical acupoint stimulation
L: M	lactulose to mannitol ratio
CRP	C-reactive protein
NSE	neuron-specific enolase
SAE	sepsis-associated encephalopathy
APACHE	acute physiologic and chronic health evaluation
CV4	Guanyuan
CLP	cecal ligation and puncture
CASP	colon ascendens stent petitonitis
BL13	Feishu
GV20/DU20	Baihui
ST25	Tianshu

(Continued)

Continued

LI11	Quchi
PC6	Neiguan
NPY	neuropeptide Y
MA	manual acupuncture
HSN	heat sensitive neurons
CB2R	cannabinoid CB2 receptor
CAP	Cholinergic anti-inflammatory pathway
α7nAChR	α7 nicotinic acetylcholine receptors
Ach	acetylcholine
CK-MB	creatine kinase MB
NO	nitric oxide
MPO	myeloperoxidase
BL32	Ciliao
LI4	Hegu
DVC	the dorsal vagal complex
AP	acute pancreatitis
NEI	the nerve endocrine immune system
ALI	acute lung injury
MDA	malondialdehyde
SOD	superoxide dismutase
HO-1	heme oxygenase-1
W/D	wet/dry
iNOS	nitric oxide synthase
Nrf2	nuclear factor erythroid-2 related factor-2
ARE	antioxidant response element
ERK1/2	extracellular signal regulated kinases1/2
SIRT1	sirtuin 1
ACE2	angiotensin-converting enzyme 2
RAS	the renin-angiotensin system
AT II	alveolar type II cell
SAE	sepsis-associated encephalopathy
ChAT	choline acetyltransferase
AChE	acetylcholinesterase
eNOS	endothelial nitric oxide
Aβ	β–peptide
H2O2	hydrogen peroxide
CAT	catalase
GSH	glutathione
TJ	tight junction
sIgA	secretory immunoglobulin A

(Continued)

10.3389/fimmu.2023.1242640

Continued

SAKI	sepsis-associated acute kidney injury
SDH	succinate dehydrogenase
ALP	alkaline phosphatase
DU26	Renzhong
PI3K	phosphoinositide 3-kinase
BUN	blood urea nitrogen
Cr	creatinine
NAG	N-acetyl-glucosaminidase
ALT	alanine aminotransferase
AST	aspartate aminotransferase
LDH	lactate dehydrogenase
G-6-Pase	Glucose-6-phosphatase
5' –Nase	5'- Nucleotidase
XOD	xanthine oxidase

frontiers | Frontiers in Immunology

TYPE Review
PUBLISHED 06 October 2023
DOI 10.3389/fimmu.2023.1171834

OPEN ACCESS

EDITED BY
Alessandra Stasi,
University of Bari Aldo Moro, Italy

REVIEWED BY
Gianvito Caggiano,
University of Bari Aldo Moro, Italy
Undurti Narasimha Das,
UND Life Sciences LLC, United States

*CORRESPONDENCE
Xin Liu
liux0704@tmmu.edu.cn
Xiaoli Li
lixiaoli@cqmu.edu.cn

†These authors have contributed equally to this work

RECEIVED 22 February 2023
ACCEPTED 15 September 2023
PUBLISHED 06 October 2023

CITATION
Zhang L, Shi X, Qiu H, Liu S, Yang T, Li X and Liu X (2023) Protein modification by short-chain fatty acid metabolites in sepsis: a comprehensive review.
Front. Immunol. 14:1171834.
doi: 10.3389/fimmu.2023.1171834

Protein modification by short-chain fatty acid metabolites in sepsis: a comprehensive review

Liang Zhang[1,2,3†], Xinhui Shi[1,2,3†], Hongmei Qiu[1,2,3], Sijia Liu[1,2,3], Ting Yang[1,2,3], Xiaoli Li[1,2,3*] and Xin Liu[4*]

[1]Department of Pharmacology, College of Pharmacy, Chongqing Medical University, Chongqing, China, [2]Chongqing Key Laboratory of Drug Metabolism, Chongqing, China, [3]Key Laboratory for Biochemistry and Molecular Pharmacology of Chongqing, Chongqing, China, [4]Medical Research Center, Southwest Hospital, Third Military Medical University, Chongqing, China

Sepsis is a major life-threatening syndrome of organ dysfunction caused by a dysregulated host response due to infection. Dysregulated immunometabolism is fundamental to the onset of sepsis. Particularly, short-chain fatty acids (SCFAs) are gut microbes derived metabolites serving to drive the communication between gut microbes and the immune system, thereby exerting a profound influence on the pathophysiology of sepsis. Protein post-translational modifications (PTMs) have emerged as key players in shaping protein function, offering novel insights into the intricate connections between metabolism and phenotype regulation that characterize sepsis. Accumulating evidence from recent studies suggests that SCFAs can mediate various PTM-dependent mechanisms, modulating protein activity and influencing cellular signaling events in sepsis. This comprehensive review discusses the roles of SCFAs metabolism in sepsis associated inflammatory and immunosuppressive disorders while highlights recent advancements in SCFAs-mediated lysine acylation modifications, such as substrate supplement and enzyme regulation, which may provide new pharmacological targets for the treatment of sepsis.

KEYWORDS

sepsis, short-chain fatty acids (SCFAs), protein post-translational modifications (PTMs), immunity, inflammation

1 Introduction

Sepsis, according to the latest criteria (Sepsis 3.0) is defined a life-threatening organ dysfunction syndrome caused by a dysregulated host response due to infection or infectious agents. It serves as one of the most common complications in patients with clinical trauma/burns and infections while ranks a leading cause of death in critically ill units (1). An estimated number of 31.5 million cases and 5.3 million deaths are recorded worldwide in a single year, making sepsis as a prominent health problem for the global medical community (2). Sepsis is traditionally recognized as a two- stage syndrome which manifests with hyperinflammation and immune suppression. More recently, it is

suggested that sepsis may manifest concurrent hyperinflammation and immune suppression (3). In recent years, substantial progress has been made in revealing the mechanisms that drives the development of sepsis, especially in the areas of metabolisms and epigenetics (4). Remarkably, profound alterations in intracellular metabolites and protein epigenetic markers have been identified as key regulatory mechanisms for the initiation of inflammation and immunosuppression as well as their phenotypic transformation. These findings hold significant implications for understanding the immunopathology of sepsis and the search for potential drug intervention targets.

The primary events of sepsis include infection, inflammation induced by infection, immune dysregulation, and organ dysfunction. Sepsis also involves various events that are secondary to those primary changes. During sepsis, notably changes in host metabolism have been detected, such as hyperglycemia, aberrant lipid metabolism, and amino acid metabolism disorders, leading to significant alterations in the level and activity of cellular metabolites that result in immune dysfunction (5, 6). The modified levels of metabolites can affect the pathophysiological process of sepsis by either affecting the activity of enzymes or otherwise altering protein structures and interactions (7, 8). The protein post-translational modifications (PTMs), as a result of an altered metabolism, represent one of the main causes of functional diversity of mammalian protein molecules, and are thus involved in the regulation of protein function and activity by inducing covalent binding of proteins to different functional metabolites (such as acetate, butyrate and lactate) (9). The regulatory machinery of protein PTMs mainly include substrates, modifying enzymes and de-modifying enzymes, among which the substrates are directly derived from the transformation of cell-related metabolites (10, 11). For instance, lactate can serve as a substrate for lactylation, while acetyl-CoA can be utilized as a substrate for acetylation modification (12, 13). Additionally, certain metabolites act as endogenous inhibitors of chromatin-modifying enzymes, thereby influencing the levels of PTMs by modulating the activity of modifying and de-modifying enzymes (14, 15). For instance, butyrate is a metabolite that regulates PTMs by inhibiting histone deacetylase (HDAC) activity(16). Importantly, PTMs can occur in histones, affecting the regulation of gene expression, as well as in non-histone proteins, influencing their function or interactions with other proteins (17, 18). Histone modification includes methylation, acetylation, phosphorylation and other forms, which can regulate gene transcriptional activity and chromatin structure by changing the chemical structure of histone (19–21). The role of histone modification in the pathogenesis and development of sepsis is multifaceted, encompassing the regulation of inflammatory factor expression, modulation of immune cell function and differentiation, and regulation of cell apoptosis and survival (22–24). PTMs can also influence the activity of themselves or interactive proteins by acting on non-histone proteins, thereby regulating the level of autophagy and nuclear translocation that may intervene in the progression of sepsis (25, 26). Furthermore, metabolite-dependent PTMs may affect the short- and long-term immunosuppressive state by providing rapid and prolonged responses that counteract the overreaction of circulating acute pro-inflammatory cytokines in sepsis patients (27).

In recent years, the significance of intestinal flora and their metabolites in inflammatory and metabolism-related diseases has gained increasing recognition(28). Among these, short-chain fatty acids (SCFAs), obtained by the flora through fermentation of food fibers, have received considerable attention, particularly in their regulatory roles in metabolism, maintenance of the intestinal mucosal barrier, and immune homeostasis (29, 30). SCFAs and its corresponding acyl coenzyme A are located at the crossroads of metabolic pathways and play an important role in various cellular processes. It has been observed that SCFAs can play a signal transduction role through covalent or non-covalent binding to proteins and can also bind to modifying enzymes to mediate post-translational modification of proteins (31). Moreover, SCFAs have been found to exert major regulatory effects in sepsis, including affecting gene expression, enhancing phagocytosis of macrophages, altering cell proliferation and function, and inhibiting the activity of HDAC (32–36). Several recent studies have demonstrated that there were significant differences in SCFAs levels in the feces of severe septic patients and in murine models of sepsis induced by cecal ligation and puncture (CLP) (37, 38). Therefore, the disorder of SCFAs is secondary to changes in the primary event of sepsis, and changes in SCFAs levels may further affect the formation of PTMs, which in turn may mediate the primary event of sepsis.

In this review, we have provided a summary of the metabolic mechanisms involved in the inflammatory and immunosuppressive phases of sepsis, with a particular focus on the roles of SCFAs metabolism. We have also discussed recent advances in SCFAs-mediated lysine acylation modifications.

2 The intricate pathophysiology of sepsis and the underlying metabolic mechanisms

The pathogenesis of sepsis is a complex phenomenon, involving a multitude of factors spanning from the molecular to the organ level. This intricate interplay encompasses issues such as infection, inflammation, immunity, coagulation, and tissue damage (3). Cytokine storm is an early manifestation of sepsis, which primarily arises from macrophages engulfing pathogens and subsequently releasing a myriad of inflammatory cytokines, thereby triggering the body's inflammatory response (39). In the later stages of sepsis, immunosuppression assumes a dominant role, characterized by the downregulation of pro-inflammatory factors, secondary infections, and increased apoptosis and autophagy of immune cells (40–42). Apoptosis of immune cells is a major factor in the development of immunosuppression in sepsis(43). Notably, sepsis is also suggested to manifest concurrent hyperinflammation and immune suppression that further increase the intricateness of this syndrome (3).

The alterations in the levels of relevant metabolites during sepsis can interfere with inflammatory and immune processes by regulating the levels of PTMs. Clinical investigations have shown that metabolic reprogramming during sepsis leads to profound

changes in glucose, lipid, and fatty acid metabolism (44). Among these, glucose metabolic reprogramming occurs during sepsis when glycolytic pathways are enhanced in response to cellular biosynthesis and bioenergy requirements, thereby promoting cell growth, differentiation, and effector functions (45). Second, lipid production is an important adaptive response to normal tissue function. Clinical studies have found that cholesterol and lipoprotein levels vary markedly in patients with inflammation, with patients with severe sepsis having lower levels of cholesterol, including high-density lipoprotein (HDL), low-density lipoprotein (LDL) and apolipoprotein A-I (Apo A-I), as well as high levels of triglycerides (TGs) and free fatty acids (FFA) (46). Consequently, HDL and LDL are considered to be important modulators of the host immune response during sepsis. At the same time, sepsis induces the release of lipid mediators, many of which activate nuclear receptors. For instance, peroxisome proliferator-activated receptor (PPAR) α, a nuclear receptor activated by fatty acids (FAs), controls lipid metabolism and inflammation. Paumelle et al. found that PPARα deficiency led to a pro-inflammatory response and reduced survival in the CLP model, which impaired the adaptive metabolic shift from glucose to fatty acid (FAs) utilization (47).

Beyond the major metabolic pathways, some specific metabolic pathways and their products are also significantly altered in sepsis, such as SCFAs. During sepsis, increased inflammatory factors lead to intestinal epithelial cell apoptosis and increased intestinal wall permeability (48). In addition, sepsis induces kidney injury, with a sharp increase in urea, sodium, and water leading to intestinal wall edema and disruption of tight junction proteins in colonic epithelial cells. Inflammatory cytokines as well as urea retention damage the intestinal barrier, leading to bacterial translocation through the portal vein or mesenteric lymphatic system, causing a systemic inflammatory response and eventually leading to multiple organ failure and death (49, 50). Due to the effects of antibiotics, parenteral nutrition and systemic inflammation, the number of anaerobic bacteria in the intestinal flora is significantly down-regulated, accompanied by the significant down-regulation of intestinal metabolites SCFAs (48, 51). Studies have shown that SCFAs play an important role in immune regulation and inflammation suppression (52). For example, SCFAs can regulate the function of immune cells by activating G protein-coupled receptors, inhibit the release of inflammatory mediators, and mitigating the inflammatory response (53). SCFAs can also promote intestinal barrier function and regulate intestinal flora balance, potentially conferring effects against the occurrence and progression of sepsis (54). Furthermore, both murine models and *in vitro* experiments have demonstrated notable alterations in SCFAs levels within immune cells, strongly correlating with sepsis progression. For example, one study revealed fecal SCFAs levels were significantly downregulated in a rat sepsis model induced by CLP, while the levels of TNF-α, IL-1β, IL-6, and other inflammatory factors in the hippocampus were markedly upregulated (55). Additionally, exogenous supplementation of SCFAs in lipopolysaccharide (LPS)-stimulated primary rat neutrophils not only significantly suppressed the levels of TNF-α and nitric oxide synthase by inhibiting the activation of nuclear factor κB (NF-κB), but also inhibited the activity of HDAC, potentially influencing inflammation progression through the modulation of specific PTMs (56).

3 Gut microbiota and microbiota derived SCFAs

Gut microbiota refers to the community of various microorganisms present in the human gut, including bacteria, archaea, fungi, and viruses, plays a crucial role in human health (57). Recent studies have highlighted its involvement in various biological processes, such as the regulation of tumor cell immunogenicity and innate immune functions, particularly in tumor cells and in macrophages (58, 59). In addition, the interplay between the intestinal microbiota, local immunity, and gut integrity has emerged as a key determinant in disease development (60). During sepsis, factors like intestinal hypoperfusion, intestinal cell apoptosis, systemic cytokine storms, and intestinal dysbiosis contribute to the disruption of intestinal cell permeability, promoting the migration of flora and the transfer of inflammatory mediators, leading to multiple organ dysfunction syndrome and systemic inflammatory response (61, 62). Gai et al. found that there was an imbalance of flora 12 hours after CLP in the mouse model, with significant reductions in Firmicutes and Bacteroidetes (63). Giridharan et al. found that acetate, propionate and butyrate were significantly down-regulated in the CLP model group compared with the control group (55). Thus, disruption of gut microbiota during sepsis leads to secondary down-regulation of SCFAs levels. Meanwhile, SCFAs, metabolites of the gut microbiota, could reshape intestinal dysbiosis, reduce the release of inflammatory cytokines, and improve survival rates in CLP-induced model (54). Therefore, the stability of gut microbiota is crucial for the production of SCFAs and host immune regulation. Meanwhile, SCFAs as products in turn maintain the intestinal ecological balance and participate in the regulation of immune response.

Acetate, propionate, and butyrate are the primary SCFAs found in the gut, accounting for more than 95% of SCFAs, of the total SCFAs composition, with an estimated ratio of approximately 3:1:1 (64). The relative abundance of these SCFAs varies depending on factors such as the host's diet, microbiome composition, and tissue location, as they are produced by specific microbial communities in different regions of the gut (65). Acetate, the most abundant SCFAs, is extensively produced in the gut and can be metabolized and transported by the intestinal epithelium and liver, serving as an energy source (66). Gut bacteria can convert pyruvate to acetate by either acetyl-CoA or the Wood-Ljungdahl pathway (67, 68). The production of propionate mainly occurs in the large intestine and is produced by bacteria such as Bacteroides and Clostridium anaerobes (69). In addition, the succinate pathway is an important pathway for the production of propionic acid by human gut microbiota, and methylmalonyl-CoA is the key enzyme in the succinate pathway. Propionic acid can also be generated by the acrylate pathway and the propylene glycol pathway (70, 71). Propionate can be absorbed by the intestinal epithelium and transported to the liver, where it is further

metabolized into glucose or fatty acids (72). Butyrate is formed by condensation and subsequent reduction of two acetyl-CoA molecules to butyrate, which can be converted to butyrate by phospho-transbutyrylase and butyrate kinase (73). Butyrate can be absorbed by intestinal epithelial cells and metabolized in the liver as ketone bodies or carbon dioxide (74). Studies have shown that the concentration of SCFAs in the intestine ranges from 20 to 140 mM, with extremely high concentrations in the proximal colon (70 to 140 mM), and relatively low concentrations in the distal colon (20 to 70 mM) and distal ileum (20 to 40 mM), depending on the presence of infection/inflammation in the host (32, 75). In addition, studies have found that the production of gut-derived SCFAs can be regulated by changing the proportion of SCFAs -producing flora in the gut (76). At present, the main ways to regulate the structure of gut microbiota include changing the host dietary structure (Mediterranean diet), direct intake of probiotics or prebiotics to regulate gut microbiota (77–79). In conclusion, gut microbiota plays a crucial role in the generation of SCFAs.

As the most abundant metabolite of the intestinal microbiota in the intestinal lumen, SCFAs play a multifaceted role in the regulation of the host immune system (80). Firstly, SCFAs serve as a vital energy source for colon and ileal cells, influencing the expression of genes involved in intestinal epithelial barrier function and defense mechanisms (32). Second, modulate the function of key immune cells such as macrophages, neutrophils, dendritic cells, and even adipocytes, thereby impacting inflammation progression through the regulation of TNF-α, IL-10, and IL-4 levels in adipose tissue (81). Thirdly, SCFAs exert their immunomodulatory effects by inhibiting HDAC activity and activating specific receptors, namely, free fatty acid receptors type 2 and 3 (FFA2 and FFA3 receptors) and G protein-coupled receptor 109A (GPR109A) (82). These mechanisms collectively contribute to the regulation of immune responses and the formation of various post-translational modifications involved in cellular processes.

4 The relationship between sepsis and SCFAs metabolism

4.1 Changes in SCFAs levels in sepsis and their relationship to disease progression or regression

The pivotal pathway responsible for the production of SCFAs has been found to be intricately linked with the presence of microbiota (80). Notably, a recent study has demonstrated that individuals with diminished gut microbiota diversity face an elevated susceptibility to sepsis (83, 84). Furthermore, in an observational investigation involving critically ill patients with non-abdominal infections, perturbations in the gut microbiome have been shown to predispose individuals to sepsis by enabling the proliferation of pathogens, promoting an aberrant immune response, and impeding the production of beneficial SCFAs (85). Additionally, the concentration of propionic acid in serum has been found to increase in tandem with the severity of sepsis, suggesting that serum propionate holds significant potential as a predictor and prognostic biomarker for septic patients (86). Consequently, alterations in SCFAs levels during sepsis may result from an imbalance in intestinal flora, thereby inducing immune dysregulation and damage to the intestinal epithelial barrier. This, in turn, exacerbates the detrimental cycle of immune dysregulation prompted by the inflammatory response to sepsis.

Furthermore, Liao et al. have observed a significant downregulation of acetic acid and propionic acid in the CLP-induced model relative to the sham group. Remarkably, exogenous supplementation of SCFAs has been shown to substantially increase acetic acid and propionic acid levels while significantly downregulating the levels of IL-1β, IL-6, and TNF-α (38). Similarly, Li et al. have discovered that in mice subjected to the CLP model, SCFAs levels are significantly reduced, accompanied by considerable alterations in the gut microbiota. Notably, exogenous SCFAs administration has been found to enhance intestinal barrier integrity and significantly downregulate IL-1β, TNF-α, and IL-6 levels in mice (87). Although SCFAs may have potential value in the prevention and treatment of sepsis, its feasibility for the treatment of clinical patients should be verified by human trials.

4.2 The regulatory effect of SCFAs on sepsis

SCFAs exert multiple modulatory effects on the pathophysiology of sepsis. First, SCFAs are a key source of energy for colon and ileal cells and affect intestinal epithelial barrier and defense functions by regulating related gene expression (68). Wang et al. found that butyrate provides energy to colonic intestinal epithelial cells, regulates intestinal gene expression, inhibits the intestinal inflammation induced by LPS (88). Zhan et al. have demonstrated that SCFAs hinder pathogen invasion by supplying energy and regulating the barrier function and immune status of the host intestine (89). Secondly, SCFAs intervene in the inflammatory storm phase during sepsis by regulating the production of immune cytokines (Table 1). At present, a number of studies have found that SCFAs can significantly down-regulate the levels of a variety of pro-inflammatory mediators (38, 90, 92, 93). For example, Vinolo et al. found that butyrate and propionate can reduce the expression of TNF-α and nitric oxide synthase (NOS) in primary mouse neutrophils induced by LPS (56). Similarly, Wang et al. demonstrated that butyrate significantly decreased the levels of TNF-α, IL-1β and IL-6 in LPS-injected mice (91). In another study, butyrate treatment was shown to inhibit the levels of nitric oxide, IL-6, and IL-12 inflammatory mediators in LPS-stimulated bone marrow-derived macrophage (BMDM) cells by inhibiting HDAC (7). Thirdly, SCFAs could regulate sepsis by regulating PTMs. For example, in $CD8^+$ T cells within a low-glucose tumor environment, acetate facilitates histone acetylation to enhance the transcription of the IFN-γ gene and cytokine production, thereby modulating the progression of inflammation (94). In addition, acetate can supplement acetyl-CoA, which promotes the acetylation of GAPDH to enhance its activity, thereby promoting glycolysis, so as to promote rapid memory CD8(+) T cell response and enhance the immune response (95). Taken together, these findings suggest that

TABLE 1 SCFAs regulate inflammation by regulating the production of immune cytokines.

SCFAs	Model	Pro-/anti-inflammatory	Signaling pathway	Ref
Acetate	LPS-induced	anti-	TNF-α↓	(90)
Butyrate	LPS-induced	anti-	CO↓, IL-6↓, IL-12↓	(7)
Butyrate	LPS-induced	anti-	IL-6↓, TNF-α↓, IL-1β↓, IL-10↑	(91)
Propionate	LPS-induced	anti-	iNOS↓, NF-kB↓, COX-2↓	(92)
Butyrate	CLP-induced	anti-	iNOS↓, COX-2↓	(59)
Acetate Propionate Butyrate	CLP-induced	anti-	IL-6↓, TNF-α↓, IL-1β↓	(38)
Acetate Propionate Butyrate	CLP-induced	anti-	IL-18↓, NLRP3↓, IL-1β↓	(54)
Butyrate	CLP-induced	anti-	NF-kB↓, IL-6↓, TNF-α↓, IL-1β↓	(93)

The symbols "↑" represent increase. The symbols "↓" represent decrease.

SCFAs can suppress the inflammatory response, and that the absence of SCFAs and the reaction of SCFAs with PTMs are secondary events of the inflammatory response in sepsis.

4.3 The mechanism of SCFAs regulating post-translational modification of proteins in sepsis

PTMs represent a crucial pathway for regulating protein function, and significant changes in phosphorylation, ubiquitination, methylation, and acylation have been observed during and after sepsis (96–98). Lysine acylation includes long chain acylation and short chain acylation. Protein acylation is involved in a variety of cellular processes, such as protein stability, protein subcellular localization, enzyme activity, transcriptional activity, protein-protein interaction and protein-DNA interaction (99). Among them, protein lysine acylation exerts important and unique regulatory roles. Studies have indicated that lysine acylation can regulate the development of sepsis by regulating the activity of modifying enzymes, targeting innate sensors and downstream signaling molecules (100, 101).

Interestingly, the most substrates of these novel lysine acylation modification are SCFAs, such as acetate, malonate, crotonic acid and 2-hydroxyisobutyric acid, among which lysine acetylation (Kac), lysine malonylation (Kmal), lysine crotonylation (Kcr) and lysine 2-hydroxyisobutyrylation (Khib) play crucial roles in inflammation and immunity. Consequently, SCFAs may participate in regulating the immune response during sepsis by influencing the corresponding acylation modification levels (102–105). To simplify the intricate regulation of SCFAs-mediated PTMs on the immune system, this review will combine current research to elucidate the mechanism by which SCFAs affect PTMs through two primary pathways: i: SCFAs as inhibitors of HDAC that regulate the level of lysine acylation modification and participate in the regulation of sepsis; ii. SCFAs as substrates for lysine post-translational modification that regulate the level of modification and participate in the regulation of sepsis.

4.3.1 SCFAs as inhibitors of HDAC

4.3.1.1 Methylation

Protein lysine methylation is a dynamic process that plays a vital role in various biological processes, such as DNA damage repair, cell growth, metabolism, and signal transduction (106). The dynamic lysine methylation system comprises three key components: protein lysine methyltransferases (PKMTs), which add methylation marks; methyl-binding domains (MBDs), which participate in methylation events with biological outcomes; and lysine-specific demethylases (KDMs), responsible for the removal of methylation marks (107).

In the context of early sepsis, protein lysine methylation assumes a critical role in the epigenetic regulation of innate immunity. Xia et al. discovered that Ash1l, an H3K4 methyltransferase, suppressed the expression of TNF-α and IL-6 by promoting H3K4 methylation at the Tnfaip3 promoter in mice injected with LPS (108). Interestingly, SCFAs also regulate inflammation progression and immune cell functional expression by modulating lysine methylation modifications. Kaye et al. observed that in hypertensive mice, acetate activated DNA methylation in Treg cell regions, enhancing the anti-inflammatory effects of immune cells by regulating Treg cell proliferation (109). Additionally, Chang et al. found that in LPS-stimulated BMDM cells, exogenous addition of butyrate could inhibit the methylation modification of the GPR41/43 promoter region, thereby suppressing the expression of GPR41/43 and reducing host inflammatory damage (7). Collectively, the methylation of histone and non-histone lysine significantly influences the function of immune cells during sepsis. SCFAs regulate the levels of inflammatory and anti-inflammatory factors by inhibiting HDAC activity, thereby affecting methylation levels and interfering with the transcriptional activities of transcription factors. Hence, SCFAs hold promise as potential therapeutic agents for early sepsis treatment.

4.3.1.2 Acetylation

Lysine acetylation modifications are a universally recognized group of PTMs that that have the potential to impact protein function through various mechanisms. These mechanisms include the regulation of protein stability, enzymatic activity, subcellular localization, interplay with other post-translational modifications, and the control of protein-protein and protein-DNA interactions (110). Among these, the diverse HAT/KAT and HDAC/KDAC enzymes are widely involved in biological cellular processes, and the lysine acetylation or deacetylation they induce in cells may contribute to the development of several diseases.

SCFAs play a role in the regulation of lysine acetylation modifications by inhibiting HDAC activity. This interference with HDAC activity has been shown to impact the progression of inflammation in various diseases (111–118). Notably, Luu et al. discovered that in experimental mouse models of colitis, valerate promotes the acetylation of histone H4 at the IL-10 promoter by providing acetyl-CoA and inhibiting HDAC activity. This, in turn, induces the production of IL-10 in lymphocytes, playing an anti-inflammatory immunomodulatory role (119). Moreover, Park et al. found that acetate upregulates the acetylation modification of p70 S6 kinase by inhibiting HDAC activity. This promotes the differentiation of T cells into effector T cells and regulatory T cells, consequently reducing anti-CD3-induced inflammation in an IL-10-dependent manner (120). Meanwhile, Yang et al. discovered that in anti-CD3-activated $CD4^+$ cells, butyrate upregulates histone acetylation on the IL-22 promoter, facilitating HIF1α binding to this region. This ultimately promotes the production of IL-22, safeguarding the host from inflammation (121). Therefore, SCFAs can regulate inflammatory and immune processes by regulating protein acetylation modification, which may potentially exert a similar effect on inhibiting hyperinflammation in sepsis. In conclusion, facilitate the acetylation of both histone and non-histone proteins by inhibiting HDAC activity. This regulation of lysine acetylation contributes to the innate immune response of the host and participates in the immune pathogenesis of sepsis. Consequently, targeting key lysine acetylation sites to inhibit inflammation progression represents an important approach to the treatment and intervention of sepsis.

4.3.1.3 Crotonylation

Lysine crotonylation (Kcr) modification is a highly conserved protein modification that has evolved from histone lysine acetylation (Kac). Although crotonylation and acetylation have distinct biological characteristics, they share the same regulatory enzymes. Crotonylation modification plays a role in regulating diverse biological processes and the development of various diseases, including gene expression, spermatogenesis, cell cycle regulation, and the pathogenesis of conditions ranging from depression to cancer (122–125). In addition to intracellular crotonyl-CoA, the regulation of Kcr also involves the addition and removal of modified writers and erasers, respectively, contributing to homeostasis (126). Histone acetyltransferases (HATs), such as p300/CBP, possess significant histone crotonyl transferase (HCT) activity, highlighting their role in crotonylation modification (127).

It has been also demonstrated that crotonylation is involved in sepsis. Sabari et al. found that crotonyl-CoA supplementation in macrophages led to a substantial increase in histone H3K18Cr. Additionally, knockdown of ACSS2, an enzyme involved in crotonyl-CoA synthesis, reduced the expression of histone H3K18Cr and inflammatory genes in LPS-stimulated RAW264.7 cells (128). This suggests a close association between crotonylation and sepsis, with the possibility of modulating inflammatory progression through the regulation of crotonylation. Furthermore, SCFAs are involved in regulating Kcr modification levels by inhibiting HDAC activity. Fellows et al. demonstrated that exogenous butyrate supplementation inhibited HDAC activity in colonic epithelial cells, resulting in the upregulation of histone H3K18cr modification and influencing the cell cycle. This finding further underscores the connection between SCFAs and chromatin signaling (129). Collectively, the levels of lysine Kcr modification undergo significant changes following LPS stimulation, and SCFAs participate in the regulation of Kcr by inhibiting HDAC activity. This suggests that SCFAs may impact sepsis through the modulation of Kcr modification. Therefore, it is crucial to further investigate the mechanisms underlying histone and non-histone Kcr modification targets in sepsis for the development of effective treatments.

4.3.2 SCFAs as substrates for lysine acylation modification

4.3.2.1 Lysine 2-hydroxyisobutyrylation

Lysine 2-hydroxyisobutyrylation (Khib) is a novel histone acylation modification first identified in 2014 with 2-hydroxybutyrate and its cozymoylated form 2-hydroxyisobutyl CoA as the substrates (130–132). The 2-hydroxybutyric acid is a typical SCFAs detected in micromolar concentrations in a variety of human biological fluids. Of note, its high occurrence in the urine of obese patients was found associated with the abundance of specific taxa of the gut microbiota (133, 134). Similar to other types of PTMs, khib also maintains a dynamic balance by adding and removing writers and erasers respectively. Huang et al. demonstrated that Esa1p and its human homolog TIP60 from yeast cells can regulate khib proteinogenesis and act as writers for khib (130). Additionally, the lysine acetyltransferase p300, mentioned earlier, exhibits enzymatic activity not only for lysine acetylation but also for lysine butyrylation, propionylation, and crotonylation (135–137a).

Although khib occurs in diverse cellular proteins, it has only emerged to realize that it may exert mutifaced roles physiological and pathological conditions. For instance, Yamazaki et al. found that the serum level of 2-HIBA was significantly up-regulated in a mouse model of periodontitis through metabolomics (138). Similarly, Tsoukalas et al. found statistically significant differences in the metabolite levels of 2-hydroxyisobutyric acid in urine of rheumatoid arthritis patients through metabolomics (139). Therefore, as a SCFAs, the level of 2-hydroxyisobutyric acid is significantly up-regulated in a variety of diseases involving inflammation, suggesting that the change of its level has an important relationship with the development of inflammation.

Notably, the occurrence of khib is also strongly associated with inflammatory regulation. Ge et al. found that in the skin tissue of patients with psoriasis, the proteins encoded by S100A9, FUBP1 and SERPINB2 genes have significant khib with proteins in the PI3K-Akt signaling pathway (137b). Among them, S100A9 is a potential target for the treatment of sepsis, and further investigation is needed to determine if its khib is involved in sepsis progression (140). In addition, Dong et al. analyzed khib occurrence in key enzymes of the glycolytic pathway in blood monocytes from end-stage renal disease patients, which may affect immune cell numbers and induce immune senescence by influencing glycolytic function (141). Furthermore, Xie et al. found high enrichment of khib in blood monocytes from lupus erythematosus patients during the antigen processing and presentation process and leukocyte migration pathways. This suggests that khib is involved in inflammation regulation by affecting the khib level of key proteins in these pathways (142). Although there is no direct reported relationship between khib and sepsis, khib is essentially involved in the regulation of various inflammation-related diseases, implicating the necessity to further elucidate the specific mechanism of immune function regulated by khib-modified histone or non-histone proteins and discover new targets for sepsis treatment.

4.3.2.2 Lysine malonylation

Lysine malonylation (Kmal) is a highly conserved acylation modification that was initially discovered in 2011 (143). Its modified substrates include malonate and malonyl-CoA. The occurrence of Kmal relies on the addition of malonyl groups to lysine by malonyl-CoA, resulting in its charge changed from +1 to -1. Of note, malonate is also a typical SCFAs which participates in the regulation of mammalian glycolytic physiological processes (144, 145). Similar to other acylation modifications, the extent of Kmal modification is governed by the de-modifying enzyme. For example, Nishida et al. unveiled that SIRT5 functions as a global regulator of lysine malonylation and orchestrates the energy cycle through the glycolytic pathway (146).

Kmal is also implicated in regulating intracellular inflammatory and immune events. In a study conducted by Lee et al., it was discovered that malonate profoundly hindered the activation of the p38 MAPK/NF-κB pathway in LPS-stimulated microglia, thereby exerting an anti-inflammatory effect (147). Additionally, Park et al. observed that malonate significantly downregulated the expression of ROS-induced NF-κB and inflammation-related cytokines (IL-6, COX-2, and TNF-α) in HaCaT cells(148). Hence, it is plausible that malonate, acting as a SCFAs, modulates the innate immune response through the inhibition of the inflammatory cascade. Interestingly, Galván-Peña et al. demonstrated that the level of Kmal was significantly upregulated in LPS-stimulated BMDM cells. Notably, malonylation mass spectrometry revealed the presence of malonylation modifications at the lysine 213 site on GAPDH. Under normal circumstances, GAPDH binds to and represses the translation of various mRNAs associated with inflammation, including the one encoding TNFα. However, upon malonylation modification of GAPDH, it dissociates from the TNFα mRNA, thereby promoting its translation (149). Furthermore, Qu et al. (150) found that atractylodin inhibits the malonylation of GAPDH and subsequently suppresses the level of TNF-α in LPS-induced RAW264.7 cells. Consequently, Kmal modification may play a pivotal role in the regulation of sepsis. The identification of novel targets of Kmal-modified histones or non-histones holds great significance for the treatment of sepsis.

Figure 1 An overview on the effects of SCFAs on signaling pathways and protein post-translational modifications during sepsis. The binding of LPS or TNF-α to their respective receptors triggers the activation of Toll-like receptor 4 (TLR4), MAPK and nuclear factor kappa B (NF-κB) signaling pathways, leading to the release of cytokines, which plays a crucial role in sepsis development. However, SCFAs, predominantly acetate, propionate, and butyrate, exert anti-inflammatory effects by

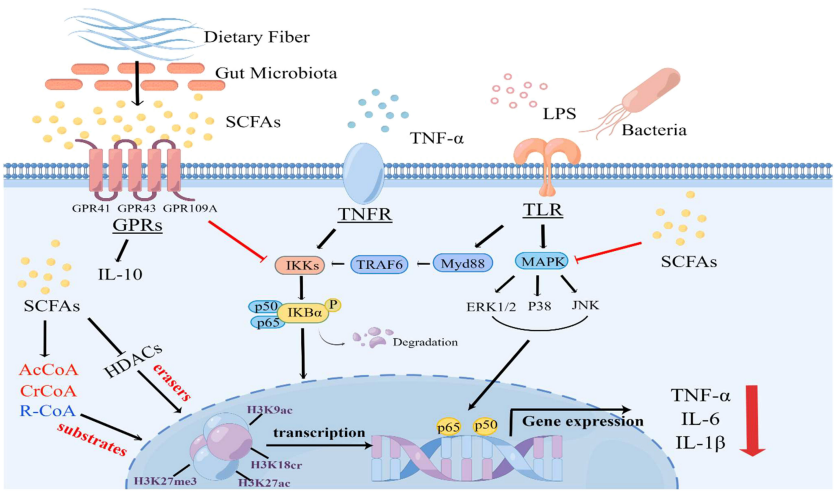

FIGURE 1
An overview on the effects of SCFAs on signaling pathways and protein post-translational modifications during LPS or TNFα-induced sepsis.

activating G protein-coupled receptor (GPR) 41, GPR43, and GPR109A receptors or inhibiting the activation of NF-κB and mitogen-activated protein kinase (MAPK) signaling pathways. Furthermore, SCFAs can serve as substrates for protein post-translational modifications and inhibit the activity of HDAC, thereby regulating the levels of various lysine acylation modifications. This inhibition of HDAC activity leads to the transcriptional downregulation of inflammatory factors and actively participates in immune regulation within the body (By Figdraw).

5 Summary and perspectives

As a byproduct of intestinal bacteria and a metabolite, SCFAs actively participate in the regulation of the host's immune function, playing a crucial role in sepsis and inflammatory diseases. Furthermore, PTMs are closely associated with key stages of sepsis, exerting their influence on the regulation of cytokine storms and immune suppression by inhibiting or reversing the transcription of pro-inflammatory genes. Interestingly, both the epigenetic changes caused by PTMs and the immunosuppressive state of sepsis are long-lasting conditions. In our review, we have focused on the role of SCFAs, which may have a significant impact on the regulation of lysine acylation modifications in sepsis. There is mounting evidence suggesting that SCFAs can modulate innate and adaptive immune responses by regulating lysine acylation modifications (Table 2).

In this review, we have summarized the research progress regarding SCFAs in the pathological processes of inflammation and sepsis by their impact on PTMs. While host metabolism and immune regulation have garnered significant attention, further experiments are required to elucidate the specific mechanisms through which SCFAs regulate different lysine acylation

TABLE 2 Regulation of protein post-translational modifications by SCFAs in sepsis.

SCFAs	Histone/ non-histone	PTMs changes	Model	Roles	Ref
Acetate	NIP45	Methylation	T-cell	Acetate alters DNA methylation in the region of activated Treg cells, regulates Treg cell proliferation and enhances the anti-inflammatory effect of immune cells.	(109)
Acetate	Foxp3 H3K9ac	Acetylation	T-cell	Acetate may increase acetylation of the Foxp3 promoter through HDAC9 inhibition by increasing the number and function of T regulatory cells and significant airway inflammatory responses.	(117)
Acetate	p70-S6K	Acetylation	T-cell	The inhibitory effect of SCFA on HDAC in T-cells increases acetylation of p70 S6 kinase and promotes T-cell differentiation into effector and regulatory T-cells, thereby promoting immunity or immune tolerance depending on the immune environment.	(120)
propionate	H3K9ac	Acetylation	cTregs	Propionic acid treatment of cTregs enhanced histone H3K9ac through inhibition of HDAC, which in turn affected the immune status of cTregs.	(115)
Pentanoate	H4	Acetylation	Th17 cell	Pentanoate promotes histone H4 acetylation by providing acetyl coenzyme A and inhibiting the activity of HDAC, induces IL-10 production by lymphocytes by increasing acetylation at the IL-10 promoter, and improves anti-inflammatory capacity.	(119)
Butyrate	H3	Acetylation	$CD4^+$ T cells	Exogenous addition of butyrate enhances histone H3 acetylation in the promoter and conserved non-coding sequence regions of the Foxp3 locus, induces differentiation of mouse colonic T-cells and ameliorates the development of colitis.	(118)
Butyrate	H3K9ac/ H3K9me3	Acetylation	$CD4^+$ T cells	Butyrate protects the host from inflammation by increasing the binding of HIF1α to the IL-22 promoter through histone modifications and promoting IL-22 production.	(121)
Butyrate	H3K9ac	Acetylation	BMDM	Butyrate maintains tolerance to intestinal microbiota by inhibiting the activity of HDAC, promoting Nos2, IL-6 and H3K9ac, the promoter region of the IL12b gene, and by down-regulating the release of pro-inflammatory factors that reduce the response of macrophages to commensal bacteria.	(7)
Butyrate	GPR41/ GPR43	Methylation	Cecal Tissues	Butyrate inhibits the methylation of the GPR41/43 promoter region and thus the expression of GPR41/43, reducing inflammatory damage.	(103)
Butyrate	H3K18cr	Crotonylation	Colon epithelial cell	Butyrate promotes histone crotonylation by inhibiting the activity of HDAC in colonic epithelial cells.	(129)
Butyrate/ Propionate	Foxp3	Acetylation	peripheral regulatory T-cell	Butyrate and propionate increase acetylation of Foxp3 to promote extrathymic Treg cell differentiation by inhibiting HDAC activity.	(104)
Butyrate/ Propionate	H4K12ac	Acetylation	BMDM	Treatment of bone marrow cells with butyrate and propionate resulted in upregulation of H4K12ac on the PU.1 promoter, inhibiting the expression of PU.1 and RelB and thus preventing DC development.	(111)
isobutyric/ propionic	H3K27ac/ H3K27me3	Acetylation	T-cell	SCFAs regulates host antiviral innate immune response by increasing histone acetylation and decreasing repressive histone methylation to coordinate viral transcriptional activation.	(116)

modifications and the interplay between these modifications in sepsis-induced inflammation and immune suppression. Building upon the current research progress, we propose a scientific hypothesis that exogenous supplementation of SCFAs can regulate the levels of lysine acylation modifications, thereby restoring the immune response function of host immune cells and reversing host immunosuppression. With the advancement of metabolomics and proteomics technologies, it becomes increasingly feasible to explore the molecular targets of different lysine acylation modifications regulated by SCFAs during the immunosuppression stage of sepsis. Consequently, targeting lysine acylation regulated by SCFAs emerges as a potential therapeutic strategy for treating immunosuppression in sepsis, although further clinical trials are necessary to validate its feasibility in the future.

Author contributions

LZ and XS collected documents, wrote the manuscript and drew the mechanism figures. HQ collected documents and made tables. SL and TY polished the language and revised the manuscript. XLL and XL conceived ideas, designed the structure of the manuscript and revised the manuscript. All authors read and approved the submitted version. All authors contributed to the article.

Funding

This project is supported by grants from the National Natural Science Foundation of China (81873955 and 82172133) and Chongqing National Natural Science Program (csct2020jcyj-msxmX0223 and csct2022nscq-msx0214).

Conflict of interest

The authors declare that the research was conducted in the absence of any commercial or financial relationships that could be construed as a potential conflict of interest.

Publisher's note

All claims expressed in this article are solely those of the authors and do not necessarily represent those of their affiliated organizations, or those of the publisher, the editors and the reviewers. Any product that may be evaluated in this article, or claim that may be made by its manufacturer, is not guaranteed or endorsed by the publisher.

References

1. Cecconi M, Evans L, Levy M, Rhodes A. Sepsis and septic shock. *Lancet* (2018) 392(10141):75–87. doi: 10.1016/s0140-6736(18)30696-2

2. van Vught LA, Klein Klouwenberg PM, Spitoni C, Scicluna BP, Wiewel MA, Horn J, et al. Incidence, risk factors, and attributable mortality of secondary infections in the intensive care unit after admission for sepsis. *Jama* (2016) 315(14):1469–79. doi: 10.1001/jama.2016.2691

3. van der Poll T, Shankar-Hari M, Wiersinga WJ. The immunology of sepsis. *Immunity* (2021) 54(11):2450–64. doi: 10.1016/j.immuni.2021.10.012

4. Domínguez-Andrés J, Novakovic B, Li Y, Scicluna BP, Gresnigt MS, Arts RJW, et al. The itaconate pathway is a central regulatory node linking innate immune tolerance and trained immunity. *Cell Metab* (2019) 29(1):211–220.e215. doi: 10.1016/j.cmet.2018.09.003

5. Spitzer JJ, Bagby GJ, Mészáros K, Lang CH. Alterations in lipid and carbohydrate metabolism in sepsis. *JPEN J Parenter Enteral Nutr* (1988) 12(6 Suppl):53s–8s. doi: 10.1177/014860718801200604

6. Marik PE, Raghavan M. Stress-hyperglycemia, insulin and immunomodulation in sepsis. *Intensive Care Med* (2004) 30(5):748–56. doi: 10.1007/s00134-004-2167-y

7. Chang PV, Hao L, Offermanns S, Medzhitov R. The microbial metabolite butyrate regulates intestinal macrophage function via histone deacetylase inhibition. *Proc Natl Acad Sci USA* (2014) 111(6):2247–52. doi: 10.1073/pnas.1322269111

8. Yang K, Fan M, Wang X, Xu J, Wang Y, Tu F, et al. Lactate promotes macrophage HMGB1 lactylation, acetylation, and exosomal release in polymicrobial sepsis. *Cell Death Differ* (2022) 29(1):133–46. doi: 10.1038/s41418-021-00841-9

9. Seet BT, Dikic I, Zhou MM, Pawson T. Reading protein modifications with interaction domains. *Nat Rev Mol Cell Biol* (2006) 7(7):473–83. doi: 10.1038/nrm1960

10. Zheng YG, Wu J, Chen Z, Goodman M. Chemical regulation of epigenetic modifications: opportunities for new cancer therapy. *Med Res Rev* (2008) 28(5):645–87. doi: 10.1002/med.20120

11. Zhao Y, Garcia BA. Comprehensive catalog of currently documented histone modifications. *Cold Spring Harb Perspect Biol* (2015) 7(9):a025064. doi: 10.1101/cshperspect.a025064

12. Shen Y, Wei W, Zhou DX. Histone acetylation enzymes coordinate metabolism and gene expression. *Trends Plant Sci* (2015) 20(10):614–21. doi: 10.1016/j.tplants.2015.07.005

13. Zhang D, Tang Z, Huang H, Zhou G, Cui C, Weng Y, et al. Metabolic regulation of gene expression by histone lactylation. *Nature* (2019) 574(7779):575–80. doi: 10.1038/s41586-019-1678-1

14. Yang M, Soga T, Pollard PJ. Oncometabolites: linking altered metabolism with cancer. *J Clin Invest* (2013) 123(9):3652–8. doi: 10.1172/jci67228

15. Diehl KL, Muir TW. Chromatin as a key consumer in the metabolite economy. *Nat Chem Biol* (2020) 16(6):620–9. doi: 10.1038/s41589-020-0517-x

16. He J, Zhang P, Shen L, Niu L, Tan Y, Chen L, et al. Short-chain fatty acids and their association with signalling pathways in inflammation, glucose and lipid metabolism. *Int J Mol Sci* (2020) 21(17):6356. doi: 10.3390/ijms21176356

17. Millán-Zambrano G, Burton A, Bannister AJ, Schneider R. Histone post-translational modifications - cause and consequence of genome function. *Nat Rev Genet* (2022) 23(9):563–80. doi: 10.1038/s41576-022-00468-7

18. Lee JM, Hammarén HM, Savitski MM, Baek SH. Control of protein stability by post-translational modifications. *Nat Commun* (2023) 14(1):201. doi: 10.1038/s41467-023-35795-8

19. Hirota T, Lipp JJ, Toh BH, Peters JM. Histone H3 serine 10 phosphorylation by Aurora B causes HP1 dissociation from heterochromatin. *Nature* (2005) 438 (7071):1176–80. doi: 10.1038/nature04254

20. Isbel L, Iskar M, Durdu S, Weiss J, Grand RS, Hietter-Pfeiffer E, et al. Readout of histone methylation by Trim24 locally restricts chromatin opening by p53. *Nat Struct Mol Biol* (2023) 30(7):948–57. doi: 10.1038/s41594-023-01021-8

21. Wu K, Fan D, Zhao H, Liu Z, Hou Z, Tao W, et al. Dynamics of histone acetylation during human early embryogenesis. *Cell Discovery* (2023) 9(1):29. doi: 10.1038/s41421-022-00514-y

22. Weiterer S, Uhle F, Lichtenstern C, Siegler BH, Bhuju S, Jarek M, et al. Sepsis induces specific changes in histone modification patterns in human monocytes. *PloS One* (2015) 10(3):e0121748. doi: 10.1371/journal.pone.0121748

23. Ostuni R, Natoli G, Cassatella MA, Tamassia N. Epigenetic regulation of neutrophil development and function. *Semin Immunol* (2016) 28(2):83–93. doi: 10.1016/j.smim.2016.04.002

24. Patel BV, Lee T, O'Dea K. CLUSTERINg circulating histones in sepsis. *Am J Respir Crit Care Med* (2023) 208(2):125–7. doi: 10.1164/rccm.202305-0935ED

25. Wei S, Gao Y, Dai X, Fu W, Cai S, Fang H, et al. SIRT1-mediated HMGB1 deacetylation suppresses sepsis-associated acute kidney injury. *Am J Physiol Renal Physiol* (2019) 316(1):F20–31. doi: 10.1152/ajprenal.00119.2018

26. Sun M, Li J, Mao L, Wu J, Deng Z, He M, et al. p53 deacetylation alleviates sepsis-induced acute kidney injury by promoting autophagy. *Front Immunol* (2021) 12:685523. doi: 10.3389/fimmu.2021.685523

27. McCall CE, Yoza B, Liu T, El Gazzar M. Gene-specific epigenetic regulation in serious infections with systemic inflammation. *J Innate Immun* (2010) 2(5):395–405. doi: 10.1159/000314077

28. Saad MJ, Santos A, Prada PO. Linking gut microbiota and inflammation to obesity and insulin resistance. *Physiol (Bethesda)* (2016) 31(4):283–93. doi: 10.1152/physiol.00041.2015

29. Yue X, Wen S, Long-Kun D, Man Y, Chang S, Min Z, et al. Three important short-chain fatty acids (SCFAs) attenuate the inflammatory response induced by 5-FU and maintain the integrity of intestinal mucosal tight junction. *BMC Immunol* (2022) 23(1):19. doi: 10.1186/s12865-022-00495-3

30. Wang J, Zhu N, Su X, Gao Y, Yang R. Gut-microbiota-derived metabolites maintain gut and systemic immune homeostasis. *Cells* (2023) 12(5):2296. doi: 10.3390/cells12050793

31. Huang H, Tang S, Ji M, Tang Z, Shimada M, Liu X, et al. p300-mediated lysine 2-hydroxyisobutyrylation regulates glycolysis. *Mol Cell* (2018) 70(4):663–678.e666. doi: 10.1016/j.molcel.2018.04.011

32. Tan J, McKenzie C, Potamitis M, Thorburn AN, Mackay CR, Macia L. The role of short-chain fatty acids in health and disease. *Adv Immunol* (2014) 121:91–119. doi: 10.1016/b978-0-12-800100-4.00003-9

33. Lin MY, de Zoete MR, van Putten JP, Strijbis K. Redirection of epithelial immune responses by short-chain fatty acids through inhibition of histone deacetylases. *Front Immunol* (2015) 6:554. doi: 10.3389/fimmu.2015.00554

34. Sanford JA, Zhang LJ, Williams MR, Gangoiti JA, Huang CM, Gallo RL. Inhibition of HDAC8 and HDAC9 by microbial short-chain fatty acids breaks immune tolerance of the epidermis to TLR ligands. *Sci Immunol* (2016) 1(4):eaah4609. doi: 10.1126/sciimmunol.aah4609

35. Wu T, Li H, Su C, Xu F, Yang G, Sun K, et al. Microbiota-derived short-chain fatty acids promote LAMTOR2-mediated immune responses in macrophages. *mSystems* (2020) 5(6):eaah4609. doi: 10.1128/mSystems.00587-20

36. Liu J, Jin Y, Ye Y, Tang Y, Dai S, Li M, et al. The neuroprotective effect of short chain fatty acids against sepsis-associated encephalopathy in mice. *Front Immunol* (2021) 12:626894. doi: 10.3389/fimmu.2021.626894

37. Valdés-Duque BE, Giraldo-Giraldo NA, Jaillier-Ramírez AM, Giraldo-Villa A, Acevedo-Castaño I, Yepes-Molina MA, et al. Stool short-chain fatty acids in critically ill patients with sepsis. *J Am Coll Nutr* (2020) 39(8):706–12. doi: 10.1080/07315724.2020.1727379

38. Liao H, Li H, Bao H, Jiang L, Du J, Guo Y, et al. Short chain fatty acids protect the cognitive function of sepsis associated encephalopathy mice via GPR43. *Front Neurol* (2022) 13:909436. doi: 10.3389/fneur.2022.909436

39. Boyd JH, Russell JA, Fjell CD. The meta-genome of sepsis: host genetics, pathogens and the acute immune response. *J Innate Immun* (2014) 6(3):272–83. doi: 10.1159/000358835

40. Borouchaki A, de Roquetaillade C, Barthelemy R, Mebazaa A, Chousterman BG. Immunotherapy to treat sepsis induced-immunosuppression: Immune eligibility or outcome criteria, a systematic review. *J Crit Care* (2022) 72:154137. doi: 10.1016/j.jcrc.2022.154137

41. Liu D, Huang SY, Sun JH, Zhang HC, Cai QL, Gao C, et al. Sepsis-induced immunosuppression: mechanisms, diagnosis and current treatment options. *Mil Med Res* (2022) 9(1):56. doi: 10.1186/s40779-022-00422-y

42. Torres LK, Pickkers P, van der Poll T. Sepsis-induced immunosuppression. *Annu Rev Physiol* (2022) 84:157–81. doi: 10.1146/annurev-physiol-061121-040214

43. Yao RQ, Ren C, Zheng LY, Xia ZF, Yao YM. Advances in immune monitoring approaches for sepsis-induced immunosuppression. *Front Immunol* (2022) 13:891024. doi: 10.3389/fimmu.2022.891024

44. Preau S, Vodovar D, Jung B, Lancel S, Zafrani L, Flatres A, et al. Energetic dysfunction in sepsis: a narrative review. *Ann Intensive Care* (2021) 11(1):104. doi: 10.1186/s13613-021-00893-7

45. Iida J, Ishii S, Nakajima Y, Sessler DI, Teramae H, Kageyama K, et al. Hyperglycaemia augments lipopolysaccharide-induced reduction in rat and human macrophage phagocytosis via the endoplasmic stress-C/EBP homologous protein pathway. *Br J Anaesth* (2019) 123(1):51–9. doi: 10.1016/j.bja.2019.03.040

46. Cappi SB, Noritomi DT, Velasco IT, Curi R, Loureiro TC, Soriano FG. Dyslipidemia: a prospective controlled randomized trial of intensive glycemic control in sepsis. *Intensive Care Med* (2012) 38(4):634–41. doi: 10.1007/s00134-011-2458-z

47. Paumelle R, Haas JT, Hennuyer N, Baugé E, Deleye Y, Mesotten D, et al. Hepatic PPARα is critical in the metabolic adaptation to sepsis. *J Hepatol* (2019) 70(5):963–73. doi: 10.1016/j.jhep.2018.12.037

48. Zhang J, Ankawi G, Sun J, Digvijay K, Yin Y, Rosner MH, et al. Gut-kidney crosstalk in septic acute kidney injury. *Crit Care* (2018) 22(1):117. doi: 10.1186/s13054-018-2040-y

49. Dominguez JA, Coopersmith CM. Can we protect the gut in critical illness? The role of growth factors and other novel approaches. *Crit Care Clin* (2010) 26(3):549–65. doi: 10.1016/j.ccc.2010.04.005

50. Vaziri ND, Yuan J, Rahimi A, Ni Z, Said H, Subramanian VS. Disintegration of colonic epithelial tight junction in uremia: a likely cause of CKD-associated inflammation. *Nephrol Dial Transplant* (2012) 27(7):2686–93. doi: 10.1093/ndt/gfr624

51. Hayakawa M, Asahara T, Henzan N, Murakami H, Yamamoto H, Mukai N, et al. Dramatic changes of the gut flora immediately after severe and sudden insults. *Dig Dis Sci* (2011) 56(8):2361–5. doi: 10.1007/s10620-011-1649-3

52. Kim CH. Complex regulatory effects of gut microbial short-chain fatty acids on immune tolerance and autoimmunity. *Cell Mol Immunol* (2023) 20(4):341–50. doi: 10.1038/s41423-023-00987-1

53. Wang A, Li Z, Sun Z, Zhang D, Ma X. Gut-derived short-chain fatty acids bridge cardiac and systemic metabolism and immunity in heart failure. *J Nutr Biochem* (2023) 120:109370. doi: 10.1016/j.jnutbio.2023.109370

54. Lou X, Xue J, Shao R, Yang Y, Ning D, Mo C, et al. Fecal microbiota transplantation and short-chain fatty acids reduce sepsis mortality by remodeling antibiotic-induced gut microbiota disturbances. *Front Immunol* (2022) 13:1063543. doi: 10.3389/fimmu.2022.1063543

55. Giridharan VV, Generoso JS, Lence L, Candiotto G, Streck E, Petronilho F, et al. A crosstalk between gut and brain in sepsis-induced cognitive decline. *J Neuroinflamm* (2022) 19(1):114. doi: 10.1186/s12974-022-02472-4

56. Vinolo MA, Rodrigues HG, Hatanaka E, Sato FT, Sampaio SC, Curi R. Suppressive effect of short-chain fatty acids on production of proinflammatory mediators by neutrophils. *J Nutr Biochem* (2011) 22(9):849–55. doi: 10.1016/j.jnutbio.2010.07.009

57. Sorboni SG, Moghaddam HS, Jafarzadeh-Esfehani R, Soleimanpour S. A comprehensive review on the role of the gut microbiome in human neurological disorders. *Clin Microbiol Rev* (2022) 35(1):e0033820. doi: 10.1128/cmr.00338-20

58. Deng H, Li Z, Tan Y, Guo Z, Liu Y, Wang Y, et al. A novel strain of Bacteroides fragilis enhances phagocytosis and polarises M1 macrophages. *Sci Rep* (2016) 6:29401. doi: 10.1038/srep29401

59. Zhang H, Xu J, Wu Q, Fang H, Shao X, Ouyang X, et al. Gut microbiota mediates the susceptibility of mice to sepsis-associated encephalopathy by butyric acid. *J Inflammation Res* (2022) 15:2103–19. doi: 10.2147/jir.S350566

60. Yang W, Cong Y. Gut microbiota-derived metabolites in the regulation of host immune responses and immune-related inflammatory diseases. *Cell Mol Immunol* (2021) 18(4):866–77. doi: 10.1038/s41423-021-00661-4

61. Mittal R, Coopersmith CM. Redefining the gut as the motor of critical illness. *Trends Mol Med* (2014) 20(4):214–23. doi: 10.1016/j.molmed.2013.08.004

62. Chancharoenthana W, Sutnu N, Visitchanakun P, Sawaswong V, Chitcharoen S, Payungporn S, et al. Critical roles of sepsis-reshaped fecal virota in attenuating sepsis severity. *Front Immunol* (2022) 13:940935. doi: 10.3389/fimmu.2022.940935

63. Gai X, Wang H, Li Y, Zhao H, He C, Wang Z, et al. Fecal microbiota transplantation protects the intestinal mucosal barrier by reconstructing the gut microbiota in a murine model of sepsis. *Front Cell Infect Microbiol* (2021) 11:736204. doi: 10.3389/fcimb.2021.736204

64. Fernandes J, Su W, Rahat-Rozenbloom S, Wolever TM, Comelli EM. Adiposity, gut microbiota and faecal short chain fatty acids are linked in adult humans. *Nutr Diabetes* (2014) 4(6):e121. doi: 10.1038/nutd.2014.23

65. Hamer HM, Jonkers D, Venema K, Vanhoutvin S, Troost FJ, Brummer RJ. Review article: the role of butyrate on colonic function. *Aliment Pharmacol Ther* (2008) 27(2):104–19. doi: 10.1111/j.1365-2036.2007.03562.x

66. MaChado MG, Patente TA, Rouillé Y, Heumel S, Melo EM, Deruyter L, et al. Acetate Improves the Killing of Streptococcus pneumoniae by Alveolar Macrophages via NLRP3 Inflammasome and Glycolysis-HIF-1α Axis. *Front Immunol* (2022) 13:773261. doi: 10.3389/fimmu.2022.773261

67. Ragsdale SW, Pierce E. Acetogenesis and the Wood-Ljungdahl pathway of CO (2) fixation. *Biochim Biophys Acta* (2008) 1784(12):1873–98. doi: 10.1016/j.bbapap.2008.08.012

68. Koh A, De Vadder F, Kovatcheva-Datchary P, Bäckhed F. From dietary fiber to host physiology: short-chain fatty acids as key bacterial metabolites. *Cell* (2016) 165(6):1332–45. doi: 10.1016/j.cell.2016.05.041

69. Nogal A, Valdes AM, Menni C. The role of short-chain fatty acids in the interplay between gut microbiota and diet in cardio-metabolic health. *Gut Microbes* (2021) 13(1):1–24. doi: 10.1080/19490976.2021.1897212

70. Hetzel M, Brock M, Selmer T, Pierik AJ, Golding BT, Buckel W. Acryloyl-CoA reductase from Clostridium propionicum. An enzyme complex of propionyl-CoA dehydrogenase and electron-transferring flavoprotein. *Eur J Biochem* (2003) 270(5):902–10. doi: 10.1046/j.1432-1033.2003.03450.x

71. Scott KP, Martin JC, Campbell G, Mayer CD, Flint HJ. Whole-genome transcription profiling reveals genes up-regulated by growth on fucose in the human gut bacterium "Roseburia inulinivorans". *J Bacteriol* (2006) 188(12):4340–9. doi: 10.1128/jb.00137-06

72. Xie L, Alam MJ, Marques FZ, Mackay CR. A major mechanism for immunomodulation: Dietary fibres and acid metabolites. *Semin Immunol* (2023) 66:101737. doi: 10.1016/j.smim.2023.101737

73. Louis P, Duncan SH, McCrae SI, Millar J, Jackson MS, Flint HJ. Restricted distribution of the butyrate kinase pathway among butyrate-producing bacteria from the human colon. *J Bacteriol* (2004) 186(7):2099–106. doi: 10.1128/jb.186.7.2099-2106.2004

74. Wang X, Sun Z, Yang T, Lin F, Ye S, Yan J, et al. Sodium butyrate facilitates CRHR2 expression to alleviate HPA axis hyperactivity in autism-like rats induced by

prenatal lipopolysaccharides through histone deacetylase inhibition. *mSystems* (2023) 8 (4):e0041523. doi: 10.1128/msystems.00415-23

75. Topping DL, Clifton PM. Short-chain fatty acids and human colonic function: roles of resistant starch and nonstarch polysaccharides. *Physiol Rev* (2001) 81(3):1031–64. doi: 10.1152/physrev.2001.81.3.1031

76. Lecerf JM, Dépeint F, Clerc E, Dugenet Y, Niamba CN, Rhazi L, et al. Xylo-oligosaccharide (XOS) in combination with inulin modulates both the intestinal environment and immune status in healthy subjects, while XOS alone only shows prebiotic properties. *Br J Nutr* (2012) 108(10):1847–58. doi: 10.1017/s0007114511007252

77. Le Leu RK, Winter JM, Christophersen CT, Young GP, Humphreys KJ, Hu Y, et al. Butyrylated starch intake can prevent red meat-induced O6-methyl-2-deoxyguanosine adducts in human rectal tissue: a randomised clinical trial. *Br J Nutr* (2015) 114(2):220–30. doi: 10.1017/s0007114515001750

78. Ghosh TS, Shanahan F, O'Toole PW. The gut microbiome as a modulator of healthy ageing. *Nat Rev Gastroenterol Hepatol* (2022) 19(9):565–84. doi: 10.1038/s41575-022-00605-x

79. Haskey N, Estaki M, Ye J, Shim RK, Singh S, Dieleman LA, et al. A Mediterranean Diet Pattern improves intestinal inflammation concomitant with reshaping of the bacteriome in ulcerative colitis: A randomized controlled trial. *J Crohns Colitis* (2023) jjad073. doi: 10.1093/ecco-jcc/jjad073

80. Yao Y, Cai X, Fei W, Ye Y, Zhao M, Zheng C. The role of short-chain fatty acids in immunity, inflammation and metabolism. *Crit Rev Food Sci Nutr* (2022) 62(1):1–12. doi: 10.1080/10408398.2020.1854675

81. Al-Lahham S, Roelofsen H, Rezaee F, Weening D, Hoek A, Vonk R, et al. Propionic acid affects immune status and metabolism in adipose tissue from overweight subjects. *Eur J Clin Invest* (2012) 42(4):357–64. doi: 10.1111/j.1365-2362.2011.02590.x

82. Fellows R, Varga-Weisz P. Chromatin dynamics and histone modifications in intestinal microbiota-host crosstalk. *Mol Metab* (2020) 38:100925. doi: 10.1016/j.molmet.2019.12.005

83. MacFie J, O'Boyle C, Mitchell CJ, Buckley PM, Johnstone D, Sudworth P. Gut origin of sepsis: a prospective study investigating associations between bacterial translocation, gastric microflora, and septic morbidity. *Gut* (1999) 45(2):223–8. doi: 10.1136/gut.45.2.223

84. Graspeuntner S, WasChina S, Künzel S, Twisselmann N, Rausch TK, Cloppenborg-Schmidt K, et al. Gut dysbiosis with bacilli dominance and accumulation of fermentation products precedes late-onset sepsis in preterm infants. *Clin Infect Dis* (2019) 69(2):268–77. doi: 10.1093/cid/ciy882

85. Xu W, Zhong M, Pan T, Qu H, Chen E. Gut microbiota and enteral nutrition tolerance in non-abdominal infection septic ICU patients: an observational study. *Nutrients* (2022) 14(24):5342. doi: 10.3390/nu14245342

86. Weng J, Wu H, Xu Z, Xi H, Chen C, Chen D, et al. The role of propionic acid at diagnosis predicts mortality in patients with septic shock. *J Crit Care* (2018) 43:95–101. doi: 10.1016/j.jcrc.2017.08.009

87. Li Z, Zhang F, Sun M, Liu J, Zhao L, Liu S, et al. The modulatory effects of gut microbes and metabolites on blood-brain barrier integrity and brain function in sepsis-associated encephalopathy. *PeerJ* (2023) 11:e15122. doi: 10.7717/peerj.15122

88. Wang H, Chen H, Lin Y, Wang G, Luo Y, Li X, et al. Butyrate glycerides protect against intestinal inflammation and barrier dysfunction in mice. *Nutrients* (2022) 14 (19):3991. doi: 10.3390/nu14193991

89. Zhan Z, Tang H, Zhang Y, Huang X, Xu M. Potential of gut-derived short-chain fatty acids to control enteric pathogens. *Front Microbiol* (2022) 13:976406. doi: 10.3389/fmicb.2022.976406

90. Masui R, Sasaki M, Funaki Y, Ogasawara N, Mizuno M, Iida A, et al. G protein-coupled receptor 43 moderates gut inflammation through cytokine regulation from mononuclear cells. *Inflammation Bowel Dis* (2013) 19(13):2848–56. doi: 10.1097/01.MIB.0000435444.14860.ea

91. Wang F, Liu J, Weng T, Shen K, Chen Z, Yu Y, et al. The Inflammation Induced by Lipopolysaccharide can be Mitigated by Short-chain Fatty Acid, Butyrate, through Upregulation of IL-10 in Septic Shock. *Scand J Immunol* (2017) 85(4):258–63. doi: 10.1111/sji.12515

92. Filippone A, Lanza M, Campolo M, Casili G, Paterniti I, Cuzzocrea S, et al. The anti-inflammatory and antioxidant effects of sodium propionate. *Int J Mol Sci* (2020) 21 (8):3026. doi: 10.3390/ijms21083026

93. Fu J, Li G, Wu X, Zang B. Sodium butyrate ameliorates intestinal injury and improves survival in a rat model of cecal ligation and puncture-induced sepsis. *Inflammation* (2019) 42(4):1276–86. doi: 10.1007/s10753-019-00987-2

94. Qiu J, Villa M, Sanin DE, Buck MD, O'Sullivan D, Ching R, et al. Acetate promotes T cell effector function during glucose restriction. *Cell Rep* (2019) 27 (7):2063–74.e2065. doi: 10.1016/j.celrep.2019.04.022

95. Balmer ML, Ma EH, Bantug GR, Grählert J, Pfister S, Glatter T, et al. Memory CD8(+) T cells require increased concentrations of acetate induced by stress for optimal function. *Immunity* (2016) 44(6):1312–24. doi: 10.1016/j.immuni.2016.03.016

96. Sun Y, Varambally S, Maher CA, Cao Q, Chockley P, Toubai T, et al. Targeting of microRNA-142-3p in dendritic cells regulates endotoxin-induced mortality. *Blood* (2011) 117(23):6172–83. doi: 10.1182/blood-2010-12-325647

97. Cao L, Zhu T, Lang X, Jia S, Yang Y, Zhu C, et al. Inhibiting DNA methylation improves survival in severe sepsis by regulating NF-κB pathway. *Front Immunol* (2020) 11:1360. doi: 10.3389/fimmu.2020.01360

98. Eyenga P, Rey B, Eyenga L, Sheu SS. Regulation of oxidative phosphorylation of liver mitochondria in sepsis. *Cells* (2022) 11(10):1598. doi: 10.3390/cells11101598

99. Shang S, Liu J, Hua F. Protein acylation: mechanisms, biological functions and therapeutic targets. *Signal Transduct Target Ther* (2022) 7(1):396. doi: 10.1038/s41392-022-01245-y

100. Mowen KA, David M. Unconventional post-translational modifications in immunological signaling. *Nat Immunol* (2014) 15(6):512–20. doi: 10.1038/ni.2873

101. Zhang F, Qi L, Feng Q, Zhang B, Li X, Liu C, et al. HIPK2 phosphorylates HDAC3 for NF-κB acetylation to ameliorate colitis-associated colorectal carcinoma and sepsis. *Proc Natl Acad Sci USA* (2021) 118(28):e2021798118. doi: 10.1073/pnas.2021798118

102. Schliehe C, Flynn EK, Vilagos B, Richson U, Swaminanthan S, Bosnjak B, et al. The methyltransferase Setdb2 mediates virus-induced susceptibility to bacterial superinfection. *Nat Immunol* (2015) 16(1):67–74. doi: 10.1038/ni.3046

103. Chang G, Ma N, Zhang H, Wang Y, Huang J, Liu J, et al. Sodium butyrate modulates mucosal inflammation injury mediated by GPR41/43 in the cecum of goats fed a high concentration diet. *Front Physiol* (2019) 10:1130. doi: 10.3389/fphys.2019.01130

104. Campbell C, McKenney PT, Konstantinovsky D, Isaeva OI, Schizas M, Verter J, et al. Bacterial metabolism of bile acids promotes generation of peripheral regulatory T cells. *Nature* (2020) 581(7809):475–9. doi: 10.1038/s41586-020-2193-0

105. Yamada N, Karasawa T, Kimura H, Watanabe S, Komada T, Kamata R, et al. Ferroptosis driven by radical oxidation of n-6 polyunsaturated fatty acids mediates acetaminophen-induced acute liver failure. *Cell Death Dis* (2020) 11(2):144. doi: 10.1038/s41419-020-2334-2

106. Wu Z, Connolly J, Biggar KK. Beyond histones - the expanding roles of protein lysine methylation. *FEBS J* (2017) 284(17):2732–44. doi: 10.1111/febs.14056

107. Kaniskan HU, Martini ML, Jin J. Inhibitors of protein methyltransferases and demethylases. *Chem Rev* (2018) 118(3):989–1068. doi: 10.1021/acs.chemrev.6b00801

108. Xia M, Liu J, Wu X, Liu S, Li G, Han C, et al. Histone methyltransferase Ash1l suppresses interleukin-6 production and inflammatory autoimmune diseases by inducing the ubiquitin-editing enzyme A20. *Immunity* (2013) 39(3):470–81. doi: 10.1016/j.immuni.2013.08.016

109. Kaye DM, Shihata WA, Jama HA, Tsyganov K, Ziemann M, Kiriazis H, et al. Deficiency of prebiotic fiber and insufficient signaling through gut metabolite-sensing receptors leads to cardiovascular disease. *Circulation* (2020) 141(17):1393–403. doi: 10.1161/circulationaha.119.043081

110. Wang M, Lin H. Understanding the function of mammalian sirtuins and protein lysine acylation. *Annu Rev Biochem* (2021) 90:245–85. doi: 10.1146/annurev-biochem-082520-125411

111. Singh N, Thangaraju M, Prasad PD, Martin PM, Lambert NA, Boettger T, et al. Blockade of dendritic cell development by bacterial fermentation products butyrate and propionate through a transporter (Slc5a8)-dependent inhibition of histone deacetylases. *J Biol Chem* (2010) 285(36):27601–8. doi: 10.1074/jbc.M110.102947

112. Feng T, Cao AT, Weaver CT, Elson CO, Cong Y. Interleukin-12 converts Foxp3 + regulatory T cells to interferon-γ-producing Foxp3+ T cells that inhibit colitis. *Gastroenterology* (2011) 140(7):2031–43. doi: 10.1053/j.gastro.2011.03.009

113. Arpaia N, Campbell C, Fan X, Dikiy S, van der Veeken J, deRoos P, et al. Metabolites produced by commensal bacteria promote peripheral regulatory T-cell generation. *Nature* (2013) 504(7480):451–5. doi: 10.1038/nature12726

114. Furusawa Y, Obata Y, Fukuda S, Endo TA, Nakato G, Takahashi D, et al. Commensal microbe-derived butyrate induces the differentiation of colonic regulatory T cells. *Nature* (2013) 504(7480):446–50. doi: 10.1038/nature12721

115. Smith PM, Howitt MR, Panikov N, Michaud M, Gallini CA, Bohlooly YM, et al. The microbial metabolites, short-chain fatty acids, regulate colonic Treg cell homeostasis. *Science* (2013) 341(6145):569–73. doi: 10.1126/science.1241165

116. Das B, Dobrowolski C, Shahir AM, Feng Z, Yu X, Sha J, et al. Short chain fatty acids potently induce latent HIV-1 in T-cells by activating P-TEFb and multiple histone modifications. *Virology* (2015) 474:65–81. doi: 10.1016/j.virol.2014.10.033

117. Thorburn AN, McKenzie CI, Shen S, Stanley D, Macia L, Mason LJ, et al. Evidence that asthma is a developmental origin disease influenced by maternal diet and bacterial metabolites. *Nat Commun* (2015) 6:7320. doi: 10.1038/ncomms8320

118. Takahashi D, Hoshina N, Kabumoto Y, Maeda Y, Suzuki A, Tanabe H, et al. Microbiota-derived butyrate limits the autoimmune response by promoting the differentiation of follicular regulatory T cells. *EBioMedicine* (2020) 58:102913. doi: 10.1016/j.ebiom.2020.102913

119. Luu M, Pautz S, Kohl V, Singh R, Romero R, Lucas S, et al. The short-chain fatty acid pentanoate suppresses autoimmunity by modulating the metabolic-epigenetic crosstalk in lymphocytes. *Nat Commun* (2019) 10(1):760. doi: 10.1038/s41467-019-08711-2

120. Park J, Kim M, Kang SG, Jannasch AH, Cooper B, Patterson J, et al. Short-chain fatty acids induce both effector and regulatory T cells by suppression of histone deacetylases and regulation of the mTOR-S6K pathway. *Mucosal Immunol* (2015) 8 (1):80–93. doi: 10.1038/mi.2014.44

121. Yang W, Yu T, Huang X, Bilotta AJ, Xu L , Lu Y, et al. Intestinal microbiota-derived short-chain fatty acids regulation of immune cell IL-22 production and gut immunity. *Nat Commun* (2020) 11(1):4457. doi: 10.1038/s41467-020-18262-6

122. Liu S, Yu H, Liu Y, Liu X, Zhang Y, Bu C, et al. Chromodomain protein CDYL acts as a crotonyl-coA hydratase to regulate histone crotonylation and spermatogenesis. *Mol Cell* (2017) 67(5):853–866.e855. doi: 10.1016/j.molcel.2017.07.011

123. Chan JC, Maze I. Histone crotonylation makes its mark in depression research. *Biol Psychiatry* (2019) 85(8):616–8. doi: 10.1016/j.biopsych.2019.01.025

124. Tang X, Chen XF, Sun X, Xu P, Zhao X, Tong Y, et al. Short-chain enoyl-coA hydratase mediates histone crotonylation and contributes to cardiac homeostasis. *Circulation* (2021) 143(10):1066–9. doi: 10.1161/circulationaha.120.049438

125. Wang S, Mu G, Qiu B, Wang M, Yu Z, Wang W, et al. The function and related diseases of protein crotonylation. *Int J Biol Sci* (2021) 17(13):3441–55. doi: 10.7150/ijbs.58872

126. Jiang G, Li C, Lu M, Lu K, Li H. Protein lysine crotonylation: past, present, perspective. *Cell Death Dis* (2021) 12(7):703. doi: 10.1038/s41419-021-03987-z

127. Liu X, Wei W, Liu Y, Yang X, Wu J, Zhang Y, et al. MOF as an evolutionarily conserved histone crotonyltransferase and transcriptional activation by histone acetyltransferase-deficient and crotonyltransferase-competent CBP/p300. *Cell Discov* (2017) 3:17016. doi: 10.1038/celldisc.2017.16

128. Sabari BR, Tang Z, Huang H, Yong-Gonzalez V, Molina H, Kong HE, et al. Intracellular crotonyl-CoA stimulates transcription through p300-catalyzed histone crotonylation. *Mol Cell* (2015) 58(2):203–15. doi: 10.1016/j.molcel.2015.02.029

129. Fellows R, Denizot J, Stellato C, Cuomo A, Jain P, Stoyanova E, et al. Microbiota derived short chain fatty acids promote histone crotonylation in the colon through histone deacetylases. *Nat Commun* (2018) 9(1):105. doi: 10.1038/s41467-017-02651-5

130. Huang H, Luo Z, Qi S, Huang J, Xu P, Wang X, et al. Landscape of the regulatory elements for lysine 2-hydroxyisobutyrylation pathway. *Cell Res* (2018) 28 (1):111–25. doi: 10.1038/cr.2017.149

131. Huang S, Tang D, Dai Y. Metabolic functions of lysine 2-hydroxyisobutyrylation. *Cureus* (2020) 12(8):e9651. doi: 10.7759/cureus.9651

132. Wang N, Jiang Y, Peng P, Liu G, Qi S, Liu K, et al. Quantitative proteomics reveals the role of lysine 2-hydroxyisobutyrylation pathway mediated by tip60. *Oxid Med Cell Longev* (2022) 2022:4571319. doi: 10.1155/2022/4571319

133. Li M, Wang B, Zhang M, Rantalainen M, Wang S, Zhou H, et al. Symbiotic gut microbes modulate human metabolic phenotypes. *Proc Natl Acad Sci USA* (2008) 105 (6):2117–22. doi: 10.1073/pnas.0712038105

134. Calvani R, Miccheli A, Capuani G, Tomassini Miccheli A, Puccetti C, Delfini M, et al. Gut microbiome-derived metabolites characterize a peculiar obese urinary metabotype. *Int J Obes (Lond)* (2010) 34(6):1095–8. doi: 10.1038/ijo.2010.44

135. Zhao S, Zhang X, Li H. Beyond histone acetylation-writing and erasing histone acylations. *Curr Opin Struct Biol* (2018) 53:169–77. doi: 10.1016/j.sbi.2018.10.001

136. Dong H, Zhai G, Chen C, Bai X, Tian S, Hu D, et al. Protein lysine de-2-hydroxyisobutyrylation by CobB in prokaryotes. *Sci Adv* (2019) 5(7):eaaw6703. doi: 10.1126/sciadv.aaw6703

137. Ge H, Li B, Chen W, Xu Q, Chen S, Zhang H, et al. Differential occurrence of lysine 2-hydroxyisobutyrylation in psoriasis skin lesions. *J Proteomics* (2019) 205:103420. doi: 10.1016/j.jprot.2019.103420

138. Yamazaki K, Miyauchi E, Kato T, Sato K, Suda W, Tsuzuno T, et al. Dysbiotic human oral microbiota alters systemic metabolism via modulation of gut microbiota in germ-free mice. *J Oral Microbiol* (2022) 14(1):2110194. doi: 10.1080/20002297.2022.2110194

139. Tsoukalas D, Fragoulakis V, Papakonstantinou E, Antonaki M, Vozikis A, Tsatsakis A, et al. Prediction of autoimmune diseases by targeted metabolomic assay of urinary organic acids. *Metabolites* (2020) 10(12):502. doi: 10.3390/metabo10120502

140. Zhao B, Lu R, Chen J, Xie M, Zhao X, Kong L. S100A9 blockade prevents lipopolysaccharide-induced lung injury via suppressing the NLRP3 pathway. *Respir Res* (2021) 22(1):45. doi: 10.1186/s12931-021-01641-y

141. Dong J, Li Y, Zheng F, Chen W, Huang S, Zhou X, et al. Co-occurrence of protein crotonylation and 2-hydroxyisobutyrylation in the proteome of end-stage renal disease. *ACS Omega* (2021) 6(24):15782–93. doi: 10.1021/acsomega.1c01161

142. Xie T, Dong J, Zhou X, Tang D, Li D, Chen J, et al. Proteomics analysis of lysine crotonylation and 2-hydroxyisobutyrylation reveals significant features of systemic lupus erythematosus. *Clin Rheumatol* (2022) 41(12):3851–8. doi: 10.1007/s10067-022-06254-4

143. Peng C, Lu Z, Xie Z, Cheng Z, Chen Y, Tan M, et al. The first identification of lysine malonylation substrates and its regulatory enzyme. *Mol Cell Proteomics* (2011) 10(12):M111.012658. doi: 10.1074/mcp.M111.012658

144. Li J, Zhao S, Zhou X, Zhang T, Zhao L, Miao P, et al. Inhibition of lipolysis by mercaptoacetate and etomoxir specifically sensitize drug-resistant lung adenocarcinoma cell to paclitaxel. *PloS One* (2013) 8(9):e74623. doi: 10.1371/journal.pone.0074623

145. Chen XF, Chen X, Tang X. Short-chain fatty acid, acylation and cardiovascular diseases. *Clin Sci (Lond)* (2020) 134(6):657–76. doi: 10.1042/cs20200128

146. Nishida Y, Rardin MJ, Carrico C, He W, Sahu AK, Gut P, et al. SIRT5 regulates both cytosolic and mitochondrial protein malonylation with glycolysis as a major target. *Mol Cell* (2015) 59(2):321–32. doi: 10.1016/j.molcel.2015.05.022

147. Lee H, Jang JH, Kim SJ. Malonic acid suppresses lipopolysaccharide-induced BV2 microglia cell activation by inhibiting the p38 MAPK/NF-κB pathway. *Anim Cells Syst (Seoul)* (2021) 25(2):110–8. doi: 10.1080/19768354.2021.1901781

148. Park C, Park J, Kim WJ, Kim W, Cheong H, Kim SJ. Malonic acid isolated from pinus densiflora inhibits UVB-induced oxidative stress and inflammation in haCaT keratinocytes. *Polymers (Basel)* (2021) 13(5):816. doi: 10.3390/polym13050816

149. Galván-Peña S, Carroll RG, Newman C, Hinchy EC, Palsson-McDermott E, Robinson EK, et al. Malonylation of GAPDH is an inflammatory signal in macrophages. *Nat Commun* (2019) 10(1):338. doi: 10.1038/s41467-018-08187-6

150. Qu L, Lin X, Liu C, Ke C, Zhou Z, Xu K, et al. Atractylodin attenuates dextran sulfate sodium-induced colitis by alleviating gut microbiota dysbiosis and inhibiting inflammatory response through the MAPK pathway. *Front Pharmacol* (2021) 12:665376. doi: 10.3389/fphar.2021.665376

Frontiers in Immunology

Explores novel approaches and diagnoses to treat immune disorders.

The official journal of the International Union of Immunological Societies (IUIS) and the most cited in its field, leading the way for research across basic, translational and clinical immunology.

Discover the latest Research Topics

See more →

Frontiers

Avenue du Tribunal-Fédéral 34
1005 Lausanne, Switzerland
frontiersin.org

Contact us

+41 (0)21 510 17 00
frontiersin.org/about/contact